

ISSN 1881-7815 Online ISSN 1881-7823

BST

BioScience Trends

Volume 18, Number 5
October, 2024



www.biosciencetrends.com

BST

BioScience Trends



ISSN: 1881-7815
Online ISSN: 1881-7823

CODEN: BTIRCZ
Issues/Year: 6
Language: English
Publisher: IACMHR Co., Ltd.

BioScience Trends is one of a series of peer-reviewed journals of the International Research and Cooperation Association for Bio & Socio-Sciences Advancement (IRCA-BSSA) Group. It is published bimonthly by the International Advancement Center for Medicine & Health Research Co., Ltd. (IACMHR Co., Ltd.) and supported by the IRCA-BSSA.

BioScience Trends devotes to publishing the latest and most exciting advances in scientific research. Articles cover fields of life science such as biochemistry, molecular biology, clinical research, public health, medical care system, and social science in order to encourage cooperation and exchange among scientists and clinical researchers.

BioScience Trends publishes Original Articles, Brief Reports, Reviews, Policy Forum articles, Communications, Editorials, News, and Letters on all aspects of the field of life science. All contributions should seek to promote international collaboration.

Editorial Board

Editor-in-Chief:

Norihiro KOKUDO
National Center for Global Health and Medicine, Tokyo, Japan

Co-Editors-in-Chief:

Xishan HAO
Tianjin Medical University, Tianjin, China
Takashi KARAKO
National Center for Global Health and Medicine, Tokyo, Japan
John J. ROSSI
Beckman Research Institute of City of Hope, Duarte, CA, USA

Hongen LIAO
Tsinghua University, Beijing, China
Misao MATSUSHITA
Tokai University, Hiratsuka, Japan
Fanghua QI
Shandong Provincial Hospital, Ji'nan, China
Ri SHO
Yamagata University, Yamagata, Japan
Yasuhiko SUGAWARA
Kumamoto University, Kumamoto, Japan
Ling WANG
Fudan University, Shanghai, China

Senior Editors:

Tetsuya ASAKAWA
The Third People's Hospital of Shenzhen, Shenzhen, China
Yu CHEN
The University of Tokyo, Tokyo, Japan
Xunjia CHENG
Fudan University, Shanghai, China
Yoko FUJITA-YAMAGUCHI
Beckman Research Institute of the City of Hope, Duarte, CA, USA
Jianjun GAO
Qingdao University, Qingdao, China
Na HE
Fudan University, Shanghai, China

Proofreaders:

Curtis BENTLEY
Roswell, GA, USA
Thomas R. LEBON
Los Angeles, CA, USA

Editorial and Head Office

Pearl City Koishikawa 603,
2-4-5 Kasuga, Bunkyo-ku, Tokyo 112-0003, Japan
E-mail: office@biosciencetrends.com

BioScience Trends

Editorial and Head Office

Pearl City Koishikawa 603, 2-4-5 Kasuga, Bunkyo-ku,
Tokyo 112-0003, Japan

E-mail: office@biosciencetrends.com
URL: www.biosciencetrends.com

Editorial Board Members

Girdhar G. AGARWAL
(Lucknow, India)

Hirotsugu AIGA
(Geneva, Switzerland)

Hidechika AKASHI
(Tokyo, Japan)

Moazzam ALI
(Geneva, Switzerland)

Ping AO
(Shanghai, China)

Hisao ASAMURA
(Tokyo, Japan)

Michael E. BARISH
(Duarte, CA, USA)

Boon-Huat BAY
(Singapore, Singapore)

Yasumasa BESSHO
(Nara, Japan)

Generoso BEVILACQUA
(Pisa, Italy)

Shiuan CHEN
(Duarte, CA, USA)

Yi-Li CHEN
(Yiwu, China)

Yue CHEN
(Ottawa, Ontario, Canada)

Naoshi DOHMAE
(Wako, Japan)

Zhen FAN
(Houston, TX, USA)

Ding-Zhi FANG
(Chengdu, China)

Xiao-Bin FENG
(Beijing, China)

Yoshiharu FUKUDA
(Ube, Japan)

Rajiv GARG
(Lucknow, India)

Ravindra K. GARG
(Lucknow, India)

Makoto GOTO
(Tokyo, Japan)

Demin HAN
(Beijing, China)

David M. HELFMAN
(Daejeon, Korea)

Takahiro HIGASHI
(Tokyo, Japan)

De-Fei HONG
(Hangzhou, China)

De-Xing HOU
(Kagoshima, Japan)

Sheng-Tao HOU
(Guanzhou, China)

Xiaoyang HU
(Southampton, UK)

Yong HUANG
(Ji'ning, China)

Hirofumi INAGAKI
(Tokyo, Japan)

Masamine JIMBA
(Tokyo, Japan)

Chun-Lin JIN
(Shanghai, China)

Kimataka KAGA
(Tokyo, Japan)

Michael Kahn
(Duarte, CA, USA)

Kazuhiro KAKIMOTO
(Osaka, Japan)

Kiyoko KAMIBEPPU
(Tokyo, Japan)

Haidong KAN
(Shanghai, China)

Kenji KARAKO
(Tokyo, Japan)

Bok-Luel LEE
(Busan, Korea)

Mingjie LI
(St. Louis, MO, USA)

Shixue LI
(Ji'nan, China)

Ren-Jang LIN
(Duarte, CA, USA)

Chuan-Ju LIU
(New York, NY, USA)

Lianxin LIU
(Hefei, China)

Xinqi LIU
(Tianjin, China)

Daru LU
(Shanghai, China)

Hongzhou LU
(Guanzhou, China)

Duan MA
(Shanghai, China)

Masatoshi MAKUUCHI
(Tokyo, Japan)

Francesco MAROTTA
(Milano, Italy)

Yutaka MATSUYAMA
(Tokyo, Japan)

Qingyue MENG
(Beijing, China)

Mark MEUTH
(Sheffield, UK)

Michihiro Nakamura
(Yamaguchi, Japan)

Munehiro NAKATA
(Hiratsuka, Japan)

Satoko NAGATA
(Tokyo, Japan)

Miho OBA
(Odawara, Japan)

Xianjun QU
(Beijing, China)

Carlos SAINZ-FERNANDEZ
(Santander, Spain)

Yoshihiro SAKAMOTO
(Tokyo, Japan)

Erin SATO
(Shizuoka, Japan)

Takehito SATO
(Isehara, Japan)

Akihito SHIMAZU
(Tokyo, Japan)

Zhifeng SHAO
(Shanghai, China)

Xiao-Ou SHU
(Nashville, TN, USA)

Sarah Shuck
(Duarte, CA, USA)

Judith SINGER-SAM
(Duarte, CA, USA)

Raj K. SINGH
(Dehradun, India)

Peipei SONG
(Tokyo, Japan)

Junko SUGAMA
(Kanazawa, Japan)

Zhipeng SUN
(Beijing, China)

Hiroshi TACHIBANA
(Isehara, Japan)

Tomoko TAKAMURA
(Tokyo, Japan)

Tadatoshi TAKAYAMA
(Tokyo, Japan)

Shin'ichi TAKEDA
(Tokyo, Japan)

Sumihito TAMURA
(Tokyo, Japan)

Puay Hoon TAN
(Singapore, Singapore)

Koji TANAKA
(Tsu, Japan)

John TERMINI
(Duarte, CA, USA)

Usa C. THISYAKORN
(Bangkok, Thailand)

Toshifumi TSUKAHARA
(Nomi, Japan)

Mudit Tyagi
(Philadelphia, PA, USA)

Kohjiro UEKI
(Tokyo, Japan)

Masahiro UMEZAKI
(Tokyo, Japan)

Junming WANG
(Jackson, MS, USA)

Qing Kenneth WANG
(Wuhan, China)

Xiang-Dong WANG
(Boston, MA, USA)

Hisashi WATANABE
(Tokyo, Japan)

Jufeng XIA
(Tokyo, Japan)

Feng XIE
(Hamilton, Ontario, Canada)

Jinfu XU
(Shanghai, China)

Lingzhong XU
(Ji'nan, China)

Masatake YAMAUCHI
(Chiba, Japan)

Aitian YIN
(Ji'nan, China)

George W.-C. YIP
(Singapore, Singapore)

Xue-Jie YU
(Galveston, TX, USA)

Rongfa YUAN
(Nanchang, China)

Benny C-Y ZEE
(Hong Kong, China)

Yong ZENG
(Chengdu, China)

Wei ZHANG
(Shanghai, China)

Wei ZHANG
(Tianjin, China)

Chengchao ZHOU
(Ji'nan, China)

Xiaomei ZHU
(Seattle, WA, USA)

(as of June 2024)

Editorial

- 404-408 **Strengthening medical facility responses to respiratory infectious diseases: Global trends, challenges, and innovations post-COVID-19.**
Xiaohe Li, Bing Han, Yafan Chen, Hongzhou Lu
- 409-412 **Blocking progression from intervenable mild cognitive impairment to irreversible dementia, what can we do?**
Yaohan Peng, Peipei Song, Takashi Karako, Tetsuya Asakawa

Review

- 413-430 **Exploring the multiple therapeutic mechanisms and challenges of mesenchymal stem cell-derived exosomes in Alzheimer's disease.**
Ya-nan Ma, Xiqi Hu, Kenji Karako, Peipei Song, Wei Tang, Ying Xia
- 431-443 **Management of non-alcoholic fatty liver disease-associated hepatocellular carcinoma.**
Peijun Xu, Maoyun Liu, Miao Liu, Ai Shen

Original Article

- 444-456 **How spousal cognitive functioning affects the level of depression in middle-aged and older adults: An instrumental variable study based on CHARLS in China.**
Zheng Wang, Ting Li, Jingbin Zhang, Cordia Chu, Shasha Yuan
- 457-464 **Sorafenib combined with TACE improves survival in patients with hepatocellular carcinoma with vascular invasion.**
Zhiqiang Han, Ruyun Han, Yimeng Wang, Kangwei Zhu, Xiangdong Tian, Ping Chen, Tianqiang Song, Lu Chen
- 465-475 **FNDC5/Irisin mitigates high glucose-induced neurotoxicity in HT22 cell *via* ferroptosis.**
Lingling Yang, Xiaohan Zhou, Tian Heng, Yinghai Zhu, Lihuan Gong, Na Liu, Xiuqing Yao, Yaxi Luo
- 476-481 **Imaging of pulmonary cryptococcosis with consolidations or diffuse infiltrates suggests longer clinical treatment in non-HIV patients.**
Yi Su, Yao Zhang, Qingqing Wang, Bijie Hu, Jue Pan
- 482-491 **Ligustrazine alleviates the progression of coronary artery calcification by inhibiting caspase-3/GSDME mediated pyroptosis.**
Honghui Yang, Guian Xu, Qingman Li, Lijie Zhu

Letter to the Editor

- 492-494 **Financial inclusion and financial gerontology in Japan's aging society.**
Shotaro Kinoshita, Kohei Komamura, Taishiro Kishimoto

Strengthening medical facility responses to respiratory infectious diseases: Global trends, challenges, and innovations post-COVID-19

Xiaohe Li^{1,§}, Bing Han^{2,3,§}, Yafan Chen^{1,4}, Hongzhou Lu^{1,*}

¹ National Clinical Research Centre for Infectious Diseases, The Third People's Hospital of Shenzhen and The Second Affiliated Hospital of Southern University of Science and Technology, Shenzhen, Guangdong, China;

² Beijing Ditan Hospital, Capital Medical University, Beijing, China;

³ Beijing Quality Control and Improvement Center of Infectious Diseases, Beijing, China;

⁴ Health Science Center, Shenzhen University, Shenzhen, Guangdong, China.

SUMMARY Respiratory infectious diseases have long been a serious public health problem. This study explores the significance of respiratory infectious disease prevention and control systems worldwide, particularly during and after the COVID-19 pandemic. The epidemiology of many respiratory diseases such as influenza changed over the past two years, and the incidence of pathogens such as *Mycoplasma pneumoniae* and *Bordetella pertussis* has also increased. Based on influenza surveillance data in China, the influenza season in 2023 was notably delayed and extended, with A(H1N1) pdm09 being the predominant strain. This editorial also reviewed the gradual establishment of China's infectious disease prevention and control system following the 2003 SARS outbreak, highlighting the role of medical facilities in managing public health emergencies, conducting infectious disease pre-screening, and reporting cases to networks in real time. In the future, China will further develop an intelligent, multi-trigger infectious disease surveillance and early warning system to increase the early detection of unknown infectious diseases and optimize the allocation of medical resources. A robust infectious disease control system is crucial to addressing future pandemic threats.

Keywords respiratory infectious disease, influenza, coronavirus disease 2019 (COVID-19), respiratory infectious disease prevention and control system, infectious disease surveillance

Respiratory infectious diseases pose a major global public health challenge, contributing significantly to the overall disease burden. The prevention and control of common respiratory infectious diseases, such as influenza and tuberculosis, remains a critical issue. Compounding this, the emergence of new and unpredictable outbreaks – including severe acute respiratory syndrome (SARS), Middle East respiratory syndrome (MERS), avian influenza in humans, and most recently, coronavirus disease 2019 (COVID-19) – further threatens public health and socio-economic stability worldwide.

Prevalence of respiratory infectious diseases

Following the relaxation of COVID-19 prevention and control measures worldwide, shifts in the epidemiological trends of respiratory infectious diseases have been observed (1). In addition to influenza viruses and respiratory syncytial viruses, novel coronaviruses

have emerged as a significant pathogen responsible for epidemics of respiratory infectious diseases (2). Concurrently, the number of patients infected with other pathogens, such as *Mycoplasma pneumoniae* and *Bordetella pertussis*, have increased following the emergence of pandemic-causing novel coronaviruses (3).

The epidemiology of influenza, the most prevalent respiratory infectious disease in the past, underwent a notable transformation prior to the emergence of the COVID-19 pandemic (Figure 1). According to data from the World Health Organization (WHO), the number of influenza cases remained relatively stable before the start of the COVID-19 pandemic. In 2020-2021, however, the global spread of COVID-19 led to a significant reduction in the annual transmission of influenza viruses worldwide. In 2021, the global number of influenza cases reached a historic low of 662,862, marking a decline from the previous year. However, the number of influenza cases globally increased significantly in

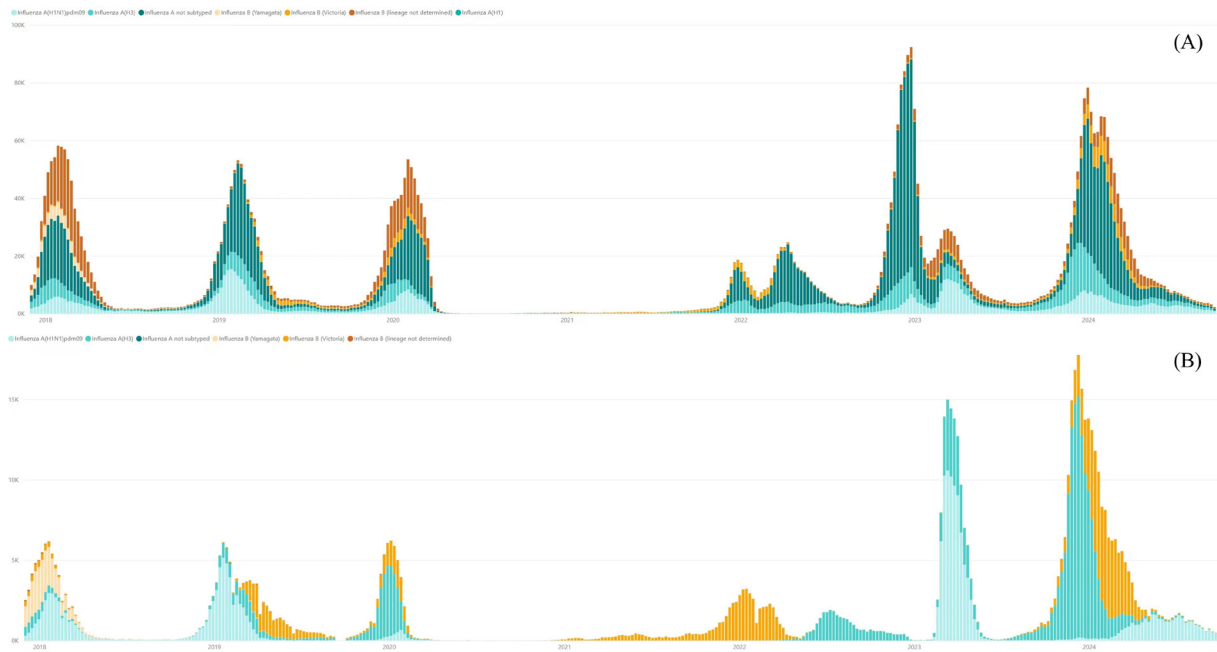


Figure 1. Instances of global influenza detection by subtype, 2018-2024, reported to FluNet, GISRS (2024-09-29) (A), Instances of influenza detection by subtype in China, 2018-2024, reported to FluNet, GISRS (2024-09-29) (B).

September 2023 and 2024, reaching levels well above those observed historically. In addition, the seasonality of influenza viruses shifted before and after the start of the COVID-19 pandemic. The timing of annual global influenza circulation in 2020 differed from that of any season observed previously. Influenza activity peaked in late January-early February 2020 and continued into early April 2020. For the remainder of 2020, influenza activity was either absent or minimal compared to that in previous years. However, the subsequent years, 2023 and 2024, witnessed a delayed and significantly prolonged influenza season. From mid-February to the end of April 2023, China experienced a wave of influenza epidemics predominantly involving the A(H1N1)pdm09 subtype. These seasonal epidemics occurred approximately two months later than the previous winter and spring influenza seasons (4). Moreover, the subspecies causing influenza epidemics differed. Of the 33,118,831 samples of respiratory viruses collected globally during inpatient and outpatient surveillance, 19% (614,907) were positive for influenza between early November 2019 and the end of December 2020. Of these positive samples, 63% were subtyped as influenza A and 37% (229,639) as influenza B. In contrast to the situation during the 2019–2020 COVID-19 pandemic, the 2023 and 2024 influenza seasons are predominantly characterized by untyped influenza A, and to a lesser extent, subtype A(H3N2). Data from the Global Influenza Surveillance and Response System (GISRS) indicate that the 2022–2023 influenza season in the EU/EEA countries was characterized by a co-pandemic of A(H1N1) pdm09, A(H3N2), and B/Victorian lineage viruses, with the A(H3N2) subtype predominating in 2024 (5). In 2022, an

influenza outbreak primarily caused by the B(Victoria) lineage occurred in northern China. After May 2022, the influenza epidemic season in the southern provinces of China predominantly involved the A(H3N2) subtype. From mid-February to the end of April 2023, a wave of influenza predominantly caused by the A(H1N1) pdm09 subtype was observed in the country. In the 2024 influenza season in China, epidemics caused by both the A(H3N2) and B(Victoria) lineage viruses occurred simultaneously.

The infection trends for the novel coronavirus warrant attention. According to the Centers for Disease Control and Prevention (CDC), both the nucleic acid positivity rate and mortality rate in the United States exhibited a seasonal pattern as of August 2024, with peaks in July–August and December–January, followed by a gradual decline beginning in March. The initial pandemic peak occurred between March and June 2020, with cases steadily rising in the months that followed. In the first week of January 2021, weekly deaths reached a record high of 25,974. Another surge in cases occurred in July 2021, driven by the spread of the Delta variant. The emergence of the Omicron variant in late 2021 and early 2022 led to a resurgence in cases, with a positivity rate of 30.5% in the first week of January 2022. However, widespread vaccination helped mitigate severe outcomes, keeping the proportion of severe cases relatively low. Over the past two years, the rise in incidence and mortality rates has stabilized (Figure 2A) (6). As of August 31, 2024, the cumulative number of confirmed cases in the United States surpassed 100 million, with over 1.2 million deaths. In December 2022, China announced a relaxation of its strict containment

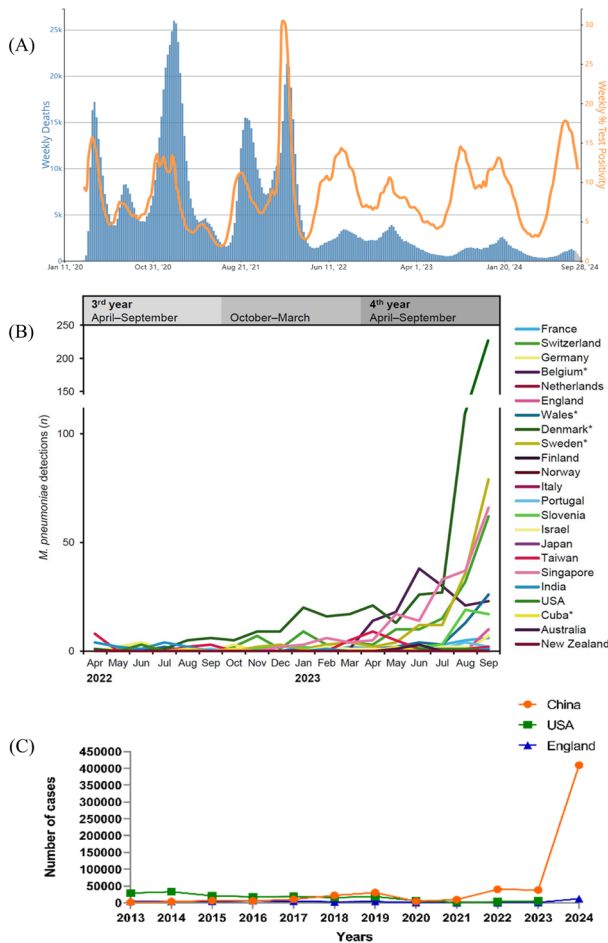


Figure 2: Provisional COVID-19 Deaths and COVID-19 Nucleic Acid Amplification Test (NAAT) Percent Positivity, by Week, in the United States, Reported to the CDC (through August 2024) (A); Mycoplasma pneumoniae detection by PCR worldwide since the start of the global prospective surveillance. Time in years and 6-month periods since the introduction of non-pharmaceutical interventions are indicated at the top of the graph. *National surveillance. Detection during the 3rd year was previously reported (B); The number of Pertussis cases in the United States, United Kingdom, and China, 2013-2024 (2024-07) (C).

policy, transitioning to a strategy of coexisting with the virus. From December 2022 to January 2023, China experienced a sharp surge in cases, with daily confirmed infections reaching several million. Despite this rebound, the proportion of severe cases declined, highlighting the effectiveness of China’s vaccination efforts. By October 2023, China had reported approximately 120 million cumulative confirmed cases and around 60,000 deaths. The overall mortality rate has significantly decreased since the early stages of the pandemic. As of April 2024, the national COVID-19 positivity rate remains low (2).

Global surveillance data for *M. pneumoniae* indicate that the global incidence of *M. pneumoniae* before the COVID-19 epidemic was 8.61%, and in the early 2020s the number of *M. pneumoniae* cases decreased yearly due to the strict NPIs (non-pharmaceutical interventions) implemented during the epidemic, to 1.69% in 2020 to 2021 and 0.70% in 2021 to 2022 (7). More than three

years after the implementation of restrictive measures during the COVID-19 pandemic, *M. pneumoniae* has re-emerged in both Europe and Asia (Figure 2B)(8). Since August 2023, there has been a notable surge in the incidence of *M. pneumoniae* cases in Denmark, Sweden, Singapore, and Switzerland (7). Similar changes in epidemiological trends have also been noted in China (8). *M. pneumoniae* triggered multiple outbreaks in Shanghai (9), Guangzhou (10), and Chongqing (11) after the COVID-19 pandemic, and especially among children (12).

Pertussis is an ancient infectious disease caused by *B. pertussis* that has historically had a low prevalence in countries around the world. Since 2023, the United States, the United Kingdom, and China have seen a significant rise in pertussis cases, with incidence far exceeding historical levels (Figure 2C) (13). This phenomenon has been particularly pronounced in China. Over the past year, reported pertussis cases in China have surged dramatically. In June 2023, there were 1,512 cases, though that number rose sharply to 15,275 by January 2024. This upward trend accelerated in the subsequent months, with the number of cases soaring to 91,272 in April and 97,669 in May—levels that are considerably higher than those observed historically.

Given the impact of the COVID-19 pandemic and the associated prevention and control measures, as well as the emergence of pathogen mutations and other factors, there have been changes in the pathogen spectrum and the epidemiological pattern of respiratory infectious diseases. This has resulted in the emergence of a number of new infectious diseases that have yet to exhibit clear epidemiological trends. Consequently, the threat to human health from Disease X will persist in the future. Therefore, development of a robust and comprehensive infectious disease prevention and control system is crucial.

How medical facilities respond to respiratory infections

In China, medical facilities act as the primary line of defense against respiratory infectious diseases. Effective prevention and control hinge on several key factors: monitoring and early warning systems for common respiratory infections, prompt identification of novel infectious diseases, and strategic allocation of medical resources. In response to the SARS outbreak in 2003, China progressively developed a comprehensive system for preventing and controlling respiratory infectious diseases centered around medical facilities. This system has been instrumental in enhancing the country’s response to such health threats.

1. *Establish a Management System for Public Health Emergencies:* The State Council introduced the Emergency Regulations for Public Health Emergencies in May 2003 and the National Emergency Plan for Public Health Emergencies in January 2006. These frameworks

classify public health emergencies into four levels based on their nature, severity, and scope: especially major (Level I), major (Level II), moderate (Level III), and general (Level IV). This classification system has established a national emergency response system and clarified the responsibilities of the various agencies involved.

2. *Pre-screen and Triage Infectious Diseases in Medical Facilities*: On September 13, 2004, and February 18, 2005, the former Ministry of Health issued the Notice on the Establishment of Infectious Disease Departments in General Hospitals above Level II and the Management Measures for Pre-screening and Triage of Infectious Diseases in Medical Facilities. These regulations mandate that general hospitals at Level II and above establish dedicated infectious disease departments to handle pre-screening and triage. This initiative aims to enable early identification of infectious diseases, designate specific departments for treatment, and minimize further transmission within healthcare settings.

3. *Enable Direct Reporting of Infectious Disease Information in Medical Facilities*: Post-SARS, China developed a network-based infectious disease reporting system for real-time reporting from primary medical facilities or county/district disease control centers to the Chinese Center for Disease Control and Prevention via the Internet. Infectious Disease Information Management Standards were established to enhance the reporting process and improve data quality. This system facilitates real-time monitoring of respiratory infectious diseases, such as influenza, COVID-19, pulmonary tuberculosis, and pneumonic plague, providing timely and accurate diagnostic and clinical information to aid in outbreak prevention and control.

4. *Conduct Surveillance of Unexplained Pneumonia*: In July 2004 and August 2007, the former Ministry of Health introduced the Implementation Plan for (Trial) National Surveillance of Unexplained Pneumonia Cases and the National Surveillance, Investigation, and Management Plan for Unexplained Pneumonia Cases. These plans initiated nationwide monitoring of unexplained pneumonia cases and clusters, enabling rapid identification of new pathogens. Notably, human infections with H7N9 avian influenza and the novel coronavirus were swiftly detected. For example, following the first reported H7N9 case in Shanghai in March 2013, specimens were analyzed, leading to the isolation of three strains of the virus within two weeks. Similarly, in December 2019, the Wuhan outbreak of unexplained pneumonia prompted immediate government action, including pathogen identification and international dissemination of the novel coronavirus's genetic sequence by January 10, 2020, showcasing a rapid response from initial detection to global alert.

5. *Enhance Intelligent Multi-point Trigger Monitoring and Early Warning Systems*: On August 30, 2024, the National Center for Disease Control and

Prevention issued the Guiding Opinions on Establishing and Improving the Intelligent Multi-point Trigger Infectious Disease Monitoring and Early Warning System. This initiative aims to unify the monitoring of clinical syndromes, laboratory surveillance of pathogens, and risk factors associated with vectors, host animals, and the environment, alongside effective monitoring of societal attitudes. By 2030, the goal is to develop a rapid, scientifically efficient monitoring and early warning system that significantly improves sensitivity and accuracy in detecting newly emerging infectious diseases, unexplained illness clusters, and key infectious diseases, achieving internationally advanced levels of epidemic detection, assessment, and warning capabilities.

Currently, China has established an effective system for preventing and controlling respiratory infectious diseases, centered on monitoring, diagnosis, and clinical outcomes at medical facilities. Future efforts will aim to further enhance the monitoring of infectious disease, clinical syndromes, and laboratory surveillance of pathogens. These improvements depend on the reliability of diagnostic practices across all levels of medical facilities.

In 2023, the National Health Commission introduced quality control indicators for influenza, which include metrics such as the positivity rate of laboratory diagnosis before antiviral therapy and the mortality rate among patients hospitalized with severe influenza. These indicators are designed to guide medical facilities in managing quality control related to etiological diagnosis, appropriate use of medication, and treatment of severe cases. Future indicators will also address diseases such as tuberculosis and COVID-19 with the aim of improving the diagnostic accuracy of respiratory infections.

These measures are expected to enhance China's capabilities in monitoring, warning of, and detecting unknown infectious diseases while ensuring the rational and effective allocation of medical resources.

Funding: Supported by grants from the Shenzhen Fund for High-level Key Clinical Specialties in Guangdong Province (no. SZGSP011), the Shenzhen Clinical Research Center for Emerging Infectious Diseases (nos. LCYSSQ20220823091203007 and LCYSSQ20220823091203007), the Shenzhen High level Hospital Construction Fund, and High-level Public Health Technical Talents Construction Project from Beijing Municipal Health Commission (No.2022-01-02).

Conflict of Interest: The authors have no conflicts of interest to disclose.

References

1. Hamid S, Winn A, Parikh R, Jones JM, McMorro M, Prill MM, Silk BJ, Scobie HM, Hall AJ. Seasonality of respiratory syncytial virus - United States, 2017-2023.

- MMWR Morb Mortal Wkly Rep. 2023; 72:355-361.
- Han B, Li XM, Li R, *et al.* Epidemiological surveillance of acute respiratory infections based on targeted metagenomic next generation sequencing during the flu season after COVID-19 pandemic in Beijing. *J Infect.* 2024; 89:106188.
 - Wang MH, Hu ZX, Feng LZ, Yu HJ, Yang J. Epidemic trends and prevention and control of seasonal influenza in China after the COVID-19 pandemic. *Zhonghua Yi Xue Za Zhi.* 2024; 104:559-565. (in Chinese)
 - Ma GF, Zhu J, Cao HJ, Jiang Y. Epidemiological analysis of influenza virus in China from 2013 to 2018. *J Pathogen Bio.* 2019; 14:73-77. (in Chinese)
 - Broberg EK, Svartström O, Riess M, Kraus A, Vukovikj M, Melidou A. Co-circulation of seasonal influenza A(H1N1)pdm09, A(H3N2) and B/Victoria lineage viruses with further genetic diversification, EU/EEA, 2022/23 influenza season. *Euro Surveill.* 2024; 29.
 - US Centers for Disease Control and Prevention. COVID Data Tracker. <https://covid.cdc.gov/covid-data-tracker/#datatracker-home> (accessed September 17, 2024).
 - Meyer Sauter PM, Beeton ML, Uldum SA, *et al.* Mycoplasma pneumoniae detections before and during the COVID-19 pandemic: Results of a global survey, 2017 to 2021. *Euro Surveill.* 2022; 27.
 - Meyer Sauter PM, Beeton ML. Mycoplasma pneumoniae: Delayed re-emergence after COVID-19 pandemic restrictions. *Lancet Microbe.* 2024; 5:e100-e101.
 - Zhu X, Liu P, Yu H, Wang L, Zhong H, Xu M, Lu L, Jia R, Su L, Cao L, Zhai X, Wang Y, Xu J. An outbreak of Mycoplasma pneumoniae in children after the COVID-19 pandemic, Shanghai, China, 2023. *Front Microbiol.* 2024; 15:1427702.
 - Li Y, Wu M, Liang Y, Yang Y, Guo W, Deng Y, Wen T, Tan C, Lin C, Liu F, Lin Y, Chen Q. Mycoplasma pneumoniae infection outbreak in Guangzhou, China after COVID-19 pandemic. *Virology.* 2024; 21:183.
 - You J, Zhang L, Chen W, Wu Q, Zhang D, Luo Z, Fu Z. Epidemiological characteristics of Mycoplasma pneumoniae in hospitalized children before, during, and after COVID-19 pandemic restrictions in Chongqing, China. *Front Cell Infect Microbiol.* 2024; 14:1424554.
 - Wei M, Li S, Lu X, Hu K, Li Z, Li M. Changing respiratory pathogens infection patterns after COVID-19 pandemic in Shanghai, China. *J Med Virol.* 2024; 96:e29616.
 - gov.uk. Confirmed cases of pertussis in England by month. <https://www.gov.uk/government/publications/pertussis-epidemiology-in-england-2024/confirmed-cases-of-pertussis-in-england-by-month> (accessed September 17, 2024).
- Received September 15, 2024; Revised October 12, 2024; Accepted October 15, 2024.
- §These authors contributed equally to this work.
*Address correspondence to:
Hongzhou Lu, Department of Infectious Diseases, National Clinical Research Center for Infectious Diseases, Shenzhen Third People's Hospital, Shenzhen 518112, Guangdong Province, China.
E-mail: luhongzhou@fudan.edu.cn
- Released online in J-STAGE as advance publication October 17, 2024.

Blocking progression from intervenable mild cognitive impairment to irreversible dementia, what can we do?

Yaohan Peng¹, Peipei Song^{2,3,*}, Takashi Karako^{2,3,*}, Tetsuya Asakawa^{4,*}

¹Key Laboratory of Plateau Hypoxia Environment and Life and Health, Xizang Minzu University, Xianyang, Shaanxi, China;

²National Center for Global Health and Medicine, Tokyo, Japan;

³National College of Nursing, Japan, Tokyo, Japan;

⁴Institute of Neurology, National Clinical Research Center for Infectious Diseases, The Third People's Hospital of Shenzhen, Shenzhen, Guangdong, China.

SUMMARY With the rapid growth of the elderly population, dementia has become a global challenge that governments must address. Given the incurable nature of dementia, rehabilitation interventions starting in the mild cognitive impairment (MCI) stage may offer a solution. For a rehabilitation intervention to be implemented as early as possible, existing problems of identification of MCI and development of MCI-specific forms of rehabilitation must be addressed. Use of computer technologies such as virtual reality and artificial intelligence might be helpful in overcoming these problems. Multi-disciplinary integrated approaches to rehabilitation should be the direction that dementia-related rehabilitation takes in the future. In addition to early rehabilitation, prevention of cognitive decline through the development of public community-based services for the elderly might be a more reasonable approach.

Keywords dementia, mild cognitive impairment, virtual reality, rehabilitation, elderly care facilities

1. Background

Dementia is a pathophysiological state characterized by a decline in cognitive domains including memory, attention, movement, language, communication, and executive function. It is usually caused by a spectrum of diseases, such as Alzheimer's disease (AD), vascular dementia, dementia with Lewy bodies, and Parkinson's disease-related dementia. Dementia markedly impacts activities of daily living (ADL) and quality of life (QOL), with dementia-related death being frequently reported (1). Todd *et al.* reported that the median survival time from dementia onset ranges from 3.3 to 11.7 years, with most studies indicating 7-11.7 years (2). This implies that patients with dementia must live for an extended period in a state requiring care, significantly increasing the burden on their families and society. Dementia has become a global public health concern with aging of the population. Dementia typically progresses through seven stages (Figure 1). Once patients reach the dementia stage, existing treatments have minimal impact on their functional activities and QOL (3). Mild cognitive impairment (MCI) is the initial stage before mild dementia, where cognitive impairment is mild and does not affect the ability for self-care. The annual

conversion rate of MCI to dementia is reportedly 10-15%, approximately four times that for individuals with normal cognition. Over 80% of individuals develop dementia after six years (4). Nonetheless, intervention in the MCI stage might be beneficial, particularly with early rehabilitation (5,6). In this regard, the MCI stage might be the only stage when intervention could prove useful. Thus, timely identification of MCI and subsequent effective interventions might be the only useful approach for dementia so far.

2. Identification of MCI

Identifying cognitive impairment, and MCI in particular, is a challenge. Over 50% of individuals with dementia are left undiagnosed or diagnosed late in primary care settings (7). Several factors contribute to this issue:

i) Most widely-used neuropsychological tools for dementia, such as the Montreal Cognitive Assessment (MoCA) and Mini-Mental State Examination (MMSE), are investigator-reported scales. Although some objective tasks are included, some items remain subjective (8). Importantly, the thresholds for MCI are questionable. A recent study reported that the conversion rate from MCI to AD increased to 84% when the MCI threshold was set

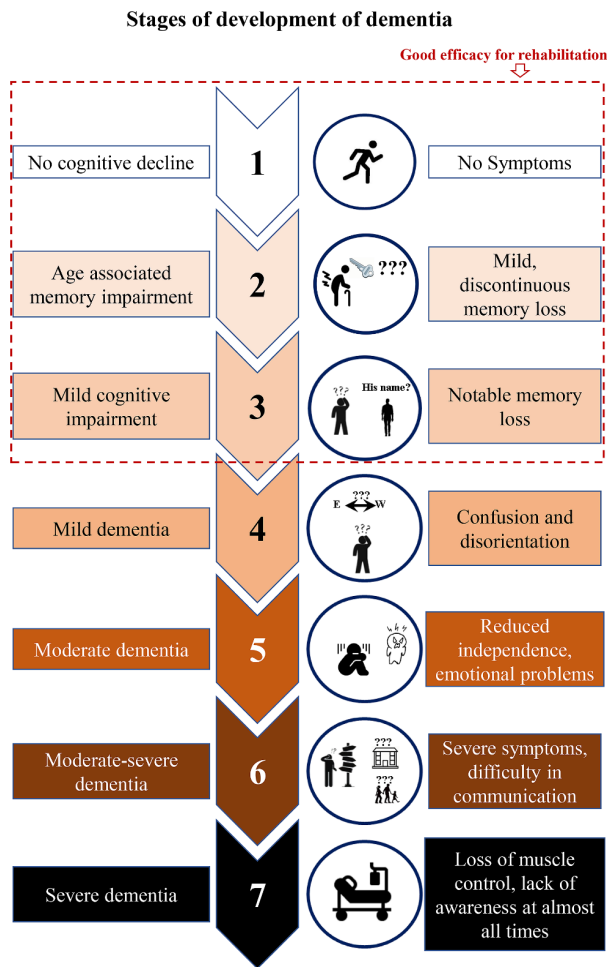


Figure 1. Stages of dementia.

to 22.85 (vs. the recommended 16). Since the threshold to identify MCI is crucial, a better threshold for MCI was proposed for clinical settings according to the subtypes of dementia (9).

ii) Compliance with dementia-related tests is questionable, as patients' individual status and environment may greatly influence diagnosis. For example, the elderly commonly have age-related hearing loss (ARHL). Whether the poor performance in these tests is due to ARHL is still uncertain (as an example, they cannot properly hear the investigator's questions) (10).

iii) Biomarkers like amyloid-beta (A β) and tau protein have been found to predict the progression from MCI to AD, but the actual diagnostic value of those biomarkers still requires further verification. A study reported that the combination of A β 1-42 and Tau had a high sensitivity of 95% and a specificity of 83% in predicting the progression of MCI to AD (6).

iv) Functional neuroimaging, such as positron emission tomography and functional magnetic resonance imaging (fMRI), might be helpful in identifying MCI. For example, a previous study by the current authors identified an MCI-related pattern of brain changes (11).

However, such methods need to be verified further with robust evidence. Moreover, the prohibitive expense of these examinations might preclude their verification in a large-scale clinical trial, as well as their clinical use.

Thanks to advances in computer technologies in medicine, evaluation of an individual's behaviors has become possible, including evaluating cognitive changes in real time and remotely (12). Virtual reality (VR) equipment can be used to develop many objective tasks. Wearable sensor-based equipment can be used to check a patient's trajectory in real time. Apps for a smart device can be developed to assess cognitive functions. All of the acquired data can be transmitted wirelessly and compiled on a server in the cloud, and then the technologies of artificial intelligence (AI) and machine learning can be used to analyze these data, hopefully constituting an AI-based approach to diagnosing MCI.

3. Rehabilitation interventions for MCI

Compared to patients who have been labeled as "handicapped" or "disabled", patients with MCI commonly exhibit a mild decline in cognitive functions and ADL that might be amenable to intervention and reversible with rehabilitation (13,14). Cognitive training has been found to be effective in modulating cortical and subcortical neural functions, maintaining a resilient and healthy cognitive state, preventing cognitive decline, and delaying the progression of cognitive impairment in patients with MCI (15). Therefore, rehabilitation for MCI patients should be initiated rapidly after the diagnosis is confirmed. Several principles should be considered in clinical settings for MCI rehabilitation:

i) The principle of humanity, which means that forms of rehabilitation should be devised to minimize the burden of intervention. They should be friendly, inclusive, and sustainable. Psychological and emotional support is also indispensable.

ii) The principle of goal-directed rehabilitation. Setting a reasonable rehabilitation goal is important. Rehabilitation goals should be set in conjunction with the patient's expectations along with the patient's physical condition. Patients with MCI, and even patients with mild-to-moderate dementia, may help to set the rehabilitation goal (16).

iii) The principle of personalization. This is crucial to the patient's adherence to the rehabilitation plan. Lissek and Suchan reported on Maximizing Cognition (MAXCOG), a home-based four-session individualized face-to-face cognitive rehabilitation intervention (15). This personalized rehabilitation plan achieved satisfactory efficiency in patients with MCI and early dementia (15).

Multi-disciplinary integrated approaches to rehabilitation should be the future direction for dementia-related rehabilitation. Older patients often suffer from multiple frailty-related conditions (17).

Accordingly, a comprehensive rehabilitation plan is indispensable. For instance, physical exercise is commonly combined with psychological rehabilitation and nutritional interventions for patients with MCI, which helps to improve the patient's overall status. Buele *et al.* reported that dual intervention (sequentially conducting motor and cognitive training in sessions of 40 min per day, twice a week for 6 weeks) improved cognitive function in patients with MCI, and their MoCA-S scores increased from 22.36 to 25.29 (18). The efficacy of combining other technologies and cognitive rehabilitation to treat MCI was widely reported, including computer technologies and non-invasive brain stimulation (NIBS) (19). The combination of NIBS and computer-assisted cognitive rehabilitation should be useful in preventing cognitive decline in healthy older adults (20). VR is a booming technology, and its value in cognitive rehabilitation has been reported (21). Recently, Porras-Garcia *et al.* reviewed immersive VR training for patients with cognitive impairment and depression (3). They noted that use of VR training can help patients overcome the negative emotions. Improvement in the domains of attention and memory can be achieved by stimulating neurotransmitters, including the cholinergic and dopaminergic systems. The advantages of this VR-based rehabilitation lie in the full compliance of patients. First, the VR technology allows a therapist to design a full-fledged, fun rehabilitation program based on the patient's condition and requirements and to maximize the patient's motivation to participate. Second, home-based telerehabilitation could be developed, and it might be easily accepted by the elderly. Third, VR-based rehabilitation may be subtly designed to focus on training in ADL and compensatory cognitive-behavioral memory (3). Thus, VR-based tools could be used in cognitive rehabilitation.

4. Problems in elderly care facilities

Elderly care facilities, such as nursing homes (NHs), are set up to provide 24-hour professional nursing care for older people who cannot be cared for at home but who do not require hospitalization. The original intent behind a NH is to reduce the burden on families and improve the QOL of these older people. However, older people in NHs are more likely to develop cognitive problems. A meta-analysis of 53 studies covering 17 countries reported that the overall prevalence of MCI in older people in NHs was significantly higher than that in the general community (21.2% vs. 17.3%) (22). Reasons for that might be a lack of care, a worse mood due to being alone, and being in an unfamiliar environment. However, given the increasing older population, such community-based nursing and group rehabilitation might be the trends of the future. Thus, more humane and friendly elderly care facilities need to be established. To that end, here are several suggestions based on the

status quo of NHs and the current authors' experience:

i) Establishment of a family-style NH. This novel NH provides fast, effective, flexible care. More importantly, it allows patients to be in a family-like environment, including friendly people, familiar furniture, interesting programs, and positive social interactions. In addition, the NH should be conveniently located to meet with family members. Such an NH would help to improve the well-being of residents, help to maintain their mental health longer, and also help to prevent further decline. Indeed, such small-scale, family-style care facilities have been increasingly established in developed countries such as Sweden, the Netherlands, and the United States (23).

ii) Professionalization of nursing staff and criteria for care. First, the quality of care depends on the nurse-patient relationship and the caregiver's ability to communicate and interact with older people, which helps to create needs-oriented care and a respectful and reliable relationship between the caregiver and the elderly patient. Second, criteria for care need to be established and rigorously followed. In this regard, appropriate training and education of the staff of NH is indispensable.

5. Conclusion

With the rapid growth of the elderly population, the problem of dementia has become a tough nut to crack but will have to be faced by governments worldwide. Due to the incurable nature of dementia thus far, rehabilitation interventions starting in the MCI stage might be a solution. Beyond these, prevention of cognitive decline might be more reasonable. Development of public community-based services for the elderly might be a useful solution, since a study reported that a 10% enhancement in the coverage of community-based services might lead to a 1.4% reduction in the probability of residence in an NH (24). Indeed, now is the right time to seriously think about how to fight dementia.

Funding: This work was supported by the Shenzhen High-level Hospital Construction Fund (No.23274G1001)

Conflict of Interest: The authors have no conflicts of interest to disclose.

References

1. Garcia-Ptacek S, Kareholt I, Cermakova P, Rizzuto D, Religa D, Eriksdotter M. Causes of death according to death certificates in individuals with dementia: A cohort from the Swedish Dementia Registry. *J Am Geriatr Soc.* 2016; 64:e137-e142.
2. Todd S, Barr S, Roberts M, Passmore AP. Survival in dementia and predictors of mortality: A review. *Int J Geriatr Psychiatry.* 2013; 28:1109-1124.
3. Porras-Garcia B, Rojas-Rincon J, Adams A, Garolera

- M, Chang R. Immersive virtual reality cognitive training for improving cognition and depressive symptoms among older adults. Current evidence and future recommendations. A systematic review. *Cyberpsychol Behav Soc Netw*. 2024.
4. Reparaz-Escudero I, Izquierdo M, Bischoff-Ferrari HA, Martinez-Lage P, Saez de Asteasu ML. Effect of long-term physical exercise and multidomain interventions on cognitive function and the risk of mild cognitive impairment and dementia in older adults: A systematic review with meta-analysis. *Ageing Res Rev*. 2024; 100:102463.
 5. Liu H, Wu M, Huang H, Chen X, Zeng P, Xu Y. Comparative efficacy of non-invasive brain stimulation on cognition function in patients with mild cognitive impairment: A systematic review and network meta-analysis. *Ageing Res Rev*. 2024;102508.
 6. DeCarli C. Mild cognitive impairment: Prevalence, prognosis, aetiology, and treatment. *Lancet Neurol*. 2003; 2:15-21.
 7. de Sola-Smith K, Gilissen J, van der Steen JT, Mayan I, Van den Block L, Ritchie CS, Hunt LJ. Palliative care in early dementia. *J Pain Symptom Manage*. 2024; 68:e206-e227.
 8. Asakawa T, Fang H, Sugiyama K, Nozaki T, Kobayashi S, Hong Z, Suzuki K, Mori N, Yang Y, Hua F, Ding G, Wen G, Namba H, Xia Y. Human behavioral assessments in current research of Parkinson's disease. *Neurosci Biobehav Rev*. 2016; 68:741-772.
 9. Ilardi CR, Menichelli A, Michelutti M, Cattaruzza T, Federico G, Salvatore M, Iavarone A, Manganotti P. On the clinimetrics of the Montreal Cognitive Assessment: Cutoff analysis in patients with mild cognitive impairment due to Alzheimer's disease. *J Alzheimers Dis*. 2024; 101:293-308.
 10. Asakawa T, Yang Y, Xiao Z, Shi Y, Qin W, Hong Z, Ding D. Stumbling blocks in the investigation of the relationship between age-related hearing loss and cognitive impairment. *Perspect Psychol Sci*. 2024; 19:137-150.
 11. Li X, Wang F, Liu X, Cao D, Cai L, Jiang X, Yang X, Yang T, Asakawa T. Changes in Brain function networks in patients with amnesic mild cognitive impairment: A resting-state fMRI study. *Front Neurol*. 2020; 11:554032.
 12. Asakawa T, Sugiyama K, Nozaki T, Sameshima T, Kobayashi S, Wang L, Hong Z, Chen S, Li C, Namba H. Can the latest computerized technologies revolutionize conventional assessment tools and therapies for a neurological disease? The example of Parkinson's disease. *Neurol Med Chir (Tokyo)*. 2019; 59:69-78.
 13. Bellelli F. Cognitive interventions: Symptomatic or disease-modifying treatments in the brain? *JAR Life*. 2024; 13:60-64.
 14. Veronese N, Soysal P, Demurtas J, *et al*. Physical activity and exercise for the prevention and management of mild cognitive impairment and dementia: A collaborative international guideline. *Eur Geriatr Med*. 2023; 14:925-952.
 15. Lissek V, Suchan B. Preventing dementia? Interventional approaches in mild cognitive impairment. *Neurosci Biobehav Rev*. 2021; 122:143-164.
 16. Dutzi I, Schwenk M, Kirchner M, Bauer JM, Hauer K. "What would you like to achieve?" Goal-setting in patients with dementia in geriatric rehabilitation. *BMC Geriatr*. 2019; 19:280.
 17. Asakawa T, Karako T. Facing frailty: Are you ready? *Biosci Trends*. 2023; 17:249-251.
 18. Buele J, Aviles-Castillo F, Del-Valle-Soto C, Varela-Aldas J, Palacios-Navarro G. Effects of a dual intervention (motor and virtual reality-based cognitive) on cognition in patients with mild cognitive impairment: A single-blind, randomized controlled trial. *J Neuroeng Rehabil*. 2024; 21:130.
 19. Yang T, Liu W, He J, Gui C, Meng L, Xu L, Jia C. The cognitive effect of non-invasive brain stimulation combined with cognitive training in Alzheimer's disease and mild cognitive impairment: A systematic review and meta-analysis. *Alzheimers Res Ther*. 2024; 16:140.
 20. Takakura T. Nutrition, Exercise, and cognitive rehabilitation for dementia prevention. *Juntendo Iji Zasshi*. 2024; 70:9-22.
 21. Chan JYC, Liu J, Chan ATC, Tsoi KKF. Exergaming and cognitive functions in people with mild cognitive impairment and dementia: A meta-analysis. *NPJ Digit Med*. 2024; 7:154.
 22. Chen P, Cai H, Bai W, Su Z, Tang YL, Ungvari GS, Ng CH, Zhang Q, Xiang YT. Global prevalence of mild cognitive impairment among older adults living in nursing homes: A meta-analysis and systematic review of epidemiological surveys. *Transl Psychiatry*. 2023; 13:88.
 23. D'Cunha NM, Isbel S, Bail K, Gibson D. 'It's like home' - A small-scale dementia care home and the use of technology: A qualitative study. *J Adv Nurs*. 2023; 79:3848-3865.
 24. Long KH, Smith C, Petersen R, Emerson J, Ransom J, Mielke MM, Hass S, Leibson C. Medical and nursing home costs: From cognitively unimpaired through dementia. *Alzheimers Dement*. 2022; 18:393-407.
- Received September 25, 2024; Accepted October 8, 2024.
- *Address correspondence to:*
Peipei Song and Takashi Karako, National Center for Global Health and Medicine, 1-21-1 Toyama, Shinjuku-ku, Tokyo 162-8655, Japan.
E-mail: psong@it.ncgm.go.jp; politang-ky@umin.ac.jp
- Tetsuya Asakawa, Institute of Neurology, National Clinical Research Center for Infectious Diseases, The Third People's Hospital of Shenzhen, No. 29 Bulan Road, Shenzhen 518112, Guangdong, China.
E-mail: asakawat1971@gmail.com
- Released online in J-STAGE as advance publication October 11, 2024.

Exploring the multiple therapeutic mechanisms and challenges of mesenchymal stem cell-derived exosomes in Alzheimer's disease

Ya-nan Ma¹, Xiqi Hu¹, Kenji Karako², Peipei Song^{3,*}, Wei Tang^{2,3}, Ying Xia^{1,*}

¹Department of Neurosurgery, Haikou Affiliated Hospital of Central South University Xiangya School of Medicine, Haikou, China;

²Department of Surgery, Graduate School of Medicine, The University of Tokyo, Tokyo, Japan;

³National Center for Global Health and Medicine, Tokyo, Japan.

SUMMARY Alzheimer's disease (AD) is a severe neurodegenerative disorder, and the current treatment options are limited. Mesenchymal stem cell-derived exosomes (MSC-Exos) have garnered significant attention due to their unique biological properties, showcasing tremendous potential as an acellular alternative therapy for AD. MSC-Exos exhibit excellent biocompatibility and low immunogenicity, enabling them to effectively cross the blood-brain barrier (BBB) and deliver therapeutic molecules directly to target cells. They are highly efficacious in delivering nucleic acid-based drugs. Moreover, the production process of MSC-Exos benefits from a high proliferation capacity and multilineage differentiation potential, allowing for production while maintaining a stable composition. Despite the significant theoretical advantages of MSC-Exos, their clinical use still faces multiple challenges, including cross-contamination during isolation and purification processes, the complexity of their components, and the presence of potential adverse paracrine factors. Future research needs to focus on optimizing separation and purification techniques, enhancing delivery methods to improve therapeutic efficacy, and performing detailed analyses of the components of MSC-Exos. In summary, MSC-Exos hold promise as an effective option for the treatment of AD and other neurodegenerative diseases, driving their clinical research and use in related fields.

Keywords mesenchymal stem cell-derived exosomes, Alzheimer's disease, drug delivery, blood-brain barrier, immunogenicity, cell therapy

1. Introduction

Alzheimer's disease (AD) is a neurodegenerative disorder characterized by progressive cognitive decline, primarily affecting the elderly population. According to the World Health Organization, approximately 55 million people worldwide suffer from dementia, with AD being the most common form, accounting for 60% to 70% of cases (1). As global aging accelerates, the incidence of AD continues to rise, making it a serious public health issue that poses a heavy burden on patients, their families, and society.

The exact pathogenesis of AD remains unclear; however, growing evidence suggests that the progression of the disease is closely linked to multiple pathological changes. Among these, the deposition of β -amyloid ($A\beta$) is considered a hallmark of AD. $A\beta$ accumulates between neurons, forming plaques that disrupt neuronal function and ultimately lead to neuronal death. In addition to $A\beta$ accumulation, the abnormal phosphorylation of tau protein is regarded as a critical pathological mechanism

in AD, leading to the formation of neurofibrillary tangles that further exacerbate neurodegeneration. Moreover, neuroinflammation plays a crucial role in the progression of AD. Excessive inflammatory responses not only damage neurons but also contribute to the aggregation of $A\beta$ and tau, creating a vicious cycle that accelerates disease progression.

Current treatment options for AD primarily focus on managing symptoms. Commonly used drugs include cholinesterase inhibitors and NMDA receptor antagonists (2,3). However, these treatments have been largely ineffective in halting the progression of the disease, underscoring the urgent need for new therapeutic strategies. Targeting the multiple pathological mechanisms of AD and integrating modern biomedical technologies to develop novel therapies has thus become a major area of research (4).

Over the past few years, mesenchymal stem cells (MSCs) and the exosomes secreted by them have gained considerable attention in the field of regenerative medicine. MSCs are adult stem cells with the capacity

for self-renewal and multipotent differentiation and are found in various tissues such as bone marrow, adipose tissue, and the umbilical cord (5-7). Mesenchymal stem cell-derived exosomes (MSC-Exos) are small vesicles secreted by MSCs that contain numerous bioactive molecules, including proteins, lipids, and RNA. These exosomes mediate intercellular communication and regulate various biological processes (8). Research has shown that MSC-Exos have promising therapeutic potential in a variety of diseases, demonstrating anti-inflammatory, immunomodulatory, neuroprotective, and regenerative properties.

MSC-Exos can protect neurons through various mechanisms, including reducing the toxicity of A β and tau proteins and preventing neuronal apoptosis. Studies suggest that the growth factors and antioxidant molecules contained within exosomes significantly enhance neuronal survival rates. Given that neuroinflammation plays a major role in AD pathology, MSC-Exos also exhibit the ability to modulate immune cell function, effectively suppressing excessive inflammatory responses and thereby reducing neuronal damage. In addition, MSC-Exos can promote the proliferation and differentiation of neural stem cells, aiding in the restoration of neural networks. This points to a novel therapeutic approach for AD treatment.

Although preliminary studies have indicated that MSC-Exos may offer benefits to patients with AD, their use in AD treatment remains in the exploratory phase, with several challenges yet to be addressed. These challenges include the processes of preparation, purification, and storage, as well as ensuring consistency and efficacy in clinical use. At present, there are various methods for exosome preparation and purification, but many are costly, operationally complex, and have limited efficiency. Therefore, there is an urgent need to develop more efficient and cost-effective technologies for isolating and purifying exosomes to increase their yield and purity. The bioactivity of MSC-Exos largely depends on their specific components. However, a comprehensive analysis of the precise proteins, RNA, and lipids present within MSC-Exos is still lacking. In this regard, evaluating the efficacy and safety of MSC-Exos, while ensuring consistency in quality and therapeutic outcomes for clinical use, is a key focus for future research.

In conclusion, MSC-Exos represent a promising and innovative therapeutic strategy for AD treatment. By further exploring their multiple therapeutic mechanisms, we can gain a deeper understanding of their potential in combating AD. As research advances, the clinical translation of MSC-Exos could significantly improve the quality of life for patients with AD and reduce the social burden of the disease. The aim of this study was to provide new insights and directions for future research, fostering the development and use of MSC-Exos in the field of neurodegenerative diseases.

2. Pathological mechanisms of AD

AD is a complex neurodegenerative disorder primarily characterized by memory impairment, cognitive decline, and loss of daily living abilities. While the exact mechanisms underlying AD remain unclear, mounting research indicates that its pathology involves multiple interrelated factors, including the deposition of A β , abnormal tau protein phosphorylation, neuroinflammation, and neurodegeneration.

2.1. A β deposition

A β deposition is a hallmark pathological feature of AD. A β is generated through the cleavage of amyloid precursor protein (APP) by β - and γ -secretases (9). Under normal physiological conditions, APP metabolism is tightly regulated. In patients with AD, however, this balance is disrupted, resulting in the overproduction and aggregation of A β , which subsequently forms amyloid plaques (Figure 1). Research has demonstrated that A β deposition impairs neuronal function and induces cell death by triggering oxidative stress, releasing pro-inflammatory factors, and ultimately causing neuronal dysfunction.

A β aggregation occurs in three stages: monomers, oligomers, and fibrils, with oligomers being the most toxic form. Oligomeric A β binds to neuronal cell membranes, disrupting intracellular signaling pathways and leading to calcium homeostasis imbalances, ultimately resulting in apoptosis. Moreover, amyloid plaque deposition is closely associated with microglial activation. Microglia, the immune cells of the central nervous system, respond to A β deposition by attempting to clear the harmful substance. However, excessive microglial activation can trigger neuroinflammation, creating a vicious cycle that exacerbates neuronal damage.

2.2. Tau protein phosphorylation

Tau protein, a microtubule-associated protein primarily found in neurons, plays a key role in stabilizing microtubules and facilitating intracellular transport. In AD, tau undergoes abnormal hyperphosphorylation, causing it to detach from microtubules and aggregate into neurofibrillary tangles (NFTs), another major pathological hallmark of AD closely linked to cognitive impairment (10).

Research has shown that tau hyperphosphorylation is regulated by several kinases, including glycogen synthase kinase 3 β (GSK-3 β) and cyclin-dependent kinase 5 (Cdk5) (11,12). These kinases are influenced by A β deposition, which further promotes tau phosphorylation. Tau aggregation disrupts intracellular signaling and metabolic pathways, leading to neurodegeneration (Figure 1). Studies indicate that abnormal tau phosphorylation not only directly contributes to neuronal death but also plays a

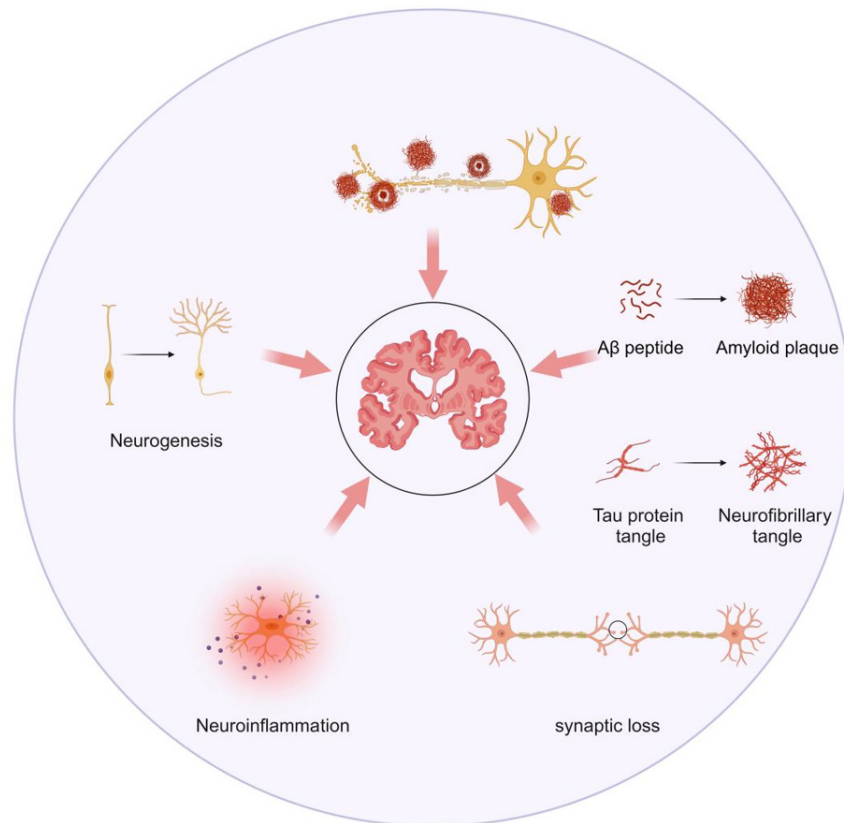


Figure 1. Pathogenesis of Alzheimer's disease. The progression of Alzheimer's disease is driven by various interconnected factors, such as A β deposition, abnormal tau protein phosphorylation, neuroinflammation, and neurodegeneration.

significant role in synaptic dysfunction and neural network disruption.

2.3. Neuroinflammation

Neuroinflammation plays a dual role in AD progression. Initially, the inflammatory response may be protective, aimed at clearing cellular damage or pathogens. As the disease advances, however, chronic inflammation persists, leading to further neuronal damage and death. Microglia and astrocytes, the primary immune cells of the central nervous system, are central to the inflammatory response in AD.

Activated microglia release various pro-inflammatory cytokines, including tumor necrosis factor- α (TNF- α), interleukin-1 β (IL-1 β), and interleukin-6 (IL-6), that can induce neuronal apoptosis and synaptic damage (13). In addition, chronic inflammation can accelerate AD pathology by influencing A β metabolism and tau phosphorylation (Figure 1). Studies have shown that inhibiting neuroinflammation can alleviate cognitive impairment in mouse models of AD, suggesting that targeting neuroinflammation may be a therapeutic approach to AD treatment.

2.4. Neurodegeneration

Neurodegeneration is the final consequence of AD and is

marked by the loss of neurons, synaptic dysfunction, and the breakdown of neural networks. This process is driven by a combination of A β deposition, abnormal tau protein aggregation, and chronic neuroinflammation. As neurons are lost, patients experience progressive cognitive decline, manifesting in memory loss, diminished learning capacity, and impaired executive functions (14).

Neurodegeneration in AD is often accompanied by a reduced capacity for neuronal regeneration, which is associated with impaired neural stem cell function and a lack of growth factors. Research has indicated that decreased neural stem cell activity and reduced neurogenesis may contribute to the neurodegenerative processes observed in the brain of patients with AD (15). Consequently, restoring neural stem cell function and promoting neurogenesis represent promising directions for future AD therapies.

3. General characteristics of exosomes

3.1. Biogenesis of exosomes

Exosomes are small membrane-bound vesicles secreted by cells, ranging in diameter from 30 to 150 nm. The process of exosome biogenesis primarily involves the inward budding of the plasma membrane, leading to the formation of multivesicular bodies (MVBs) within the cell. This process begins with the invagination of

the plasma membrane, which captures surface proteins and soluble proteins from the extracellular environment, thus marking the start of exosome biogenesis. In addition, the Golgi apparatus and the endoplasmic reticulum contribute to the formation and fusion of early endosomes (ESE) (16-18). As these early endosomes mature into late endosomes, a secondary invagination occurs, resulting in the formation of intraluminal vesicles (ILVs), which are the precursors of exosomes. The size and number of ILVs vary depending on the extent of invagination. Some MVBs fuse with lysosomes or autophagosomes, leading to the degradation of their contents, while others fuse with the plasma membrane, releasing ILVs into the extracellular space, where they become exosomes (18,19). Once MVBs fuse with the plasma membrane, the ILVs are released into the extracellular space as exosomes that possess a lipid bilayer structure similar to that of the plasma membrane (16,20). Figure 2 provides an illustration of this process. Proteins involved in exosome biogenesis include Ras-related proteins (Rab GTPases), ESCRT proteins, exosome marker proteins (e.g., TSG101, flotillin, ceramide, and Alix), and exosome surface proteins (e.g., integrins, immunomodulatory proteins, and tetraspanins) (17,21,22). Alterations in the function of Rab and ESCRT proteins can indirectly affect the autophagic-lysosomal pathway and vesicular transport from the Golgi apparatus, thereby impacting exosome biogenesis. Moreover, factors such as cell type, culture conditions, and the genomic health of cells can influence key regulatory factors of exosome biogenesis both *in vivo* and *in vitro* (17).

3.2. Composition of exosomes

Exosomes consist of lipids, proteins, nucleic acids, and metabolites, reflecting the characteristics and physiological state of their donor cells. Their membrane structure consists of a lipid bilayer rich in cholesterol, sphingolipids, and ceramides (lipid rafts), which not only maintain structural integrity but also play a pivotal role in exosome formation and signal transduction (23-24).

Exosomes contain a variety of proteins, including ESCRT proteins and Rab GTPases, which participate in their biogenesis. In addition, exosomes carry marker proteins such as TSG101, flotillin, ceramide, and Alix and surface proteins like integrins, immunomodulatory proteins, and tetraspanins (17,21,22). Cell-specific proteins, such as MHC class I and II molecules, are also present in exosomes and reflect the unique characteristics of their donor cells (25).

Moreover, exosomes contain various nucleic acids, including DNA, mRNA, and non-coding RNA, with microRNA (miRNA) being the most abundant. These nucleic acids can be transferred to recipient cells *via* exosomes, influencing gene expression and cellular functions (26,27). In addition, exosomes carry small metabolites, such as growth factors and cytokines, that play critical roles in cellular metabolism and signal transduction (26,28,29). The composition of exosomes can vary depending on the cell type, cellular state, and environmental factors.

3.3. Exosome isolation and purification

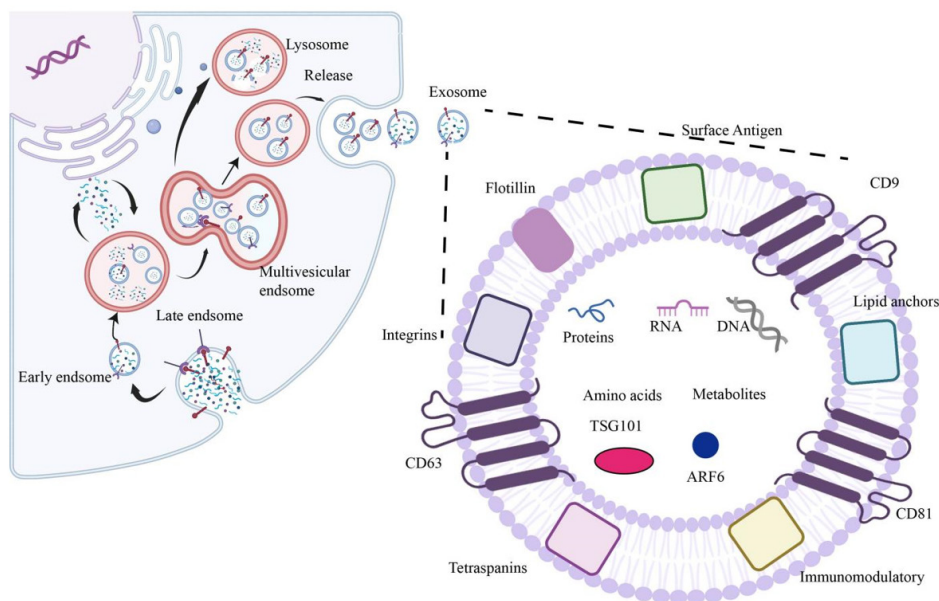


Figure 2. The process of exosome biogenesis. Exosome biogenesis begins with the invagination of the plasma membrane, capturing surface and extracellular proteins to form MVBs. The Golgi apparatus and endoplasmic reticulum aid in the formation of early endosomes, which mature into late endosomes. During this process, ILVs are formed as exosome precursors. Some MVBs fuse with lysosomes or autophagosomes for degradation, while others fuse with the plasma membrane, releasing ILVs as exosomes into the extracellular space with a lipid bilayer similar to the plasma membrane. Abbreviations: ILVs: intraluminal vesicles; MVBs: multivesicular bodies.

Isolating exosomes is a critical step in studying their functions and potential uses. Currently, there are several effective methods of isolation, including differential ultracentrifugation, size- and molecular weight-based ultrafiltration, polymer precipitation, washing separation, immunomagnetic bead separation, microfluidic separation, and mass spectrometry. Each method has its own set of advantages and disadvantages.

Differential ultracentrifugation is the most commonly used technique, separating particles by altering or gradually increasing centrifugation speeds. This method has been widely used for exosome isolation and purification (30). While it requires specialized equipment and can be time-consuming, it yields relatively pure exosomes (31). Another variation is density gradient centrifugation, which uses sucrose or cesium chloride to establish a density gradient that helps separate exosomes from other components. Although this method enhances exosome purity, it is labor-intensive and time-consuming, and repeated centrifugation or exposure to high centrifugal forces may irreversibly damage the vesicles (32,33). Ultrafiltration, based on size and molecular weight, uses membranes with varying pore sizes to filter cell culture supernatants. Although this method is simple and fast, it may cause damage to or loss of exosome structures. It is efficient, economical, and easy to perform, making it suitable for large-scale processing, but the ultrafiltration membranes can become clogged, and excessive pressure during the process can lead to exosome denaturation (34). Polymer precipitation involves adding solvents to a solution to alter the polarity and solubility of components, causing exosomes to precipitate. This method, which utilizes commercially available kits, enhances exosome separation from biological fluids (35,36). Immunomagnetic bead separation uses the specific binding between antibodies and exosome surface markers for isolation. It is a fast and highly specific method with a high yield and purity (37,38). However, the process is expensive and can affect the functionality of exosomes. Microfluidic separation allows precise control and manipulation of micro-scale fluids for exosome isolation in micron/nanometer-sized spaces. This technology is also widely used in cancer diagnosis and detection (39-41). Size exclusion chromatography (SEC) separates exosomes based on particle size using a gel filtration column. This method preserves exosome bioactivity, is time-efficient, cost-effective, and highly reproducible. However, it has relatively low recovery rates and purity (42). Given the advantages and limitations of each method, combining multiple approaches may help maximize exosome enrichment. One of the main challenges to clinical use of exosomes is the reproducibility of the isolation techniques, thus requiring further optimization and standardization.

Exosome yield is influenced by various factors, with cell type being one of the most critical. Different cells,

such as tumor cells, immune cells, and stem cells, differ significantly in exosome yield and content (43,44). For example, MSCs secrete large amounts of exosomes, whereas immature dendritic cells produce fewer (45,46). In addition, the growth stage and physiological state of the cells affect exosome secretion. Under conditions of starvation, stress, or hypoxia, certain cell types may increase exosome production (47,48).

Culture conditions, including medium composition, pH, and temperature, also influence exosome secretion (49). Cell seeding density and growth density further affect yield (50). To optimize exosome yield, several strategies can be used. Biochemical strategies (*e.g.*, LPS, BMP-2, HIF-1 α , interferon- γ (IFN- γ), and TNF- α), physical strategies (*e.g.*, hypoxia, heat stress, and starvation), mechanical strategies (*e.g.*, shear stress and 3D culture), and instrumental strategies (*e.g.*, hollow fiber bioreactors and stirred-tank bioreactors) can significantly enhance exosome production. Optimizing these techniques can not only increase exosome yield but also modulate their properties (51).

3.4. Characterization of exosomes

The characterization of exosomes is a crucial step in understanding their functions and mechanisms of action. Current methods primarily focus on analyzing the size, morphology, surface charges, and contents of exosomes. Common techniques for determining exosome size include nanoparticle tracking analysis (NTA), dynamic light scattering (DLS), and tunable resistive pulse sensing (TRPS) (40).

NTA measures the size and concentration of exosomes by tracking the Brownian motion of particles in a liquid (52). One key advantage of NTA is that it can detect a variety of extracellular vesicles (EVs), including exosomes, with relatively simple sample preparation. In addition, the sample can be recovered after measurement. Fluorescently labeled antibodies may also be used to detect EV antigens. However, a significant limitation is the difficulty in distinguishing exosomes from contaminants, such as proteins (52-54).

DLS, in contrast, analyzes the scattered light of particles in suspension to determine their size and is often used to measure the average particle size and distribution of exosomes (54). Its benefit lies in its ability to measure particles ranging from 1 nm to 6 μ m, which makes it ideal for measuring particles in suspension (55).

TRPS measures electrical resistance changes when particles pass through a membrane with tunable pore sizes, allowing for single-particle characterization and concentration measurement of exosomes. However, TRPS is susceptible to issues like system instability, pore clogging, and sensitivity (56).

To analyze exosome morphology, transmission electron microscopy (TEM) and scanning electron microscopy (SEM) are frequently used. TEM is a high-

resolution imaging technique that uses an electron beam to penetrate the sample, making it ideal for visualizing EV morphology and measuring vesicle diameter. Despite its utility, TEM requires complex sample preparation and is not suitable for rapid analysis of large sample quantities, as it may cause morphological changes in EVs (57). In contrast, SEM scans the sample's surface with an electron beam, quickly generating high-resolution images (53). SEM offers the advantage of fast imaging and direct observation of solid samples without the need for complex sectioning or staining. However, it cannot be used directly on liquid samples, and sample vacuum stability must also be considered.

Exosome contents are typically analyzed in terms of proteomics, lipidomics, and genomics. Common methods include Western blotting, ELISA, flow cytometry, mass spectrometry, and PCR (53,58). These techniques can be used together to obtain comprehensive information about exosomes, including their morphology, size, concentration, surface markers, and molecular composition. In practice, researchers often use a combination of methods such as NTA, TEM, and Western blotting to ensure accurate exosome characterization.

3.5. Exosome heterogeneity

Exosome heterogeneity manifests in their origin, size, composition, and effects on recipient cell functions. Different cells secrete exosomes with diverse biological characteristics (42,59,60). Nearly all human cell types, including adipocytes, macrophages, olfactory mucosa cells, dendritic cells, stem cells, and tumor cells, are capable of releasing exosomes.

The size heterogeneity of exosomes may result from uneven invagination of the plasma membrane during biogenesis or contamination with other types of extracellular vesicles during isolation (61). These size differences can influence exosome density. In addition, exosomes contain various biomolecules such as proteins, lipids, RNA, and DNA, although the abundance of these molecules varies between exosomes (62-65). Notably, there are significant differences in protein and RNA composition between exosomes derived from different sources. Exosome impacts on recipient cells are closely related to surface receptor expression. For example, in cancer therapy, exosomes may either inhibit or promote tumor progression depending on their origin (66). The cellular microenvironment and biological characteristics of the donor cells also influence exosome cargo and markers, making exosome heterogeneity a key focus of research. Exosomes are found in various bodily fluids, such as blood, tears, saliva, amniotic fluid, and even breast milk, where they act as stable disease biomarkers that are useful for clinical liquid biopsies (67-69).

3.6. Exosome uptake and biodistribution

Exosomes reach their target cells through various mechanisms, including membrane fusion, receptor-mediated interactions, and endocytosis. Membrane fusion involves the direct release of exosomal contents into the cytoplasm of recipient cells when the exosome membrane merges with the recipient cell membrane. Proteins like SNAREs, Rab family proteins, exosomal lipid domains, integrins, and adhesion molecules are crucial to this fusion process (70,71). Receptor-mediated interactions occur when transmembrane ligands on the exosome surface bind to recipient cell receptors, triggering downstream signaling cascades in pathways that are often involved in immune regulation and apoptosis (72,73).

Endocytosis is another major uptake mechanism, allowing exosomes to be internalized by recipient cells. This can occur through clathrin-mediated endocytosis, phagocytosis, or lipid raft-mediated endocytosis. These processes may occur simultaneously and are not mutually exclusive (74,75). After internalization, exosomal cargo is released into the cytoplasm, depending on factors like the exosome's origin, cargo, and the metabolic state of the recipient cell (76). For instance, research has demonstrated that oncogenic signaling induced by mutant KRAS expression promotes the uptake of exosomes by human pancreatic cancer cells *via* macrophages (77,78). In contrast, human melanoma cells have been found to internalize exosome contents through plasma membrane fusion (79), while neurosecretory PC12 cells (derived from rat adrenal medullary tumors) exhibit a higher dependency on lectin-mediated endocytosis for exosomal cargo uptake (80).

The biodistribution of exogenous exosomes is influenced by factors such as the route of administration, exosome size, and surface composition. Different routes result in distinct distribution patterns. For instance, intravenously administered exosomes primarily accumulate in the liver, spleen, lungs, and gastrointestinal tract but are quickly cleared from circulation (81,82). Oral administration allows exosomes to reach multiple organs, including the brain (83), while intranasal administration efficiently delivers exosomes to the brain (84,85). Intratumoral injection ensures exosomes remain within tumors longer (86).

Exosome size also plays a role in biodistribution, with larger vesicles accumulating in bones, lymph nodes, and the liver (61). In addition, surface molecular composition influences *in vivo* distribution. For example, rabies virus glycoprotein (RVG) can direct exosomes to the brain (87), while cancer-derived exosomes rich in mannose and sialic acid target specific cell types (88). Another notable example involves RVG, which has been found to direct exosomal delivery specifically to the brain (87). Moreover, glycoproteins enriched with mannose and sialic acid on the surface of cancer cells have been identified as key contributors to the targeting of specific cell types (88). Glioblastoma-derived

exosomes, which are rich in phosphatidylethanolamine, show a greater propensity to target glioblastoma cells, while sphingomyelin-rich melanoma-derived exosomes demonstrate enhanced targeting capabilities within the tumor microenvironment (79).

3.7. Storage of exosomes

The storage of exosomes is essential to maintaining their stability and biological functionality. To prevent degradation, exosomes are typically stored at low temperatures. Common methods of preservation include cryopreservation, freeze-drying, and spray-drying. The optimal storage temperature is -80°C , which ensures long-term stability, whereas storage at 4°C may result in compromised biological activity and reduced protein content (89,90). For short-term storage, -20°C may suffice.

Non-permeable disaccharide cryoprotectants such as sucrose and trehalose are often used to enhance exosome protection during low-temperature storage (91). Freeze-drying, which converts exosomes into a stable powder form, is another effective method of long-term preservation that also aids in transportation. Freeze-drying (using lyophilization) removes moisture, preventing degradation, and studies suggest that exosomes treated with cryoprotectants can retain their protein and RNA activity for up to four weeks at room temperature (92).

Spray-drying offers another way to convert exosomes into dry powder, enhancing their stability and facilitating their transport (93). Prior to use, exosome quality needs to be assessed, including particle size and concentration, to ensure their integrity and activity.

3.8. The role and therapeutic potential of exosomes in neurodegenerative disorders

Exosomes play a crucial role in the pathogenesis of neurodegenerative diseases, largely by promoting or mitigating the aggregation of misfolded or unfolded proteins in the brain (94-96). Research has indicated that exosomes facilitate disease progression by spreading and aggregating misfolded proteins. For example, exosomes have been implicated in the transmission of the infectious prion protein PrP^{Sc}, which is associated with prion diseases (97). In AD, Tau and A β amyloid proteins have been detected in exosomes derived from cerebrospinal fluid (CSF) of patients (for Tau) and from the culture supernatants of mouse and human cells (for A β). Exosomes are also involved in propagating Tau aggregation pathology (98,99). In HeLa and Neuro-2a cells, APP cleavage occurs in early endosomes, leading to the release of A β into the extracellular space *via* exosomes (98). However, whether exosomes promote the oligomerization of neurotoxic A β *in vivo* remains unclear, and this warrants further investigation.

In addition to their role in the spread of misfolded proteins, exosomes have also been found to engage in the clearance of such proteins, acting as detoxifying agents and having a neuroprotective effect. By inhibiting the formation of neurotoxic oligomers or facilitating their expulsion from the cell, exosomes contribute to cellular protection (100,101). For instance, in APP transgenic mice, dysfunction of neuron-secreted exosomes, specifically in relation to endothelin-converting enzyme 1/2 (ECE1/2), leads to an accumulation of oligomeric A β within exosomes, accelerating the spread of A β amyloid (102). A similar phenomenon has been observed in Parkinson's disease (PD) and other proteinopathies, where exosomes from the CSF of patients with PD contain aggregates of α -synuclein (103). Moreover, α -synuclein inhibits the endosomal sorting complex required for transport (ESCRT) system, thereby limiting its intracellular degradation and promoting intercellular propagation (104). In amyotrophic lateral sclerosis (ALS) and frontotemporal degeneration, cytoplasmic aggregation of TDP-43 is a hallmark pathology. In TDP-43 A325T transgenic mice, the secretion of exosomes facilitates the clearance of TDP-43 from neuronal cell bodies (105).

While the primary role of exosomes in neurodegenerative diseases is related to regulating misfolded proteins, other components, such as nucleic acids, also contribute to disease progression or amelioration (106). Importantly, exosomes can cross the BBB, making them a promising therapeutic approach for neurodegenerative disorders (107).

3.9. Comparison of MSC therapy and MSC-Exos therapy

Research has shown that MSCs derived from bone marrow, adipose tissue, and dental pulp can differentiate into neurons (7,108,109). In addition, MSCs play a crucial role in tissue repair and regeneration through paracrine signaling. By secreting a variety of bioactive factors, MSCs regulate the behavior of surrounding cells, promoting tissue repair, anti-inflammatory responses, immune modulation, and angiogenesis. Specifically, MSCs secrete growth factors (such as TGF- β , VEGF, and epidermal growth factor (EGF)), anti-inflammatory and immune-modulating factors (such as IL-10, TGF- β , Prostaglandin E2 (PGE2), and Indoleamine 2,3-dioxygenase (IDO)), angiogenic factors (such as VEGF, FGF, and PDGF), and anti-apoptotic and antioxidant factors (such as HGF and IGF-1), all of which provide vital support to damaged neurons and which enhance neural tissue repair and regeneration (110). Due to their ability to differentiate into neurons and their potent immunosuppressive and pro-angiogenic properties, MSCs have emerged as a promising treatment strategy for neurological disorders (111).

However, several safety concerns must be addressed when using MSCs in clinical settings. Factors such as

donor age, genetic characteristics, and medical history significantly influence the therapeutic potential of MSCs (112). This is particularly important for autologous MSC transplantation in elderly patients, where age-related changes, such as diminished proliferation and differentiation potential, may reduce therapeutic efficacy (112). Although MSCs typically exhibit low immunogenicity, they can still trigger immune responses (113). In addition, MSCs from different sources may exhibit varying immunogenic profiles, requiring close monitoring of potential immune reactions, especially in allogeneic transplants. MSCs are generally considered to have low tumorigenic potential, but there is still a risk of abnormal proliferation or transformation in certain *in vivo* microenvironments, particularly in long-term cultures or with genetically modified MSCs (112,114). The behavior of MSCs may also vary depending on the tissue and disease context; in some cancer environments, MSCs have been found to promote tumor growth and metastasis. Therefore, a thorough understanding and monitoring of MSC behavior in specific pathological settings is critical.

Moreover, when MSCs are used in combination with immunosuppressive drugs, respiratory and gastrointestinal infections have occurred in some patients, indicating that MSCs should not be used concurrently with other immunosuppressive therapies (112,114). In contrast, MSC-Exos contain bioactive factors that regulate immune responses, vascular function, and neuronal repair. Due to their nanoscale size and lipid-encapsulated structure, MSC-Exos can easily penetrate neural tissues and reach target cells (115). The exosomal membrane, which is rich in cholesterol, sphingolipids, ceramides, and lipid raft proteins, protects the exosomal

contents from degradation. In addition, adhesion molecules such as CD29, CD44, and CD73 expressed on MSC-Exos promote their migration to inflamed or damaged tissues. Once they reach their destination, MSC-Exos directly fuse with cell membranes, delivering their contents into the cytoplasm of target cells and modulating their phenotype and function (116). MSC-Exos contain nucleic acids, proteins (such as cytokines and chemokines), and lipids that can alter the phenotype, function, and viability of neuronal and immune cells (116). Thus, MSC-Exos play an important role in treating neuroinflammatory diseases.

Importantly, no adverse effects have been observed in animal models or patients treated with MSC-Exos, suggesting that these exosomes could serve as a safer alternative to MSC therapy for treating inflammatory and degenerative neurological diseases (115). MSC-Exos inherit the therapeutic properties of MSCs, including anti-inflammatory, immune-modulatory, and regenerative effects, and they represent a viable alternative to MSC therapy while mitigating the risks associated with MSC use (Table 1).

4. Use of MSC-Exos in AD

MSC-Exos have a neuroprotective effect against AD *via* a variety of mechanisms, including the clearance of abnormal protein accumulations, alleviation of inflammation, and reduction of oxidative stress. Collectively, these effects significantly alleviate the pathological changes associated with AD and improve cognitive ability (Table 2).

4.1. Clearance of abnormal protein accumulation

Table 1. Comparison of MSC therapy and MSC-Exos therapy

Characteristics	MSC therapy	MSC-Exos therapy
Mechanism	Regeneration and repair <i>via</i> living cells	Therapy through exosomes released by MSCs
Multilineage differentiation potential	Present	Absent
Applicability	Suitable for treating various diseases	MSC-Exos have efficacy comparable to that of stem cells but are smaller in size
Isolation	MSCs are easily isolated and are scalable for large-scale production	Lower yield in large-scale production
Safety	May induce immune responses and carry a risk of tumor formation	Minimal risk of tumor formation and immune response
Ethical concerns	Ethical issues exist	No ethical concerns
Transportation and storage	Requires strict storage and transportation conditions	Stable, suitable for long-term storage and transport
Regulatory approval	Regulatory guidelines have been established	Lacks standardized quality control and faces regulatory challenges

Abbreviations: MSC: mesenchymal stem cell; MSC-Exos: mesenchymal stem cell-derived exosomes.

A hallmark of AD pathology is the presence of A β plaques and hyperphosphorylated tau proteins, which contribute to synaptic disruption and neuronal degeneration. Therefore, clearing these abnormal proteins is crucial to improving synaptic function and neuronal survival, representing a significant therapeutic target for AD (130). Notably, MSC-Exos demonstrate the ability to modulate the levels of key proteins involved in the progression of AD.

For instance, sphingosine-1-phosphate (S1P) receptors, which are widely expressed throughout the body, play vital roles in various physiological processes, including angiogenesis, neurogenesis, immune cell trafficking, endothelial barrier function, and vascular tone regulation (131). Bone-marrow mesenchymal stem cell-derived exosomes (BMSC-Exos) can reduce A β deposition and promote cognitive recovery in mice with AD by enhancing the expression of S1P (117). In addition, neprilysin (NEP), a membrane-bound metallopeptidase capable of degrading neuropeptides and amyloid proteins, represents a potential therapeutic target for AD (132,133). Research by Elia *et al.* demonstrated that injecting BMSC-Exos into the cortex of APP/PS1 mice significantly increased the expression and activity of NEP, leading to reduced A β protein deposition in both the hippocampus and cortex (118). Similarly, Wang *et al.* administered human umbilical cord mesenchymal stem cell-derived exosomes (hUC-MSC-Exos) to 9-month-old APP/PS1 mice *via* the tail vein. This intervention resulted in a reduction in A β accumulation and neuronal loss in the hippocampus, along with improvements in cognitive function, likely mediated by its effects on the nuclear factor erythroid 2-related factor 2 (Nrf2) signaling pathway, which is a critical mediator of neuronal damage in AD (119).

Moreover, MSC-Exos have been found to possess the capability to clear pathological proteins through non-coding RNAs. The pathology of AD begins with the cleavage of APP by β -secretase (BACE), making BACE1 inhibitors potential therapeutic agents for AD (134,135). Research by Sha *et al.* revealed that microRNA-29c-3p, delivered through BMSC-Exos, suppressed BACE1 expression (120) and activated the Wnt/ β -catenin pathway, thereby lowering BACE1 levels and demonstrating efficacy against AD (136).

4.2. Anti-inflammatory effects

Neuroinflammation is a significant feature in the pathological process of AD and is primarily characterized by the abnormal activation of immune cells, such as microglia and astrocytes, within the brain, along with excessive production of inflammatory factors. In the early stages of AD, activated microglia typically exhibit an M2 phenotype, which is associated with neuroprotective and anti-inflammatory properties. As the disease progresses, however, this M2 phenotype gradually shifts towards

a pro-inflammatory M1 phenotype, exacerbating neuroinflammation and neuronal damage.

The immunomodulatory effects of MSC-Exos in the treatment of AD primarily involve the inhibition of neuroinflammation and the regulation of microglial polarization. Specifically, MSC-Exos can reduce the production of pro-inflammatory cytokines and inhibit the activation of both microglia and astrocytes. In addition, MSC-Exos promote the polarization of microglia from the M1 phenotype to the M2 phenotype, thereby mitigating neuroinflammation and facilitating neural repair, which ultimately alleviates AD-related neurodegeneration. For instance, research by Ding *et al.* demonstrated that injecting hUC-MSC-Exos in a mouse model of AD modulated the phenotype and function of microglia in APP/PS1 mice, thereby alleviating neuroinflammation (121).

Moreover, the findings of Nakano *et al.* corroborate these results, showing that miR-146a present in BMSC-Exos can inhibit TRAF6 and IRAK1 in microglia, subsequently reducing NF- κ B activity. This reduction leads to decreased gene expression of inducible nitric oxide synthase (iNOS), TNF- α , IL-1 β , and IL-6, resulting in diminished production of the pro-inflammatory M1 phenotype in microglia treated with MSC-Exos (122). In addition to miR-146a, MSC-derived miR-21 also plays a role in modulating immunity and protecting neurons. Research has indicated that hypoxia-preconditioned MSC-Exos inhibit microglial activation through miR-21, decreasing inflammatory factors (such as TNF- α and IL-1 β) while increasing the anti-inflammatory factor IL-10 (123). Thus, MSC-Exos induce anti-inflammatory effects by inhibiting activated microglia, reactive astrocytes, and the release of cytokines (137).

Importantly, overexpression or dysregulation of pro-inflammatory cytokines (such as iNOS) can promote AD pathology (138). Studies have shown that MSC-derived EVs have beneficial effects in mouse models of AD by inhibiting A β -induced iNOS expression in APP/PS1 mice (139). Moreover, research by Liu *et al.* demonstrated that direct injection of exosomes into the lateral ventricles of mice with AD significantly reduced the activation of glial cells in the hippocampus and lowered levels of pro-inflammatory markers such as IL-1 β and TNF- α . This indicates that exosomes have an inhibitory effect on inflammatory responses, potentially mitigating the damage caused by neuroinflammation (129).

In addition, Godoy *et al.* found that MSC-Exos naturally contain and carry endogenous catalase. This enzyme can be delivered to neurons *via* exosomes, providing antioxidant protection and preventing synaptic loss in neurons exposed to A β . This finding suggests that MSC-Exos may offer a novel therapeutic possibility for AD by reducing oxidative stress and its associated neuronal damage (124).

Table 2. Use of MSC-Exos in AD

Source of Exosomes	Method of extraction	Administration	Mechanism	Effect	Mouse model	Reference
BMSCs	Total exosome isolation reagent	Intravenous injection <i>via</i> the tail vein	Reduces A β deposition in mice with AD by activating the SphK/SIP signaling pathway	Promotes the recovery of cognitive function	Female double-transgenic APP/PS1 mice	(117)
BMSCs	Ultracentrifugation	Intracortical injection	BMSC-EVs enhance the expression and activity of neprilysin	Reduces A β plaque load and dystrophic neurites in the cortex and hippocampus	Male APP/PS1 mice	(118)
hUC-MSCs	Ultracentrifugation	Intravenous injection <i>via</i> the tail vein	Modulates nuclear factor E2-related factor 2 (Nrf2)	Reduces A β accumulation and neuron loss in the hippocampus and improves cognitive function	Male APP/PS1 mice	(119)
BMSCs	Ultracentrifugation	Intracerebroventricular injection	BMSC-EVs deliver miR-29c-3p to target BACE1 and activate the Wnt/ β -catenin pathway	Lowers BACE1 levels and reduces A β aggregation	SD rats injected with oligomeric A β 1-42 (5 μ g/ μ L)	(120)
hUC-MSCs	ExoQuick-TC (polymer precipitation)	Intravenous injection <i>via</i> the tail vein	Reduces acute inflammation and selectively activates microglia, increasing "M2 microglia" and decreasing "M1 microglia"	Relieves neuroinflammation, clears A β deposition, and restores cognitive function	APPswe/PS1-dE9 mice	(121)
BMSCs	MagCapture exosome isolation kit (magnetic bead-based isolation)	Intracerebroventricular injection	miR-146a reduces NF- κ B activity by inhibiting TRAF6 and IRAK1 in microglia	Promotes synaptogenesis and alleviates cognitive impairment	APP-695swe/PS1-dE9 mice	(122)
BMSCs	ExoQuick exosome precipitation solution (polymer precipitation)	Intravenous injection <i>via</i> the tail vein	miRNA-21 inhibits microglial activation, decreases inflammatory factors (TNF- α and IL-1 β), increases anti-inflammatory IL-10, enhances synaptophysin expression, and restores synaptic function	Improves learning and memory and alleviates A β pathology	Male APP/PS1 mice	(123)
BMSCs	Ultracentrifugation	NA	Catalase antioxidant protection	Reduces A β O-induced oxidative stress and synaptic damage <i>in vitro</i>	Hippocampal neurons induced by A β O	(124)
MSCs	Ultracentrifugation	Bilateral dentate gyrus injection	Stimulates neurogenesis in the ventricles	Promotes neurogenesis and recovery of cognitive function	C57BL/6 mice injected with A β aggregates in the bilateral dentate gyrus	(125)
ADMSCs	Ultracentrifugation	Intranasal administration	Upregulates genes related to neuronal neurogenesis and neurite outgrowth	Promotes neurogenesis and alleviates memory deficits	APP/PS1 mice	(126)
hWJ-MSCs	Ultracentrifugation	NA	Catalase-mediated protection	Attenuates A β O-induced oxidative stress and synaptic damage	Primary hippocampal cultures exposed to A β O	(127)
WJ-MSCs	Ultracentrifugation	Intravenous injection	Increases expression of NR2B, GluR1, GluR2, NR2A, Syp, and BDNF, all related to synaptic plasticity and memory	Significantly improves brain glucose metabolism and cognitive function	AD (JAX-006293) mice	(128)
BMSCs	Exosome isolation kit (ultrafiltration tube kit)	Intravenous/intracerebroventricular injection	Upregulates the expression of BDNF and synapse-associated proteins in the hippocampus	Improves cognitive deficits in AD mice	Male C57BL/6 mice, sporadic AD model established by streptozotocin	(129)

Abbreviations: A β O: amyloid β oligomers; AD: Alzheimer's disease; ADMSCs: adipose-derived mesenchymal stem cells; BDNF: brain-derived neurotrophic factor; BMSCs: bone-marrow mesenchymal stem cells; hUC-MSCs: human umbilical cord mesenchymal stem cells; hWJ-MSCs: human Wharton's jelly MSCs; MSCs: mesenchymal stem cells; WJ-MSCs: Wharton's jelly MSCs.

4.3. Promotion of neurogenesis

MSC-Exos have displayed the ability to alleviate the neuropathology associated with AD and improve cognitive function by promoting the proliferation and differentiation of neural stem cells, as well as by enhancing synaptic plasticity. A study has indicated that MSC-Exos can stimulate the generation of new neurons within the brain ventricles, thereby alleviating cognitive impairments caused by β 1-42 amyloid protein (125). A notable study by Ma *et al.* found that EVs secreted by adipose-derived mesenchymal stem cells (ADMSCs) and delivered intranasally rapidly entered the brain, significantly repairing neural damage and improving spatial learning and memory abilities (140).

Moreover, MSC-Exos promote the expression of nerve growth factor (NGF), which enhances the survival and functionality of neural cells. Research by Li *et al.* demonstrated that MSC-Exos upregulate NGF expression and activity, stimulating the proliferation and differentiation of adult neural stem cells. This process promotes neurogenesis and synaptic plasticity, ultimately alleviating cognitive deficits associated with AD (141).

As research on the pathological mechanisms of AD progresses, the potential use of MSCs and their derived exosomes in treating neurodegenerative diseases has garnered increasing attention. Notably, MSC-Exos demonstrate significant potential for the treatment of AD through various mechanisms, including the clearance of abnormal protein accumulation, inhibition of neuroinflammation, and promotion of neurogenesis. However, an important point to note is that most of the current research involves animal models, underscoring the need for more clinical trials to verify the efficacy and safety of MSC-Exos.

5. Advanced techniques for optimizing exosome function

With advances in research on MSC-Exos, these nanoscale vesicles have shown significant promise in regenerative medicine and disease treatment. Exosomes are essential carriers of intercellular signaling, and their bioactivity and functionality are influenced by several factors, including the physiological state of the source cells, culture conditions, and changes in the extracellular environment (142). Therefore, exploring cutting-edge technologies to optimize exosome function is crucial to enhancing their therapeutic efficacy in neurodegenerative diseases such as AD.

5.1. The impact of preconditioning techniques on exosomes

Preconditioning techniques involve manipulating the parent cells under specific culture conditions, such as hypoxia, three-dimensional (3D) culture, and serum

deprivation. In addition, biochemical stimuli like lipopolysaccharides, nitric oxide, pro-inflammatory cytokines, or exogenous genes (*e.g.*, plasmid DNA and miRNAs) can be introduced to alter the culture environment, thereby modulating the function of the cells (143-145). Recent research has indicated that hypoxia or pro-inflammatory cytokine preconditioning can be effectively used to produce MSC-Exos for the treatment of AD. For example, a study by Cui *et al.* demonstrated that exosomes derived from hypoxia-preconditioned mesenchymal stem cells (PC-MSCs) significantly increased the levels of miR-21 in the brains of mice with AD. This increase not only reduced A β deposition but also decreased pro-inflammatory cytokines such as TNF- α and IL-1 β , thereby enhancing therapeutic efficacy in transgenic mice with AD (123). Similarly, Liu *et al.* found that exosomes derived from hypoxia-preconditioned ADMSCs improved cognitive function in mice with AD by upregulating circRNA-Epc1. This modulation of microglial M1/M2 polarization reduced neuronal damage and enhanced cognitive function (146). Hypoxic preconditioning of MSCs enhances their neuroprotective effects primarily by inducing the secretion of HIF-1 α , reactive oxygen species (ROS), and anti-inflammatory cytokines (147). Moreover, preconditioning MSCs with pro-inflammatory cytokines enhances the immunomodulatory properties of MSC-Exos. For instance, Losurdo *et al.* found that MSC-Exos preconditioned with IFN γ and TNF- α suppressed microglial activation and increased dendritic spine density, thereby displaying both immunomodulatory and neuroprotective effects in AD (148).

In addition, Chen *et al.* demonstrated that preconditioning MSCs with a prostaglandin E₂ receptor 4 (EP4) antagonist inhibited the proliferation of reactive astrocytes, reduced widespread inflammation, enhanced BBB integrity, and alleviated learning and memory deficits (149). Moreover, altering MSC culture conditions, such as use of 3D culture methods, can significantly modify the miRNA and protein profiles of MSC-Exos (3D-MSC-Exos) compared to traditional two-dimensional culture systems. Studies have confirmed that 3D culture upregulates α -secretase expression and inhibits β -secretase activity, thereby reducing A β production in pathological AD cells and transgenic mice (142).

These findings suggest that preconditioning strategies can enhance MSC functionality by modifying the culture environment, thus optimizing their performance before transplantation. However, an important point is to carefully consider the effects of preconditioning on the parent cells, as changes in physiological conditions may impact therapeutic outcomes in particular. Therefore, assessing whether the components generated within exosomes can negatively affect these outcomes is essential.

5.2. Drug-loaded MSC-Exos

Loading drugs into MSC-Exos capitalized on the natural delivery capabilities of exosomes to transport therapeutic agents more effectively to targeted disease sites. Drug-loading strategies can be broadly categorized into two main approaches: the first involves loading drugs into the parent cells, which subsequently transfer these drugs to exosomes. This can be achieved by co-culturing the parent cells with the drug or by using chemical methods (e.g., liposomal transfection) to introduce the drug into the parent cells, after which the drugs are encapsulated within the exosomes (44,84,150). The second approach is direct exosome loading, where exogenous drugs are directly introduced into isolated exosomes. This method includes co-incubating the drug with isolated exosomes or using physical techniques (e.g., electroporation, low-permeability dialysis, and ultrasound treatment) and chemical methods (e.g., liposomes) to transfer the drug to exosomes (151,152).

Both approaches aim to optimize drug delivery efficiency and enhance therapeutic efficacy. Current research has shown that nucleic acids, proteins, and drugs can be effectively loaded into MSC-Exos for the treatment of AD. For instance, Zhai *et al.* successfully loaded miRNA-22 into ADMSCs, producing miRNA-22-loaded exosomes that suppressed neuroinflammation in mice with AD, resulting in improved behavioral and memory function (153). Similarly, Jahangard *et al.* loaded miR-29b into BMSCs, generating miR-29b-enriched exosomes that helped reduce A β peptide pathology in a rat model of AD (154). Moreover, Xu *et al.* used genetic engineering techniques to transfect MSCs with the gene encoding tyrosine phosphatase-2 (SHP2), resulting in exosomes enriched with SHP2. These SHP2-expressing MSC-Exos significantly induced mitophagy in neuronal cells, alleviating mitochondrial damage-induced apoptosis and NLRP3 inflammasome activation in mice with AD (155). Another study demonstrated that exosomes derived from enkephalinase gene-modified human umbilical cord mesenchymal stem cells (hUC-MSCs) significantly enhanced the effects of hUC-MSCs on memory and cognitive improvement in mice with AD (132).

The advantages of using MSC-Exos for drug loading are twofold. First, MSC-Exos possess inherent neuroprotective properties, including the ability to reduce A β accumulation, inhibit inflammatory responses, and improve neuronal function. Second, MSC-Exos have strong targeting capabilities, efficiently delivering drugs to neurons and diseased regions. In addition, they have excellent biocompatibility, lower immunogenicity, and the ability to cross the BBB, delivering therapeutic agents directly to brain tissue and influencing AD pathology. A strategy that combines the therapeutic benefits of both drugs and MSC-Exos offers new possibilities and directions for AD treatment.

5.3. Surface modification and artificial exosomes

Surface modification techniques allow for the endowment of natural exosomes with unique functions, such as targeted delivery, through genetic engineering or chemical modification of specific peptides or ligands (156). Surface functionalization can be divided into two categories: endogenous and exogenous modifications. Endogenous functionalization involves modifying the exosome surface by transfecting vectors into the parent cells. This approach preserves the essential functions and integrity of the exosomes; however, it may introduce heterogeneity and requires complex purification processes to isolate the functionalized exosomes (157). In contrast, exogenous functionalization uses physical or chemical methods to directly modify the exosome membrane. Physical methods include extrusion, sonication, and freeze-thaw cycles, while chemical methods utilize various click chemistry techniques (158). However, these methods may affect the internal cargo of the exosomes, and further research needs to be conducted to fully understand their impact on functionality, integrity, and therapeutic potential.

In addition to natural exosomes, artificial exosomes, which act as substitutes, offer greater scalability and flexibility. They can be produced through techniques such as extrusion and microfluidics (159). Artificial exosomes can retain multiple intracellular components from the parent cells, and their RNA and protein content may be double that of natural exosomes (160). During the production process, drugs and therapeutic molecules can also be loaded into artificial exosomes. However, several challenges remain for the clinical use of artificial exosomes. These include potential contamination with other organelles during purification, low encapsulation efficiency due to quality control issues, and alterations in the ratio of cellular membrane components (161). Therefore, the establishment of standard operating procedures and further exploration into their use in AD treatment are essential.

6. Therapeutic advantages and challenges

The use of MSC-Exos in the treatment of AD has gained increasing attention. As a cell-free alternative to stem cell therapy, these exosomes exhibit immense potential for the treatment of neurodegenerative diseases because of their unique biological properties and therapeutic benefits. Compared to traditional stem cells and nanocarriers, MSC-Exos offer superior biocompatibility and lower immunogenicity. Since exosomes are non-replicating entities, they eliminate the tumorigenic risks associated with cell proliferation. In addition, unlike artificial nanoparticles, they do not trigger strong immune responses, which reduces toxicity and contributes to their excellent *in vivo* stability. This safety profile makes MSC-Exos ideal for allogeneic applications, minimizing

the risk of immune rejection.

Another key advantage is their nanoscale size, which enables MSC-Exos to effectively cross the BBB—an essential feature for AD treatment. Their natural properties allow exosomes to remain stable within the body and efficiently reach their target cells. As a drug delivery system, MSC-Exos can transport therapeutic molecules directly to specific cells within brain tissue, and they display a particular affinity for packaging and delivering nucleic acid-based drugs. Moreover, engineered MSC-Exos with surface modifications can enhance targeting capabilities, further improving the efficiency of drug delivery. The high proliferative capacity and multi-differentiation potential of MSCs also make the large-scale production of consistent exosomes feasible, a critical factor for clinical use. In addition to these advantages, MSC-Exos have multiple biological effects—such as anti-inflammatory, antioxidative, immunomodulatory, and neuroprotective properties—enabling them to mitigate AD pathology through various mechanisms.

Despite these significant theoretical advantages, several challenges still impede the clinical use of MSC-Exos. First, the isolation, purification, and storage processes for MSC-Exos require further optimization and standardization. Current methods of isolation, which mainly rely on density and size, may result in cross-contamination with other biological molecules like lipoproteins and viruses, potentially compromising purification quality and therapeutic efficacy. Thus, there is an urgent need for more efficient and cost-effective isolation techniques, as well as standardized production processes, to ensure the consistency and reproducibility of MSC-Exos. In addition, the complex composition of MSC-Exos may include harmful paracrine factors that could interfere with therapeutic outcomes or cause adverse effects. To address these concerns, detailed analyses of the components within MSC-Exos need to be performed to identify and remove potential harmful factors while maintaining rigorous quality control before clinical use.

Moving forward, future research and clinical efforts should focus on addressing these challenges and further exploring the therapeutic potential of MSC-Exos in AD treatment. Developing efficient production and purification methods will help improve the yield and consistency of MSC-Exos. Moreover, investigating novel delivery methods—such as local delivery and the incorporation of biomaterials to protect and enhance exosome delivery—could significantly improve therapeutic efficacy. Grappling with these aspects collectively would position MSC-Exos to play a crucial role in treating AD and other neurodegenerative diseases, paving the way for their emergence as a viable therapeutic option.

Funding: This work was supported by a grant from the

National Natural Science Foundation of China (No. 82460268), the Hainan Provincial Center for Clinical Medical Research on Cerebrovascular Disease (NO. 0202067/0202068), and Grants-in-Aid from the Ministry of Education, Science, Sports, and Culture of Japan (24K14216).

Conflict of Interest: The authors have no conflicts of interest to disclose.

References

1. Hu X, Ma YN, Karako K, Song P, Tang W, Xia Y. Guardians of memory: The urgency of early dementia screening in an aging society. *Intractable Rare Dis Res.* 2024; 13:133-137.
2. Booker SA, Wyllie DJA. NMDA receptor function in inhibitory neurons. *Neuropharmacology.* 2021; 196:108609.
3. Marucci G, Buccioni M, Ben DD, Lambertucci C, Volpini R, Amenta F. Efficacy of acetylcholinesterase inhibitors in Alzheimer's disease. *Neuropharmacology.* 2021; 190:108352.
4. Hu X, Ma YN, Xia Y. Association between abnormal lipid metabolism and Alzheimer's disease: New research has revealed significant findings on the APOE4 genotype in microglia. *Biosci Trends.* 2024; 18:195-197.
5. Liu ZZ, Huang Y, Hong CG, Wang X, Duan R, Liu JY, He JL, Duan D, Xie H, Lu M. Autologous olfactory mucosa mesenchymal stem cells treatment improves the neural network in chronic refractory epilepsy. *Stem Cell Res Ther.* 2023; 14:237.
6. Kuang Y, Zheng X, Zhang L, Ai X, Venkataramani V, Kilic E, Hermann DM, Majid A, Bahr M, Doepfner TR. Adipose-derived mesenchymal stem cells reduce autophagy in stroke mice by extracellular vesicle transfer of miR-25. *J Extracell Vesicles.* 2020; 10:e12024.
7. Lin H, Sohn J, Shen H, Langhans MT, Tuan RS. Bone marrow mesenchymal stem cells: Aging and tissue engineering applications to enhance bone healing. *Biomaterials.* 2019; 203:96-110.
8. Harrell CR, Volarevic A, Djonov V, Volarevic V. Mesenchymal stem cell-derived exosomes as new remedy for the treatment of neurocognitive disorders. *Int J Mol Sci.* 2021; 22:1433.
9. Orobets KS, Karamyshev AL. Amyloid precursor protein and Alzheimer's disease. *Int J Mol Sci.* 2023; 24:14794.
10. Trejo-Lopez JA, Yachnis AT, Prokop S. Neuropathology of Alzheimer's disease. *Neurotherapeutics.* 2022; 19:173-185.
11. Ao C, Li C, Chen J, Tan J, Zeng L. The role of Cdk5 in neurological disorders. *Front Cell Neurosci.* 2022; 16:951202.
12. Lai S, Wang P, Gong J, Zhang S. New insights into the role of GSK-3beta in the brain: From neurodegenerative disease to tumorigenesis. *PeerJ.* 2023; 11:e16635.
13. Leng F, Edison P. Neuroinflammation and microglial activation in Alzheimer disease: Where do we go from here? *Nat Rev Neurol.* 2021; 17:157-172.
14. Marogianni C, Sokratous M, Dardiotis E, Hadjigeorgiou GM, Bogdanos D, Xiromerisiou G. Neurodegeneration and inflammation—An interesting interplay in Parkinson's disease. *Int J Mol Sci.* 2020; 21:8421.

15. Culig L, Chu X, Bohr VA. Neurogenesis in aging and age-related neurodegenerative diseases. *Ageing Res Rev.* 2022; 78:101636.
16. Hessvik NP, Llorente A. Current knowledge on exosome biogenesis and release. *Cell Mol Life Sci.* 2018; 75:193-208.
17. Mathieu M, Martin-Jaular L, Lavieu G, Thery C. Specificities of secretion and uptake of exosomes and other extracellular vesicles for cell-to-cell communication. *Nat Cell Biol.* 2019; 21:9-17.
18. van Niel G, D'Angelo G, Raposo G. Shedding light on the cell biology of extracellular vesicles. *Nat Rev Mol Cell Biol.* 2018; 19:213-228.
19. Kahlert C, Kalluri R. Exosomes in tumor microenvironment influence cancer progression and metastasis. *J Mol Med (Berl).* 2013; 91:431-437.
20. Pegtel DM, Gould SJ. Exosomes. *Annu Rev Biochem.* 2019; 88:487-514.
21. Ciardiello C, Cavallini L, Spinelli C, Yang J, Reis-Sobreiro M, de Candia P, Minciocchi VR, Di Vizio D. Focus on extracellular vesicles: New frontiers of cell-to-cell communication in cancer. *Int J Mol Sci.* 2016; 17:175.
22. Bebelman MP, Smit MJ, Pegtel DM, Baglio SR. Biogenesis and function of extracellular vesicles in cancer. *Pharmacol Ther.* 2018; 188:1-11.
23. Skryabin GO, Komelkov AV, Savelyeva EE, Tchevkina EM. Lipid rafts in exosome biogenesis. *Biochemistry (Mosc).* 2020; 85:177-191.
24. Skotland T, Hessvik NP, Sandvig K, Llorente A. Exosomal lipid composition and the role of ether lipids and phosphoinositides in exosome biology. *J Lipid Res.* 2019; 60:9-18.
25. Mashouri L, Yousefi H, Aref AR, Ahadi AM, Molaei F, Alahari SK. Exosomes: Composition, biogenesis, and mechanisms in cancer metastasis and drug resistance. *Mol Cancer.* 2019; 18:75.
26. Zhang Y, Liu Y, Liu H, Tang WH. Exosomes: Biogenesis, biologic function and clinical potential. *Cell Biosci.* 2019; 9:19.
27. Ge L, Zhang N, Li D, Wu Y, Wang H, Wang J. Circulating exosomal small RNAs are promising non-invasive diagnostic biomarkers for gastric cancer. *J Cell Mol Med.* 2020; 24:14502-14513.
28. Shelke GV, Yin Y, Jang SC, Lasser C, Wennmalm S, Hoffmann HJ, Li L, Gho YS, Nilsson JA, Lotvall J. Endosomal signalling *via* exosome surface TGFbeta-1. *J Extracell Vesicles.* 2019; 8:1650458.
29. Munich S, Sobovujanovic A, Buchser WJ, Beer-Stolz D, Vujanovic NL. Dendritic cell exosomes directly kill tumor cells and activate natural killer cells *via* TNF superfamily ligands. *Oncoimmunology.* 2012; 1:1074-1083.
30. Yang D, Zhang W, Zhang H, Zhang F, Chen L, Ma L, Larcher LM, Chen S, Liu N, Zhao Q, Tran PHL, Chen C, Veedu RN, Wang T. Progress, opportunity, and perspective on exosome isolation - Efforts for efficient exosome-based theranostics. *Theranostics.* 2020; 10:3684-3707.
31. Shao H, Im H, Castro CM, Breakefield X, Weissleder R, Lee H. New technologies for analysis of extracellular vesicles. *Chem Rev.* 2018; 118:1917-1950.
32. Xu K, Jin Y, Li Y, Huang Y, Zhao R. Recent progress of exosome isolation and peptide recognition-guided strategies for exosome research. *Front Chem.* 2022; 10:844124.
33. Melo SA, Luecke LB, Kahlert C, *et al.* Glypican-1 identifies cancer exosomes and detects early pancreatic cancer. *Nature.* 2015; 523:177-182.
34. Jalaludin I, Lubman DM, Kim J. A guide to mass spectrometric analysis of extracellular vesicle proteins for biomarker discovery. *Mass Spectrom Rev.* 2023; 42:844-872.
35. Soares Martins T, Catita J, Martins Rosa I, O AbdCES, Henriques AG. Exosome isolation from distinct biofluids using precipitation and column-based approaches. *PLoS One.* 2018; 13:e0198820.
36. Menon R, Dixon CL, Sheller-Miller S, Fortunato SJ, Saade GR, Palma C, Lai A, Guanzone D, Salomon C. Quantitative proteomics by SWATH-MS of maternal plasma exosomes determine pathways associated with term and preterm birth. *Endocrinology.* 2019; 160:639-650.
37. Doyle LM, Wang MZ. Overview of extracellular vesicles, their origin, composition, purpose, and methods for exosome isolation and analysis. *Cells.* 2019; 8:727.
38. Que RS, Lin C, Ding GP, Wu ZR, Cao LP. Increasing the immune activity of exosomes: The effect of miRNA-depleted exosome proteins on activating dendritic cell/cytokine-induced killer cells against pancreatic cancer. *J Zhejiang Univ Sci B.* 2016; 17:352-360.
39. Iliescu FS, Vrtacnik D, Neuzil P, Iliescu C. Microfluidic technology for clinical applications of exosomes. *Micromachines (Basel).* 2019; 10:392.
40. Gurunathan S, Kang MH, Jeyaraj M, Qasim M, Kim JH. Review of the isolation, characterization, biological function, and multifarious therapeutic approaches of exosomes. *Cells.* 2019; 8:307.
41. Popovic M, Mazzega E, Toffoletto B, de Marco A. Isolation of anti-extra-cellular vesicle single-domain antibodies by direct panning on vesicle-enriched fractions. *Microb Cell Fact.* 2018; 17:6.
42. Kalluri R, LeBleu VS. The biology, function, and biomedical applications of exosomes. *Science.* 2020; 367:eaau6977.
43. Tian Y, Li S, Song J, Ji T, Zhu M, Anderson GJ, Wei J, Nie G. A doxorubicin delivery platform using engineered natural membrane vesicle exosomes for targeted tumor therapy. *Biomaterials.* 2014; 35:2383-2390.
44. Alvarez-Erviti L, Seow Y, Yin H, Betts C, Lakkhal S, Wood MJ. Delivery of siRNA to the mouse brain by systemic injection of targeted exosomes. *Nat Biotechnol.* 2011; 29:341-345.
45. Chen TS, Arslan F, Yin Y, Tan SS, Lai RC, Choo AB, Padmanabhan J, Lee CN, de Kleijn DP, Lim SK. Enabling a robust scalable manufacturing process for therapeutic exosomes through oncogenic immortalization of human ESC-derived MSCs. *J Transl Med.* 2011; 9:47.
46. Yeo RW, Lai RC, Zhang B, Tan SS, Yin Y, Teh BJ, Lim SK. Mesenchymal stem cell: An efficient mass producer of exosomes for drug delivery. *Adv Drug Deliv Rev.* 2013; 65:336-341.
47. Jiang H, Zhao H, Zhang M, He Y, Li X, Xu Y, Liu X. Hypoxia induced changes of exosome cargo and subsequent biological effects. *Front Immunol.* 2022; 13:824188.
48. Kucharzewska P, Christianson HC, Welch JE, Svensson KJ, Fredlund E, Ringner M, Morgelin M, Bourseau-Guilmain E, Bengzon J, Belting M. Exosomes reflect the hypoxic status of glioma cells and mediate hypoxia-dependent activation of vascular cells during tumor development. *Proc Natl Acad Sci U S A.* 2013; 110:7312-7317.

49. Li J, Lee Y, Johansson HJ, Mager I, Vader P, Nordin JZ, Wiklander OP, Lehtio J, Wood MJ, Andaloussi SE. Serum-free culture alters the quantity and protein composition of neuroblastoma-derived extracellular vesicles. *J Extracell Vesicles*. 2015; 4:26883.
50. Yuan X, Sun L, Jeske R, Nkosi D, York SB, Liu Y, Grant SC, Meckes DG, Jr., Li Y. Engineering extracellular vesicles by three-dimensional dynamic culture of human mesenchymal stem cells. *J Extracell Vesicles*. 2022; 11:e12235.
51. Bei HP, Hung PM, Yeung HL, Wang S, Zhao X. Bone-a-Petite: Engineering exosomes towards bone, osteochondral, and cartilage repair. *Small*. 2021; 17:e2101741.
52. Dragovic RA, Gardiner C, Brooks AS, Tannetta DS, Ferguson DJ, Hole P, Carr B, Redman CW, Harris AL, Dobson PJ, Harrison P, Sargent IL. Sizing and phenotyping of cellular vesicles using nanoparticle tracking analysis. *Nanomedicine*. 2011; 7:780-788.
53. Tan F, Li X, Wang Z, Li J, Shahzad K, Zheng J. Clinical applications of stem cell-derived exosomes. *Signal Transduct Target Ther*. 2024; 9:17.
54. Szatanek R, Baj-Krzyworzeka M, Zimoch J, Lekka M, Siedlar M, Baran J. The methods of choice for extracellular vesicles (EVs) characterization. *Int J Mol Sci*. 2017; 18:1153.
55. Hoo CM, Starostin N, West P, Mecartney ML. A comparison of atomic force microscopy (AFM) and dynamic light scattering (DLS) methods to characterize nanoparticle size distributions. *Journal of Nanoparticle Research*. 2008; 10:89-96.
56. Anderson W, Lane R, Korbie D, Trau M. Observations of tunable resistive pulse sensing for exosome analysis: Improving system sensitivity and stability. *Langmuir*. 2015; 31:6577-6587.
57. Colombo M, Raposo G, Thery C. Biogenesis, secretion, and intercellular interactions of exosomes and other extracellular vesicles. *Annu Rev Cell Dev Biol*. 2014; 30:255-289.
58. Pospichalova V, Svoboda J, Dave Z, Kotrbova A, Kaiser K, Klemova D, Ilkovic L, Hampl A, Crha I, Jandakova E, Minar L, Weinberger V, Bryja V. Simplified protocol for flow cytometry analysis of fluorescently labeled exosomes and microvesicles using dedicated flow cytometer. *J Extracell Vesicles*. 2015; 4:25530.
59. Shan X, Zhang C, Mai C, Hu X, Cheng N, Chen W, Peng D, Wang L, Ji Z, Xie Y. The biogenesis, biological functions, and applications of macrophage-derived exosomes. *Front Mol Biosci*. 2021; 8:715461.
60. Li M, Li S, Du C, Zhang Y, Li Y, Chu L, Han X, Galons H, Zhang Y, Sun H, Yu P. Exosomes from different cells: Characteristics, modifications, and therapeutic applications. *Eur J Med Chem*. 2020; 207:112784.
61. Zhang H, Freitas D, Kim HS, *et al*. Identification of distinct nanoparticles and subsets of extracellular vesicles by asymmetric flow field-flow fractionation. *Nat Cell Biol*. 2018; 20:332-343.
62. Chevillet JR, Kang Q, Ruf IK, *et al*. Quantitative and stoichiometric analysis of the microRNA content of exosomes. *Proc Natl Acad Sci U S A*. 2014; 111:14888-14893.
63. Lasda E, Parker R. Circular RNAs co-precipitate with extracellular vesicles: A possible mechanism for circRNA clearance. *PLoS One*. 2016; 11:e0148407.
64. Pathan M, Fonseka P, Chitti SV, Kang T, Sanwani R, Van Deun J, Hendrix A, Mathivanan S. Vesiclepedia 2019: A compendium of RNA, proteins, lipids and metabolites in extracellular vesicles. *Nucleic Acids Res*. 2019; 47:D516-D519.
65. Keerthikumar S, Chisanga D, Ariyaratne D, Al Saffar H, Anand S, Zhao K, Samuel M, Pathan M, Jois M, Chilamkurti N, Gangoda L, Mathivanan S. ExoCarta: A web-based compendium of exosomal cargo. *J Mol Biol*. 2016; 428:688-692.
66. Liu J, Wu F, Zhou H. Macrophage-derived exosomes in cancers: Biogenesis, functions and therapeutic applications. *Immunol Lett*. 2020; 227:102-108.
67. Boukouris S, Mathivanan S. Exosomes in bodily fluids are a highly stable resource of disease biomarkers. *Proteomics Clin Appl*. 2015; 9:358-367.
68. Zhou B, Xu K, Zheng X, Chen T, Wang J, Song Y, Shao Y, Zheng S. Application of exosomes as liquid biopsy in clinical diagnosis. *Signal Transduct Target Ther*. 2020; 5:144.
69. Kluszczynska K, Czernek L, Cypryk W, Peczek L, Duchler M. Methods for the determination of the purity of exosomes. *Curr Pharm Des*. 2019; 25:4464-4485.
70. Mulcahy LA, Pink RC, Carter DR. Routes and mechanisms of extracellular vesicle uptake. *J Extracell Vesicles*. 2014; 3.
71. Prada I, Meldolesi J. Binding and fusion of extracellular vesicles to the plasma membrane of their cell targets. *Int J Mol Sci*. 2016; 17:1296.
72. Tkach M, Kowal J, Zucchetti AE, Enserink L, Jouve M, Lankar D, Saitakis M, Martin-Jaular L, Thery C. Qualitative differences in T-cell activation by dendritic cell-derived extracellular vesicle subtypes. *EMBO J*. 2017; 36:3012-3028.
73. Valadi H, Ekstrom K, Bossios A, Sjostrand M, Lee JJ, Lotvall JO. Exosome-mediated transfer of mRNAs and microRNAs is a novel mechanism of genetic exchange between cells. *Nat Cell Biol*. 2007; 9:654-659.
74. Tian T, Zhu YL, Hu FH, Wang YY, Huang NP, Xiao ZD. Dynamics of exosome internalization and trafficking. *J Cell Physiol*. 2013; 228:1487-1495.
75. Joshi BS, de Beer MA, Giepmans BNG, Zuhorn IS. Endocytosis of extracellular vesicles and release of their cargo from endosomes. *ACS Nano*. 2020; 14:4444-4455.
76. Kwok ZH, Wang C, Jin Y. Extracellular vesicle transportation and uptake by recipient cells: A critical process to regulate human diseases. *Processes (Basel)*. 2021; 9:273.
77. Kamerkar S, LeBleu VS, Sugimoto H, Yang S, Ruivo CF, Melo SA, Lee JJ, Kalluri R. Exosomes facilitate therapeutic targeting of oncogenic KRAS in pancreatic cancer. *Nature*. 2017; 546:498-503.
78. Commisso C, Davidson SM, Soydaner-Azeloglu RG, Parker SJ, Kamphorst JJ, Hackett S, Grabocka E, Nofal M, Drebin JA, Thompson CB, Rabinowitz JD, Metallo CM, Vander Heiden MG, Bar-Sagi D. Macropinocytosis of protein is an amino acid supply route in Ras-transformed cells. *Nature*. 2013; 497:633-637.
79. Parolini I, Federici C, Raggi C, Lugini L, Palleschi S, De Milito A, Coscia C, Iessi E, Logozzi M, Molinari A, Colone M, Tatti M, Sargiacomo M, Fais S. Microenvironmental pH is a key factor for exosome traffic in tumor cells. *J Biol Chem*. 2009; 284:34211-34222.
80. Tian T, Zhu YL, Zhou YY, Liang GF, Wang YY, Hu FH, Xiao ZD. Exosome uptake through clathrin-mediated endocytosis and macropinocytosis and mediating miR-21

- delivery. *J Biol Chem.* 2014; 289:22258-22267.
81. Murphy DE, de Jong OG, Brouwer M, Wood MJ, Lavieu G, Schifferers RM, Vader P. Extracellular vesicle-based therapeutics: Natural *versus* engineered targeting and trafficking. *Exp Mol Med.* 2019; 51:1-12.
 82. Morishita M, Takahashi Y, Nishikawa M, Takakura Y. Pharmacokinetics of exosomes-An important factor for elucidating the biological roles of exosomes and for the development of exosome-based therapeutics. *J Pharm Sci.* 2017; 106:2265-2269.
 83. Munagala R, Aqil F, Jeyabalan J, Gupta RC. Bovine milk-derived exosomes for drug delivery. *Cancer Lett.* 2016; 371:48-61.
 84. Zhuang X, Xiang X, Grizzle W, Sun D, Zhang S, Axtell RC, Ju S, Mu J, Zhang L, Steinman L, Miller D, Zhang HG. Treatment of brain inflammatory diseases by delivering exosome encapsulated anti-inflammatory drugs from the nasal region to the brain. *Mol Ther.* 2011; 19:1769-1779.
 85. Haney MJ, Klyachko NL, Zhao Y, Gupta R, Plotnikova EG, He Z, Patel T, Piroyan A, Sokolsky M, Kabanov AV, Batrakova EV. Exosomes as drug delivery vehicles for Parkinson's disease therapy. *J Control Release.* 2015; 207:18-30.
 86. Smyth T, Kullberg M, Malik N, Smith-Jones P, Graner MW, Anchordoquy TJ. Biodistribution and delivery efficiency of unmodified tumor-derived exosomes. *J Control Release.* 2015; 199:145-155.
 87. Lentz TL, Burrage TG, Smith AL, Crick J, Tignor GH. Is the acetylcholine receptor a rabies virus receptor? *Science.* 1982; 215:182-184.
 88. Escrevente C, Keller S, Altevogt P, Costa J. Interaction and uptake of exosomes by ovarian cancer cells. *BMC Cancer.* 2011; 11:108.
 89. Yamashita T, Takahashi Y, Takakura Y. Possibility of exosome-based therapeutics and challenges in production of exosomes eligible for therapeutic application. *Biol Pharm Bull.* 2018; 41:835-842.
 90. Maroto R, Zhao Y, Jamaluddin M, Popov VL, Wang H, Kalubowilage M, Zhang Y, Luisi J, Sun H, Culbertson CT, Bossmann SH, Motamedi M, Brasier AR. Effects of storage temperature on airway exosome integrity for diagnostic and functional analyses. *J Extracell Vesicles.* 2017; 6:1359478.
 91. Bosch S, de Beaupaire L, Allard M, Mosser M, Heichette C, Chretien D, Jegou D, Bach JM. Trehalose prevents aggregation of exosomes and cryodamage. *Sci Rep.* 2016; 6:36162.
 92. Charoenviriyakul C, Takahashi Y, Nishikawa M, Takakura Y. Preservation of exosomes at room temperature using lyophilization. *Int J Pharm.* 2018; 553:1-7.
 93. Kusuma GD, Barabadi M, Tan JL, Morton DAV, Frith JE, Lim R. To protect and to preserve: Novel preservation strategies for extracellular vesicles. *Front Pharmacol.* 2018; 9:1199.
 94. Yuan L, Li JY. Exosomes in Parkinson's disease: Current perspectives and future challenges. *ACS Chem Neurosci.* 2019; 10:964-972.
 95. Howitt J, Hill AF. Exosomes in the pathology of neurodegenerative diseases. *J Biol Chem.* 2016; 291:26589-26597.
 96. Budnik V, Ruiz-Canada C, Wandler F. Extracellular vesicles round off communication in the nervous system. *Nat Rev Neurosci.* 2016; 17:160-172.
 97. Guo BB, Bellingham SA, Hill AF. Stimulating the release of exosomes increases the intercellular transfer of prions. *J Biol Chem.* 2016; 291:5128-5137.
 98. Rajendran L, Honsho M, Zahn TR, Keller P, Geiger KD, Verkade P, Simons K. Alzheimer's disease beta-amyloid peptides are released in association with exosomes. *Proc Natl Acad Sci U S A.* 2006; 103:11172-11177.
 99. Baker S, Polanco JC, Gotz J. Extracellular vesicles containing P301L mutant tau accelerate pathological tau phosphorylation and oligomer formation but do not seed mature neurofibrillary tangles in ALZ17 mice. *J Alzheimers Dis.* 2016; 54:1207-1217.
 100. Yuyama K, Sun H, Usuki S, Sakai S, Hanamatsu H, Mioka T, Kimura N, Okada M, Tahara H, Furukawa J, Fujitani N, Shinohara Y, Igarashi Y. A potential function for neuronal exosomes: Sequestering intracerebral amyloid-beta peptide. *FEBS Lett.* 2015; 589:84-88.
 101. Falker C, Hartmann A, Guett I, Dohler F, Altmeppen H, Betzel C, Schubert R, Thurm D, Wegwitz F, Joshi P, Verderio C, Krasemann S, Glatzel M. Exosomal cellular prion protein drives fibrillization of amyloid beta and counteracts amyloid beta-mediated neurotoxicity. *J Neurochem.* 2016; 137:88-100.
 102. Pacheco-Quinto J, Clausen D, Perez-Gonzalez R, Peng H, Meszaros A, Eckman CB, Levy E, Eckman EA. Intracellular metalloprotease activity controls intraneuronal Aβ aggregation and limits secretion of Aβ via exosomes. *FASEB J.* 2019; 33:3758-3771.
 103. Stuenkel A, Kunadt M, Kruse N, Bartels C, Moebius W, Danzer KM, Mollenhauer B, Schneider A. Induction of alpha-synuclein aggregate formation by CSF exosomes from patients with Parkinson's disease and dementia with Lewy bodies. *Brain.* 2016; 139:481-494.
 104. Spencer B, Kim C, Gonzalez T, Bisquertt A, Patrick C, Rockenstein E, Adame A, Lee SJ, Desplats P, Masliah E. alpha-Synuclein interferes with the ESCRT-III complex contributing to the pathogenesis of Lewy body disease. *Hum Mol Genet.* 2016; 25:1100-1115.
 105. Iguchi Y, Eid L, Parent M, Soucy G, Bareil C, Riku Y, Kawai K, Takagi S, Yoshida M, Katsuno M, Sobue G, Julien JP. Exosome secretion is a key pathway for clearance of pathological TDP-43. *Brain.* 2016; 139:3187-3201.
 106. Tsilioni I, Theoharides TC. Extracellular vesicles are increased in the serum of children with autism spectrum disorder, contain mitochondrial DNA, and stimulate human microglia to secrete IL-1β. *J Neuroinflammation.* 2018; 15:239.
 107. Cooper JM, Wiklander PB, Nordin JZ, Al-Shawi R, Wood MJ, Vitlani M, Schapira AH, Simons JP, El-Andaloussi S, Alvarez-Erviti L. Systemic exosomal siRNA delivery reduced alpha-synuclein aggregates in brains of transgenic mice. *Mov Disord.* 2014; 29:1476-1485.
 108. Han C, Wang YJ, Wang YC, Guan X, Wang L, Shen LM, Zou W, Liu J. Caveolin-1 downregulation promotes the dopaminergic neuron-like differentiation of human adipose-derived mesenchymal stem cells. *Neural Regen Res.* 2021; 16:714-720.
 109. Bonaventura G, Incontro S, Iemmolo R, La Cognata V, Barbagallo I, Costanzo E, Barcellona ML, Pellitteri R, Cavallaro S. Dental mesenchymal stem cells and neuroregeneration: A focus on spinal cord injury. *Cell Tissue Res.* 2020; 379:421-428.
 110. Volarevic V, Gazdic M, Simovic Markovic B, Jovicic N, Djonov V, Arsenijevic N. Mesenchymal stem cell-derived factors: Immuno-modulatory effects and therapeutic

- potential. *Biofactors*. 2017; 43:633-644.
111. Shariati A, Nemati R, Sadeghipour Y, Yaghoubi Y, Baghbani R, Javidi K, Zamani M, Hassanzadeh A. Mesenchymal stromal cells (MSCs) for neurodegenerative disease: A promising frontier. *Eur J Cell Biol*. 2020; 99:151097.
 112. Lukomska B, Stanaszek L, Zuba-Surma E, Legosz P, Sarzynska S, Drela K. Challenges and controversies in human mesenchymal stem cell therapy. *Stem Cells Int*. 2019; 2019:9628536.
 113. Gazdic M, Volarevic V, Arsenijevic N, Stojkovic M. Mesenchymal stem cells: A friend or foe in immune-mediated diseases. *Stem Cell Rev Rep*. 2015; 11:280-287.
 114. Volarevic V, Markovic BS, Gazdic M, Volarevic A, Jovicic N, Arsenijevic N, Armstrong L, Djonov V, Lako M, Stojkovic M. Ethical and safety issues of stem cell-based therapy. *Int J Med Sci*. 2018; 15:36-45.
 115. Guy R, Offen D. Promising opportunities for treating neurodegenerative diseases with mesenchymal stem cell-derived exosomes. *Biomolecules*. 2020; 10:1320.
 116. Harrell CR, Jovicic N, Djonov V, Arsenijevic N, Volarevic V. Mesenchymal stem cell-derived exosomes and other extracellular vesicles as new remedies in the therapy of inflammatory diseases. *Cells*. 2019; 8:1605.
 117. Scheltens P, De Strooper B, Kivipelto M, Holstege H, Chetelat G, Teunissen CE, Cummings J, van der Flier WM. Alzheimer's disease. *Lancet*. 2021; 397:1577-1590.
 118. Elia CA, Tamborini M, Rasile M, Desiato G, Marchetti S, Swuec P, Mazzitelli S, Clemente F, Anselmo A, Matteoli M, Malosio ML, Coco S. Intracerebral injection of extracellular vesicles from mesenchymal stem cells exerts reduced A β plaque burden in early stages of a preclinical model of Alzheimer's disease. *Cells*. 2019; 8.
 119. Wang H, Liu Y, Li J, Wang T, Hei Y, Li H, Wang X, Wang L, Zhao R, Liu W, Long Q. Tail-vein injection of MSC-derived small extracellular vesicles facilitates the restoration of hippocampal neuronal morphology and function in APP / PS1 mice. *Cell Death Discov*. 2021; 7:230.
 120. Sha S, Shen X, Cao Y, Qu L. Mesenchymal stem cell-derived extracellular vesicles ameliorate Alzheimer's disease in rat models *via* the microRNA-29c-3p/BACE1 axis and the Wnt/beta-catenin pathway. *Aging (Albany NY)*. 2021; 13:15285-15306.
 121. Ding M, Shen Y, Wang P, Xie Z, Xu S, Zhu Z, Wang Y, Lyu Y, Wang D, Xu L, Bi J, Yang H. Exosomes isolated from human umbilical cord mesenchymal stem cells alleviate neuroinflammation and reduce amyloid-beta deposition by modulating microglial activation in Alzheimer's disease. *Neurochem Res*. 2018; 43:2165-2177.
 122. Nakano M, Kubota K, Kobayashi E, Chikenji TS, Saito Y, Konari N, Fujimiya M. Bone marrow-derived mesenchymal stem cells improve cognitive impairment in an Alzheimer's disease model by increasing the expression of microRNA-146a in hippocampus. *Sci Rep*. 2020; 10:10772.
 123. Cui GH, Wu J, Mou FF, Xie WH, Wang FB, Wang QL, Fang J, Xu YW, Dong YR, Liu JR, Guo HD. Exosomes derived from hypoxia-preconditioned mesenchymal stromal cells ameliorate cognitive decline by rescuing synaptic dysfunction and regulating inflammatory responses in APP/PS1 mice. *FASEB J*. 2018; 32:654-668.
 124. de Godoy MA, Saraiva LM, de Carvalho LRP, *et al*. Mesenchymal stem cells and cell-derived extracellular vesicles protect hippocampal neurons from oxidative stress and synapse damage induced by amyloid-beta oligomers. *J Biol Chem*. 2018; 293:1957-1975.
 125. Reza-Zaldivar EE, Hernandez-Sapiens MA, Gutierrez-Mercado YK, Sandoval-Avila S, Gomez-Pinedo U, Marquez-Aguirre AL, Vazquez-Mendez E, Padilla-Camberos E, Canales-Aguirre AA. Mesenchymal stem cell-derived exosomes promote neurogenesis and cognitive function recovery in a mouse model of Alzheimer's disease. *Neural Regen Res*. 2019; 14:1626-1634.
 126. Ma X, Huang M, Zheng M, *et al*. ADSCs-derived extracellular vesicles alleviate neuronal damage, promote neurogenesis and rescue memory loss in mice with Alzheimer's disease. *J Control Release*. 2020; 327:688-702.
 127. Bodart-Santos V, de Carvalho LRP, de Godoy MA, Batista AF, Saraiva LM, Lima LG, Abreu CA, De Felice FG, Galina A, Mendez-Otero R, Ferreira ST. Extracellular vesicles derived from human Wharton's jelly mesenchymal stem cells protect hippocampal neurons from oxidative stress and synapse damage induced by amyloid-beta oligomers. *Stem Cell Res Ther*. 2019; 10:332.
 128. Chen YA, Lu CH, Ke CC, Chiu SJ, Jeng FS, Chang CW, Yang BH, Liu RS. Mesenchymal stem cell-derived exosomes ameliorate Alzheimer's disease pathology and improve cognitive deficits. *Biomedicines*. 2021; 9:594.
 129. Liu S, Fan M, Xu JX, Yang LJ, Qi CC, Xia QR, Ge JF. Exosomes derived from bone-marrow mesenchymal stem cells alleviate cognitive decline in AD-like mice by improving BDNF-related neuropathology. *J Neuroinflammation*. 2022; 19:35.
 130. Scheltens P, De Strooper B, Kivipelto M, Holstege H, Chetelat G, Teunissen CE, Cummings J, van der Flier WM. Alzheimer's disease. *Lancet*. 2021; 397:1577-1590.
 131. McGinley MP, Cohen JA. Sphingosine 1-phosphate receptor modulators in multiple sclerosis and other conditions. *Lancet*. 2021; 398:1184-1194.
 132. Jeong H, Kim OJ, Oh SH, Lee S, Reum Lee HA, Lee KO, Lee BY, Kim NK. Extracellular vesicles released from neprilysin gene-modified human umbilical cord-derived mesenchymal stem cell enhance therapeutic effects in an Alzheimer's disease animal model. *Stem Cells Int*. 2021; 2021:5548630.
 133. de Dios C, Bartolessis I, Roca-Agujetas V, Barbero-Camps E, Mari M, Morales A, Colell A. Oxidative inactivation of amyloid beta-degrading proteases by cholesterol-enhanced mitochondrial stress. *Redox Biol*. 2019; 26:101283.
 134. Ferreira JPS, Albuquerque HMT, Cardoso SM, Silva AMS, Silva VLM. Dual-target compounds for Alzheimer's disease: Natural and synthetic AChE and BACE-1 dual-inhibitors and their structure-activity relationship (SAR). *Eur J Med Chem*. 2021; 221:113492.
 135. Ghosh AK. BACE1 inhibitor drugs for the treatment of Alzheimer's disease: Lessons learned, challenges to overcome, and future prospects(dagger). *Glob Health Med*. 2024; 6:164-168.
 136. Parr C, Mirzaei N, Christian M, Sastre M. Activation of the Wnt/beta-catenin pathway represses the transcription of the beta-amyloid precursor protein cleaving enzyme (BACE1) *via* binding of T-cell factor-4 to BACE1 promoter. *FASEB J*. 2015; 29:623-635.
 137. Wu H, Fan H, Shou Z, Xu M, Chen Q, Ai C, Dong Y, Liu Y, Nan Z, Wang Y, Yu T, Liu X. Extracellular vesicles

- containing miR-146a attenuate experimental colitis by targeting TRAF6 and IRAK1. *Int Immunopharmacol.* 2019; 68:204-212.
138. Cinelli MA, Do HT, Miley GP, Silverman RB. Inducible nitric oxide synthase: Regulation, structure, and inhibition. *Med Res Rev.* 2020; 40:158-189.
 139. Wang SS, Jia J, Wang Z. Mesenchymal stem cell-derived extracellular vesicles suppresses iNOS expression and ameliorates neural impairment in Alzheimer's Disease mice. *J Alzheimers Dis.* 2018; 61:1005-1013.
 140. Elelu N, Bankole AA, Daphne HP, Rabi M, Ola-Fadunsin SD, Ambali HM, Cutler SJ. Molecular characterisation of *Rhipicephalus sanguineus sensu lato* ticks from domestic dogs in Nigeria. *Vet Med Sci.* 2022; 8:454-459.
 141. Mukherjee M, Dutta S, Ghosh M, Basuchowdhuri P, Datta A. Performance of the nitrogen reduction reaction on metal bound g-C(6)N(6): A combined approach of machine learning and DFT. *Phys Chem Chem Phys.* 2022; 24:17050-17058.
 142. Yang L, Zhai Y, Hao Y, Zhu Z, Cheng G. The regulatory functionality of exosomes derived from hUMSCs in 3D culture for Alzheimer's disease therapy. *Small.* 2020; 16:e1906273.
 143. Domenis R, Cifu A, Quaglia S, Pistis C, Moretti M, Vicario A, Parodi PC, Fabris M, Niazi KR, Soon-Shiong P, Curcio F. Pro inflammatory stimuli enhance the immunosuppressive functions of adipose mesenchymal stem cells-derived exosomes. *Sci Rep.* 2018; 8:13325.
 144. Liu X, Li X, Zhu W, Zhang Y, Hong Y, Liang X, Fan B, Zhao H, He H, Zhang F. Exosomes from mesenchymal stem cells overexpressing MIF enhance myocardial repair. *J Cell Physiol.* 2020; 235:8010-8022.
 145. Gala D, Mohak S, Fabian Z. Extracellular vehicles of oxygen-depleted mesenchymal stromal cells: Route to off-shelf cellular therapeutics? *Cells.* 2021; 10:2199.
 146. Liu H, Jin M, Ji M, Zhang W, Liu A, Wang T. Hypoxic pretreatment of adipose-derived stem cell exosomes improved cognition by delivery of circ-Epc1 and shifting microglial M1/M2 polarization in an Alzheimer's disease mice model. *Aging (Albany NY).* 2022; 14:3070-3083.
 147. Yin T, Liu Y, Ji W, Zhuang J, Chen X, Gong B, Chu J, Liang W, Gao J, Yin Y. Engineered mesenchymal stem cell-derived extracellular vesicles: A state-of-the-art multifunctional weapon against Alzheimer's disease. *Theranostics.* 2023; 13:1264-1285.
 148. Losurdo M, Pedrazzoli M, D'Agostino C, *et al.* Intranasal delivery of mesenchymal stem cell-derived extracellular vesicles exerts immunomodulatory and neuroprotective effects in a 3xTg model of Alzheimer's disease. *Stem Cells Transl Med.* 2020; 9:1068-1084.
 149. Chen SY, Lin MC, Tsai JS, He PL, Luo WT, Herschman H, Li HJ. EP(4) antagonist-elicited extracellular vesicles from mesenchymal stem cells rescue cognition/learning deficiencies by restoring brain cellular functions. *Stem Cells Transl Med.* 2019; 8:707-723.
 150. Xu M, Yang Q, Sun X, Wang Y. Recent advancements in the loading and modification of therapeutic exosomes. *Front Bioeng Biotechnol.* 2020; 8:586130.
 151. Wang Z, Rich J, Hao N, Gu Y, Chen C, Yang S, Zhang P, Huang TJ. Acoustofluidics for simultaneous nanoparticle-based drug loading and exosome encapsulation. *Microsyst Nanoeng.* 2022; 8:45.
 152. Wang J, Chen D, Ho EA. Challenges in the development and establishment of exosome-based drug delivery systems. *J Control Release.* 2021; 329:894-906.
 153. Zhai L, Shen H, Sheng Y, Guan Q. ADMSC Exo-microRNA-22 improve neurological function and neuroinflammation in mice with Alzheimer's disease. *J Cell Mol Med.* 2021; 25:7513-7523.
 154. Jahangard Y, Monfared H, Moradi A, Zare M, Mirnajafi-Zadeh J, Mowla SJ. Therapeutic effects of transplanted exosomes containing miR-29b to a rat model of Alzheimer's disease. *Front Neurosci.* 2020; 14:564.
 155. Xu F, Wu Y, Yang Q, Cheng Y, Xu J, Zhang Y, Dai H, Wang B, Ma Q, Chen Y, Lin F, Wang C. Engineered extracellular vesicles with SHP2 high expression promote mitophagy for Alzheimer's disease treatment. *Adv Mater.* 2022; 34:e2207107.
 156. Tian T, Zhang HX, He CP, Fan S, Zhu YL, Qi C, Huang NP, Xiao ZD, Lu ZH, Tannous BA, Gao J. Surface functionalized exosomes as targeted drug delivery vehicles for cerebral ischemia therapy. *Biomaterials.* 2018; 150:137-149.
 157. Gaurav I, Thakur A, Iyaswamy A, Wang X, Chen X, Yang Z. Factors affecting extracellular vesicles based drug delivery systems. *Molecules.* 2021; 26:1544.
 158. Rayamajhi S, Aryal S. Surface functionalization strategies of extracellular vesicles. *J Mater Chem B.* 2020; 8:4552-4569.
 159. Li YJ, Wu JY, Liu J, Xu W, Qiu X, Huang S, Hu XB, Xiang DX. Artificial exosomes for translational nanomedicine. *J Nanobiotechnology.* 2021; 19:242.
 160. Kim HY, Kwon S, Um W, Shin S, Kim CH, Park JH, Kim BS. Functional extracellular vesicles for regenerative medicine. *Small.* 2022; 18:e2106569.
 161. Le QV, Lee J, Lee H, Shim G, Oh YK. Cell membrane-derived vesicles for delivery of therapeutic agents. *Acta Pharm Sin B.* 2021; 11:2096-2113.
- Received September 8, 2024; Revised October 6, 2024; Accepted October 9, 2024.
- *Address correspondence to:*
Ying Xia, Department of Neurosurgery, Haikou Affiliated Hospital of Central South University Xiangya School of Medicine, Haikou 570208, China.
E-mail: xiaying008@163.com
- Peipei Song, National Center for Global Health and Medicine, 1-21-1 Toyama, Shinjuku-ku, Tokyo 162-8655, Japan.
E-mail: psong@it.ncgm.go.jp
- Released online in J-STAGE as advance publication October 11, 2024.

Management of non-alcoholic fatty liver disease-associated hepatocellular carcinoma

Peijun Xu¹, Maoyun Liu¹, Miao Liu^{2,*}, Ai Shen^{1,*}

¹Department of Hepatobiliary Pancreatic Cancer Center, Cancer Hospital, School of Medicine, Chongqing University, Chongqing, China;

²Department of Gastrointestinal Cancer Center, Cancer Hospital, School of Medicine, Chongqing University, Chongqing, China.

SUMMARY In recent years, with the decline in HBV and HCV infections, there has been a corresponding reduction in both the morbidity and mortality of virus-associated HCC. Nevertheless, rising living standards, coupled with the increasing prevalence of metabolic disorders like diabetes and obesity, have led to a rapid surge in non-alcoholic fatty liver disease-associated hepatocellular carcinoma (NAFLD-HCC) incidence. The mechanisms underlying the progression from NAFLD to NAFLD-HCC are multifaceted and remain incompletely understood. Current research suggests that genetic predisposition, metabolic dysregulation, lipotoxicity, oxidative stress, and inflammation are key contributing factors. Given the complexity of these mechanisms and the frequent occurrence of metabolic comorbidities like type 2 diabetes mellitus (T2DM) and cardiovascular disease in NAFLD-HCC patients, there is a pressing need for tailored therapeutic strategies, along with novel prevention, monitoring, and treatment approaches that are personalized to the patient's pathophysiology. Due to the limited depth of research, incomplete understanding of pathogenesis, and insufficient clinical data on NAFLD-HCC treatment, current therapeutic approaches largely rely on tumor staging. In this review, we synthesize current research on the pathogenesis, surveillance, diagnosis, treatment, and prevention of NAFLD-HCC, and offer perspectives for future studies, particularly regarding its underlying mechanisms.

Keywords NAFLD-HCC, NAFLD, pathogenesis, diagnosis, treatment

1. Introduction

Hepatocellular carcinoma (HCC) represents the predominant histological subtype of primary liver cancer, comprising the vast majority of cases (1). Recent global cancer statistics indicate that HCC exhibits both a high incidence and mortality rate. Non-alcoholic fatty liver disease (NAFLD) is rapidly becoming a leading cause of HCC, driven by the rising prevalence of non-alcoholic fatty liver disease and the declining incidence of chronic viral hepatitis. Current clinical studies suggest that 10~20% of NAFLD patients progress to non-alcoholic steatohepatitis (NASH), with nearly one-third of those progressing to cirrhosis and potentially HCC (2).

The development of NAFLD-HCC is a multifactorial and complex process involving numerous risk factors. Metabolic dysregulation leads to hepatic steatosis, and under the combined influence of genetic predisposition, lipotoxicity, oxidative stress, inflammation, and other mechanisms, NAFLD

progresses, leading to hepatic inflammation, fibrosis, and ultimately, the onset of NAFLD-HCC.

The incidence of NAFLD-HCC is steadily rising, highlighting the critical need for a deeper understanding of NAFLD-HCC to enhance treatment outcomes and prognosis. In this review, we summarize the current knowledge on the pathogenesis, diagnosis, surveillance, and treatment of NAFLD-HCC, and offer perspectives for future research, particularly on its underlying mechanisms.

2. Prevalence of NAFLD-HCC

HCC is the most prevalent histological type of primary liver cancer, ranking as the third leading cause of cancer-related deaths globally. It is also the primary cause of mortality in patients with chronic liver disease and cirrhosis, contributing to 7.8% of all cancer-related deaths worldwide (3). Globally, morbidity and mortality rates for HCC are two to three times higher in men than in women. Key risk factors for HCC include

chronic hepatitis B and C infections, heavy alcohol use, NAFLD, obesity, T2DM, aflatoxin exposure, and smoking (4). The highest incidence and prevalence of HCC currently occur in regions such as East Asia, North Africa, and Southeast Asia, largely due to the high burden of HBV infection, which accounts for over 50% of global HCC cases. By contrast, in North America, Europe, and Australia, non-viral etiologies like NAFLD are responsible for the majority of HCC cases. With rising hepatitis B vaccination rates, antiviral therapies, and increasing obesity rates, the prevalence of HBV-associated HCC has decreased, while NAFLD-HCC has risen from 9.9% to 13.6% (5). Globally, the prevalence of NAFLD-HCC is expected to rise in tandem with the increasing incidence of metabolic diseases, including obesity and T2DM. Presently, the highest prevalence of NAFLD-HCC is observed in countries such as the United Kingdom, Germany, Saudi Arabia, Southeast Asia, and Africa. The United States, Canada, Australia, South America, and France show slightly lower rates, while regions like China and Japan report comparatively lower prevalence (Figure 1). The annual incidence of HCC in NASH patients with cirrhosis is estimated at 0.5-2.6%, while in non-cirrhotic NAFLD patients, it is significantly lower, ranging from 0.1 to 1.3 per 1,000 patients per year. Currently, although NAFLD-HCC has a lower incidence compared to HCC from other etiologies, the rising prevalence of obesity, T2DM, and metabolic syndrome suggests that the future burden of NAFLD-HCC will surpass other liver diseases. This highlights the urgent need for a deeper understanding of NAFLD-HCC pathogenesis and the implementation of targeted measures to halt its progression.

3. Pathogenesis of NAFLD-HCC

NAFLD can progress to NAFLD-HCC (Figure 2), a multifactorial process primarily driven by genetic susceptibility, metabolic dysregulation, lipotoxicity, oxidative stress, and inflammation (Figure 3). Additionally, factors such as circadian rhythm disruption, gut microbiota dysbiosis, and alcohol or cigarette use may act as cofactors, potentially contributing to disease progression (14).

3.1. Genetic susceptibility

Recent studies increasingly demonstrate that the development of NAFLD and the elevated risk of NAFLD-HCC are linked to genetic polymorphisms in several key genes, including the patatin-like phospholipase domain-containing 3 (PNPLA3), the transmembrane 6 superfamily member 2 (TM6SF2), the membrane bound O-acyltransferase domain-containing 7 (MBOAT7) (14), and the 17- beta hydroxysteroid dehydrogenase 13 (HSD17B13) is a protective heritable factor (15).

PNPLA3: The first genome-wide association study (GWAS) on NAFLD, conducted in 2008, identified the rs738409 C>G variant in the *PNPLA3* gene, resulting in an isoleucine-to-methionine substitution at position 148 (p.I148M) (16). This variant is a key genetic factor linked to hepatic fat accumulation. Numerous recent studies continue to demonstrate that the *PNPLA3* rs738409 C>G variant is strongly associated with NAFLD, hepatic steatosis, and the severity of liver fibrosis in NAFLD, making it the most reliable genetic predictor of inter-individual variability in liver fat content

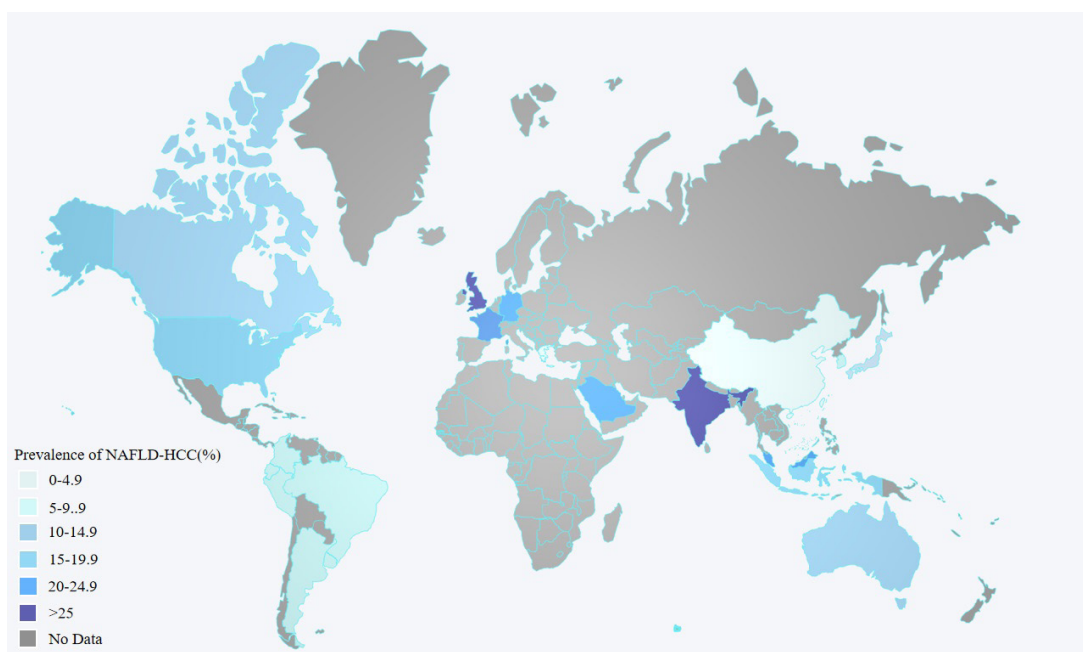


Figure 1. The Prevalence of NAFLD-HCC. The specific data comes from references, but there is still a lack of specific data for many countries (6-13).

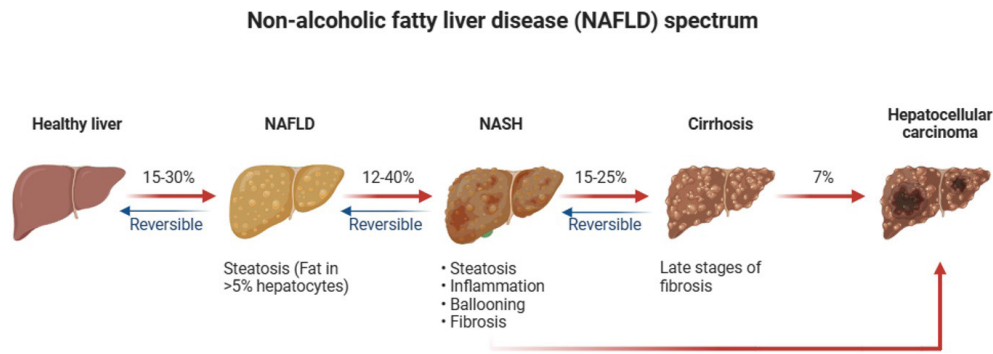


Figure 2. The progression of NAFLD-HCC. Healthy liver, NASH and Cirrhosis of liver can transform each other, but once it progresses to HCC, this progression of the disease is irreversible.

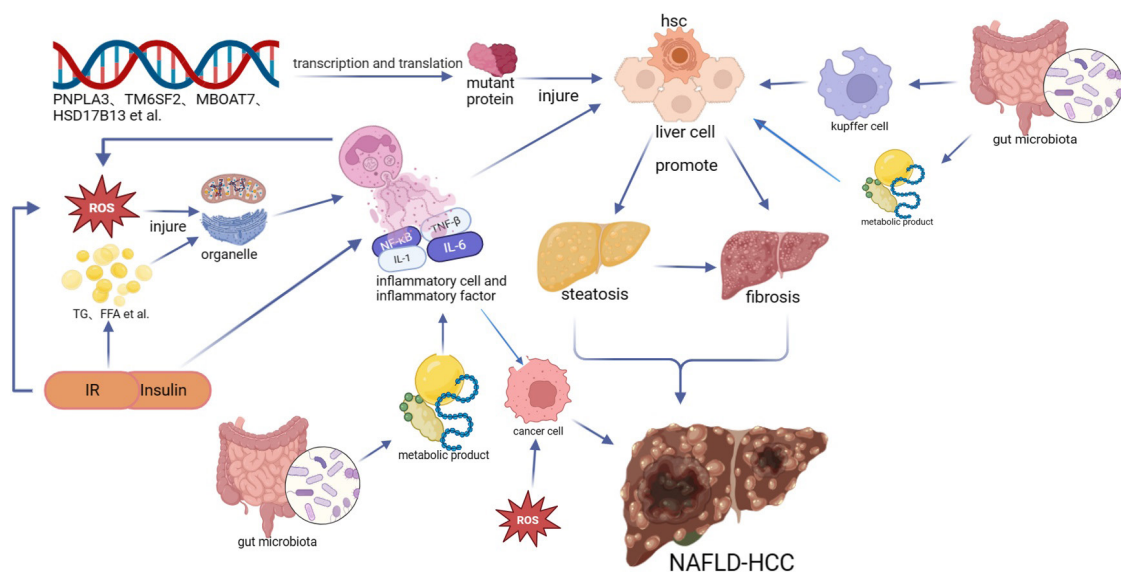


Figure 3. Proposed mechanism of NAFLD-HCC. NAFLD-HCC is mainly associated with genetic susceptibility, metabolic imbalance, lipotoxicity, oxidative stress, and inflammation.

(17). The PNPLA3 rs738409 C>G polymorphism is associated not only with hepatic steatosis, steatohepatitis, and fibrosis but also with the development of NAFLD-HCC (18). The *PNPLA3* gene encodes a 481-amino acid triacylglycerol lipase, which primarily mediates triglyceride hydrolysis in adipocytes. This enzyme is localized to the surface of the endoplasmic reticulum (ER) and lipid droplets (LD) in hepatocytes, adipocytes, and hepatic stellate cells (HSCs) (19). The PNPLA3 mutation impairs triglyceride mobilization and inhibits triglyceride release, leading to hepatic fat accumulation. Excess free fatty acids in hepatocytes disrupt the local liver immune system, triggering hepatic inflammation. Additionally, PNPLA3 mutant proteins may impair retinol release from HSCs, altering liver retinol storage and serum retinol levels, thereby directly promoting hepatic fibrosis and carcinogenesis (20).

TM6SF2: A 2014 exome-wide association study identified the rs58542926 C > T variant in the *TM6SF2* gene, resulting in a glutamate-to-lysine substitution

at position 167 (p.E167K). This variant is associated with increased serum alanine aminotransferase activity, decreased serum alkaline phosphatase activity, and reduced plasma triglyceride and very low-density lipoprotein levels (21). TM6SF2 encodes a protein that plays a crucial role in the regulation of hepatic triglyceride secretion. The E167K variant of the *TM6SF2* gene promotes hepatic lipid accumulation by enhancing hepatic lipid uptake and de novo lipogenesis, while simultaneously reducing β -oxidation and decreasing very low-density lipoprotein secretion (22). Individuals carrying the TM6SF2 rs58542926 C>T polymorphism (E167K) exhibit more pronounced hepatic steatosis, inflammation, and fibrosis. Additionally, multiple studies have confirmed the link between this genetic variant and conditions such as hepatic steatosis, NASH, and liver fibrosis (23), but the role in hepatocarcinogenesis is unknown.

MBOAT7: The MBOAT7 rs641738 C>T variant has been linked to hepatic fat accumulation, severe

liver injury, and hepatic fibrosis across multiple studies. It is also correlated with disease severity in NAFLD and NAFLD-HCC, particularly in patients without advanced liver fibrosis (24). A recent meta-analysis identified the MBOAT7 rs641738 polymorphism as being associated with increased susceptibility to HCC, particularly in Asian populations, where it contributes to hepatocarcinogenesis. The underlying mechanisms, however, warrant further investigation (25).

HSD17B13: A 2018 study identified a splice variant (rs72613567) in the *HSD17B13* gene, which encodes hydroxysteroid 17- β dehydrogenase 13, as not being associated with simple steatosis but significantly reducing the risk of NASH and hepatic fibrosis. The variant was also shown to prevent progression to advanced stages of chronic liver disease (26). This protective role was further validated by a GWAS study, which found that the protective effect of HSD17B13 was more strongly linked to NAFLD development than to the progression of liver fibrosis (27).

As research progresses, many other genes have also been identified as being involved in the development of NAFLD and NAFLD-HCC, including odd-skipped related transcription factor 1, human telomerase reverse transcriptase, programmed cell death protein 1, and ectonucleotide pyrophosphatase/phosphodiesterase 1 (14). Research on these genetic variants is enhancing our understanding of NAFLD pathogenesis and improving our capacity to mitigate the risk of HCC development.

3.2. Metabolic imbalance

Metabolic imbalance is primarily associated with fat accumulation, with insulin resistance (IR) and hyperinsulinemia being the most prevalent metabolic features of NAFLD-HCC. In the context of insulin resistance, visceral adipose tissue (AT) becomes resistant to insulin's anti-lipolytic effects, leading to the breakdown of triglycerides (TG) into free fatty acids (FFA) and glycerol. The liver absorbs FFA and converts it into TG, resulting in hepatic TG accumulation and ultimately hepatic steatosis. Additionally, insulin resistance inhibits the β -oxidation of FFA, further exacerbating lipid accumulation in the liver (28).

In addition to increased FFA production, enhanced FFA uptake by the liver, inhibition of β -oxidation, and elevated intrahepatic lipogenesis, exogenous lipids from dietary intake also contribute to increased intrahepatic TG levels. Studies have demonstrated that long-term high-fat and high-carbohydrate diets elevate intrahepatic TG production, thereby promoting hepatic steatosis and ultimately facilitating the development of NAFLD-HCC (29).

Insulin resistance and hyperinsulinemia have been shown to drive the progression of NAFLD to NAFLD-HCC and contribute to NAFLD-HCC development *via* multiple oncogenic pathways, as evidenced by numerous

animal models and human studies (30). Insulin and insulin-like growth factor (IGF)-1 increase the risk of hepatocellular carcinoma by promoting cell proliferation and inhibiting apoptosis, among other mechanisms. Hyperglycemia supplies energy for cancer cell growth and proliferation, while chronic hyperglycemia drives glycosylation reactions, producing advanced glycation end products (AGEs), activating nuclear factor κ -B (NF- κ B) and inflammatory signaling pathways, promoting reactive oxygen species (ROS) production, and inducing NAFLD-HCC (31). Additionally, IR has been shown to promote hepatic neovascularization by stimulating the formation of new blood vessels in the liver (31). Through the combined influence of these mechanisms, NAFLD can gradually progress, leading to liver fibrosis and the eventual development of NAFLD-HCC.

3.3. Lipotoxicity

Lipotoxicity refers to the accumulation of toxic lipids resulting from the dysregulation of intracellular lipid composition, primarily including cholesterol, FFA and their derivatives, as well as ceramides (32). Lipotoxicity can ultimately result in cellular damage and even cell death by disrupting the function of cellular organelles, such as the endoplasmic reticulum and mitochondria. Additionally, it can dysregulate metabolic and inflammatory pathways by directly altering intracellular signaling mechanisms.

ER is an intracellular organelle responsible for essential functions, including protein folding, lipid synthesis, and calcium storage. Lipotoxicity can lead to ER dysfunction, disrupting the protein folding process. Under ER stress, unfolded or misfolded proteins accumulate, triggering an adaptive mechanism known as the unfolded protein response to restore cellular homeostasis (33,34). If ER stress is not alleviated in a timely manner, apoptotic pathways are activated, leading to cell death.

ER stress is closely associated with the development and progression of NAFLD-HCC, increasing the risk of NASH and NAFLD-HCC independently of insulin resistance. ER stress triggers TNF-dependent steatohepatitis, ultimately promoting NAFLD-HCC by stimulating the release of tumor necrosis factor (TNF) from macrophages (35).

3.4. Oxidative stress

Oxidative stress refers to tissue damage resulting from an imbalance between oxidants and antioxidants in the body (36). Oxidative stress is closely linked to the development and progression of diseases like NAFLD, NASH, and HCC, playing a critical role in promoting liver fibrosis, cirrhosis, and HCC (37). The primary driver of oxidative stress is ROS. Under physiological conditions, partially reduced ROS are detoxified to

water, while the body maintains oxidant levels at a relatively low concentration through antioxidant defense mechanisms and repair enzymes (38). When redox balance is disrupted, excessive ROS production or impaired clearance can damage cellular macromolecules, including proteins, lipids, and nucleic acids, leading to structural dysfunction, carcinogenesis, and even cell death.

ROS accumulation plays a critical role in the development of chronic inflammation, hepatic fibrosis, necroptosis, and liver carcinogenesis (39). ROS accumulation impairs hepatocyte function and induces hepatocyte death by causing mitochondrial dysfunction and altering cell membrane permeability. Additionally, ROS promote the differentiation of HSCs into myofibroblasts, which secrete and accumulate collagen and other extracellular matrix components in the liver. This process is key in the development of liver fibrosis and plays a crucial role in promoting cirrhosis and hepatocellular carcinoma (40). When hepatic macrophages (KCs) are activated by specific stimuli, they can further promote this process by producing factors such as transforming growth factor (TGF- β) and platelet-derived growth factor (41). Liver sinusoidal endothelial cells (LSECs) protect KCs and HSCs from abnormal activation by toxic molecules in the portal vein. However, ROS accumulation leads to LSEC damage, compromising vascular endothelial function and ultimately resulting in portal hypertension (42). In response to oxidative stress, liver cells may develop adaptive survival and proliferation mechanisms, which ultimately promote cancer cell growth and contribute to the progression of NAFLD-HCC.

3.5. Inflammation

Fat accumulation in the liver leads to cellular damage, mitochondrial dysfunction, endoplasmic reticulum stress, oxidative stress, and activation of necrosis. These mechanisms trigger sterile chronic inflammation in the liver, promoting the progression of NASH and facilitating the onset and development of NAFLD-HCC (43). Inflammatory cells in chronic inflammation promote vasculogenesis and lymphangiogenesis by releasing various inflammatory factors, including interleukins (IL-6, IL-1), NF- κ B, TNF, signal transducer and activator of transcription 3, and TGF- β . These factors cause DNA damage, suppress the immune system, evade host defenses, and promote tumorigenesis and progression through various mechanisms (44). Chronic inflammation triggers the release of ROS, cytokines, chemokines, and other mediators, causing DNA damage and promoting tumor proliferation (45). As NAFLD progresses, most patients develop chronic liver inflammation. Through these complex mechanisms, NAFLD advances, leading to DNA damage, the formation of new blood vessels and lymphatic vessels, and the eventual emergence of cancer

cells, ultimately culminating in NAFLD-HCC.

3.6. Gut microorganisms

Under normal conditions, gut microorganisms maintain a stable balance, supporting various physiological processes such as energy intake, immune regulation, nutrient metabolism, and the integrity of the intestinal mucosal barrier. When this balance is disrupted by gut dysbiosis, it can lead to hepatic inflammation, fibrosis, hepatocyte proliferation, and reduced anti-tumor immunity. Mechanisms such as increased intestinal permeability, bacterial overgrowth, translocation, impaired enterohepatic bile acid circulation, and endotoxemia contribute to the development and progression of chronic liver disease and NAFLD-HCC (46). Gut microorganisms play a crucial role in regulating metabolic processes. When gut microbial homeostasis is disrupted, the microbiota can increase hepatic fat accumulation by influencing appetite, enhancing energy extraction from food, and altering the expression of genes involved in fat synthesis and oxidation. This disruption further impairs metabolic homeostasis, contributing to the onset and progression of metabolic disorders.

In cirrhosis, portal hypertension impairs the intestinal mucosal barrier, increasing intestinal permeability and allowing bacteria and bacterial metabolites to enter the liver and bloodstream *via* the portal vein. This leads to elevated endotoxin levels in the blood, which stimulate cytokine production and trigger chronic inflammation in the liver, intestines, and adipose tissue. Inflammatory cells further promote the generation of cancer cells and the progression of NAFLD-HCC by releasing various inflammatory factors and activating multiple pathways.

Disruption of homeostasis between the organism and gut microbiota allows bacterial metabolites, such as lipopolysaccharide from Gram-negative bacteria and lipoteichoic acid from Gram-positive bacteria, to activate immune responses in hepatic macrophages (Kupffer cells) *via* Toll-like receptors and other pattern recognition receptors. This leads to hepatocyte proliferation and hepatic stellate cell activation, ultimately causing hepatic inflammation, liver fibrosis, and the progression of NAFLD-HCC (47).

Beyond gut microbes, metabolites in the gut, bloodstream, and liver tissues play a key role in the progression of NAFLD and NAFLD-HCC. These metabolites include amino acids, short-chain fatty acids, and bile acids, which are strongly associated with these conditions. Bile acids, secreted by the liver and undergoing enterohepatic circulation, are influenced by gut microbiota. In obesity-related microbiota, the conversion of chenodeoxycholic acid to the hepatotoxic deoxycholic acid (DCA) is increased, leading to DCA accumulation in the liver. This accumulation induces oxidative damage to mitochondrial structures and promotes hepatocyte proliferation *via* the hepatic

mTOR pathway, contributing to liver fibrosis and HCC development (48). Bile acids can modulate the farnesoid X receptor (FXR), and FXR activation helps regulate NAFLD progression by reducing triglyceride levels, inhibiting fatty acid synthesis and uptake in the liver, mitigating inflammatory responses, and alleviating liver fibrosis (49).

4. Diagnosis of NAFLD-HCC

Early diagnosis of NAFLD-HCC is crucial for improving treatment outcomes and preventing the severe prognosis commonly associated with this condition. Over the next two decades, the global incidence of HCC is projected to rise by more than 55%, driven by the increasing prevalence of NAFLD (50). Current international guidelines recommend that all cirrhotic patients and hepatitis B patients without cirrhosis undergo abdominal ultrasound, with or without alpha-fetoprotein (AFP) testing, every six months (51). NAFLD-HCC is typically more monofocal, characterized by larger tumor volume, better differentiation, lower AFP levels, higher body weight, less pronounced early clinical presentation, a higher rate of metabolic complications, and lower rates of cirrhosis and ascites compared to HCC from other causes. Notably, 20%-30% of NAFLD-HCC cases occur in patients without cirrhosis (52). Due to the unique characteristics of NAFLD-HCC, current testing faces challenges in improving the early detection rate and enhancing patient survival. Early diagnosis of NAFLD-HCC remains particularly difficult.

Abdominal ultrasonography, a noninvasive and low-cost imaging test with high sensitivity and specificity, is recommended by many guidelines. However, despite its advantages, a meta-analysis highlighted its poor sensitivity for detecting early-stage HCC (53). This limitation is even more pronounced in NAFLD-HCC, as the presence of adiposity in NAFLD patients, leading to higher body weight and increased subcutaneous fat, impairs the ultrasound beam, reducing image quality and liver visualization. This hampers lesion detection. Nevertheless, due to its significant benefits, abdominal ultrasonography remains widely used in clinical practice for NAFLD-HCC screening.

According to current guidelines, lesions ≥ 10 mm or AFP levels > 20 ng/mL detected by ultrasound require further evaluation with more sensitive imaging techniques, such as CT, MRI, or contrast-enhanced ultrasound (54). MRI offers greater sensitivity and specificity than CT, particularly for detecting HCCs smaller than 1 cm. However, its limited availability, lengthy examination times, and high costs restrict its widespread use in clinical practice (55). In 2018, the American College of Radiology and the American Association for the Study of Liver Diseases introduced the Liver Imaging Reporting and Data System (Li-RADS) (56), applicable to both CT and MRI. The diagnosis

of HCC under Li-RADS is based on factors such as contrast perfusion and excretion, non-rim arterial phase enhancement, lesion size, tumor capsule, and growth rate, to improve lesion characterization.

Liver biopsy is an invasive procedure reserved for cases where imaging, such as CT or MRI, yields uncertain results (54), and is less frequently used in clinical practice compared to other diagnostic methods.

The primary serum biomarkers currently used for HCC diagnosis include alpha-fetoprotein (AFP), des-carboxyprothrombin (DCP), and AFP-L3. Numerous additional serum biomarkers for HCC diagnosis are under investigation, such as glypican-3 and adiponectin (57), midkine (58), and apoptosis inhibitor of macrophages (59). Effective monitoring of these serum biomarkers enhances the accuracy of NAFLD-HCC diagnosis, particularly in the absence of imaging.

In conclusion, both imaging techniques and various serum markers play a critical role in diagnosing NAFLD-HCC, particularly when combined to achieve higher sensitivity and specificity. As science and technology advance, additional diagnostic tools, including other serum biomarkers, circulating tumor DNA, genomic glycosylation, and noninvasive saliva biomarkers, show significant potential. However, these methods still require large-scale prospective studies to validate their clinical effectiveness. Moreover, it is crucial to explore more sensitive and specific diagnostic approaches based on the pathogenesis and characteristics of NAFLD-HCC to enable early diagnosis, improve treatment efficacy, and enhance patient prognosis.

5. Treatment of NAFLD-HCC

The pathogenesis of NAFLD-HCC involves multiple pathological processes and remains incompletely understood, contributing to the complexity of its treatment. Managing NAFLD-HCC often requires a multidisciplinary approach, including hepatology, oncology, radiology, and other specialties, to provide combined therapies. Currently, treatment choices for HCC are primarily based on tumor staging, with no significant differences between etiologies (60). However, patients with NAFLD-HCC often present with multiple metabolic comorbidities, such as T2DM and cardiovascular disease, which can influence the selection of treatment modalities and impact long-term survival. Therefore, it is crucial to consider the patient's overall condition and tailor treatment options to ensure individualized care.

5.1. Surgical treatment

Surgery remains the most crucial and effective treatment for early-stage liver cancer, primarily including hepatectomy and liver transplantation.

Hepatic resection is the primary curative treatment

for NAFLD-HCC. Patients with BCLC stage 0 and A, as well as CNLC stage IA, IB, and IIA, are prioritized for resection. Additionally, some patients with initially unresectable tumors may become eligible for surgery following conversion therapy (61). Retrospective studies have shown no significant differences in 5-year overall survival (OS) and recurrence-free survival (RFS) between NAFLD-HCC patients and those with other etiologies of HCC (Table 1).

Liver transplantation offers a viable treatment option for patients with liver cancer, as it can eliminate both the cancer and underlying liver disease, potentially leading to long-term survival. According to current guidelines, liver transplantation should be considered for patients with HCC who are not candidates for hepatectomy but meet the Milan criteria. These criteria include having either one lesion that is ≥ 2 cm and ≤ 5 cm or up to three lesions, each ≥ 1 cm and ≤ 3 cm, with no evidence of vascular invasion or extrahepatic metastasis (54). Many experts argue that the Milan criteria are overly stringent. Recent studies indicate that liver transplantation may be appropriate for certain patients who exceed these criteria or undergo downstaging treatment (67), with some patients achieving improved survival outcomes as a result (68). Results from the U.S. Multicenter HCC Transplant Consortium indicated no significant difference in the 1-, 3-, and 5-year cumulative incidence of recurrence (3.1%, 9.1%, and 11.5% for NAFLD-HCC vs 4.9%, 10.1%, and 12.6% for non-NAFLD-HCC; $p = 0.36$) and recurrence-free survival (87%, 76%, and 67% vs 87%, 75%, and 67%; $p = 0.97$) between patients with

NAFLD-HCC and those with non-NAFLD-HCC (69). However, a comprehensive analysis from the European Transplant Registry revealed a lower overall survival rate in NAFLD-HCC compared to HCC associated with alcoholic liver disease (70). Numerous studies have explored the long-term prognosis following liver transplantation for NAFLD-HCC (Table 2). Generally, NAFLD-HCC does not significantly affect overall survival compared to HCC from other causes after transplantation (71).

5.2. Local treatment

Ablation is a non-surgical treatment modality that utilizes thermal energy to destroy tumor tissue while preserving surrounding healthy liver tissue. It primarily includes radiofrequency ablation (RFA) and microwave ablation (MWA) and is typically applied to patients with BCLC stage 0 or stage A (60). In a study involving 520 HCC patients, including 62 with NAFLD-HCC, RFA was identified as an effective treatment modality. There were no significant differences in the 5-year recurrence rate (74% vs 77%), overall survival rate (59% vs 56%), or recurrence-free survival rate (21% vs 18%) between NAFLD-HCC patients and those with other etiologies. Moreover, RFA proved to be both safe and effective for the NAFLD-HCC population (76). MWA has been increasingly utilized in the treatment of HCC. Although MWA demonstrates improved efficacy and safety, there is a lack of data regarding the prognosis of NAFLD-HCC patients.

Table 1. Five-year overall survival (OS) and Five-year recurrence-free survival (RFS) in patients with NAFLD-HCC after liver resection

Reference	Patients	Five-year OS.	Five-year RFS.
Koh <i>et al.</i> (62)	$N = 996$ HCC patients, 844 with non-NAFLD HCC and 152 with NAFLD-HCC	70.1% vs 60.9%	45.4% vs 40.8%
Jung <i>et al.</i> (63)	$N = 426$ HCC patients, 32 with NAFLD-HCC, 200 with HBV-HCC, and 194 with HBV/NAFLD-HCC (HBV and NAFLD)	63% vs 80%	41% vs 55%
Matsumoto <i>et al.</i> (64)	$N = 784$ HCC patients, 57 with NAFLD-HCC, 727 with virus-related HCC	58.1% vs 52.8%	29.6% vs 21.3%
Yang <i>et al.</i> (65)	$N = 1,483$ HCC patients, 96 with NAFLD-HCC and 1,387 with HBV-HCC	51.4% vs 55.3%	38.8% vs 43.3%
Wakai <i>et al.</i> (66)	$N = 225$ HCC patients, 17 with NAFLD-HCC, 61 with HBV, and 147 with HCV	59% vs 57% vs 63%	66% vs 39% vs 29%

Table 2. Five-year overall survival (OS) and Five-year recurrence rates in patients with NAFLD-HCC after liver transplantation

Reference	Patients	Five-year overall survival.	Five-year recurrence rates.
Rajendran <i>et al.</i> (72)	$N = 20,672$ HCC patients, 2,071 with NASH-HCC, 18,601 with non-NASH HCC	76.3%	n/a
Lamm <i>et al.</i> (73)	$N = 7,461$ HCC patients, 1,405 with NASH-HCC, 6,086 with non-NASH HCC	80.71%	5.8%
Holzner <i>et al.</i> (74)	$N = 635$ HCC patients, 51 with NASH-HCC, 584 with non-NASH HCC	80%	14%
Sadler <i>et al.</i> (75)	$N = 929$ HCC patients, 60 with NASH-HCC, 869 with non-NASH HCC	80%	13.3%

Transarterial chemoembolization (TACE) is an interventional treatment that involves injecting chemotherapeutic agents directly into a branch of the hepatic artery supplying the tumor and subsequently embolizing that branch, leading to ischemic necrosis of the tumor tissue. Current guidelines recommend TACE as the treatment of choice for patients with BCLC stage B (51) and indicate its use in patients with CNLC stage IIB, IIIA, and select IIIB HCC (77). While TACE has been extensively studied for HCC treatment, its efficacy and safety in NAFLD-HCC remain less explored. Shamar Young *et al.* conducted TACE on 220 patients, including 30 with NAFLD-HCC, and found that the median OS and treatment-related complications in NAFLD-HCC patients were comparable to those in patients with HCC from other etiologies (78). Transarterial radioembolization (TARE) is another intraarterial therapy utilized in Western countries, but its use has not yet become widespread in China. Transarterial radioembolization (TARE) is another intraarterial therapy utilized in Western countries, but its use has not yet become widespread in China. A retrospective study involving 138 HCC patients treated with TARE, including 30 with NAFLD-HCC, found no significant differences in overall survival and local progression-free survival between NAFLD-HCC and non-NAFLD-HCC patients (79).

5.3. Adjuvant therapy

Patients with early-stage NAFLD-HCC can achieve long-term survival following treatments such as hepatectomy or ablation; In one study, the 5-year recurrence rate for NAFLD-HCC patients was approximately 69.6%. Other studies reported a recurrence rate of 44.6% for NAFLD-HCC patients (80). However, overall, the recurrence rate remains relatively high. Previous attempts at adjuvant therapy using tyrosine kinase inhibitors yielded unsatisfactory results, failing to significantly enhance recurrence-free survival and overall survival (81). However, advancements in systemic therapies and the introduction of immune checkpoint inhibitors (ICIs) are gradually improving the efficacy and safety of adjuvant treatments. The IMbrave050 trial was the first randomized controlled trial to demonstrate positive results, indicating that atilizumab combined with bevacizumab significantly improved recurrence-free survival in patients at high risk of recurrence following hepatectomy or local ablation (82). Several ongoing phase III randomized controlled trials are currently underway, notably Keynote-937 (Pembrolizumab), Checkmate-9DX (Nivolumab), EMERALD-2 (Durvalumab +/- bevacizumab), and JUPITER-04 (Toripalimab), among others (81). Subsequent studies are anticipated to yield valuable data for the adjuvant treatment of NAFLD-HCC.

5.4. Neoadjuvant therapy

The high recurrence rate of early-stage NAFLD-HCC post-treatment adversely impacts patient prognosis. Adopting neoadjuvant therapy may reduce tumor size, enhance surgical resection rates, eliminate potential micrometastases, and ultimately lower the recurrence rate (83). The incorporation of ICIs into neoadjuvant therapy has demonstrated enhanced therapeutic efficacy and safety, a conclusion supported by several trials. A key challenge in neoadjuvant therapy is determining the optimal treatment duration. If the duration is too long, patients may experience lesion progression, immune-related adverse events, and drug toxicity accumulation. Conversely, if the duration is too short, the effectiveness of neoadjuvant therapy may be significantly diminished. Therefore, further studies are needed to establish the optimal treatment duration and identify biomarkers to guide therapeutic decisions (81,84). Likewise, neoadjuvant treatment strategies for NAFLD-HCC require further exploration.

5.5. Systemic therapy

Patients with advanced (BCLC stage C) HCC, those ineligible for localized therapy, and early-stage HCC patients who have relapsed or progressed after previous treatments are eligible for systemic therapy (85). Due to the limited data on the use of systemic therapy for NAFLD-HCC, treatment approaches in these patients resemble those used for HCC associated with other etiologies. Sorafenib, a multikinase inhibitor and the first systemic treatment for HCC, was found to be more effective in patients with HCV-associated HCC, according to data from the SHARP phase III trial (86). Additionally, recent research indicated that patients with NAFLD-HCC had larger tumors and were at a more advanced stage compared to those with other etiology-associated HCC; however, the efficacy of sorafenib was similar in both groups (87).

Patients with NAFLD-HCC frequently present with comorbidities such as obesity and T2DM, often resulting in treatment with oral metformin. One study found that HCC patients undergoing long-term metformin treatment experienced worse progression-free survival and overall survival when receiving systemic therapy with sorafenib, compared to HCC patients without T2DM. In contrast, NAFLD-HCC patients treated with insulin demonstrated better responses and longer survival with sorafenib therapy. These results may be attributed to the aggressive nature of tumors induced by long-term metformin treatment and the increased resistance to sorafenib (88). However, in patients with NAFLD, metformin reduces body fat accumulation and decreases the risk of progression from NAFLD to HCC.

Recent advances in immunotherapy for HCC have led to the development of more available drugs

for treating advanced NAFLD-HCC, demonstrating improved safety and efficacy. The effectiveness and potential of ICIs in this context have been validated by several clinical trials. Single-agent anti-PD-1/anti-PD-L1 inhibitors show limited efficacy in treating NAFLD-HCC, whereas combination therapies can simultaneously target multiple immune checkpoints, making them the most extensively studied treatment option. The IMbrave150 trial demonstrated that atilizumab in combination with bevacizumab significantly improved overall and progression-free survival compared to sorafenib in patients with advanced NAFLD-HCC who had not received prior systemic therapy; however, 38% of patients experienced severe toxicity (89). The phase III HIMALAYA trial demonstrated that the combination therapy of Durvalumab and Tremelimumab resulted in improved overall survival (90,91). Both of these regimens have been approved by the FDA as first-line treatment options for patients with advanced HCC. However, the CheckMate 459 phase III randomized clinical trial found that first-line nabulizumab treatment demonstrated better efficacy and safety compared to sorafenib, although it did not significantly improve overall survival in HCC patients (92). While it has been demonstrated that the efficacy of immunotherapy diminishes in obese and NAFLD-HCC populations (93,94), current research does not allow for the differentiation of therapeutic effects of immunotherapeutic agents across various HCC etiologies.

Current studies suggest that immunotherapy and local therapies (*e.g.*, TACE, ablation, radiation therapy) may exhibit synergistic effects. In a study by Duffy *et al.*, the combination of Tremelimumab and local therapy demonstrated both the feasibility and safety of this approach, as well as improved clinical therapeutic outcomes (95). In a study by Zhu *et al.*, the combination of PD-1 inhibitors with TACE demonstrated improved downstaging rates, acceptable survival, and tolerability in patients with intermediate-stage HCC (96). Currently, numerous studies are investigating the combination of ICIs with local therapies. This approach is expected to yield more favorable results in the future, and as our understanding of its pathogenesis deepens, treatment options for NAFLD-HCC may become increasingly specialized. However, there is currently a lack of appropriate clinical studies and data on this combination therapy, necessitating further large-scale research in the future.

Overall, the intricate nature of treating NAFLD-HCC demands a comprehensive, multidisciplinary strategy. Surgical resection continues to be the cornerstone of treatment for early-stage NAFLD-HCC patients. Minimally invasive ablation methods, including RFA and MWA, alongside locoregional therapies such as TACE and TARE, provide viable alternatives for patients ineligible for surgery. Nevertheless, given the elevated recurrence rates of NAFLD-HCC, the investigation of

adjuvant therapies, particularly immune checkpoint inhibitors, has emerged as a critical research priority. In light of the current paucity of data regarding NAFLD-HCC-specific populations, future research must focus on expanding this knowledge base and refining treatment strategies to deliver more tailored, long-term management plans for affected patients.

6. Prevention of NAFLD-HCC

The development of NAFLD-HCC is primarily linked to metabolic imbalance and fat accumulation. Effective prevention strategies include weight loss and management of related metabolic comorbidities, with lifestyle modifications being the simplest and most feasible approach. According to the practice guidelines from European Association for the Study of the liver, European Association for the Study of Diabetes, and European Association for the Study of Obesity, non-pharmacological treatments — such as adopting a low-calorie, low-fat diet, engaging in moderate physical activity, and achieving weight loss — can reduce liver injury, decrease steatosis, and improve hepatic inflammation and fibrosis (97). The safety and therapeutic efficacy of medications like statins, glucagon-like peptide-1 receptor agonists, vitamin E, metformin, and PPAR agonists for managing obesity and T2DM have been supported by various studies (98). Therefore, improving metabolic imbalance, reducing body weight, and managing other related comorbidities through these medications are also viable strategies. This pharmacological therapy can help reduce hepatic steatosis, prevent the progression of NAFLD to NAFLD-HCC, and ultimately decrease the incidence of NAFLD-HCC in high-risk populations.

7. Future perspectives

In recent years, as the incidence of HBV and HCV infections has declined, the morbidity and mortality associated with virus-related HCC have also decreased. However, improvements in living standards and the rising prevalence of metabolic diseases such as diabetes mellitus and obesity have contributed to a rapid increase in NAFLD-HCC cases. Several challenges arise in the context of NAFLD-HCC, particularly in prevention efforts aimed at reducing obesity and T2DM prevalence, thereby decreasing NAFLD incidence and preventing its progression to NASH or NAFLD-HCC. Achieving this requires a deeper exploration of the pathogenesis of NAFLD-HCC to uncover its complexities and attain a comprehensive understanding of the condition.

The second challenge involves monitoring high-risk groups for NAFLD-HCC. Early-stage HCC patients tend to have a better prognosis following radical treatment, making early detection of NAFLD-HCC crucial. Achieving this objective requires the development of

more sensitive and specific biomarkers and imaging tests tailored to the pathogenesis and characteristics of NAFLD-HCC, which should be integrated into routine medical examinations to optimize surveillance strategies for NAFLD patients and those at high risk for NAFLD-HCC.

Finally, the treatment of NAFLD-HCC should focus on enhancing the efficacy of treatment modalities while minimizing complications and ensuring safety. While all current treatment options have room for improvement, management should be individualized based on the pathogenesis and characteristics of NAFLD-HCC. Systemic therapy is the recommended approach for unresectable HCC, and further investigation into the development, safety, and therapeutic efficacy of systemic therapies for NAFLD-HCC is necessary. Due to the low representation of NAFLD-HCC patients in completed studies, data on the efficacy and safety of treatment modalities are limited. Therefore, future studies should aim to include a larger proportion of this population to achieve more objective results.

In conclusion, NAFLD-HCC represents a significant challenge; however, our ongoing exploration of its pathogenesis and increasing understanding lead us to believe that future advancements in research will gradually address the issues related to the monitoring and treatment of NAFLD-HCC.

8. Conclusions

In summary, the rising prevalence of NAFLD-HCC presents a significant challenge in the context of improving patient outcomes. The interplay between metabolic imbalances, lifestyle factors, and genetic susceptibility underscores the complexity of NAFLD-HCC pathogenesis. As the understanding of these mechanisms deepens, it becomes increasingly clear that targeted prevention strategies, including lifestyle modifications and early detection methods, are essential in managing high-risk populations.

Moreover, while advancements in immunotherapy and systemic treatments offer new avenues for intervention, the integration of these therapies into clinical practice must be approached with caution. Personalized treatment plans that account for individual metabolic profiles and comorbidities, such as obesity and type 2 diabetes, are critical in optimizing therapeutic outcomes.

Furthermore, the development of sensitive biomarkers and imaging techniques will enhance the monitoring and early detection of NAFLD-HCC, potentially improving prognosis. Despite the current lack of extensive clinical data on effective treatments specifically for NAFLD-HCC, ongoing research and clinical trials are necessary to fill this knowledge gap and refine treatment strategies.

Collectively, addressing the multifaceted challenges of NAFLD-HCC through a comprehensive approach

that includes prevention, early detection, individualized treatment, and continued research will be vital in reducing the global burden of this disease and improving patient survival rates.

Funding: This work was supported by a grant from Chongqing Young and Middle aged Medical High-end Talent Project (No. YXGD202443) and Joint project of Chongqing Health Commission and Science and Technology Bureau (No.2023MSXM104).

Conflict of Interest: The authors have no conflicts of interest to disclose.

References

1. McGlynn KA, Petrick JL, El-Serag HB. Epidemiology of Hepatocellular Carcinoma. *Hepatology*. 2021; 73 Suppl 1:4-13.
2. Huang C, Zhou Y, Cheng J, Guo X, Shou D, Quan Y, Chen H, Chen H, Zhou Y. Pattern recognition receptors in the development of nonalcoholic fatty liver disease and progression to hepatocellular carcinoma: An emerging therapeutic strategy. *Front Endocrinol (Lausanne)*. 2023; 14:1145392.
3. Bray F, Laversanne M, Sung H, Ferlay J, Siegel RL, Soerjomataram I, Jemal A. Global cancer statistics 2022: GLOBOCAN estimates of incidence and mortality worldwide for 36 cancers in 185 countries. *CA Cancer J Clin*. 2024; 74:229-263.
4. Akinjemiju T, Abera S, Ahmed M, *et al*. The Burden of Primary Liver Cancer and Underlying Etiologies From 1990 to 2015 at the Global, Regional, and National Level: Results From the Global Burden of Disease Study 2015. *JAMA Oncol*. 2017; 3:1683-1691.
5. Kim DY. Changing etiology and epidemiology of hepatocellular carcinoma: Asia and worldwide. *J Liver Cancer*. 2024; 24:62-70.
6. Huang DQ, El-Serag HB, Loomba R. Global epidemiology of NAFLD-related HCC: trends, predictions, risk factors and prevention. *Nat Rev Gastroenterol Hepatol*. 2021; 18:223-238.
7. Younossi Z, Stepanova M, Ong JP, *et al*. Nonalcoholic Steatohepatitis Is the Fastest Growing Cause of Hepatocellular Carcinoma in Liver Transplant Candidates. *Clin Gastroenterol Hepatol*. 2019; 17:748-755.e743.
8. Debes JD, Chan AJ, Balderramo D, *et al*. Hepatocellular carcinoma in South America: Evaluation of risk factors, demographics and therapy. *Liver Int*. 2018; 38:136-143.
9. Dyson J, Jaques B, Chattopadhyay D, *et al*. Hepatocellular cancer: the impact of obesity, type 2 diabetes and a multidisciplinary team. *J Hepatol*. 2014; 60:110-117.
10. Pais R, Fartoux L, Goumar C, Scatton O, Wendum D, Rosmorduc O, Ratzu V. Temporal trends, clinical patterns and outcomes of NAFLD-related HCC in patients undergoing liver resection over a 20-year period. *Aliment Pharmacol Ther*. 2017; 46:856-863.
11. Ganslmayer M, Hagel A, Dauth W, Zopf S, Strobel D, Müller V, Uder M, Neurath MF, Siebler J. A large cohort of patients with hepatocellular carcinoma in a single European centre: aetiology and prognosis now and in a historical cohort. *Swiss Med Wkly*. 2014; 144:w13900.

12. Yang JD, Mohamed EA, Aziz AO, *et al.* Characteristics, management, and outcomes of patients with hepatocellular carcinoma in Africa: a multicountry observational study from the Africa Liver Cancer Consortium. *Lancet Gastroenterol Hepatol.* 2017; 2:103-111.
13. Park JW, Chen M, Colombo M, Roberts LR, Schwartz M, Chen PJ, Kudo M, Johnson P, Wagner S, Orsini LS, Sherman M. Global patterns of hepatocellular carcinoma management from diagnosis to death: the BRIDGE Study. *Liver Int.* 2015; 35:2155-2166.
14. Tovo CV, de Mattos AZ, Coral GP, Sartori GDP, Nogueira LV, Both GT, Villela-Nogueira CA, de Mattos AA. Hepatocellular carcinoma in non-alcoholic steatohepatitis without cirrhosis. *World J Gastroenterol.* 2023; 29:343-356.
15. Trépo E, Valenti L. Update on NAFLD genetics: From new variants to the clinic. *J Hepatol.* 2020; 72:1196-1209.
16. Romeo S, Kozlitina J, Xing C, Pertsemlidis A, Cox D, Pennacchio LA, Boerwinkle E, Cohen JC, Hobbs HH. Genetic variation in PNPLA3 confers susceptibility to nonalcoholic fatty liver disease. *Nat Genet.* 2008; 40:1461-1465.
17. Elmansoury N, Megahed AA, Kamal A, El-Nikhely N, Labane M, Abdelmageed M, Daly AK, Wahid A. Relevance of PNPLA3, TM6SF2, HSD17B13, and GCKR Variants to MASLD Severity in an Egyptian Population. *Genes (Basel).* 2024; 15.
18. Liu YL, Patman GL, Leathart JB, Piguat AC, Burt AD, Dufour JF, Day CP, Daly AK, Reeves HL, Anstee QM. Carriage of the PNPLA3 rs738409 C >G polymorphism confers an increased risk of non-alcoholic fatty liver disease associated hepatocellular carcinoma. *J Hepatol.* 2014; 61:75-81.
19. Takahashi Y, Dungubat E, Kusano H, Fukusato T. Pathology and Pathogenesis of Metabolic Dysfunction-Associated Steatotic Liver Disease-Associated Hepatic Tumors. *Biomedicines.* 2023; 11.
20. Liou CJ, Wu SJ, Shen SC, Chen LC, Chen YL, Huang WC. Phloretin ameliorates hepatic steatosis through regulation of lipogenesis and Sirt1/AMPK signaling in obese mice. *Cell Biosci.* 2020; 10:114.
21. Kozlitina J, Smagris E, Stender S, Nordestgaard BG, Zhou HH, Tybjaerg-Hansen A, Vogt TF, Hobbs HH, Cohen JC. Exome-wide association study identifies a TM6SF2 variant that confers susceptibility to nonalcoholic fatty liver disease. *Nat Genet.* 2014; 46:352-356.
22. Borén J, Adiels M, Björnson E, *et al.* Effects of TM6SF2 E167K on hepatic lipid and very low-density lipoprotein metabolism in humans. *JCI Insight.* 2020; 5.
23. Sookoian S, Castaño GO, Scian R, Mallardi P, Fernández Gianotti T, Burgueño AL, San Martino J, Pirola CJ. Genetic variation in transmembrane 6 superfamily member 2 and the risk of nonalcoholic fatty liver disease and histological disease severity. *Hepatology.* 2015; 61:515-525.
24. Sookoian S, Flichman D, Garaycoechea ME, Gazzi C, Martino JS, Castaño GO, Pirola CJ. Lack of evidence supporting a role of TMC4-rs641738 missense variant-MBOAT7- intergenic downstream variant-in the Susceptibility to Nonalcoholic Fatty Liver Disease. *Sci Rep.* 2018; 8:5097.
25. Lai M, Qin YL, Jin QY, Chen WJ, Hu J. Association of MBOAT7 rs641738 polymorphism with hepatocellular carcinoma susceptibility: A systematic review and meta-analysis. *World J Gastrointest Oncol.* 2023; 15:2225-2236.
26. Abul-Husn NS, Cheng X, Li AH, *et al.* A Protein-Truncating HSD17B13 Variant and Protection from Chronic Liver Disease. *N Engl J Med.* 2018; 378:1096-1106.
27. Anstee QM, Darlay R, Cockell S, *et al.* Genome-wide association study of non-alcoholic fatty liver and steatohepatitis in a histologically characterised cohort(☆). *J Hepatol.* 2020; 73:505-515.
28. Shao G, Liu Y, Lu L, Zhang G, Zhou W, Wu T, Wang L, Xu H, Ji G. The Pathogenesis of HCC Driven by NASH and the Preventive and Therapeutic Effects of Natural Products. *Front Pharmacol.* 2022; 13:944088.
29. Luukkonen PK, Sädevirta S, Zhou Y, *et al.* Saturated Fat Is More Metabolically Harmful for the Human Liver Than Unsaturated Fat or Simple Sugars. *Diabetes Care.* 2018; 41:1732-1739.
30. Chettouh H, Lequoy M, Fartoux L, Vigouroux C, Desbois-Mouthon C. Hyperinsulinaemia and insulin signalling in the pathogenesis and the clinical course of hepatocellular carcinoma. *Liver Int.* 2015; 35:2203-2217.
31. Ghazanfar H, Javed N, Qasim A, Zacharia GS, Ghazanfar A, Jyala A, Shehi E, Patel H. Metabolic Dysfunction-Associated Steatohepatitis and Progression to Hepatocellular Carcinoma: A Literature Review. *Cancers (Basel).* 2024; 16.
32. Neuschwander-Tetri BA. Hepatic lipotoxicity and the pathogenesis of nonalcoholic steatohepatitis: the central role of nontriglyceride fatty acid metabolites. *Hepatology.* 2010; 52:774-788.
33. Ron D, Walter P. Signal integration in the endoplasmic reticulum unfolded protein response. *Nat Rev Mol Cell Biol.* 2007; 8:519-529.
34. Hetz C. The unfolded protein response: controlling cell fate decisions under ER stress and beyond. *Nat Rev Mol Cell Biol.* 2012; 13:89-102.
35. Nakagawa H, Umemura A, Taniguchi K, Font-Burgada J, Dhar D, Ogata H, Zhong Z, Valasek MA, Seki E, Hidalgo J, Koike K, Kaufman RJ, Karin M. ER stress cooperates with hypernutrition to trigger TNF-dependent spontaneous HCC development. *Cancer Cell.* 2014; 26:331-343.
36. Sies H. Oxidative stress: oxidants and antioxidants. *Exp Physiol.* 1997; 82:291-295.
37. Allameh A, Niayesh-Mehr R, Aliarab A, Sebastiani G, Pantopoulos K. Oxidative Stress in Liver Pathophysiology and Disease. *Antioxidants (Basel).* 2023; 12.
38. Brand MD. The sites and topology of mitochondrial superoxide production. *Exp Gerontol.* 2010; 45:466-472.
39. Li S, Tan HY, Wang N, Zhang ZJ, Lao L, Wong CW, Feng Y. The Role of Oxidative Stress and Antioxidants in Liver Diseases. *Int J Mol Sci.* 2015; 16:26087-26124.
40. Gandhi CR. Oxidative Stress and Hepatic Stellate Cells: A PARADOXICAL RELATIONSHIP. *Trends Cell Mol Biol.* 2012; 7:1-10.
41. Kolios G, Valatas V, Kouroumalis E. Role of Kupffer cells in the pathogenesis of liver disease. *World J Gastroenterol.* 2006; 12:7413-7420.
42. Ruat M, Chavarria L, Campreciós G, Suárez-Herrera N, Montironi C, Guixé-Muntet S, Bosch J, Friedman SL, Garcia-Pagán JC, Hernández-Gea V. Impaired endothelial autophagy promotes liver fibrosis by aggravating the oxidative stress response during acute liver injury. *J Hepatol.* 2019; 70:458-469.
43. Rodríguez-Lara A, Rueda-Robles A, Sáez-Lara MJ, Plaza-Diaz J, Álvarez-Mercado AI. From Non-Alcoholic Fatty Liver Disease to Liver Cancer: Microbiota and

- Inflammation as Key Players. *Pathogens*. 2023; 12.
44. Coussens LM, Werb Z. Inflammation and cancer. *Nature*. 2002; 420:860-867.
 45. Grivennikov SI, Greten FR, Karin M. Immunity, inflammation, and cancer. *Cell*. 2010; 140:883-899.
 46. Long C, Zhou X, Xia F, Zhou B. Intestinal Barrier Dysfunction and Gut Microbiota in Non-Alcoholic Fatty Liver Disease: Assessment, Mechanisms, and Therapeutic Considerations. *Biology (Basel)*. 2024; 13.
 47. Schwabe RF, Greten TF. Gut microbiome in HCC - Mechanisms, diagnosis and therapy. *J Hepatol*. 2020; 72:230-238.
 48. Zheng Y, Wang T, Tu X, Huang Y, Zhang H, Tan D, Jiang W, Cai S, Zhao P, Song R, Li P, Qin N, Fang W. Gut microbiome affects the response to anti-PD-1 immunotherapy in patients with hepatocellular carcinoma. *J Immunother Cancer*. 2019; 7:193.
 49. Younossi ZM, Ratziu V, Loomba R, *et al*. Obeticholic acid for the treatment of non-alcoholic steatohepatitis: interim analysis from a multicentre, randomised, placebo-controlled phase 3 trial. *Lancet*. 2019; 394:2184-2196.
 50. Runggay H, Arnold M, Ferlay J, Lesi O, Cabaasag CJ, Vignat J, Laversanne M, McGlynn KA, Soerjomataram I. Global burden of primary liver cancer in 2020 and predictions to 2040. *J Hepatol*. 2022; 77:1598-1606.
 51. EASL Clinical Practice Guidelines: Management of hepatocellular carcinoma. *J Hepatol*. 2018; 69:182-236.
 52. Nguyen N, Rode A, Trillaud H, *et al*. Percutaneous radiofrequency ablation for hepatocellular carcinoma developed on non-alcoholic fatty liver disease. *Liver Int*. 2022; 42:905-917.
 53. Tzartzeva K, Obi J, Rich NE, Parikh ND, Marrero JA, Yopp A, Waljee AK, Singal AG. Surveillance Imaging and Alpha Fetoprotein for Early Detection of Hepatocellular Carcinoma in Patients With Cirrhosis: A Meta-analysis. *Gastroenterology*. 2018; 154:1706-1718.e1701.
 54. Heimbach JK, Kulik LM, Finn RS, Sirlin CB, Abecassis MM, Roberts LR, Zhu AX, Murad MH, Marrero JA. AASLD guidelines for the treatment of hepatocellular carcinoma. *Hepatology*. 2018; 67:358-380.
 55. Roberts LR, Sirlin CB, Zaiem F, Almasri J, Prokop LJ, Heimbach JK, Murad MH, Mohammed K. Imaging for the diagnosis of hepatocellular carcinoma: A systematic review and meta-analysis. *Hepatology*. 2018; 67:401-421.
 56. Marrero JA, Kulik LM, Sirlin CB, Zhu AX, Finn RS, Abecassis MM, Roberts LR, Heimbach JK. Diagnosis, Staging, and Management of Hepatocellular Carcinoma: 2018 Practice Guidance by the American Association for the Study of Liver Diseases. *Hepatology*. 2018; 68:723-750.
 57. Caviglia GP, Armandi A, Rosso C, Gaia S, Aneli S, Rolle E, Abate ML, Olivero A, Nicolosi A, Guariglia M, Ribaldone DG, Carucci P, Saracco GM, Bugianesi E. Biomarkers of Oncogenesis, Adipose Tissue Dysfunction and Systemic Inflammation for the Detection of Hepatocellular Carcinoma in Patients with Nonalcoholic Fatty Liver Disease. *Cancers (Basel)*. 2021; 13.
 58. Vongsuvan R, van der Poorten D, Iseli T, Strasser SI, McCaughan GW, George J. Midkine Increases Diagnostic Yield in AFP Negative and NASH-Related Hepatocellular Carcinoma. *PLoS One*. 2016; 11:e0155800.
 59. Shimizu T, Sawada T, Asai T, Kanetsuki Y, Hirota J, Moriguchi M, Nakajima T, Miyazaki T, Okanoue T. Hepatocellular carcinoma diagnosis using a novel electrochemiluminescence immunoassay targeting serum IgM-free AIM. *Clin J Gastroenterol*. 2022; 15:41-51.
 60. Reig M, Forner A, Rimola J, *et al*. BCLC strategy for prognosis prediction and treatment recommendation: The 2022 update. *J Hepatol*. 2022; 76:681-693.
 61. Karachaliou GS, Dimitrokallis N, Moris DP. Downstaging strategies for unresectable hepatocellular carcinoma. *World J Gastroenterol*. 2024; 30:2731-2733.
 62. Koh YX, Tan HJ, Liew YX, Syn N, Teo JY, Lee SY, Goh BKP, Goh GBB, Chan CY. Liver Resection for Nonalcoholic Fatty Liver Disease-Associated Hepatocellular Carcinoma. *J Am Coll Surg*. 2019; 229:467-478.e461.
 63. Jung YB, Yoo JE, Han DH, Kim KS, Choi JS, Kim DY, Park YN, Choi GH. Clinical and survival outcomes after hepatectomy in patients with non-alcoholic fatty liver and hepatitis B-related hepatocellular carcinoma. *HPB (Oxford)*. 2021; 23:1113-1122.
 64. Matsumoto T, Shiraki T, Tanaka G, Yamaguchi T, Park KH, Mori S, Iso Y, Ishizuka M, Kubota K, Aoki T. Comparative analysis of perioperative and long-term outcomes of patients with hepatocellular carcinoma: Nonalcoholic fatty liver disease versus viral hepatitis. *World J Surg*. 2024; 48:1219-1230.
 65. Yang T, Hu LY, Li ZL, *et al*. Liver Resection for Hepatocellular Carcinoma in Non-alcoholic Fatty Liver Disease: a Multicenter Propensity Matching Analysis with HBV-HCC. *J Gastrointest Surg*. 2020; 24:320-329.
 66. Wakai T, Shirai Y, Sakata J, Korita PV, Ajioka Y, Hatakeyama K. Surgical outcomes for hepatocellular carcinoma in nonalcoholic fatty liver disease. *J Gastrointest Surg*. 2011; 15:1450-1458.
 67. Lee S, Kim KW, Song GW, Kwon JH, Hwang S, Kim KH, Ahn CS, Moon DB, Park GC, Lee SG. The Real Impact of Bridging or Downstaging on Survival Outcomes after Liver Transplantation for Hepatocellular Carcinoma. *Liver Cancer*. 2020; 9:721-733.
 68. Lingiah VA, Niazi M, Olivo R, Paterno F, Guarrera JV, Pysopoulos NT. Liver Transplantation Beyond Milan Criteria. *J Clin Transl Hepatol*. 2020; 8:69-75.
 69. Verna EC, Phipps MM, Halazun KJ, *et al*. Outcomes in liver transplant recipients with nonalcoholic fatty liver disease-related HCC: results from the US multicenter HCC transplant consortium. *Liver Transpl*. 2023; 29:34-47.
 70. Haldar D, Kern B, Hodson J, *et al*. Outcomes of liver transplantation for non-alcoholic steatohepatitis: A European Liver Transplant Registry study. *J Hepatol*. 2019; 71:313-322.
 71. Cadar R, Lupascu Ursulescu C, Vasilescu AM, Trofin AM, Zabara M, Rusu-Andriesi D, Ciuntu B, Muzica C, Lupascu CD. Challenges and Solutions in the Management of Hepatocellular Carcinoma Associated with Non-Alcoholic Fatty Liver Disease. *Life (Basel)*. 2023; 13.
 72. Rajendran L, Murillo Perez CF, Ivanics T, Claassen M, Hansen BE, Wallace D, Yoon PD, Sapisochin G. Outcomes of liver transplantation in non-alcoholic steatohepatitis (NASH) versus non-NASH associated hepatocellular carcinoma. *HPB (Oxford)*. 2023; 25:556-567.
 73. Lamm R, Altshuler PJ, Patel K, Shaheen O, Amante AP, Civan J, Maley W, Frank A, Ramirez C, Glorioso J, Shah A, Dang H, Bodzin AS. Reduced Rates of Post-Transplant Recurrent Hepatocellular Carcinoma in Non-Alcoholic Steatohepatitis: A Propensity Score Matched Analysis.

- Transpl Int. 2022; 35:10175.
74. Holzner ML, Florman S, Schwartz ME, Tabrizian P. Outcomes of liver transplantation for nonalcoholic steatohepatitis-associated hepatocellular carcinoma. *HPB (Oxford)*. 2022; 24:470-477.
 75. Sadler EM, Mehta N, Bhat M, Ghanekar A, Greig PD, Grant DR, Yao F, Sapisochin G. Liver Transplantation for NASH-Related Hepatocellular Carcinoma Versus Non-NASH Etiologies of Hepatocellular Carcinoma. *Transplantation*. 2018; 102:640-647.
 76. Wong CR, Njei B, Nguyen MH, Nguyen A, Lim JK. Survival after treatment with curative intent for hepatocellular carcinoma among patients with vs without non-alcoholic fatty liver disease. *Aliment Pharmacol Ther*. 2017; 46:1061-1069.
 77. Xie DY, Zhu K, Ren ZG, Zhou J, Fan J, Gao Q. A review of 2022 Chinese clinical guidelines on the management of hepatocellular carcinoma: updates and insights. *Hepatobiliary Surg Nutr*. 2023; 12:216-228.
 78. Young S, Sanghvi T, Rubin N, Hall D, Roller L, Charaf Y, Golzarian J. Transarterial Chemoembolization of Hepatocellular Carcinoma: Propensity Score Matching Study Comparing Survival and Complications in Patients with Nonalcoholic Steatohepatitis Versus Other Causes Cirrhosis. *Cardiovasc Intervent Radiol*. 2020; 43:65-75.
 79. Brunson C, Struycken L, Schaub D, Ref J, Goldberg D, Hannallah J, Woodhead G, Young S. Comparative outcomes of trans-arterial radioembolization in patients with non-alcoholic steatohepatitis/non-alcoholic fatty liver disease-induced HCC: a retrospective analysis. *Abdom Radiol (NY)*. 2024; 49:2714-2725.
 80. Foerster F, Gairing SJ, Müller L, Galle PR. NAFLD-driven HCC: Safety and efficacy of current and emerging treatment options. *J Hepatol*. 2022; 76:446-457.
 81. Singal AG, Yarchoan M, Yopp A, Sapisochin G, Pinato DJ, Pillai A. Neoadjuvant and adjuvant systemic therapy in HCC: Current status and the future. *Hepatol Commun*. 2024; 8.
 82. Qin S, Chen M, Cheng AL, *et al*. Atezolizumab plus bevacizumab versus active surveillance in patients with resected or ablated high-risk hepatocellular carcinoma (IMbrave050): a randomised, open-label, multicentre, phase 3 trial. *Lancet*. 2023; 402:1835-1847.
 83. Ma YN, Jiang X, Song P, Tang W. Neoadjuvant therapies in resectable hepatocellular carcinoma: Exploring strategies to improve prognosis. *Biosci Trends*. 2024; 18:21-41.
 84. Whitham Z, Hsiehchen D. Role of Neoadjuvant Therapy Prior to Curative Resection in Hepatocellular Carcinoma. *Surg Oncol Clin N Am*. 2024; 33:87-97.
 85. Geh D, Manas DM, Reeves HL. Hepatocellular carcinoma in non-alcoholic fatty liver disease-a review of an emerging challenge facing clinicians. *Hepatobiliary Surg Nutr*. 2021; 10:59-75.
 86. Bruix J, Cheng AL, Meinhardt G, Nakajima K, De Sanctis Y, Llovet J. Prognostic factors and predictors of sorafenib benefit in patients with hepatocellular carcinoma: Analysis of two phase III studies. *J Hepatol*. 2017; 67:999-1008.
 87. Howell J, Samani A, Mannan B, Hajiev S, Motedayen Aval L, Abdelmalak R, Tam VC, Bettinger D, Thimme R, Taddei TH, Kaplan DE, Seidensticker M, Sharma R. Impact of NAFLD on clinical outcomes in hepatocellular carcinoma treated with sorafenib: an international cohort study. *Therap Adv Gastroenterol*. 2022; 15:17562848221100106.
 88. Casadei Gardini A, Faloppi L, De Matteis S, *et al*. Metformin and insulin impact on clinical outcome in patients with advanced hepatocellular carcinoma receiving sorafenib: Validation study and biological rationale. *Eur J Cancer*. 2017; 86:106-114.
 89. Finn RS, Qin S, Ikeda M, *et al*. Atezolizumab plus Bevacizumab in Unresectable Hepatocellular Carcinoma. *N Engl J Med*. 2020; 382:1894-1905.
 90. Kudo M. Durvalumab plus tremelimumab in unresectable hepatocellular carcinoma. *Hepatobiliary Surg Nutr*. 2022; 11:592-596.
 91. de Castria TB, Khalil DN, Harding JJ, O'Reilly EM, Abou-Alfa GK. Tremelimumab and durvalumab in the treatment of unresectable, advanced hepatocellular carcinoma. *Future Oncol*. 2022; 18:3769-3782.
 92. Yau T, Park JW, Finn RS, *et al*. Nivolumab versus sorafenib in advanced hepatocellular carcinoma (CheckMate 459): a randomised, multicentre, open-label, phase 3 trial. *Lancet Oncol*. 2022; 23:77-90.
 93. Pfister D, Núñez NG, Pinyol R, *et al*. NASH limits anti-tumour surveillance in immunotherapy-treated HCC. *Nature*. 2021; 592:450-456.
 94. Pinter M, Scheiner B, Peck-Radosavljevic M. Immunotherapy for advanced hepatocellular carcinoma: a focus on special subgroups. *Gut*. 2021; 70:204-214.
 95. Duffy AG, Ulahannan SV, Makorova-Rusher O, *et al*. Tremelimumab in combination with ablation in patients with advanced hepatocellular carcinoma. *J Hepatol*. 2017; 66:545-551.
 96. Zhu C, Dai B, Zhan H, Deng R. Neoadjuvant transarterial chemoembolization (TACE) plus PD-1 inhibitor bridging to tumor resection in intermediate-stage hepatocellular carcinoma patients. *Ir J Med Sci*. 2023; 192:1065-1071.
 97. EASL-EASD-EASO Clinical Practice Guidelines on the Management of Metabolic Dysfunction-Associated Steatotic Liver Disease (MASLD). *Obes Facts*. 2024; 17:374-444.
 98. Yen FS, Hou MC, Cheng-Chung Wei J, Shih YH, Hsu CY, Hsu CC, Hwu CM. Glucagon-like peptide-1 receptor agonist use in patients with liver cirrhosis and type 2 diabetes. *Clin Gastroenterol Hepatol*. 2024; 22:1255-1264. e1218.
- Received September 5, 2024; Revised October 7, 2024; Accepted October 15, 2024.
- *Address correspondence to:*
Miao Liu, Gastrointestinal Cancer Center, Chongqing University Cancer Hospital, Chongqing, China.
E-mail: liumiao782@163.com
- Ai Shen, Hepatobiliary Pancreatic Cancer Center, Chongqing University Cancer Hospital, Chongqing, China.
E-mail: shenai200808@163.com
- Released online in J-STAGE as advance publication October 18, 2024.

How spousal cognitive functioning affects the level of depression in middle-aged and older adults: An instrumental variable study based on CHARLS in China

Zheng Wang^{1,§}, Ting Li^{2,3,§}, Jingbin Zhang¹, Cordia Chu³, Shasha Yuan^{1,*}

¹Institute of Medical Information/Medical Library, Chinese Academy of Medical Sciences & Peking Union Medical College, Beijing, China;

²National Clinical Research Centre for Infectious Diseases, The Third People's Hospital of Shenzhen, Shenzhen, Guangdong, China;

³Centre for Environment and Population Health, School of Medicine and Dentistry, Griffith University, Brisbane, Australia.

SUMMARY A better understanding of the causal relationship between spousal cognitive functioning and depression levels among middle-aged and older adults is vital for effective health policymaking under the globally severe aging challenge. However, the related evidence is often limited by potential omitted-variable bias and reverse causation. This study uses an instrumental variables approach, namely the two-stage least squares (2SLS) method, to examine the impact of spousal cognitive functioning on depression levels among middle-aged and older adults in China. The data were sourced from the China Health and Retirement Longitudinal Study (CHARLS) of 2020, including a total of 3,710 couples aged 45 years and above. Depression levels were measured using the Center for Epidemiologic Studies Depression Scale (CES-D-10), while cognitive functioning was assessed using the Mini-Mental State Examination (MMSE). Spousal social participation was employed as the instrumental variable to address omitted-variable bias and reverse causation. Additionally, an interaction effect test between gender and spousal cognitive functioning was conducted. The results show that for each one-point increase in the spouse's MMSE score, the CES-D-10 score of middle-aged and older adults decreased by 17.1% to 68.2%. The OLS results indicated that women, rural residents, and middle-aged individuals were more sensitive to these changes. The interaction effect test results confirmed that women were more affected by changes in spousal cognitive functioning. However, after a more reliable 2SLS analysis, the results for age groups shifted, showing that middle-aged individuals were more sensitive to these changes, with a decrease in depression levels reaching 70.0%, compared to 60.2% for the elderly group. Nonetheless, given the prevalence of depression among the elderly, the impact of spousal cognitive decline on depression in this group should not be overlooked. Our findings highlight the importance of spousal cognitive health in managing depression among both middle-aged and older adults, with particular attention to women and rural populations.

Keywords depression, cognitive functioning, middle-aged and older adults, instrumental variables, spouse, China

1. Introduction

The Global Burden of Disease study, 2019, shows that depression affects approximately 280 million people worldwide, representing 3.8% of the population, including 5.7% of those aged 60 years and over (1). The World Health Organization (WHO) reported that depression imposes a significant economic burden globally, with annual costs approaching US\$1 trillion (2). The factors that influence depression are complex and varied, involving biological and psychological aspects.

Biological factors include genetics, changes in brain chemistry and hormonal imbalances (3-5). Psychosocial factors such as loss of a loved one, and social isolation are also recognized as important triggers of depression (6,7). Several determinants, including gender, age, education, income, residence, financial support from offspring, and health status, also have been identified as influential factors in the prevalence of depression (8-12). According to WHO, the global population aged 60 years and over is projected to rise from 1 billion in 2020 to 1.4 billion by 2030, and further to 2.1 billion by

2050 (13). China has 190 million people aged 65 years or older, constituting 13.5% of its total population. The Comprehensive mental health action plan 2013–2030 published by the WHO states that older adults are at high risk for mental health problems (14). Depression reduces the likelihood that older people will participate in social or recreational activities, which can have a serious impact on their normal lives (15). It also impairs mental and physical functioning, leading to impaired cognitive functioning, increased risk of diseases such as heart disease and stroke, and increased risk of suicide and death in older adults (16,17). Additionally, midlife is a special stage in the journey of life. On the one hand, middle-aged people have to face many pressures from society, family and their own development. On the other hand, as they grow older, they may face more health problems, such as chronic diseases and mental health problems (18). Middle-aged people are the mainstay of society, but less research has been done on the health of middle-aged people than on other age groups. According to the life course theory, experiences and health in midlife can have a profound effect on the state of affairs in old age (19). Some studies have shown that mental stress and physical health in midlife are associated with cognitive ability and risk of depression in old age (19). Therefore, health status of middle-aged people should not be ignored, but few studies have focused on midlife. The accelerating aging of the global population highlights age-related cognitive decline as a major public health concern. Based on the status described in the previous section, our study will focus on middle-aged and older adults. Several scholars have researched the impact of cognitive function on depression, but their findings on the causal relationship between the two remain inconclusive.

A study using Longitudinal Ageing Study in India (LASI) reported that older adults with depression were at a higher risk of cognitive impairment compared to their peers through multivariable analyses, but did not confirm the causal relationship (20). Chinese researchers who studied 90 outpatients and inpatients with late-life depression from the department of geriatric psychiatry of a hospital, using a longitudinal, cross-lagged model found a unidirectional relationship between depressive symptoms and cognitive decline and, so, depression might be a risk factor for cognitive decline (21). Similarly, a study in Korea using data from the Korean Longitudinal Study of Ageing (KLoSA) and a latent growth model (LGM) analysed 1,354 older adults living alone from 2016 to 2020, using the Korean version of the Minimum Mental State Examination (MMSE) scale and depression using the Korean version of the Depression Self-Assessment Scale, and found that initial higher depression levels were linked to lower cognitive function and accelerated cognitive decline (22).

In China, most of the middle-aged and older adults over 45 years primarily live with their spouses. Most

patients with cognitive impairments receive home-based health management and are cared for by family caregivers. The National Health Commission of the PRC has issued a notice on promoting the prevention and treatment of Alzheimer's disease through the "Alzheimer's Disease Prevention and Promotion Action Plan (2023–2025)", which emphasizes the importance of specialized training to enhance caregivers' skills, alleviate their caregiving stress, and boost their confidence (23). This reflects China's national-level attention to the psychological well-being of patients' families. Despite the influence of cognitive functioning on depression has been recognized, most studies on cognitive decline and depression focus predominantly on individuals. Few studies have considered the influence of spousal cognitive function on depression among middle-aged and older adults, and there are also some controversies in these conclusions. A study using data from the National Alliance for Caregiving and the American Association of Retired Persons containing 1,509 ethnically diverse study participants, utilizing multivariate regression analyses, concluded that dementia caregivers are more affected when caring for cognitively impaired individuals with dementia compared to non-dementia caregivers (24). This conclusion highlights that family dynamics, in particular spousal interactions, play a significant role in affecting mental health among the elderly. Some researchers have suggested that spousal cognitive function could influence the other spouse's mental health. A study involving 2,486 couples analyzed the interrelation between emotional and cognitive health for individuals and spouses with dyadic regression models confirming the previous point (25). Furthermore, Monin using the Actor-Partner Interdependence Model (APIM) with data from the Cardiovascular Health Study (CHS), found that one partner's depressive symptoms could predict cognitive decline of the other, but not vice versa (26). Contrarily, research using APIM and the data from the China Health and Retirement Longitudinal Study (CHARLS), 2011 to 2018 waves, indicated that lower cognitive functioning of one spouse was associated with more depressive symptoms in the other without a reciprocal relationship (10). These inconsistent results highlight the necessity for further research to elucidate the influence of spousal cognitive functioning on depression among middle-aged and older adults.

Actor-Partner Interdependence Models can reveal interactions between individuals and is essentially a correlation-based analysis. However, due to the presence of potential confounding variables and uncontrollable factors, APIM cannot determine whether such changes are causal. Therefore, it is necessary to select an appropriate research method to explore the causal relationships. The Instrumental Variables (IV) method is appropriate to overcome endogeneity bias and reveals underlying causality in the scenario mentioned before. Based on the aforementioned current state of

depression and the advantages of the instrumental variables approach over other research methods, our study employed CHARLS 2020 wave and IV method to explore whether lower spousal cognitive functioning is a cause of depression in middle-aged and older adults to further test causality and add the latest research evidence.

2. Materials and Methods

2.1. Data source

The data of our study came from the CHARLS, a representative longitudinal survey targeting middle-aged and elderly populations across China. We conducted a cross-sectional study using CHARLS 2020 data released in November 2023. All participants provided written informed consent and this study was approved by the ethics committee of Peking University (approval code: IRB00001052-11015). CHARLS 2020 includes the information pertaining to 19,395 individuals from 11,412 households across 28 provinces, autonomous regions, and municipalities. Selection criteria for our sample was guided by the study's objectives and previous research on depression, required that: *i*) both members of the couple are 45 years old or above, *ii*) both complete The Center for Epidemiological Studies Depression Scale short form (CES-D-10), *iii*) both undergo the MMSE, and *iv*) both have complete and available baseline data. Based

on these criteria, we selected a final sample of 7,420 participants, comprising 3,710 heterosexual couples aged 45 years and above. The flowchart for sample selection is presented in Figure 1.

2.2. Variables and measurement

2.2.1. Explained variable

The explained variable for this study was the level of depression, which was quantified in CHARLS by the CES-D-10 scale. The scale, which has high internal reliability and internal consistency analysis revealed that the Cronbach's alpha coefficient for the CES-D-10 scale in this study was 0.7955. The questions in CES-D-10 scale include a) I am annoyed by small things, b) I have a hard time concentrating when I do things, c) I feel depressed, d) I feel like it is a lot of work to do everything, e) I am hopeful about the future, f) I am scared, g) my sleep is not good, h) I am pleasant, i) I feel lonely, and j) I don't think I can go on with my life. The options of each question were categorized into four levels: 1 = rarely or not at all (< 1 day), 2 = not too much (1-2 days), 3 = sometimes or half the time (3-4 days), and 4 = most of the time (5-7 days). Depression scores were calculated based on established criteria, assigning scores of "0", "1", "2", and "3" to the four levels. Notably, items e) and h) were reverse scored. The total possible score was 30, with higher scores indicating

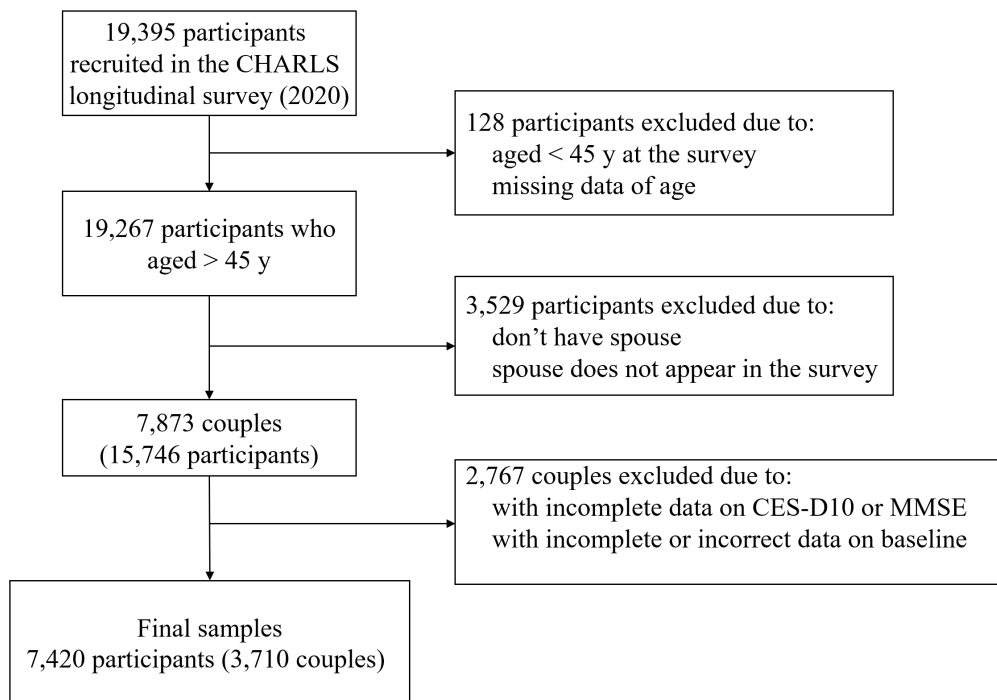


Figure 1. Flow chart of sample selection. This flowchart depicts the selection process of participants from the CHARLS longitudinal survey conducted in 2020. Out of the initial 19,395 participants, 128 were excluded due to being under 45 years of age or missing age data. From the remaining 19,267 participants, 3,529 were excluded because they did not have a spouse or their spouse did not appear in the survey. This resulted in 7,873 couples (15,746 participants) being identified. Further, 2,767 couples were excluded due to incomplete data on CES-D10 or MMSE or incomplete or incorrect baseline data. The final sample included 7,420 participants (3,710 couples).

increased levels of depression.

2.2.2. Explanatory variable

The key explanatory variable in this study is spousal cognitive functioning, which was calculated through the MMSE scale in CHARLS with a total score of 21. Higher scores represent better cognitive functioning of the respondents. Cognitive functioning consists of two components: state of mind and situational memory. A total score of 11 was obtained from the tests of date recognition, numeracy, and drawing function, while a total score of 10 was obtained from the test of situational memory using word recall.

2.2.3. Control variables

Control variables selected in this study are based on previous research on depression, including gender, age, education, annual household income, self-rated health, financial support from offspring, and residence. These factors are hypothesized to influence depression among middle-aged and older adults.

2.2.4. Instrumental variable

Instrumental variables must correlate with endogenous explanatory variables. Extensive evidence has explored the link between social participation and cognitive function. For instance, a longitudinal study in the United States from 1982–1994 found that individuals without social ties had a 137% increased risk of cognitive decline compared to their socially engaged counterparts, after adjusting for control variables (27). Additionally, a study in Taiwan from 1989–2000 found that older

adults engaged in one to two social activities were 13% less likely to fail cognitive tests (28). And compared to those uninvolved in social activities, engagement in three or more activities reduced the likelihood of failing these tests by 33%. A previous study, using Health, Aging, and Retirement in Europe (SHARE), identified a strong positive correlation between various types of social participation and cognitive functioning in older adults (29). Therefore, we imported the spousal social participation as an instrumental variable, because it aligns with the principle that instrumental variables should correlate with endogenous explanatory variables. In this context, social participation is linked to their cognitive function, which may subsequently affect spousal depression through its impact on their own cognitive functioning. This selection also meets the exclusivity criterion because the control variables in this study are unaffected by spousal social participation. In conclusion, choosing spousal social participation as the instrumental variable in this study is reliable.

To enhance data comparability, we standardized spousal social participation and obtained a standardized score. First, we calculated the score derived by assigning one point for each of the eight different social activities in which spouses participated. The standardized score was then calculated by subtracting the mean score from the total score and dividing the result by the standard deviation.

The detailed measurement of the variables used in this study are presented in Table 1.

The variables and their relationships involved in this study are shown in Figure 2. Standardized score of spouses' social participation serves as an instrumental variable, influencing depression levels indirectly through its effect on spousal cognitive functioning. Control

Table 1. Variables and their measurements

Variable	Variable type	Measurement
Explained variable		
Depression level	continuous	CES-D-10 scale score out of 30, the higher the score the higher the level of depression.
Explanatory variable		
Spousal cognitive functioning	continuous	Spouse's MMSE scale score out of 21, with higher scores associated with better cognitive functioning.
Control variables		
Gender	binary	1 = male, 0 = female.
Age	continuous	One full year of life.
Education	ordered categorical	1 = below primary school, 2 = primary school, 3 = middle school, 4 = High school and above.
Annual household income	continuous	RMB, in logarithms.
Self-rated health	ordered categorical	1 = poor, 2 = rather poor, 3 = average, 4 = good, 5 = excellent.
Financial support from offspring	binary	0 = no, 1 = yes.
Residence	binary	0 = urban, 1 = rural.
Instrumental variable		
Standardised score of spousal social participation	continuous	Each participation in one of the 8 social activities counts as 1 point. The score is calculated as (total score - mean)/standard deviation. 8 social activities include: visiting, playing mahjong, offering help, dancing, club activities, volunteer activities, going to school or training, other socialising.

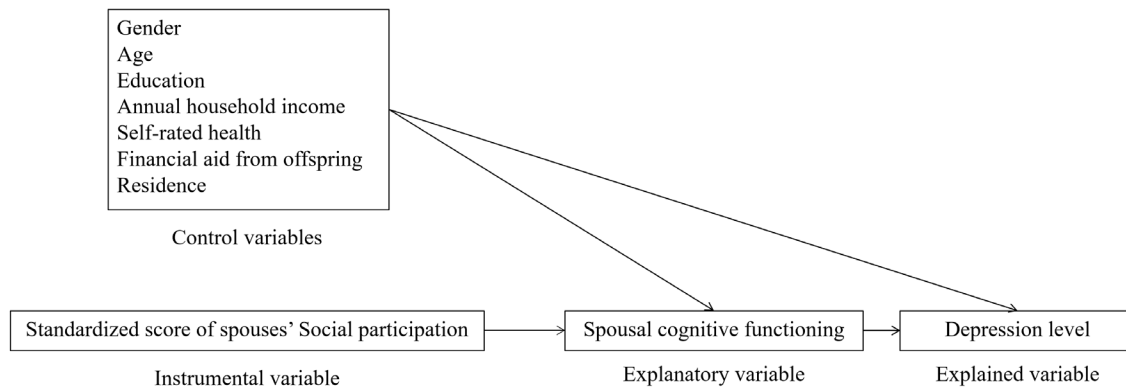


Figure 2. Causal diagram of this research. This figure illustrates the conceptual framework used to examine the impact of spousal cognitive functioning on depression levels, incorporating both control and instrumental variables. The standardized score of spouses' social participation is utilized as the instrumental variable to explain spousal cognitive functioning, which is the key explanatory variable in the model. The control variables include gender, age, education, annual household income, self-rated health, financial aid from offspring, and residence. These factors are controlled for in the analysis to isolate the effect of spousal cognitive functioning on depression levels, which is the primary explained variable.

variables, including gender, age, education, annual household income, self-rated health, financial aid from offspring, and residence, are incorporated to adjust for confounding factors that may affect the relationship between spousal cognitive functioning and depression levels.

2.3. Statistical analysis

2.3.1. Descriptive statistics

Descriptive statistics were used to characterize the sample. We calculated means or proportion of each variable for the overall sample and stratified by gender, residence, and age groups (< 60 years and ≥ 60 years). Depending on the variable type, differences between groups were assessed using either chi-square (χ^2) tests or *t*-tests, with *p*-values reported to determine statistical significance.

2.3.2. Ordinary least squares

The association between the cognitive abilities of spouses in middle-aged and older populations and their respective depression levels were analyzed using an Ordinary Least Squares (OLS) regression model. The model is defined as follows:

$$Depression_i = \beta_0 + \beta_1 s_{_c i} + \beta_2 X_i + \epsilon_i \quad (1)$$

where, *s_c* is the abbreviation for *spouse_cognition* and *Depression_i* represents the depression degree of individual *i*, and *s_c_i* represents the cognitive ability of individual *i*'s spouse. The variable *X_i* includes additional covariates, such as gender, age, and education, that could potentially influence the depression degree. The model also features β_0 as the intercept, β_1 as the coefficient for the explanatory variable, β_2 as the coefficient for the

control variable and ϵ_i to account for residual errors. This model structure allows for analysis of how spousal cognitive functioning impacts an individual's depression while controlling for other significant demographic and personal factors. To address potential heteroskedasticity issues within the dataset, the regression model was enhanced with the robust option. Additionally, the OLS regression was conducted stratified by gender, region, and age groups to explore responses to different demographic populations to changes of spousal cognitive functioning.

Because men and women may exhibit different behavioural patterns in caring for their cognitively impaired spouses during their lives, it was necessary to explore whether there was an interaction effect between gender and spousal cognitive functioning. In conducting OLS regression analyses, we specifically conducted an OLS regression in the overall sample that included an interaction term between gender and spousal cognitive functioning in order to explore whether the effect of spousal cognitive functioning on depression differed significantly between genders, and thus to clarify which gender was more sensitive to this effect.

2.3.3. Instrumental variable

Endogeneity of explanatory variables presents a significant challenge for OLS. Two primary factors contribute to the endogeneity of spousal cognitive functioning. The first is the presence of omitted variables such as couple's rapport, lifestyle habits, and genetics. These factors are difficult to measure but may influence both depression and spousal cognitive ability. Second, the other source of endogeneity is the issue of reverse causality, which means depression could potentially affect spousal cognitive functioning. To address these issues and derive more robust regression outcomes, the instrumental variable method was employed to better

ascertain the causal relationships between the variables.

In this study, the two-stage least squares (2SLS) approach within the instrumental variable framework was used. Reliability of the 2SLS estimates is based on validity of the chosen instrumental variable. The first-stage model is as follows:

$$s_c_i = \alpha_0 + \alpha_1 s_scfsp_i + \alpha_2 X_i + v_i \quad (2)$$

where s_scfsp stands for spouse_ standardised score for social participation and s_scfsp_i is the instrumental variable of our research. X_i encompasses covariates influencing depression as mentioned in Equation (1). In the second stage of 2SLS, the predicted value s_c_i of Equation (2) is used to replace s_c_i of Equation (1). And then, using OLS Equation (1), the regression coefficients determined by 2SLS can be obtained. 2SLS also introduces the robust option and performs stratified analysis.

When implementing 2SLS, the statistically significant coefficient for the instrumental variables in the first-stage regression indicate a correlation with the endogenous explanatory variable. Additionally, the validity of instrumental variable is further supported by specific test statistics such as the Cragg-Donald Wald F value, the Kleibergen-Paap rk Wald F value for the weak identification test, and the Kleibergen-Paap rk LM value for the under identification test. In addition, to quantitatively validate the exogeneity of the instrumental variable, we employed the Union of Confidence Intervals (UCI) method proposed by Conley *et al.*, setting the g_{min} value to -1 and the g_{max} value to 1 (30).

Following the preparation of data and methods, the study's parameters were estimated using Stata 17.0 software, ensuring rigorous and precise analysis results.

3. Results

3.1. Summary statistics

Descriptive statistics for each variable are presented in Table 2, with additional details available in Supplemental Tables S1-S3 (<https://www.biosciencetrends.com/action/getSupplementalData.php?ID=212>) of the Appendix. The mean of the CES-D-10 score in the overall sample is 7.63, suggesting a mild level of depression. Statistically significant differences in depression levels were observed between genders, residential areas, and age groups.

The average cognitive function score for the study sample was 13.11. Females scored higher on average (13.35) compared to males (12.87). Urban middle-aged and elderly individuals (13.77) also exhibited higher cognitive function scores than their rural counterparts (12.54). Furthermore, individuals aged < 60 years (13.66) displayed higher cognitive scores than those aged \geq 60 years (12.50). Given that the main explanatory variable of this study is spousal cognitive

functioning, that information is represented in Table 2. The spousal cognitive function score for men was calculated based on the cognitive scores of females, and vice versa for women, as presented in Supplemental Table S1-S3 (<https://www.biosciencetrends.com/action/getSupplementalData.php?ID=212>). The standardized score for spousal social participation was found to be higher among urban and individuals aged < 60 years compared to rural and older adults aged \geq 60 years, and no significant differences were observed between genders.

3.2. Ordinary least squares regression

The outcomes of the OLS regression analysis conducted in this study are presented in Table 3. Model (1) from Table 3 indicates that the regression coefficient for spousal cognitive functioning is significantly negative. Specifically, for each one-point increase of spousal cognitive functioning, the depression scores of middle-aged and older adults decreased by 17.1%. Further analysis in models (2) and (3) reveals that depression of females is more sensitive to changes in spousal cognitive functioning: a one-point increase in spousal cognitive functioning results in a 20.8% decrease of depression scores, compared to a 15.1% decrease for males. According to model (4) and (5), older adults show more

Table 2. Summary of statistics

Variable	Overall, n = 7,420
Explained variables	
CES-D-10 Depression Scale Score, Mean (SD)	7.63 (6.084)
Explanatory variable	
Spousal cognitive functioning, Mean (SD)	13.11 (3.13)
Control variables	
Gender, n (%)	
Male	3,710 (50.00)
Female	3,710 (50.00)
Age, Mean (SD)	60.33 (8.19)
Education, n (%)	
Below primary school	1,192 (26.85)
Primary school	1,819 (24.51)
Middle school	2,246 (30.27)
High school and above	1,363 (18.37)
Logarithm of annual household income, Mean (SD)	8.58 (3.98)
Self-rated health, n (%)	
Poor	372 (5.01)
Rather poor	1,173 (15.81)
General	3,917 (52.79)
Good	1,007 (13.57)
Excellent	951 (12.82)
Financial support from offspring, n (%)	
Yes	6,028 (81.24)
No	1,392 (18.76)
Residence, n (%)	
Rural	3,980 (53.64)
Urban	3,440 (46.36)
Instrumental variable	
Standardised score of spousal social participation, Mean (SD)	0.00 (1.00)

Table 3. Ordinary least squares regression result

Variable	Overall (1)	Female (2)	Male (3)	< 60 years (4)	≥ 60 years (5)	Urban (6)	Rural (7)
Spousal cognitive functioning	-0.171*** (0.022)	-0.208*** (0.033)	-0.151*** (0.027)	-0.150*** (0.032)	-0.178*** (0.031)	-0.149*** (0.032)	-0.191*** (0.031)
Gender	-1.522*** (0.129)	/	/	-1.535*** (0.172)	-1.541*** (0.196)	-1.233*** (0.173)	-1.807*** (0.191)
Age	-0.008 (0.009)	-0.0176 (0.013)	-0.000 (0.011)	0.062* (0.026)	-0.027 (0.018)	-0.029* (0.012)	0.009 (0.013)
Education							
Primary school	-0.912*** (0.189)	-1.165*** (0.246)	-0.365 (0.263)	-1.121*** (0.278)	-0.710** (0.265)	-1.326*** (0.302)	-0.574* (0.244)
Middle school	-1.443*** (0.181)	-1.860*** (0.250)	-0.775** (0.252)	-1.859*** (0.262)	-1.049*** (0.260)	-1.407*** (0.280)	-1.467*** (0.243)
High school and above	-1.778*** (0.200)	-2.234*** (0.319)	-1.144*** (0.279)	-2.040*** (0.304)	-1.692*** (0.277)	-1.957*** (0.284)	-1.600*** (0.314)
Self-rated health							
Rather poor self-reported health	-3.250*** (0.422)	-3.140*** (0.452)	-3.388*** (0.449)	-3.738*** (0.632)	-2.821*** (0.564)	-3.822*** (0.751)	-2.918*** (0.514)
General self-reported health	-6.194*** (0.392)	-6.028*** (0.419)	-6.335*** (0.406)	-6.476*** (0.579)	-5.896*** (0.531)	-6.718*** (0.709)	-5.830*** (0.474)
Good self-reported health	-8.482*** (0.408)	-8.646*** (0.488)	-8.366*** (0.446)	-8.819*** (0.593)	-8.042*** (0.569)	-8.985*** (0.720)	-8.148*** (0.512)
Excellent self-reported health	-9.251*** (0.408)	-9.470*** (0.483)	-9.061*** (0.450)	-9.494*** (0.596)	-9.040*** (0.561)	-9.729*** (0.723)	-8.924*** (0.503)
Logarithm of annual household income	-0.020 (0.017)	-0.034 (0.025)	-0.008 (0.022)	-0.077** (0.027)	0.001 (0.022)	-0.011 (0.021)	-0.058 (0.028)
Residence	0.956*** (0.132)	1.023*** (0.199)	0.853*** (0.179)	0.701*** (0.179)	1.176*** (0.200)	/	/
Financial support for children	-0.011 (0.158)	0.194 (0.237)	-0.227 (0.210)	0.068 (0.196)	-0.287 (0.270)	-0.187 (0.208)	0.265 (0.244)
_cons	17.904** (0.823)	19.035* (1.162)	15.294** (1.185)	15.025* (1.653)	18.761** (1.483)	19.396*** (1.245)	17.901*** (1.092)
R ²	0.228	0.216	0.193	0.234	0.224	0.205	0.214
Obs	7,420	3,710	3,710	3,862	3,558	3,440	3,980

* $p < 0.05$, ** $p < 0.01$, *** $p < 0.001$; robust standard errors in brackets.

sensitive responses with depression scores decreasing by 17.8% for every one-point increase of spousal cognitive functioning. Finally, the comparison between models (6) and (7) demonstrates that the depression scores of rural middle-aged and older adults are more profoundly affected by spousal cognitive functioning, with depression scores decreasing by a 19.1% reduction for each one-point increase of spousal cognitive functioning.

The OLS regression results after adding the interaction terms for gender and spousal cognitive functioning are shown in Table 4. Regression coefficients for the other variables after the addition of the interaction term are in the same direction of sign and have essentially equal values as before the interaction term was added. The regression coefficient with the addition of the interaction is 0.096, with a p -value of less than 0.05, and the effect of spousal cognition on depression is significantly different between genders. The regression coefficient of the interaction term is positive, which means that for men, the effect of spousal cognition on depression is weaker and women are more sensitive to this change. Fitted line plot (Figure 3) visualizes this result, with women experiencing a higher decline

in depression than men as their spouse's cognitive functioning improves.

3.3. Two-stage least squares regression

To mitigate the effects of potential unknown variables and reverse causality, our study imported the standardized score of spousal social participation as the instrumental variable in the 2SLS analysis. The results affirm that the first-stage instrumental variable was significantly correlated with depression scores in all models, as presented in Table 5. The p -value corresponding to Kleibergen-Paap rk LM was below 0.1 and both Kleibergen-Paap rk Wald F and Cragg-Donald Wald F value both were greater than the critical value of 19.93 for the test at the 10% level, thus rejecting that the instrumental variable is the assumption of weak identification (31,32). Additionally, in the result of UCI, we found that the robust 95% CI for the coefficient of spousal social participation is (-4.828, 3.285), which includes the coefficient found in Table 5 for the overall sample in the first stage: 0.305. It indicates that the instrumental variable meets the requirement of

Table 4. Ordinary least squares regression with interaction effects: impact of spousal cognitive functioning and gender on depression levels

Variable	Overall
Spousal cognitive functioning	-0.226*** (0.034)
Gender	-2.793*** (0.593)
Age	-0.007 (0.009)
Education	
Primary school	-0.887*** (0.190)
Middle school	-1.427*** (0.181)
High school and above	-1.771*** (0.200)
Self-rated health	
Rather poor self-reported health	-3.249*** (0.422)
General self-reported health	-6.185*** (0.392)
Good self-reported health	-8.472*** (0.408)
Excellent self-reported health	-9.248*** (0.408)
Logarithm of annual household income	-0.019 (0.017)
Residence	0.969*** (0.133)
Financial support for children	-0.010 (0.158)
Gender*Spousal cognitive functioning	0.096* (0.043)
_cons	18.541 (0.874)
R ²	0.228
Obs	7,420

* $p < 0.05$, ** $p < 0.01$, *** $p < 0.001$; robust standard errors in brackets.

exogeneity. These results confirm the adequacy of the standardized score of spousal social participation as an instrumental variable and the reliability of the 2SLS regression results.

The regression coefficient of spousal cognitive functioning on depression levels of middle-aged and older adults were significant in all models and showed a consistent direction with the OLS results, as shown in Table 5. The introduction of the instrumental variable amplified the effect. In the overall sample, each point increase in the spousal cognitive functioning score was associated with a 68.2% decrease in the depression score. The subgroup analysis of 2SLS maintains the relationship between the magnitude of the regression coefficients between genders as well as between urban and rural areas, however, the age groups changed. The absolute value of the explanatory variable's regression coefficients was larger in the middle-aged group than in the older group. The finding from 2SLS, which offers a more robust estimation of causality, indicated that the

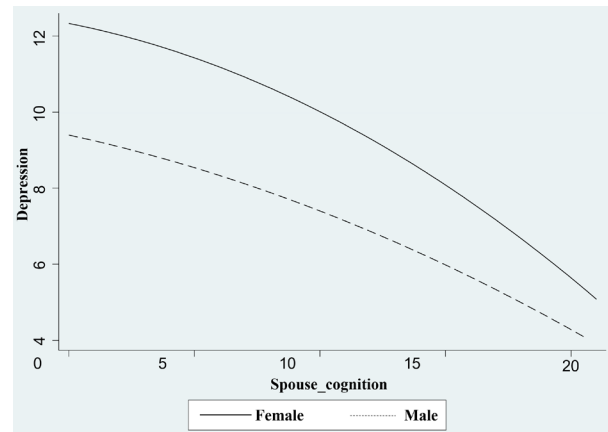


Figure 3. Interaction effect of spousal cognition and gender on depression. This figure illustrates the interaction between spousal cognition and gender on depression levels. The y-axis represents the level of depression, while the x-axis represents spousal cognitive functioning. The solid line corresponds to females, and the dotted line corresponds to males. The graph demonstrates that as spousal cognition increases, depression levels decrease for both genders. However, the effect is more pronounced for females, indicating a stronger negative association between spousal cognition and depression in women compared to men.

causality is more pronounced in the middle-aged group.

4. Discussion

Depression is becoming more common among middle-aged and older adults as the global population ages, so it is critical to determine factors that affect mental health of this population. Concurrently, the growing disease burden associated with low cognitive function in these age groups is influencing the psychological wellbeing of family members, particularly spouses. This study employed the instrumental variable method to confirm the causal relationship between spousal cognitive functioning and depression levels in middle-aged and older adults.

First, the findings reveal that higher spousal cognitive functioning correlates with lower depression levels. Our findings align with previous studies that have explored the relationship between spousal cognitive functioning and depression (33,34). However, our study extends these findings by using an instrumental variable approach to address potential endogeneity, providing more robust evidence of causality. Our findings are also inconsistent with the results of some previous studies, a Korean study showing that emotional distress effects spouse's cognitive impairment or that the cognitive ability impacts spouses' emotional distress (35). Additionally, the study identified a difference in sensitivity to spousal cognitive functioning's impact on depression between different groups including genders, age groups, and residential areas.

Theories such as emotional contagion and role tension provide valuable frameworks for understanding

Table 5. Two-stage least squares regression

Variable	Overall (1)	Female (2)	Male (3)	< 60 years (4)	≥ 60 years (5)	Urban (6)	Rural (7)
Spousal cognitive functioning	-0.682*** (0.205)	-0.751** (0.289)	-0.565* (0.273)	-0.700* (0.304)	-0.602* (0.274)	-0.512* (0.254)	-0.956** (0.359)
Other control variables	Yes	Yes	Yes	Yes	Yes	Yes	Yes
Coefficients of regression instrumental variables in the first stage	0.305***	0.305***	0.308***	0.266***	0.360***	0.312***	0.282***
Kleibergen-Paap rk LM	82.742***	49.933***	38.438***	39.601***	43.295***	53.916***	28.745***
Cragg-Donald Wald F	77.952***	46.688***	36.267***	38.237***	40.603***	50.056***	27.840***
Kleibergen-Paap rk Wald F	85.886***	51.744***	39.911***	40.721***	44.900***	56.680***	29.198***
R ²	0.167	0.159	0.143	0.168	0.180	0.172	0.081
Obs	7,420	3,710	3,710	3,862	3,558	3,440	3,980

* $p < 0.05$, ** $p < 0.01$, *** $p < 0.001$; robust standard errors in brackets.

interpersonal dynamics and mental health, in particular in the context of interspousal interactions and their influence on depression (35,36). Negative emotions such as depression and frustration often stem from one partner's cognitive dysfunction, which can be transmitted to the other partner. This transmit potentially leads to shared depressive symptoms. Furthermore, the physically healthy spouse may face multiple role tensions that encompass caregiving responsibilities, financial strains, and the balancing of personal emotional needs. The low cognitive functioning of one spouse not only diminishes their quality of life but also imposes a substantial psychological and emotional burden on the caregiver. The physically healthy spouse often shoulders the responsibility of daily care, emotional support, and managing behavioural and emotional changes of the affected partner. These responsibilities will deplete their time and energy, possibly leading to mental health challenges and triggering depression (34,37,38).

Moreover, our study found differences in this effect among different groups of middle-aged and older adults. First, in the overall sample, empirical findings of this study indicate that a one-point increase in spousal cognitive functioning scores is associated with a significant reduction in depression levels, ranging from 17.1% to 68.2%. Our study provides causal validation for previous research, while offering a contrast to Monin's conclusions (10,26). Typically, a decline in cognitive functioning is paralleled by a deterioration in daily behavioural abilities. Within the Chinese familial structure, physical and mental disease in one spouse frequently necessitates that the other spouse assume caregiving duties. This role not only consumes considerable time and energy but also leads to heightened depression levels. From the perspective of individual-social relationship theory, the influence of spousal cognitive dysfunction on depression in middle-aged and older adults is significant. This reflects the profound impact that social relationships and structures have on individual mental health. In this context, spousal interactions and relationships are critical forms of social capital that significantly affect mental wellbeing.

Cognitive dysfunction in a spouse may reduce their capacity to offer emotional and practical support, thereby weakening the overall social support system. The absence or reduction of such support is a crucial factor in the increase of depressive symptoms among middle-aged and older adults (39). Moreover, because spouses typically share similar living environments and habits, cognitive dysfunction in one partner may inadvertently impact the other through these shared lifestyle factors (40).

In terms of gender-specific differences, females exhibit higher depression levels and are more sensitive to their spouse's cognitive functioning change. Empirical study demonstrated that a one-point increase in their spousal cognitive function is associated with a 20.8–75.1% reduction in depression levels among females, a more substantial decrease compared to the 15.1–56.5% range observed in males. The result of the interaction effects test also support this view. A number of current studies have explored the reasons for this phenomenon. This is consistent with a number of previous studies in which wives' depression was found to be more sensitive to husbands' cognitive functioning (38,41). Previous research indicates that women bear a greater burden in caring for their spouses and tend to have lower levels of subjective wellbeing and physical health (42,43). Furthermore, the responsibilities of caregiving often diminish the time women can devote to engaging in social activities, which are known to positively influence mental health. Females also tend to experience higher emotional distress and responsibility when dealing with their spouse's cognitive dysfunction, heightening their depression risk. Previous research has corroborated this, indicating that female family caregivers generally suffer more adverse effects on their emotional and mental health compared to their male counterpart (44).

Second, in our study, inconsistency exists between the results of OLS and 2SLS in different age groups. In the OLS, depression was more likely to be influenced by spousal cognitive functioning in the middle-aged group, whereas the results were reversed in the 2SLS. In the middle-aged group, endogeneity problems were

more pronounced in this group due to multiple social pressures that may have underestimated the effect of spousal cognitive functioning on depressive symptoms in the OLS. 2SLS corrected for potential endogeneity problems, including possible problems of reverse causation or omitted variables, to provide more reliable causality estimates. According to the 2SLS regression results, the level of depression in middle-aged adults is more significantly impacted by spousal cognitive functioning compared to older adults. A one-point increase in spousal cognitive functioning scores results in a 70.0% reduction in depression levels in middle-aged adults, as opposed to a 60.2% decrease in older adults. Middle-aged adults often face multiple pressures from career development, child-rearing, and elderly care. When the cognitive function of their spouse declines, they are required to undertake additional caregiving responsibilities, increasing their daily life burdens and potentially affecting their mental health. Consequently, the depressive responses of middle-aged adults to their spousal cognitive decline may be more sensitive and complex than those observed in older adults. In contrast, older adults, typically retired, no longer shoulder extensive social and professional responsibilities. Thus, the direct impact of a spousal cognitive functioning decline on their mental health may be less severe. However, while the impact of cognitive decline on the mental health of older adults is less pronounced than in middle-aged individuals, it still warrants attention. Older adults are more prone to physical health issues and tend to have fewer social interactions, spending more time with their spouses daily. Consequently, spousal declining cognitive function is likely to exacerbate their depression. It causes a greater burden of disease in the elderly population than it does in middle-aged people; therefore, for middle-aged people, attention should be paid to detecting early symptoms of cognitive decline and implementing cognitive function training. This not only keeps their own cognitive health strong, but also reduces the psychological burden and depression of their spouses. Community-level psychological counselling services and support groups should also be available to assist them in managing the mental health challenges posed by their spousal cognitive decline. For the elderly, the government should enact policies to establish a robust social support network and provide home care training. This training is designed to teach older adults how to better care for spouses with declining cognitive function and reduce their caregiving burden. Additionally, establishing community service centres focused on the mental health of older adults could provide psychological counselling, emotional support, and other services to help them deal with the psychological stress caused by spousal cognitive decline.

Third, depression in middle-aged and older adults in urban compared to rural areas respond differently to spousal cognitive functioning decline. Our analysis

revealed that a one-point increase of spousal cognitive function resulted in a 14.9–51.2% reduction in depression among urban middle-aged and older adults, whereas in rural counterparts, the decrease ranged from 19.1–91.6%. The effect was markedly stronger among the rural middle-aged and older adults. This disparity can likely be attributed to the less-developed social support networks in rural areas, which increase older adults' reliance on family members, in particular spouses. When a spouse's cognitive function declines in these settings, the increased isolation can exacerbate depression risk (45). In many rural societies, there is a cultural expectation for middle-aged and elderly individuals, especially women, to care for their ailing spouses. As spousal cognitive functioning deteriorates, the care burden of females increases, leading to increased stress and potential depression due to lack of external support (42). The regression coefficients of the OLS regression model (6) and (7) for the gender in our study have also shown evidence of this. Moreover, healthcare resources are often scarce in rural areas, compounding the challenges faced by older adults and their spouses in accessing necessary treatments and support for cognitive impairment or depression (46).

Besides, other factors also have an impact on the level of depression in middle-aged and older Adults. The empirical findings of this study highlight several factors that influence depression levels in middle-aged and older adults. Higher education levels are generally associated with improved cognitive processing and problem-solving abilities, which enable individuals to manage stress and challenges more effectively (47). Additionally, better-educated individuals often adopt healthier lifestyles, including regular exercise, healthy diet, and smoking cessation (48). They may also enjoy higher social status and self-efficacy (49). All of the above are associated with reduced depression levels, corroborating previous research findings (9). Self-rated health is another critical determinant of depression. Individuals with poorer health ratings are more likely to exhibit depressive symptoms, a conclusion consistent with an analysis using the China Family Panel Studies database (8). This association may stem from negative self-perceptions that lead to diminished mood and a reduced sense of self-worth (50). Furthermore, the study identified several demographic-specific factors significantly impacting depression levels. Age was a notable influence among the middle-aged and urban populations, and annual household income significantly affected middle-aged and rural populations.

Based on our study and previous studies, certain interventions for spouses of middle-aged and older adults with cognitive decline are necessary. In addition to depressive conditions, spouses of patients with cognitive decline also face problems with their own nutritional status and need to be monitored on an ongoing basis for their mental health and nutritional status (51). In

addition, their depression stems in part from the patients' communication deficits, and existing research has shown that improving their communication skills can help improve their psychological status (52,53). There are also a number of interventions such as Mindfulness-Based Intervention (MBI), dementia care partner resilience (CP-R) and telephone counselling that have been shown to be effective in improving the psychological status of caregivers with cognitive impairment, and deserve to be further promoted in the future (54-56).

Previous research examining the factors influencing depression among couples typically employed the APIM, which can verify correlations between variables but not causality. In contrast, our study employs the instrumental variable method, which can address the challenges posed by unmeasurable potential variables and reverse causation. This approach effectively mitigates endogeneity bias, thereby uncovering underlying causal relationships.

Some limitations also exist in our study. First, depression was assessed by the CES-D-10 scale, and spousal cognitive functioning was measured by MMSE scale scores. Although both scales are extensively used in clinical research, they do not encompass all dimensions of depression or cognitive functioning. Second, our study excluded the non-completion of the scale in the population, who may have lower cognitive functioning and higher risk of depression, which resulted in a study sample that did not fully reflect the actual situation of the middle-aged and elderly population and caused some underestimation. Additionally, these scale scores are derived from individual self-reports and may be subject to subjective bias. Despite efforts to control for a variety of variables through the study design and use of instrumental variables to address endogeneity in spousal cognitive functioning, the potential for unobserved variables remains. Factors such as spousal emotional bonds and lifestyle habits might concurrently influence levels of depression in middle-aged and older adults and their spousal cognitive functioning. Our analysis was conducted using the CHARLS database from China, and its applicability may be constrained by specific cultural and social contexts. Consequently, environmental and cultural differences should be considered when extrapolating these findings to other settings.

5. Conclusion

This study determined the impact of spousal cognitive functioning on depression levels in middle-aged and older adults based on the CHARLS2020 wave. Using an instrumental variables approach, we highlighted differences in this effect across population groups. The findings demonstrated that enhanced spousal cognitive functioning is significantly linked to reduced depression levels among middle-aged and older adults, in particular in female, middle-aged, rural populations. Besides,

additional support is crucial to mitigate the negative impact of spousal cognitive decline on the mental health of older adults. Because cognitive decline is more prevalent in older adults, these supports ensure their wellbeing.

Acknowledgements

We would like to express our sincere gratitude to Peking University for providing CHARLS data and to those involved in data collection and management.

Funding: This work was supported by a grant from National Natural Science Foundation of China (72304282), Ministry of Education Social Science Foundation (22YJC630196) and Shenzhen Clinical Research Center for Emerging Infectious Diseases (No.LCYSSQ20220823 091203007)&Shenzhen High-level Hospital Construction Fund.

Conflict of Interest: The authors have no conflicts of interest to disclose.

References

1. Institute of Health Metrics and Evaluation. Global Health Data Exchange (GHDx). <https://vizhub.healthdata.org/gbd-results/> (accessed May 6, 2024).
2. World Health Organization. Depression. https://www.who.int/health-topics/depression/#tab=tab_2 (accessed May 6, 2024).
3. Zhu JH, Bo HH, Liu BP, Jia CX. The associations between DNA methylation and depression: A systematic review and meta-analysis. *J Affect Disord.* 2023; 327:439-450.
4. Grace AA. Dysregulation of the dopamine system in the pathophysiology of schizophrenia and depression. *Nat Rev Neurosci.* 2016; 17:524-532.
5. Wachowska K, Gałeczki P. Inflammation and cognition in depression: A narrative review. *J Clin Med.* 2021; 10:5859.
6. Heeke C, Franzen M, Hofmann H, Knaevelsrud C, Lenferink LIM. A latent class analysis on symptoms of prolonged grief, post-traumatic stress, and depression following the loss of a loved one. *Front Psychiatry.* 2022; 13:878773.
7. Domènech-Abella J, Lara E, Rubio-Valera M, Olaya B, Moneta MV, Rico-Urbe LA, Ayuso-Mateos JL, Mundó J, Haro JM. Loneliness and depression in the elderly: the role of social network. *Soc Psychiatry Psychiatr Epidemiol.* 2017; 52:381-390.
8. Yu J, Li J, Cuijpers P, Wu S, Wu Z. Prevalence and correlates of depressive symptoms in Chinese older adults: A population-based study. *Int J Geriatr Psychiatry.* 2012; 27:305-312.
9. Cohen AK, Nussbaum J, Weintraub MLR, Nichols CR, Yen IH. Association of adult depression with educational attainment, aspirations, and expectations. *Prev Chronic Dis.* 2020; 17:E94.
10. Li Y, Wu Q, Guo L, Weerawardena NS, Luo F, Yu B. Dyadic effects of cognitive function on depressive symptoms among middle-aged and older Chinese couples.

- Int J Geriatr Psychiatry. 2023; 38:e5909.
11. Saha A, Mandal B, Muhammad T, Ali W. Decomposing the rural–urban differences in depression among multimorbid older patients in India: Evidence from a cross-sectional study. *BMC psychiatry*. 2024; 24:60.
 12. Wu Y, Dong W, Xu Y, Fan X, Su M, Gao J, Zhou Z, Niessen L, Wang Y, Wang X. Financial transfers from adult children and depressive symptoms among mid-aged and elderly residents in China-evidence from the China health and retirement longitudinal study. *BMC Public Health*. 2018; 18:882.
 13. World Health Organization. Ageing and health. <https://www.who.int/zh/news-room/fact-sheets/detail/ageing-and-health> (accessed May 6, 2024)
 14. World Health Organization. Comprehensive mental health action plan 2013–2030. <https://www.who.int/publications/i/item/9789240031029> (accessed May 6, 2024).
 15. Holtfreter K, Reisig MD, Turanovic JJ. Depression and infrequent participation in social activities among older adults: the moderating role of high-quality familial ties. *Aging Ment Health*. 2017; 21:379-388.
 16. Chiao C, Weng LJ, Botticello AL. Social participation reduces depressive symptoms among older adults: An 18-year longitudinal analysis in Taiwan. *BMC Public Health*. 2011; 11:292.
 17. Centers for Disease Control and Prevention (CDC). Suicide among older persons--United States, 1980-1992. *MMWR Morb Mortal Wkly Rep*. 1996; 45:3-6.
 18. Johnson PJ, Mentzer KM, Jou J, Upchurch DM. Unmet healthcare needs among midlife adults with mental distress and multiple chronic conditions. *Aging Ment Health*. 2022; 26:775-783.
 19. Wickrama KAS, Lee S, Klopach ET, Wickrama T. Stressful work conditions, positive affect, and physical health of middle-aged couples: A dyadic analysis. *Stress Health*. 2019; 35:382-395.
 20. Muhammad T, Meher T. Association of late-life depression with cognitive impairment: Evidence from a cross-sectional study among older adults in India. *BMC Geriatr*. 2021; 21:364.
 21. Wu Z, Zhong X, Peng Q, Chen B, Zhang M, Zhou H, Mai N, Huang X, Ning Y. Longitudinal association between cognition and depression in patients with late-life depression: A cross-lagged design study. *Front Psychiatry*. 2021; 12:577058.
 22. Park S, Jeong K, Lee S. A study on the longitudinal relationship between changes in depression and cognitive function among older adults living alone. *Healthcare (Basel)*. 2023; 11:2712.
 23. National Health Commission of the PRC. Notice on promoting the prevention and treatment of Alzheimer's disease through the "Alzheimer's Disease Prevention and Promotion Action Plan (2023-2025)". https://www.gov.cn/zhengce/zhengceku/202306/content_6886277.htm (accessed August 29, 2024). (in Chinese)
 24. Ory MG, Hoffman RR, 3rd, Yee JL, Tennstedt S, Schulz R. Prevalence and impact of caregiving: A detailed comparison between dementia and nondementia caregivers. *Gerontologist*. 1999; 39:177-185.
 25. Lee J, Paddock SM, Feeney K. Emotional distress and cognitive functioning of older couples: A dyadic analysis. *J Aging Health*. 2012; 24:113-140.
 26. Monin JK, Doyle M, Van Ness PH, Schulz R, Marottoli RA, Birditt K, Feeney BC, Kershaw T. Longitudinal associations between cognitive functioning and depressive symptoms among older adult spouses in the cardiovascular health study. *Am J Geriatr Psychiatry*. 2018; 26:1036-1046.
 27. Bassuk SS, Glass TA, Berkman LF. Social disengagement and incident cognitive decline in community-dwelling elderly persons. *Ann Intern Med*. 1999; 131:165-173.
 28. Gleib DA, Landau DA, Goldman N, Chuang Y-L, Rodríguez G, Weinstein M. Participating in social activities helps preserve cognitive function: An analysis of a longitudinal, population-based study of the elderly. *Int J Epidemiol*. 2005; 34:864-871.
 29. Engelhardt H, Buber I, Skirbekk V, Prskawetz A. Social involvement, behavioural risks and cognitive functioning among older people. *Ageing & Society*. 2010; 30:779-809.
 30. Conley TG, Hansen CB, Rossi PE. Plausibly Exogenous. *Rev Econ Stat*. 2012; 94:260-272.
 31. Kleibergen F, Paap R. Generalized reduced rank tests using the singular value decomposition. *J Econom*. 2006; 133:97-126.
 32. Stock J, Yogo M. Testing for Weak Instruments in Linear IV Regression. In: Identification and Inference for Econometric Models (Donald WKA, ed. Cambridge University Press, New York, 2005; pp. 80-108.
 33. Skarupski KA, de Leon CF, McCann JJ, Bienias JL, Wilson RS, Evans DA. Is lower cognitive function in one spouse associated with depressive symptoms in the other spouse? *Aging Ment Health*. 2006; 10:621-630.
 34. Tower RB, Kasl SV, Moritz DJ. The influence of spouse cognitive impairment on respondents' depressive symptoms: The moderating role of marital closeness. *J Gerontol B Psychol Sci Soc Sci*. 1997; 52:S270-S278.
 35. Hatfield E, Cacioppo JT, Rapson RL. Emotional contagion. *Curr Dir Psychol Sci*. 1993; 2:96-100.
 36. Tang J, Yu G, Yao X. Emotional contagion in the online depression community. *Healthcare (Basel)*. 2021; 9:1609.
 37. Braun M, Scholz U, Bailey B, Perren S, Hornung R, Martin M. Dementia caregiving in spousal relationships: A dyadic perspective. *Aging Ment Health*. 2009; 13:426-436.
 38. Moritz DJ, Kasl SV, Berkman LF. The health impact of living with a cognitively impaired elderly spouse: Depressive symptoms and social functioning. *J Gerontol*. 1989; 44:S17-S27.
 39. SapranaVICIUTE-Zabazlajeva L, Luksiene D, Virviciute D, Bobak M, Tamosiunas A. Link between healthy lifestyle and psychological well-being in Lithuanian adults aged 45–72: A cross-sectional study. *BMJ Open*. 2017; 7:e014240.
 40. Umberson D, Williams K, Powers DA, Liu H, Needham B. You make me sick: Marital quality and health over the life course. *J Health Soc Behav*. 2006; 47:1-16.
 41. Kim W, Lee T-H, Shin J, Park E-C. Depressive symptoms in spouse caregivers of dementia patients: A longitudinal study in South Korea. *Geriatr Gerontol Int*. 2017; 17:973-983.
 42. Pinquart M, Sörensen S. Gender differences in caregiver stressors, social resources, and health: An updated meta-analysis. *J Gerontol B Psychol Sci Soc Sci*. 2006; 61:P33-P45.
 43. Seeman TE, Lusignolo TM, Albert M, Berkman L. Social relationships, social support, and patterns of cognitive aging in healthy, high-functioning older adults: MacArthur studies of successful aging. *Health Psychol*. 2001; 20:243-255.

44. Schulz R, Sherwood PR. Physical and Psychological and mental health effects of family caregiving. *Am J Nurs.* 2008; 108(9 Suppl):23-7; quiz 27.
45. Pitkala KH, Routasalo P, Kautiainen H, Sintonen H, Tilvis RS. Effects of socially stimulating group intervention on lonely, older people's cognition: A randomized, controlled trial. *Am J Geriatr Psychiatry.* 2011; 19:654-663.
46. Conwell Y, Duberstein PR, Cox C, Herrmann JH, Forbes NT, Caine ED. Relationships of age and axis I diagnoses in victims of completed suicide: A psychological autopsy study. *Am J Psychiatry.* 1996; 153:1001-1008.
47. Ross CE, Mirowsky J. Refining the association between education and health: The effects of quantity, credential, and selectivity. *Demography.* 1999; 36:445-460.
48. Hamer M, Stamatakis E, Mishra G. Psychological distress, television viewing, and physical activity in children aged 4 to 12 years. *Pediatrics.* 2009; 123:1263-1268.
49. Schuller T, Preston J, Hammond C, Brassett-Grundy A, Bynner J. The benefits of learning: The impact of education on health, family life and social capital. Routledge, 2004; pp. 1-224.
50. Mavaddat N, Kinmonth AL, Sanderson S, Surtees P, Bingham S, Khaw KT. What determines Self-Rated Health (SRH)? A cross-sectional study of SF-36 health domains in the EPIC-Norfolk cohort. *J Epidemiol Community Health.* 2011; 65:800-806.
51. Jeon SY, Kim JL. Caregiving for a spouse with cognitive impairment: Effects on nutrition and other lifestyle factors. *J Alzheimers Dis.* 2021; 84:995-1003.
52. Williams CL, Newman D, Hammar LM. Preliminary study of a communication intervention for family caregivers and spouses with dementia. *Int J Geriatr Psychiatry.* 2018; 33:e343-e349.
53. Folder N, Power E, Rietdijk R, Christensen I, Togher L, Parker D. The effectiveness and characteristics of communication partner training programs for families of people with dementia: A systematic review. *Gerontologist.* 2024; 64:gnad095.
54. Liu Z, Sun YY, Zhong BL. Mindfulness-based stress reduction for family carers of people with dementia. *Cochrane Database Syst Rev.* 2018; 8:Cd012791.
55. Zhou Y, Hasdemir D, Ishado E, Borson S, Sadak T. Validation and expansion of a behavioral framework for dementia care partner resilience (CP-R). *Dementia (London).* 2023; 22:1392-1419.
56. Lins S, Hayder-Beichel D, Rucker G, Motschall E, Antes G, Meyer G, Langer G. Efficacy and experiences of telephone counselling for informal carers of people with dementia. *Cochrane Database Syst Rev.* 2014; 2014:Cd009126.

Received July 22, 2024; Revised September 4, 2024; Accepted September 17, 2024.

§These authors contributed equally to this work.

*Address correspondence to:

Shasha Yuan, Institute of Medical Information/Medical Library, Chinese Academy of Medical Sciences & Peking Union Medical College, No. 3 Yabao Road, Chaoyang District, Beijing 100020, China
E-mail: yuanshasha417@163.com

Released online in J-STAGE as advance publication September 22, 2024.

Sorafenib combined with TACE improves survival in patients with hepatocellular carcinoma with vascular invasion

Zhiqiang Han^{1,2,§}, Ruyuan Han^{1,3,§}, Yimeng Wang^{1,3,§}, Kangwei Zhu^{1,3}, Xiangdong Tian^{1,4}, Ping Chen^{1,3,*}, Tianqiang Song^{1,3,*}, Lu Chen^{1,3,5,*}

¹ Tianjin Medical University Cancer Institute and Hospital, National Clinical Research Center for Cancer, National Key Laboratory of Druggability Evaluation and Systematic Translational Medicine, Tianjin Key Laboratory of Digestive Cancer, Tianjin's Clinical Research Center for Cancer, Tianjin, China;

² Department of Anesthesiology, Tianjin Medical University Cancer Institute and Hospital, Tianjin, China;

³ Department of Hepatobiliary Cancer, Liver cancer research center, Tianjin Medical University Cancer Institute and Hospital, Tianjin, China;

⁴ Department of Endoscopy, Tianjin Medical University Cancer Institute and Hospital, Tianjin, China;

⁵ Department of Hepato-Biliary-Pancreatic Surgery, National Center for Global Health and Medicine, Tokyo, Japan.

SUMMARY Sorafenib is a recommended first-line therapy for advanced hepatocellular carcinoma (HCC). However, when used as monotherapy in patients in advanced stages, the prognosis remains suboptimal. This study aimed to evaluate the impact of transcatheter arterial chemoembolization (TACE) on survival outcomes in patients with advanced HCC treated with sorafenib, as well as to identify which subgroups may benefit most from the addition of TACE. This single-institution retrospective study included 92 patients diagnosed with Barcelona Clinic liver cancer (BCLC) stage C HCC who received sorafenib between August 2011 and December 2016. We assessed the influence of different treatment modalities on prognosis using multivariable regression analysis. Patients were categorized into three subgroups: those with vascular invasion, those with distant metastasis, and those with both risk factors. Baseline comparisons indicated no significant differences in clinical characteristics among the three groups. Survival analysis showed no statistically significant difference in overall survival (OS) between the subgroups. However, in the overall cohort of patients with BCLC stage C, multifactorial Cox regression analysis identified pre-treatment alpha-fetoprotein (AFP) levels ($p = 0.020$), alkaline phosphatase (ALP) levels ($p = 0.034$), and the absence of combination TACE therapy ($p = 0.008$) as independent risk factors affecting OS. Further subgroup Cox analyses revealed that the lack of combination TACE therapy was an independent risk factor for OS in both the vascular invasion group and the group with both risk factors. In conclusion, for patients with advanced HCC receiving sorafenib, the addition of TACE may enhance long-term survival, particularly in those with vascular invasion.

Keywords sorafenib, transcatheter arterial chemoembolization, hepatocellular carcinoma, cancer therapy

1. Introduction

Hepatocellular carcinoma (HCC) is one of the most prevalent malignant tumors worldwide (1). Early-stage liver cancer can be effectively treated through radical surgery or liver transplantation (2). However, due to the insidious nature of liver cancer, most patients are diagnosed at an advanced stage, missing the optimal window for surgical intervention (3,4). The advanced stage, classified as Barcelona Clinic liver cancer (BCLC) stage C, encompasses patients with vascular invasion, metastasis, or both, which are associated with poor prognostic indicators (5). For patients with BCLC

stage C, the introduction of the targeted therapeutic agent sorafenib represents a significant advancement in treatment (6). Sorafenib, recognized as the first targeted agent to improve the long-term prognosis of patients with advanced HCC, has demonstrated its efficacy in a multicenter phase 3 clinical trial (7). Consequently, it is considered a first-line treatment option for advanced liver cancer in many clinical guidelines (5,8).

However, the prognosis for patients with advanced HCC treated solely with sorafenib remains suboptimal (9). Consequently, several studies are exploring the use of sorafenib in combination with other therapies to enhance the prognosis of advanced liver cancer (10,11).

However, there is a paucity of research investigating the combination of sorafenib with interventional therapies. As a result, it remains controversial whether patients with advanced HCC are appropriate candidates for sorafenib combined with transcatheter arterial chemoembolization (TACE) therapy. This study aims to compare the efficacy of sorafenib combined with TACE therapy against sorafenib monotherapy, investigating whether the addition of TACE can improve outcomes for patients with advanced HCC.

Advanced HCC involves vascular invasion and distant metastasis, both of which significantly impact the prognosis. In large prospective cohorts of patients with BCLC stage C, survival rates vary significantly (12). The primary goal of the staging system is to classify patients into subgroups based on prognosis and tailor treatments accordingly. However, the current staging has limitations, and further subdivisions are needed for greater precision (5). This study aims to analyze patients with advanced HCC with varying risk factors to identify prognostic differences between subgroups and explore appropriate treatment options for each.

2. Materials and Methods

2.1. Patients

We retrospectively reviewed the records of 182 patients with BCLC stage C liver cancer who received sorafenib treatment between August 2011 and December 2016 at Tianjin Medical University Cancer Institute and Hospital (Figure 1). All patients were classified

according to the BCLC staging system. The inclusion criteria were: (1) treatment with sorafenib and (2) availability of complete follow-up data and adequate clinical pathology information. Patients ($n = 30$) lacking adequate clinical information were excluded, as were those with BCLC stage B ($n = 23$) or Child-Pugh class C cirrhosis ($n = 37$). Ultimately, 92 patients met the inclusion criteria and were included in the analysis. To ensure objectivity, all researchers were blinded to clinical outcomes during data collection. This study followed the principles of the Declaration of Helsinki (revised in 2013) and was approved by the Ethical Committee of Tianjin Medical University Cancer Institute and Hospital, with the requirement for informed consent waived. All data were anonymized to protect patient identities before analysis.

2.2. Classification of vascular invasion and metastasis

Patients were classified into three groups based on tumor characteristics: (1) vascular invasion only ($n = 24$), (2) metastasis only ($n = 48$), and (3) both vascular invasion and metastasis ($n = 20$). Vascular invasion was further subdivided into four categories: involvement of the branch portal vein alone ($n = 21$), the left, right, or main portal trunk ($n = 9$), the hepatic vein ($n = 4$), and combined involvement of the portal and hepatic veins ($n = 10$). Metastasis was categorized into three groups: lymph node metastasis alone ($n = 25$), distant organ metastasis alone ($n = 7$), and both types ($n = 36$). It is important to differentiate vascular invasion from vascular thrombosis, which is characterized by arterial enhancement, portal vein dilation, or the formation of

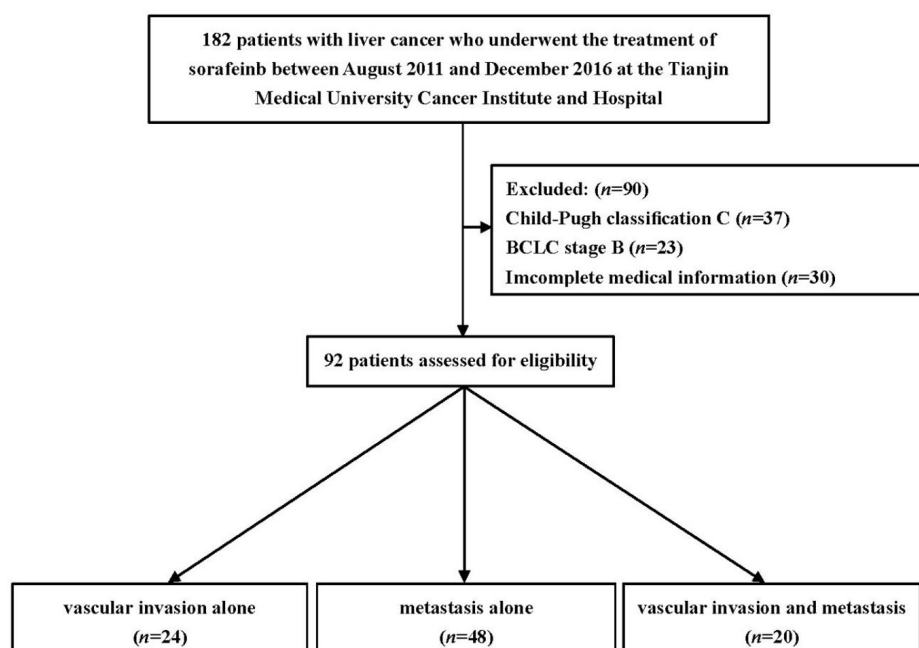


Figure 1. Flowchart of patient selection. BCLC, Barcelona Clinic Liver Cancer.

new thrombi adjacent to the tumor. Metastatic lymph nodes were diagnosed through histological examination or radiographic evidence of enlarged nodes.

2.3. Clinical characteristics of patients with BCLC stage C liver cancer

The data collected included demographic information (sex) and clinical history, such as pre-treatment alpha-fetoprotein (AFP), total bilirubin (TBIL), alkaline phosphatase (ALP), albumin (ALB), alanine aminotransferase (ALT), aspartate aminotransferase (AST), prothrombin time (PT) levels, hepatitis B virus/hepatitis C virus (HBV/HCV) status, liver cirrhosis, and ascites. Additionally, information regarding adjuvant therapies, including TACE and surgical history, was documented.

2.4. Postoperative management

Patients were followed up every three months with serum AFP measurements and imaging studies, which included magnetic resonance imaging (MRI), computed tomography (CT), or ultrasound. Overall survival (OS) was calculated from the initiation of sorafenib treatment; both clinical data and follow-up outcomes were meticulously recorded. We considered follow-up periods shorter than three months to be lost to follow-up. For patients who survived the follow-up period, the date of the last follow-up was recorded.

2.5. Statistical analysis

Patient data were analyzed using IBM SPSS Statistics for Windows (version 29.0; IBM Corp., Armonk, NY, USA). Continuous variables were compared

using unpaired *t*-tests, while categorical variables were analyzed using Mann–Whitney *U* tests. OS was estimated using the Kaplan–Meier method, with significance between groups assessed using the log-rank test. Multivariable analyses for OS were conducted, incorporating all significant variables identified through univariate analysis and utilizing Cox proportional hazards regression analysis. All statistical tests were two-sided, with a significance level set at $p < 0.05$.

3. Results

3.1. Baseline clinical characteristics and prognostic factors of 92 patients with BCLC stage C HCC

The demographics, clinical characteristics, and adjuvant therapies of all patients with BCLC stage are summarized in Table 1. Among the 92 patients, 82 were male, and 31 received TACE. Additionally, 65 patients had a history of chronic hepatitis virus B infection, while three had chronic hepatitis C infection. The numbers of patients with vascular invasion, metastasis, and both conditions were 24, 48, and 20, respectively. No statistically significant difference in OS was observed among the three groups (vascular invasion vs. metastasis, $p = 0.678$; vascular invasion vs. both, $p = 0.637$; metastasis vs. both, $p = 0.995$; Figure 2A). Furthermore, the differences in baseline clinical characteristics among the vascular invasion group, the metastasis group, and the group with both risk factors were not statistically significant. We then incorporated these clinical characteristics into the subsequent survival analysis. Univariate analysis identified four clinical characteristics — pre-treatment AFP, ALP, non-co-application of TACE, and the surgical history — as risk factors related to the survival of patients with BCLC

Table 1. Baseline clinical characteristics in the 92 HCC patients with BCLC stage C

BCLC stage C HCC patients (<i>n</i> = 92)	Vascular invasion (<i>n</i> = 24)	Metastasis (<i>n</i> = 48)	Both (<i>n</i> = 20)	<i>p</i> -value
Sex male/female	22/2	42/6	18/2	0.859
HBV (Yes/No)	18/6	32/16	15/5	0.684
HCV (Yes/No)	1/23	2/46	0/20	0.653
Liver cirrhosis (Yes/No)	19/5	33/15	15/5	0.629
PT(sec) >13.7/≤13.7	1/23	3/45	1/19	0.931
Pre-medication AFP (ng/mL)				0.312
>20/≤20	17/7	32/16	17/3	
TBIL (μmol/L) >21/≤21	12/12	23/25	11/9	0.869
ALB(g/L) >40/≤40	13/11	22/26	9/11	0.771
ALP (U/L) >125/≤125	13/11	21/27	13/7	0.266
ALT(U/L) >40/≤40	16/8	24/24	11/9	0.410
AST(U/L) >40/≤40	17/7	25/23	15/5	0.123
Accompanied by TACE				0.069
Yes	4	21	6	
No	20	27	14	
History of surgery (Yes/No)	10/14	24/24	7/13	0.501

HBV, hepatitis B virus; HCV, hepatitis C virus; PT, prothrombin time; AFP, alpha fetoprotein; TBIL, total bilirubin; ALB, albumin; ALP, alkaline phosphatase; ALT, alanine aminotransferase; AST, aspartate aminotransferase; TACE, transcatheter arterial chemoembolization; HCC, hepatocellular carcinoma; BCLC, Barcelona Clinic liver cancer.

stage C. Specifically, pre-treatment AFP ($p = 0.020$, hazard ratio [HR] = 1.9; 95% confidence interval [CI], 1.1–3.1), ALP ($p = 0.034$, HR = 1.6; 95% CI, 1.0–2.5), and non-co-application of TACE ($p = 0.008$, HR = 2.1; 95% CI, 1.2–3.5) emerged as independent risk factors associated with OS in all patients with BCLC stage C (Table 2 and Figures 2B, 2C, and 2D). Notably, patients who received TACE demonstrated a better OS rate compared to those who did not. As highlighted in the introduction, vascular invasion and metastasis were

identified as key risk factors in patients with BCLC stage C. Consequently, we divided the patients into three subgroups: those with vascular invasion, those with metastasis, and those with both risk factors. Our research further analyzed the survival effects of sorafenib in combination with TACE on patients with BCLC stage C liver cancer across these different subgroups.

3.2. Prognostic factors related to OS rates in patients with BCLC stage C HCC and vascular invasion alone

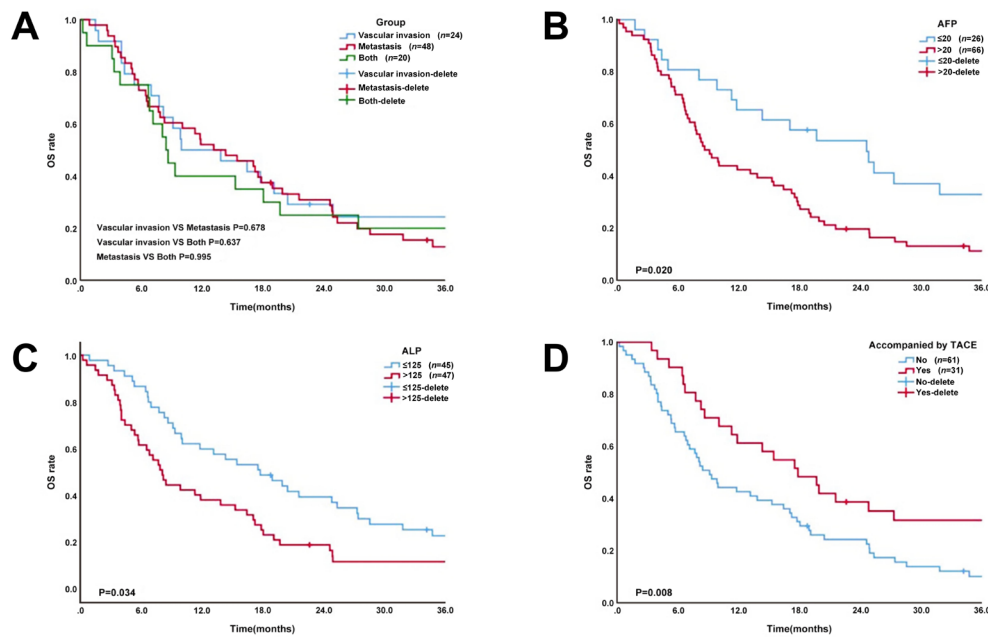


Figure 2. OS rates among patients with patients with BCLC stage C HCC. (A) Kaplan-Meier OS curves for subgroups of patients with advanced stage. (B) Kaplan-Meier OS curves based on AFP levels. (C) Kaplan-Meier OS curves based on ALP levels. (D) Kaplan-Meier OS curves comparing patients who received TACE with those who did not. (AFP, alpha fetoprotein; ALP, alkaline phosphatase; TACE, transcatheter arterial chemoembolization; OS, overall survival; HCC, hepatocellular carcinoma; BCLC, Barcelona Clinic liver cancer).

Table 2. Univariate and multivariate analysis of prognostic factors associated with OS in all 92 HCC patients with BCLC stage C

BCLC stage C HCC patients (n = 92)	Number	Univariate Analysis		Multivariate Analysis	
		three-year OS (%)	p-value	HR (95% CI)	p-value
Sex male/female	82/10	16.4/30.0	0.602		
HBV (Yes/No)	65/27	18.6/14.8	0.698		
HCV (Yes/No)	3/89	33.3/16.8	0.800		
Liver cirrhosis (Yes/No)	67/25	18.1/16.0	0.868		
PT(sec) >13.7/≤13.7	5/87	0.0/18.5	0.117		
Pre-medication AFP (ng/mL)			0.007*		0.020*
>20/≤20	66/26	11.3/33.0		1.9 (1.1,3.1)	
TBIL (μmol/L) >21/≤21	46/46	21.7/12.8	0.601		
ALB(g/L) >40/≤40	44/48	16.0/18.8	0.766		
ALP (U/L) >125/≤125	47/45	12.0/23.0	0.040*	1.6 (1.0,2.5)	0.034*
ALT(U/L) >40/≤40	51/41	22.7/10.3	0.137		
AST(U/L) >40/≤40	57/35	14.0/22.6	0.086		
Accompanied by TACE			0.001*	2.1 (1.2,3.5)	0.008*
Yes	31	31.7			
No	61	10.1			
History of surgery (Yes/No)	41/51	12.9/20.8	0.046*		0.515

HBV, hepatitis B virus; HCV, hepatitis C virus; PT, prothrombin time; AFP, alpha fetoprotein; TBIL, total bilirubin; ALB, albumin; ALP, alkaline phosphatase; ALT, alanine aminotransferase; AST, aspartate aminotransferase; TACE, transcatheter arterial chemoembolization; OS, overall survival; CI, confidence interval; HCC, hepatocellular carcinoma; BCLC, Barcelona Clinic liver cancer.

The variables included in the univariate and Cox multivariate analyses for patients with BCLC stage C and vascular invasion alone are summarized in Table 3. Following the univariate analysis for OS, the final multivariate model identified only one independent prognostic factor: the presence of TACE. The multivariate analysis indicated that patients in the TACE group had a significantly better OS rate compared to those in the non-TACE group (HR = 8.5; 95% CI, 1.1–65.3; $p = 0.040$; Figure 3A).

3.3. Prognostic factors related to OS rates in patients with BCLC stage C HCC and metastasis alone

The variables included in the univariate and Cox multivariate analyses for patients with BCLC stage C and metastasis alone are summarized in Table 4. After conducting the univariate analysis for OS, the final multivariate model revealed that there were no independent prognostic factors. However, the univariate analysis indicated that ALP level was a significant

Table 3. Univariate and multivariate analysis of prognostic factors associated with OS in 24 patients with BCLC stage C HCC with vascular invasion

Patients with vascular invasion ($n = 24$)	Number	Univariate Analysis		Multivariate Analysis	
		three-year OS (%)	p -value	HR (95% CI)	p -value
Sex male/female	22/2	26.5/0.0	0.159		
HBV Yes/No	18/6	20.8/33.3	0.389		
HCV Yes/No	1/23	0.0/25.4	0.495		
Liver cirrhosis Yes/No	19/5	19.7/40.0	0.895		
PT(sec) >13.7/≤13.7	1/23	0.0/25.4	0.042*	6.1(0.6,58.4)	0.119
Pre-medication AFP (ng/mL) >20/≤20	17/7	8.8/57.1	0.065		
TBIL (μmol/L) >21/≤21	12/12	25.0/22.2	0.885		
ALB(g/L) >40/≤40	13/11	20.5/27.3	0.858		
ALP (U/L) >125/≤125	13/11	20.5/27.3	0.991		
ALT(U/L) >40/≤40	16/8	25.0/25.0	0.601		
AST(U/L) >40/≤40	17/7	11.8/57.1	0.078		
Accompanied by TACE			0.014*	8.5(1.1,65.3)	0.040*
Yes	4	75.0			
No	20	15.0			
History of surgery Yes/No	10/14	10.0/35.7	0.259		

HBV, hepatitis B virus; HCV, hepatitis C virus; PT, prothrombin time; AFP, alpha fetoprotein; TBIL, total bilirubin; ALB, albumin; ALP, alkaline phosphatase; ALT, alanine aminotransferase; AST, aspartate aminotransferase; TACE, transcatheter arterial chemoembolization; OS, overall survival; CI, confidence interval; HCC, hepatocellular carcinoma; BCLC, Barcelona Clinic liver cancer.

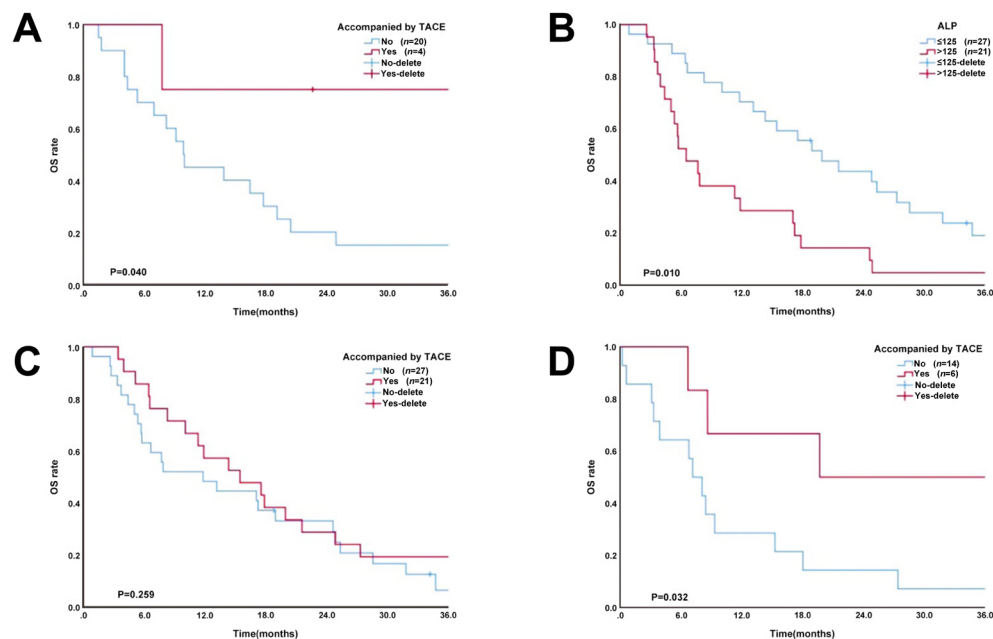


Figure 3. OS rates in subgroups of patients with BCLC stage C HCC. (A) Kaplan-Meier OS curves for the vascular invasion group, categorized by TACE treatment. **(B)** Kaplan-Meier OS curves for the metastasis group, based on ALP levels. **(C)** Kaplan-Meier OS curves for the metastasis group, categorized by TACE treatment. **(D)** Kaplan-Meier OS curves for patients with both risk factors categorized by TACE treatment. (TACE, transcatheter arterial chemoembolization; ALP, alkaline phosphatase; OS, overall survival; HCC, hepatocellular carcinoma; BCLC, Barcelona Clinic liver cancer).

risk factor ($p = 0.010$; Figure 3B). Regarding TACE, no statistically significant difference was found in the metastasis subgroup (Figure 3C).

3.4. Prognostic factors related to OS rates in patients with BCLC stage C HCC with both vascular invasion and metastasis

The variables included in the univariate and Cox multivariate analyses for patients with BCLC stage C, vascular invasion, and metastasis are summarized in Table 5. Following the univariate analysis for OS,

the final multivariate model again identified "presence of TACE," as an independent prognostic factor. The multivariate analysis demonstrated that patients in the non-TACE group had a significantly worse OS rate compared to those in the TACE group (HR = 4.1; 95% CI, 1.1–14.8; $p = 0.032$; Figure 3D).

4. Discussion

HCC is one of the most prevalent malignant tumors worldwide, ranking as the sixth most common cancer and the third leading cause of cancer-related

Table 4. Univariate and multivariate analysis of prognostic factors associated with OS in 48 patients with BCLC stage C HCC with metastasis

Patients with vascular invasion (n = 48)	Number	Univariate Analysis		Multivariate Analysis	
		three-year OS (%)	p-value	HR (95% CI)	p-value
Sex male/female	42/6	14.3/33.3	0.599		
HBV (Yes/No)	32/16	13.5/12.5	0.892		
HCV (Yes/No)	2/46	50.0/11.1	0.471		
Liver cirrhosis (Yes/No)	33/15	19.7/0.0	0.154		
PT(sec) >13.7/≤13.7	3/45	0.0/13.8	0.668		
Pre-medication AFP (ng/mL)					
>20/≤20	32/16	12.5/21.1	0.109		
TBIL (μmol/L) >21/≤21	23/25	13.0/13.5	0.721		
ALB(g/L) >40/≤40	22/26	10.4/15.4	0.392		
ALP (U/L) >125/≤125	21/27	4.8/19.0	0.010*		
ALT(U/L) >40/≤40	24/24	23.1/0.0	0.105		
AST(U/L) >40/≤40	25/23	12.0/12.9	0.381		
Accompanied by TACE			0.259		
Yes	21	19.0			
No	27	6.2			
History of surgery (Yes/No)	24/24	13.0/12.5	0.512		

HBV, hepatitis B virus; HCV, hepatitis C virus; PT, prothrombin time; AFP, alpha fetoprotein; TBIL, total bilirubin; ALB, albumin; ALP, alkaline phosphatase; ALT, alanine aminotransferase; AST, aspartate aminotransferase; TACE, transcatheter arterial chemoembolization; OS, overall survival; CI, confidence interval; HCC, hepatocellular carcinoma; BCLC, Barcelona Clinic liver cancer.

Table 5. Univariate and multivariate analysis of prognostic factors associated with OS in 20 patients with BCLC stage C HCC with vascular invasion and metastasis

Patients with vascular invasion (n = 20)	Number	Univariate Analysis		Multivariate Analysis	
		three-year OS (%)	p-value	HR (95% CI)	p-value
Sex male/female	18/2	16.7/50.0	0.432		
HBV (Yes/No)	15/5	26.7/0.0	0.200		
HCV (Yes/No)	0/20	20.0			
Liver cirrhosis (Yes/No)	15/5	13.3/40.0	0.234		
PT(sec) >13.7/≤13.7	1/19	0.0/21.1	0.004*	14.0 (0.9,224.1)	0.063
Pre-medication AFP (ng/mL)					
>20/≤20	17/3	17.6/33.3	0.325		
TBIL (μmol/L) >21/≤21	11/9	36.4/0.0	0.202		
ALB(g/L) >40/≤40	9/11	22.2/18.2	0.735		
ALP (U/L) >125/≤125	13/7	15.4/28.6	0.535		
ALT(U/L) >40/≤40	11/9	18.2/22.2	0.970		
AST(U/L) >40/≤40	15/5				
Accompanied by TACE			0.017*	4.1 (1.1,14.8)	0.032*
Yes	6	50.0			
No	14	7.1			
History of surgery (Yes/No)	7/13	14.3/23.1	0.052		

HBV, hepatitis B virus; HCV, hepatitis C virus; PT, prothrombin time; AFP, alpha fetoprotein; TBIL, total bilirubin; ALB, albumin; ALP, alkaline phosphatase; ALT, alanine aminotransferase; AST, aspartate aminotransferase; TACE, transcatheter arterial chemoembolization; OS, overall survival; CI, confidence interval; HCC, hepatocellular carcinoma; BCLC, Barcelona Clinic liver cancer.

mortality globally (1). Due to its insidious onset and rapid progression, most patients are diagnosed with either locally advanced disease or distant metastasis, corresponding to advanced BCLC stage C, which includes portal vein thrombosis, lymph node involvement, or extrahepatic metastasis (2). This advanced stage accounts for a significant proportion of cases, with 50% to 60% of patients receiving their initial clinical diagnosis at this point, often when the disease has already reached a severe state. In the absence of effective intervention, OS is typically short, contributing to the stagnation of improvements in liver cancer prognosis in recent years (13).

Sorafenib is an oral multi-kinase inhibitor that targets several receptor tyrosine kinases, including vascular endothelial growth factor receptor-2, vascular endothelial growth factor receptor-3, platelet-derived growth factor beta, and members of the Raf family of serine or threonine kinases, thereby exerting its anti-tumor effects (14,15). It was the first targeted drug demonstrated to be effective in treating advanced HCC (16). Although newer therapies, such as lenvatinib and durvalumab, have emerged, they have yet to show significantly superior efficacy compared to sorafenib in phase III clinical trials (5,17). While studies indicate that combinations such as camrelizumab plus rivoceranib may yield better outcomes than sorafenib alone, this does not suggest that sorafenib cannot be enhanced when combined with other treatments (18). Consequently, sorafenib remains a key option in the treatment of liver cancer and continues to be recommended as a first-line therapy for advanced HCC in many clinical guidelines (19).

TACE involves injecting chemotherapeutic agents and embolic materials into the main artery supplying the tumor, leading to localized tumor necrosis (20). However, because this technique primarily induces ischemic necrosis, it may stimulate the upregulation of angiogenic factors such as vascular endothelial growth factor and platelet-derived growth factor beta, potentially contributing to tumor recurrence or metastasis (21). The ability of sorafenib to inhibit these pro-angiogenic effects following TACE suggests that combining sorafenib with TACE could enhance the anti-tumor effect (22,23). Recent studies have shown that this combination significantly improves the prognosis of patients with advanced HCC compared to TACE alone. However, since TACE is not typically recommended for patients in advanced stages, its efficacy in this setting remains uncertain. Therefore, it cannot be conclusively assumed that adding TACE to sorafenib therapy will yield better outcomes than sorafenib monotherapy (24,25).

Our study found that the combination of sorafenib and TACE significantly improved prognosis compared to sorafenib alone in all patients with advanced HCC. Multifactorial analysis indicated that not using TACE

was an independent risk factor affecting OS. Therefore, combining TACE with sorafenib may lead to better outcomes for patients with advanced HCC.

To further identify the patient groups that may benefit most from TACE, we conducted a subgroup analysis. The results revealed no significant difference in prognosis between the vascular invasion group, the distant metastasis group, and the group with both risk factors. However, the absence of TACE was an independent risk factor for prognosis in both the vascular invasion group and the group with both risk factors, but not in the distant metastasis group. This suggests that TACE is particularly appropriate for patients with advanced HCC who exhibit vascular invasion.

Several limitations of our study should be acknowledged. First, it was a retrospective study, with data collected from 92 patients over a 10-year period. The small sample size is a common limitation in studies focusing on patients with BCLC stage C HCC treated with sorafenib, largely due to the rarity of the disease. Second, treatment plans and standards were influenced by physician experience and patient preferences, which could have affected the study outcomes. Consequently, randomized controlled trials are needed to provide more definitive comparisons. Finally, our analysis focused solely on short-term survival.

In conclusion, despite its limitations, this study offers valuable insights for clinical treatment, owing to the rigor of its experimental design. First, for patients with advanced HCC, there was no significant difference in prognosis among those vascular invasions, distant metastases, or both risk factors. Therefore, stratifying patients with advanced disease based on these risk factors may be unreliable. Secondly, for patients with advanced disease who have vascular invasion, combining TACE with sorafenib therapy may yield better efficacy.

Funding: This work was supported by the National Natural Science Foundation of China (Grants 82373365 and 82173317), Natural Science Foundation of Tianjin (23JCYBJC00600) and the Tianjin Key Medical Discipline Construction Project (TJYXZDXK-009A).

Conflict of Interest: The authors have no conflicts of interest to disclose.

References

1. Sung H, Ferlay J, Siegel RL, Laversanne M, Soerjomataram I, Jemal A, Bray F. Global Cancer Statistics 2020: GLOBOCAN Estimates of Incidence and Mortality Worldwide for 36 Cancers in 185 Countries. *CA Cancer J Clin.* 2021; 71:209-249.
2. Yang JD, Hainaut P, Gores GJ, Amadou A, Plymoth A, Roberts LR. A global view of hepatocellular carcinoma: trends, risk, prevention and management. *Nat Rev*

- Gastroenterol Hepatol. 2019; 16:589-604.
3. Song T, Lang M, Ren S, Gan L, Lu W. The past, present and future of conversion therapy for liver cancer. *Am J Cancer Res.* 2021; 11:4711-4724.
 4. Sun HC, Zhou J, Wang Z, *et al.* Chinese expert consensus on conversion therapy for hepatocellular carcinoma (2021 edition). *Hepatobiliary Surg Nutr.* 2022; 11:227-252.
 5. Reig M, Forner A, Rimola J, *et al.* BCLC strategy for prognosis prediction and treatment recommendation: The 2022 update. *J Hepatol.* 2022; 76:681-693.
 6. Llovet JM, Ricci S, Mazzaferro V, *et al.* Sorafenib in advanced hepatocellular carcinoma. *The N Engl J Med.* 2008; 359:378-390.
 7. Cheng AL, Kang YK, Chen Z, *et al.* Efficacy and safety of sorafenib in patients in the Asia-Pacific region with advanced hepatocellular carcinoma: a phase III randomised, double-blind, placebo-controlled trial. *Lancet Oncol.* 2009; 10:25-34.
 8. Bruix J, Chan SL, Galle PR, Rimassa L, Sangro B. Systemic treatment of hepatocellular carcinoma: An EASL position paper. *J Hepatol.* 2021; 75:960-974.
 9. Chen Q, Sun Q, Zhang J, Li B, Feng Q, Liu J. Cost-effectiveness analysis of Tislelizumab vs Sorafenib as the first-line treatment of unresectable hepatocellular carcinoma. *PloS One.* 2024; 19:e0295090.
 10. Schmid I, Häberle B, Albert MH, Corbacioglu S, Fröhlich B, Graf N, Kammer B, Kontny U, Leuschner I, Scheel-Walter HG, Scheurlen W, Werner S, Wiesel T, von Schweinitz D. Sorafenib and cisplatin/doxorubicin (PLADO) in pediatric hepatocellular carcinoma. *Pediatr Blood Cancer.* 2012; 58:539-544.
 11. Jouve JL, Lecomte T, Bouché O, *et al.* Pravastatin combination with sorafenib does not improve survival in advanced hepatocellular carcinoma. *J Hepatol.* 2019; 71:516-522.
 12. Giannini EG, Bucci L, Garuti F, *et al.* Patients with advanced hepatocellular carcinoma need a personalized management: A lesson from clinical practice. *Hepatology (Baltimore, Md).* 2018; 67:1784-1796.
 13. Ganesan P, Kulik LM. Hepatocellular Carcinoma: New Developments. *Clin Liver Dis.* 2023; 27:85-102.
 14. Patidar Y, Chandel K, Condati NK, Srinivasan SV, Mukund A, Sarin SK. Transarterial Chemoembolization (TACE) Combined With Sorafenib versus TACE in Patients With BCLC Stage C Hepatocellular Carcinoma - A Retrospective Study. *J Clin Exp Hepatol.* 2022; 12:745-754.
 15. Abdelrahim M, Victor D, Esmail A, Kodali S, Graviss EA, Nguyen DT, Moore LW, Saharia A, McMillan R, Fong JN, Uosef A, Elshawwaf M, Heyne K, Ghobrial RM. Transarterial Chemoembolization (TACE) Plus Sorafenib Compared to TACE Alone in Transplant Recipients with Hepatocellular Carcinoma: An Institution Experience. *Cancers.* 2022; 14.
 16. Man S, Luo C, Yan M, Zhao G, Ma L, Gao W. Treatment for liver cancer: From sorafenib to natural products. *Eur J Med Chem.* 2021; 224:113690.
 17. Kudo M, Finn RS, Qin S, *et al.* Lenvatinib versus sorafenib in first-line treatment of patients with unresectable hepatocellular carcinoma: a randomised phase 3 non-inferiority trial. *Lancet (London, England).* 2018; 391:1163-1173.
 18. Qin S, Chan SL, Gu S, *et al.* Camrelizumab plus rivoceranib versus sorafenib as first-line therapy for unresectable hepatocellular carcinoma (CARES-310): a randomised, open-label, international phase 3 study. *Lancet (London, England).* 2023; 402:1133-1146.
 19. Gordan JD, Kennedy EB, Abou-Alfa GK, *et al.* Systemic Therapy for Advanced Hepatocellular Carcinoma: ASCO Guideline. *J Clin Oncol.* 2020; 38:4317-4345.
 20. Wang J, Xu H, Wang Y, Feng L, Yi F. Efficacy and Safety of Drug-Eluting Bead TACE in the Treatment of Primary or Secondary Liver Cancer. *Can J Gastroenterol Hepatol.* 2023; 2023:5492931.
 21. Llovet JM, De Baere T, Kulik L, Haber PK, Gretten TF, Meyer T, Lencioni R. Locoregional therapies in the era of molecular and immune treatments for hepatocellular carcinoma. *Nat Rev Gastroenterol Hepatol.* 2021; 18:293-313.
 22. Gorodetski B, Chapiro J, Schernthaner R, *et al.* Advanced-stage hepatocellular carcinoma with portal vein thrombosis: conventional versus drug-eluting beads transcatheter arterial chemoembolization. *Eur Radiol.* 2017; 27:526-535.
 23. Jiang E, Shangguan AJ, Chen S, Tang L, Zhao S, Yu Z. The progress and prospects of routine prophylactic antiviral treatment in hepatitis B-related hepatocellular carcinoma. *Cancer Lett.* 2016; 379:262-267.
 24. Kudo M, Ueshima K, Ikeda M, *et al.* Randomised, multicentre prospective trial of transarterial chemoembolisation (TACE) plus sorafenib as compared with TACE alone in patients with hepatocellular carcinoma: TACTICS trial. *Gut.* 2020; 69:1492-1501.
 25. Fan W, Zhu B, Chen S, Wu Y, Zhao X, Qiao L, Huang Z, Tang R, Chen J, Lau WY, Chen M, Li J, Kuang M, Peng Z. Survival in Patients With Recurrent Intermediate-Stage Hepatocellular Carcinoma: Sorafenib Plus TACE vs TACE Alone Randomized Clinical Trial. *JAMA Oncol.* 2024; 10:1047-1054.
- Received September 17, 2024; Revised October 12, 2024; Accepted October 15, 2024.
- [§]These authors contributed equally to this work.
- *Address correspondence to:
 Lu Chen, Tianqiang Song, and Ping Chen, Department of Hepatobiliary Cancer, Liver cancer research center, Tianjin Medical University Cancer Institute and Hospital, National Clinical Research Center for Cancer, National Key Laboratory of Druggability Evaluation and Systematic Translational Medicine, Tianjin Key Laboratory of Digestive Cancer, Tianjin's Clinical Research Center for Cancer, Tianjin 300060, China.
 E-mail: chenlu@tmu.edu.cn (LC); tjchi@hotmail.com (TS); chenping@tjmuch.com (PC)
- Released online in J-STAGE as advance publication October 18, 2024.

FNDC5/Irisin mitigates high glucose-induced neurotoxicity in HT22 cell *via* ferroptosis

Lingling Yang^{1,§}, Xiaohan Zhou^{1,§}, Tian Heng¹, Yinghai Zhu^{1,2}, Lihuan Gong¹, Na Liu¹, Xiuqing Yao^{1,3,4,*}, Yaxi Luo^{1,*}

¹Department of Rehabilitation, The Second Affiliated Hospital of Chongqing Medical University, Chongqing, China;

²Department of Rehabilitation, The Central Hospital of Enshi Tujia and Miao Autonomous Prefecture, Enshi Clinical College of Wuhan University, Enshi, China;

³Chongqing Municipality Clinical Research Center for Geriatric Medicine, Chongqing, China;

⁴Department of Rehabilitation Therapy, Chongqing Medical University, Chongqing, China.

SUMMARY Diabetes-induced neuropathy represents a major etiology of dementia, highlighting an urgent need for the development of effective therapeutic interventions. In this study, we explored the role of fibronectin type III domain containing 5 (FNDC5)/Irisin in mitigating hyperglycemia-induced neurotoxicity in HT22 cells and investigated the underlying mechanisms. Our findings reveal that high glucose conditions are neurotoxic, leading to reduced viability of HT22 cells and increased apoptosis. Furthermore, the elevated expression of the intracellular ferroptosis marker Acyl-CoA Synthetase Long Chain Family Member 4 (ACSL4), along with increased levels of ferrous ions and malondialdehyde (MDA), suggests that high glucose conditions may induce ferroptosis in HT22 cells. FNDC5/Irisin treatment effectively mitigates high glucose-induced neurotoxicity and ferroptosis in HT22 cells. Mechanistically, FNDC5/Irisin enhances cellular antioxidant capacity, regulates ACSL4 expression, and improves intracellular redox status, thereby inhibiting ferroptosis and increasing HT22 cell survival under high-glucose conditions. These results highlight the neuroprotective potential of FNDC5/Irisin in high glucose environments, offering a promising avenue for developing treatments for diabetes-related neurodegenerative diseases.

Keywords high-glucose environment, neurotoxicity, FNDC5/Irisin, ferroptosis

1. Introduction

Type 2 diabetes mellitus (T2DM) comprises approximately 96% of all diabetes cases (1-4). Notably, the prevalence of mild cognitive impairment among individuals with T2DM reaches as high as 45% (5), a major contributor to dementia and a potentially modifiable risk factor (6). As such, diabetes-induced brain aging and cognitive decline are significant complications, underscoring the importance of investigating the mechanisms underlying hyperglycemia-driven cognitive dysfunction for the prevention and amelioration of diabetic brain injury.

Studies have identified ferroptosis as a key driver of diabetic cognitive dysfunction, with increased iron deposition observed in the brains of patients with T2DM and cognitive impairment (7). Excess iron catalyzes the Fenton reaction, resulting in the overproduction of reactive oxygen species (ROS), which subsequently depletes glutathione, triggers lipid peroxidation, and

exhausts endogenous antioxidant defenses, ultimately leading to neuronal ferroptosis, synaptic dysfunction, and cognitive decline (8). Inhibition of ferroptosis has been shown to mitigate hippocampal neuronal damage and synaptic plasticity impairments, effectively improving cognitive function (9-11). These findings suggest that high-glucose-induced neurotoxicity is closely associated with ferroptosis, highlighting the inhibition of ferroptosis as a promising therapeutic strategy for alleviating cognitive deficits in T2DM.

The FNDC5 gene is highly expressed in the hippocampus and cortex of C57BL/6 mice (12). Its cleaved form, irisin, has been detected in the cerebrospinal fluid (13,14). Studies suggest that FNDC5/irisin plays a critical role in cognitive and memory functions (14,15). Furthermore, FNDC5/irisin attenuates high-glucose-induced cytotoxicity via the AMPK-insulin receptor signaling pathway (16-18). In addition, irisin has been implicated in ferroptosis regulation in a mouse model of sepsis-associated encephalopathy, where

FNDC5/irisin reduced Fe²⁺, ROS, malondialdehyde (MDA), and acyl-CoA synthetase long-chain family member 4 (ACSL4) levels, thereby inhibiting ferroptosis and improving learning and memory functions (19). However, whether FNDC5/irisin can mitigate high-glucose-induced neurotoxicity by inhibiting ferroptosis remains unclear and warrants further investigation.

In this study, we observed that high glucose conditions induced neurotoxicity and triggered ferroptosis in HT22 cells. Irisin treatment effectively mitigated high glucose-induced neurotoxicity and ferroptosis. Additionally, we found that high glucose reduced the expression of FNDC5 in HT22 cells. Overexpression of FNDC5 attenuated high glucose-induced neurotoxicity, enhanced synaptic plasticity, and inhibited ferroptosis. Exogenous irisin supplementation also effectively alleviated hyperglycemic neurotoxicity and ferroptosis in the context of reduced FNDC5 expression. In summary, our data suggest that FNDC5/irisin exerts neuroprotective effects through the inhibition of ferroptosis under high glucose conditions, providing new insights into diabetes-induced cognitive impairment.

2. Materials and Methods

2.1. Cell culture and glucose treatment

HT22 murine hippocampal cells were kindly provided by the Chongqing Key Laboratory of Translational Medicine for Cognitive Development and Learning and Memory Disorders, Institute of Pediatrics, Children's Hospital of Chongqing Medical University. The cells were cultured in Dulbecco's modified Eagle's medium supplemented with 10% fetal bovine serum, 100 U/mL penicillin and 100 µg/mL streptomycin. For high glucose treatment, 750 mM stock solution of high glucose was prepared with D-(+)-glucose and glucose-free medium and diluted to different concentrations with glucose-free complete medium. 25 µg of Irisin lyophilized powder was added with 250 µL of glucose-free medium and mixed slowly up and down to make a stock solution of Irisin at a concentration of 100 ng/mL, and then diluted to gradient dilution with the corresponding glucose-concentrated medium according to the need of the experiments. All cells were cultured in a humidified cell culture incubator (Thermo Fisher) at 37°C with 5% CO₂.

2.2. Cell transfection

Plasmid transfection sequences were designed by Shanghai Genechem Co., For gene overexpression, the FNDC5 overexpression plasmid (CMV enhancer-MCS-3flag-polyA-EF1A-zsGreen-sv40-puromycin) was constructed by cloning the corresponding coding sequence into the GV657 vector. For knockdown, the FNDC5 knockdown plasmid (hU6-MCS-CBh-gcGFP-

IRES-puromycin) was constructed by cloning the corresponding coding sequence into the GV493 vector. lipofectamine 3000 reagent (Invitrogen, cat # L3000015, USA) was used for cell transfection according to the manufacturer's instructions. 48 hours after transfection, cells were used for further experiments.

2.3. Chemicals

Irisin (# 8880) purchased from R&D, fetal bovine serum (#10099141C), penicillin-streptomycin (#15140122), 0.25% Trypsin-EDTA(1×) (#25200056), basic DMEM (#C11995500BT), DMEM, glucose free (#11966025), Opti-MEM™ I serum reduced media (#31985062) purchased from Gibco, bovine serum albumin (#A8020), D-(+)-glucose (#G6152), D-Mannitol (#M4125), ferroptosis inhibitor ferrostatin-1 (fer-1) (#SML0583) purchased from sigma, ferroptosis inducer Erastin (#HY-15763) purchased from MCE.

2.4. CCK-8 assay

The CCK-8 (MCE, #HY-K0301, USA) assay kit was used to assess cell viability precisely according to the instructions. HT22 cells were intervened as required for the experiment, and the medium was replaced with CCK-8 working solution containing 10% CCK-8 reagent after treatment. Cells were incubated at 37°C for 1 hour. A microplate reader measured the absorbance (450 nm) of each well.

2.5. FerroOrange staining

Intracellular Fe²⁺ was detected using a FerroOrange probe (DOJINDO, #F374, Japan). After treatment according to the experimental protocol, the culture medium was discarded, HT22 cells were washed three times with PBS solution, and the FerroOrange working solution with a final concentration of 1 µmol/L was diluted with DMEM and processed for 30 minutes at 37°C in a 5% CO₂ incubator, nuclei were stained by adding 5 µl of Hoechst 33342 (Beyotime, # C1025, China) staining solution, incubated for 5 min at room temperature and protected from light. Finally, the stained cells were observed using a fluorescence microscope.

2.6. Iron measurement

Intracellular ferrous iron levels were assessed using an iron assay kit (Elabscience, #E-BC-K881-M, China). Prior to the experiment, the standard protectant was mixed with the buffer as required. After the indicated treatments, HT22 cells were harvested to lysed cells by adding 0.2 mL of buffer per 1×10⁶ cells, centrifuged at 15,000×g for 10 min, and the supernatant was taken for ferrous iron measurement assay. Experimental procedures strictly followed the manufacturer's instructions.

2.7. MDA measurement

Intracellular MDA concentration was assessed using a Lipid Peroxidation MDA Assay Kit (Beyotime, #S0131, China). After the indicated treatments, HT22 cells were harvested and lysed in RIPA lysate. Cell lysates were centrifuged at 15,000 rpm for 10 min, and the supernatant was collected for subsequent experiments. The MDA measurement procedure strictly followed the manufacturer's instructions.

2.8. ROS level detection

Dilute DCFH-DA (Beyotime, #S0033S, China) with serum-free culture medium according to 1:1,000 to give a final concentration of 10 $\mu\text{mol/L}$. An appropriate amount was added to the well plate, covered with the sample, and incubated for 20 min at 37°C in a cell culture incubator. Using a flow cytometric analyzer, set the excitation wavelength of 488 nm and the emission wavelength of 525 nm to detect the intensity of fluorescence after stimulation. All experimental operations were performed in strict accordance with the reagent instructions.

2.9. Annexin V-FITC PI apoptosis

HT22 cell death was assessed using the Annexin V - FITC PI Apoptosis Kit (Lianke, #AT101, China), which has strict instructions for use. According to the experimental design, digested with matching trypsin for 5-10 minutes at room temperature after intervention, added pre-cooled PBS, mixed by gentle blowing, collected into tubes and centrifuged, resuspended by adding 500 μL of Apoptosis Positive Control Reagent, incubated on ice for 30 minutes, resuspended by adding an appropriate amount of pre-cooled 1 \times Binding Solution, and added the same number of untreated live cells to mix with it. Added 1 \times Binding Solution to reach a total volume of 1.5 mL, the suspension was divided equally into three tubes: a blank control tube, a PI single-stained tube, and an Annexin V-FITC single-stained tube. Annexin V-FITC (5 μL) or PI (10 μL) was added to the single-stained tubes, while both Annexin V-FITC (5 μL) and PI (10 μL) were added to the tubes containing samples to be examined. Incubate the tubes for 5 min at room temperature and avoiding light, and then turn on the flow cytometer, and detect the samples through the FITC (Ex = 488 nm, Em = 530 nm) and PI (Ex = 535 nm, Em = 615 nm) channels.

2.10. Immunofluorescence

Cell culture plates used for immunofluorescence experiments were previously coated with 1% gelatin aqueous solution. After cell intervention, 4% paraformaldehyde was added to fix it for 15 min, 0.3% Triton X-100 was added, treated for 15 min, blocked with 5% goat serum, and incubated for 1 hour

at 37°C. Finally, the samples were incubated with the primary antibody against microtubule-associated protein 2 (MAP2) (Abcam, #ab183830, dilution 1:500) at 4°C overnight. The next day, samples were washed three times with PBST and incubated with anti-rabbit IgG (Invitrogen, #A21207, USA, Alexa Fluor 594, dilution 1:100) secondary antibody for 60 min at room temperature. The nuclei were then stained with DAPI (Beyotime, #C1005, China) solution for 5 minutes. Images were acquired using an orthogonal fluorescence microscope.

2.11. Western blot assays

Total cellular proteins were extracted using SDS lysis buffer supplemented with protease and phosphatase inhibitors, followed by protein electrophoresis. ACSL4 antibody (Santa Cruz Biotechnology, #sc-365230, diluted at 1:100), postsynaptic density protein 95 (PSD95) antibody (Invitrogen, #MA1-046, diluted at 1:500), FNDC5 antibody (Abcam, #ab174833, diluted at 1:1,000), β -actin antibody (Abcam, #ab115777, diluted at 1:1,000), were all shaken overnight and incubated. Next day, the samples were washed 5 times with PBST and incubated with goat anti-mouse HRP coupled secondary antibody (Proteintech, #20000838, dilution ratio 1:10,000) or goat anti-rabbit HRP coupled secondary antibody (zsbio, #ZB-2301, dilution ratio 1:5,000) for 1 hour at room temperature.

2.12. Statistical analysis

Data were presented as mean \pm standard deviation (mean \pm SD). All data were assessed for normality using appropriate statistical tests. Unpaired two-tailed *t* tests were used for comparing two independent groups, and one-way ANOVA was used for multiple group comparisons. Differences were considered statistically significant at $*(P < 0.05)$, $** (P < 0.01)$, and $*** (P < 0.001)$.

3. Results

3.1. High-glucose microenvironment induced neurotoxicity in HT22 cells

To investigate the effect of high glucose on HT22 cell viability, we treated cells with glucose concentrations of 25 mM (control group), 50 mM, and 75 mM (high glucose groups). Cell viability was assessed at 12, 24, 36, and 48 hours. High glucose treatments (50 mM and 75 mM) significantly inhibited HT22 cell proliferation and reduced cell viability at 36 hours (Figure 1A). Flow cytometry analysis revealed an apoptosis rate of 16.88% in HT22 cells at 36 hours with 75 mM glucose treatment, compared to 5.03% in the control group (Figure 1B). MAP2 immunofluorescent staining showed that 75

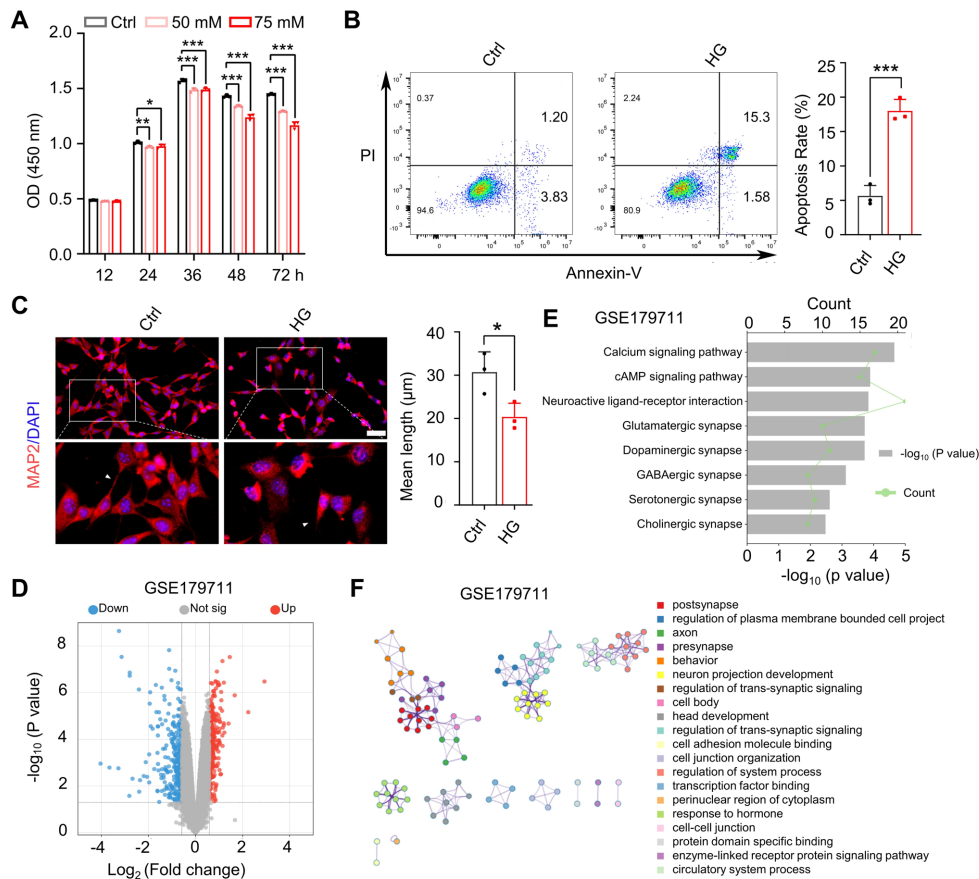


Figure 1. High-glucose microenvironment induced neurotoxicity in HT22 cells. (A) Cellular viability of HT22 cells was assessed at 12, 24, 36, 48, 72 hour after interventions with 25mM, 50mM, 75mM glucose . (B) Apoptosis rate analysis of HT22 cells was conducted using flow cytometry after high glucose (HG) interventions (C) Representative images of immunofluorescence staining of MAP2 (red) and DAPI (blue) were obtained after 36 hours of exposure to 75 mM high glucose. Scale bar = 50 µm. The mean neurite length, as indicated by MAP2 staining, was quantified. (D) Volcano plot displaying differentially expressed genes in the cerebral cortex of control mice and mice with impaired glucose tolerance in dataset GSE179711; (E) Analysis of the KEGG signaling pathway differential expression genes; (F) Analysis of the GO signaling pathway differential expression genes. Each experiment was conducted in triplicate. Statistical analyses were performed including unpaired Student's *t*-tests and one-way ANOVA. *(*P* < 0.05), **(*P* < 0.01), and ***(*P* < 0.001).

mM glucose treatment for 36 hours reduced the length of neurite in HT22 cells (Figure 1C). Additionally, we analyzed RNA sequencing data from the cerebral cortex of mice with impaired glucose tolerance using the GSE179711 dataset (20) from the GEO database. Differential gene screening was performed with a fold change cutoff of 1.5 (Figure 1D). KEGG (Figure 1E) and GO pathway enrichment analyses (Figure 1F) indicated that the differential genes were primarily involved in the regulation of neural synapses and behavioral performance. These results are consistent with our findings that high glucose affects synaptic function and exerts neurotoxic effects.

3.2. High glucose triggers ferroptosis in HT22 cells

Based on the latest research, high glucose induces ferroptosis in mouse brain neurons (21). To investigate whether high glucose-induced neurotoxicity in HT22 cells is mediated by ferroptosis, we assessed intracellular Fe²⁺ and MDA levels at various time points following 75 mM high glucose intervention. We found a significant

increase in ferrous ion levels at 36 hours (Figure 2A). Correspondingly, MDA levels increased progressively, peaking at 36 hours (Figure 2B). The occurrence of ferroptosis was further supported by a significant rise in ROS levels at 36 hours (Figure 2C). These results suggest that 75 mM high glucose intervention for 36 hours may induce ferroptosis in HT22 cells.

To further investigate high glucose-induced neurodegeneration in HT22 cells via ferroptosis, we selected Fer-1, a ferroptosis inhibitor known to effectively counter the ferroptosis cascade by interfering with lipid peroxidation and reducing oxidative stress. We treated high glucose-cultured HT22 cells with 1 µM Fer-1 (22) and observed that Fer-1 treatment significantly reduced intracellular MDA levels (Figure 2D) and decreased the accumulation of intracellular ferrous ions (Figure 2E). Additionally, Fer-1 treatment notably suppressed the expression of the ferroptosis marker protein ACSL4 induced by high glucose (Figure 2F). Using CCK8 assays, we found that Fer-1 treatment increased the viability of high glucose-treated cells (Figure 2G) and elevated the protein expression

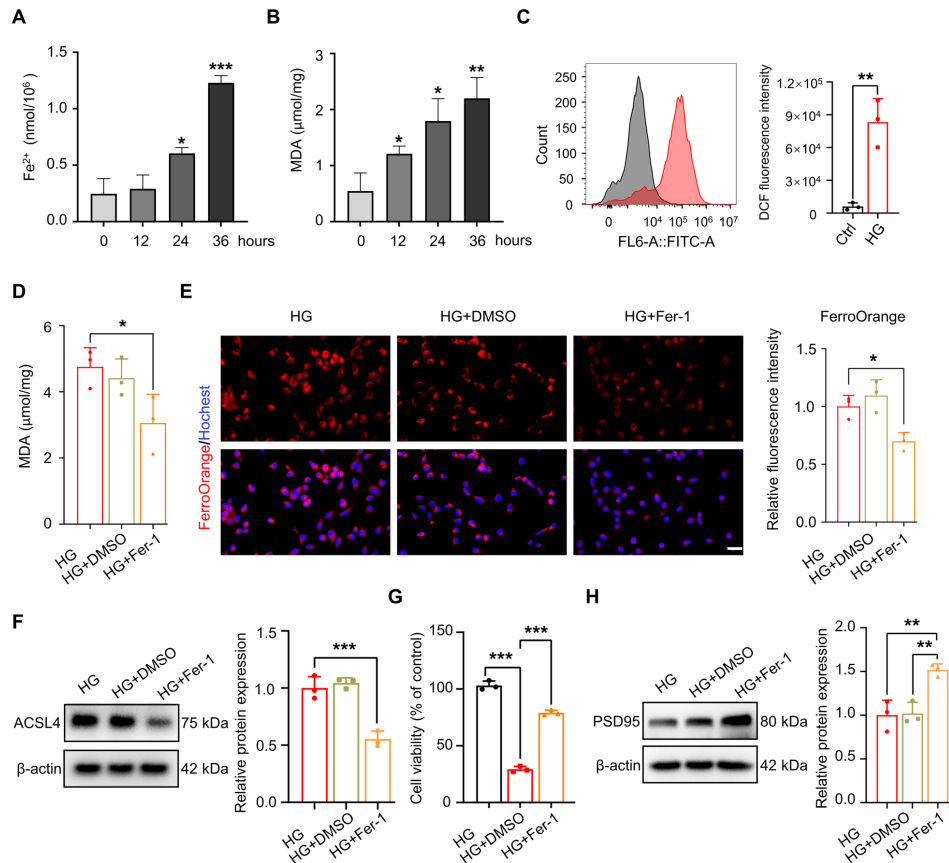


Figure 2. High glucose triggers ferroptosis in HT22 cells. Assessment of intracellular ferrous ion levels in HT22 cells following 75 mM glucose treatment at various time points ($n = 3$). (B) Assessment of MDA levels in HT22 cells following 75 mM glucose treatment at various time points ($n = 3$). (C) Measurement of ROS levels in HT22 cells after 36 hours of 75 mM glucose treatment using flow cytometry ($n = 3$). (D) Assessment of intracellular MDA levels in HT22 cells under high glucose conditions following treatment with iron death inhibitor Fer-1 ($n = 3$). (E) Intracellular ferrous ion levels in HT22 cells under high glucose conditions following treatment with Fer-1. Intracellular ferrous ions (FerroOrange, red) and nuclei (Hoechst, blue) was performed. Scale bar = 50 μm . (F) ACSL4 protein levels in HT22 cells under high glucose conditions following treatment with Fer-1. (G) Assessment of cellular activity in HT22 cells under high glucose conditions using CCK8 following treatment with Fer-1. (H) PSD95 protein levels in HT22 cells under high glucose conditions following treatment with Fer-1. Data are expressed as mean \pm SD, each experiment was conducted in triplicate. Statistical analyses were performed including unpaired Student's t -tests. * ($P < 0.05$), ** ($P < 0.01$), and *** ($P < 0.001$).

of the synaptic marker PSD95 (Figure 2H). These results indicate that Fer-1 inhibit high glucose-induced ferroptosis and neurotoxicity, highlighting ferroptosis as a critical mechanism underlying high glucose-induced cytotoxicity in HT22 cells.

3.3. Exogenous irisin ameliorated high glucose-induced neurotoxicity and ferroptosis

Studies have reported that irisin can effectively improve insulin resistance and regulate glucose homeostasis (23), highlighting its positive role in ameliorating hyperglycaemic toxicity. However, whether irisin can exert neuroprotective effects by mitigating hyperglycaemia-induced ferroptosis remains unclear. Therefore, we explored the effects of irisin on HT22 cells in a hyperglycaemic environment. We first determined the effective concentration and safe dosage of irisin. Figure 3A illustrates a decline in cell activity in the high glucose environment, while no significant changes were noted in the mannitol osmolality control group. Notably,

treatment with irisin from 0.1 to 10 nM significantly enhanced cell activity under high glucose conditions, with the most pronounced therapeutic effect observed at 5 nM irisin ($P < 0.05$). Therefore, 5 nM irisin was chosen for subsequent experiments (Figure 3A).

To validate the effect of irisin on HT22 cells in a high glucose environment, we examined cell activity and neurite length. We found that irisin significantly reduced the cell apoptosis rate (Figure 3B), increased neurite length (Figure 3C), and elevated PSD95 protein expression (Figure 3D), indicating that irisin exerts neuroprotective effects on HT22 cells under high glucose conditions. Subsequently, we investigated whether irisin could alleviate high glucose-induced ferroptosis in HT22 cells. We observed that irisin significantly decreased MDA levels (Figure 3E), intracellular ROS levels (Figure 3F), and intracellular ferrous ion levels (Figure 3G-H). In conclusion, irisin exerts neuroprotective effects in a high glucose environment by effectively inhibiting high glucose-induced intracellular iron overload, oxidative stress, and ferroptosis.

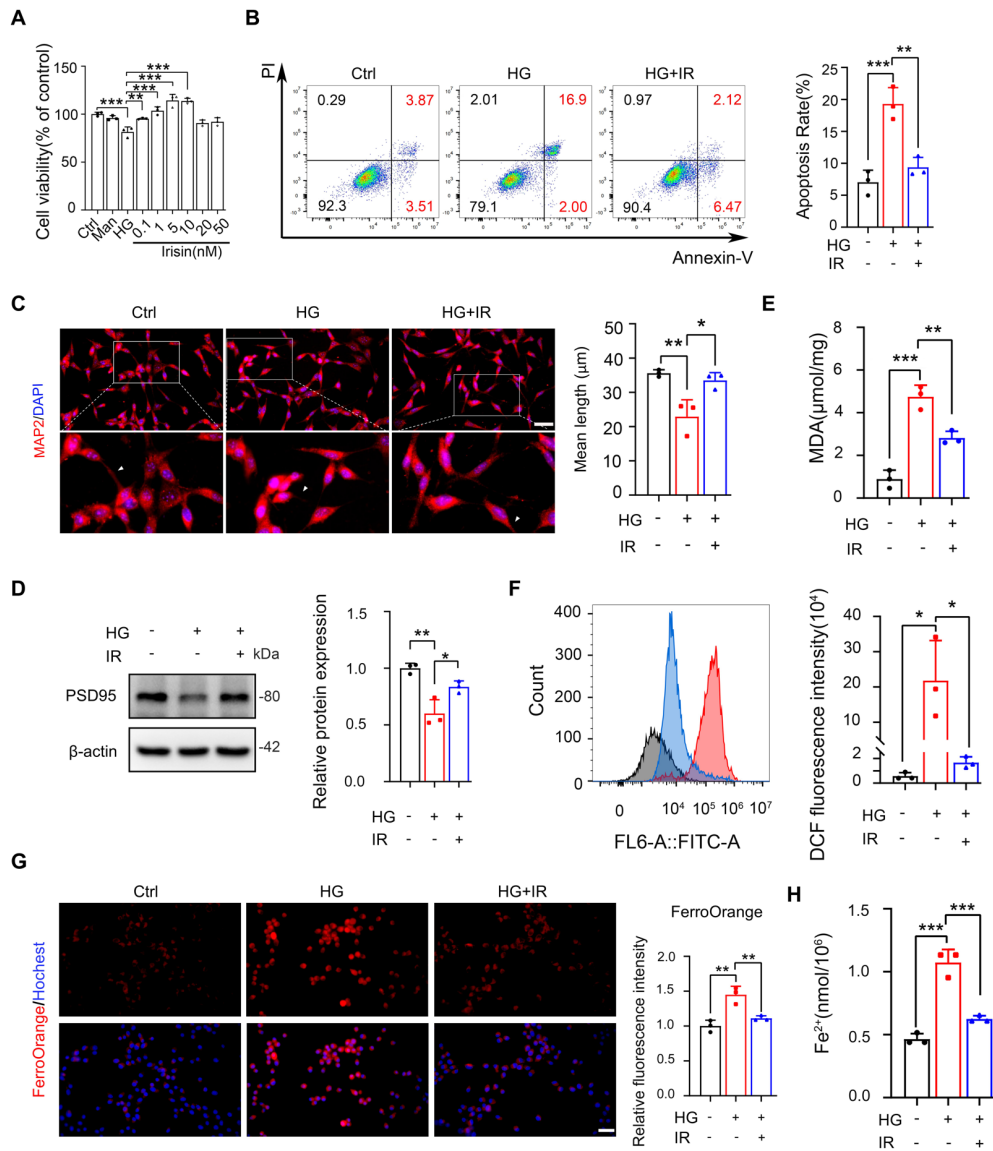


Figure 3. Exogenous irisin ameliorated high glucose-induced neurotoxicity and ferroptosis. (A) Assessment of cellular activity in HT22 cells treated with varying concentrations of irisin under high glucose conditions, using 50 nM mannitol as an osmotic control. (B) Assessment of apoptosis rate in HT22 cells treated with 5 nM irisin under high glucose conditions by flow cytometry. (C) Representative images of immunofluorescence staining of MAP2 (red) and DAPI (blue). Scale bar = 50 μ m. The mean neurite length, as indicated by MAP2 staining, was quantified. (D) Protein levels of PSD95 in HT22 cells treated with 5 nM irisin under high glucose conditions. (E) Quantitative intracellular MDA levels in HT22 cells after treated with 5 nM irisin under high glucose conditions. (F) Flow cytometry detection of intracellular ROS levels in HT22 cells after treated with 5 nM irisin under high glucose conditions. (G) Intracellular ferrous fluorescence intensity of HT22 cells after treated with 5 nM irisin under high glucose conditions. Intracellular ferrous ions (FerroOrange, red) and nuclei (Hoechst, blue) was performed to count the average fluorescence intensity. Scale bar = 50 μ m. (H) Quantitative levels of intracellular ferrous iron in HT22 cells after treated with 5 nM irisin under high glucose conditions. Each experiment was conducted in triplicate, data are expressed as mean \pm SD. Statistical analyses were performed including unpaired Student's *t*-tests and one-way ANOVA. * ($P < 0.05$), ** ($P < 0.01$), and *** ($P < 0.001$).

3.4. FNDC5 overexpression mitigated high glucose-induced neurotoxicity and ferroptosis

Irisin is derived from the FNDC5 protein through proteolytic cleavage of its extracellular fragment and is subsequently secreted into the peripheral circulation. Our findings demonstrated that exogenous irisin exerts a neuroprotective effect on HT22 cells in a high glucose environment. This prompted us to investigate whether the expression of endogenous FNDC5 could have a similar impact. We first examined the protein expression

of FNDC5 in HT22 cells under high glucose conditions and found that high glucose treatment inhibited FNDC5 expression compared to the control (Figure 4A). Based on this observation, we overexpressed FNDC5 in HT22 cells using plasmid transfection (Supplementary Figures S1. A-C, <https://www.biosciencetrends.com/action/getSupplementalData.php?ID=216>). Flow cytometry analysis revealed that FNDC5 overexpression decreased the apoptosis rate of HT22 cells in a high glucose environment (Figure 4B), improved the average length of neurite (Figure 4C), and increased the protein expression

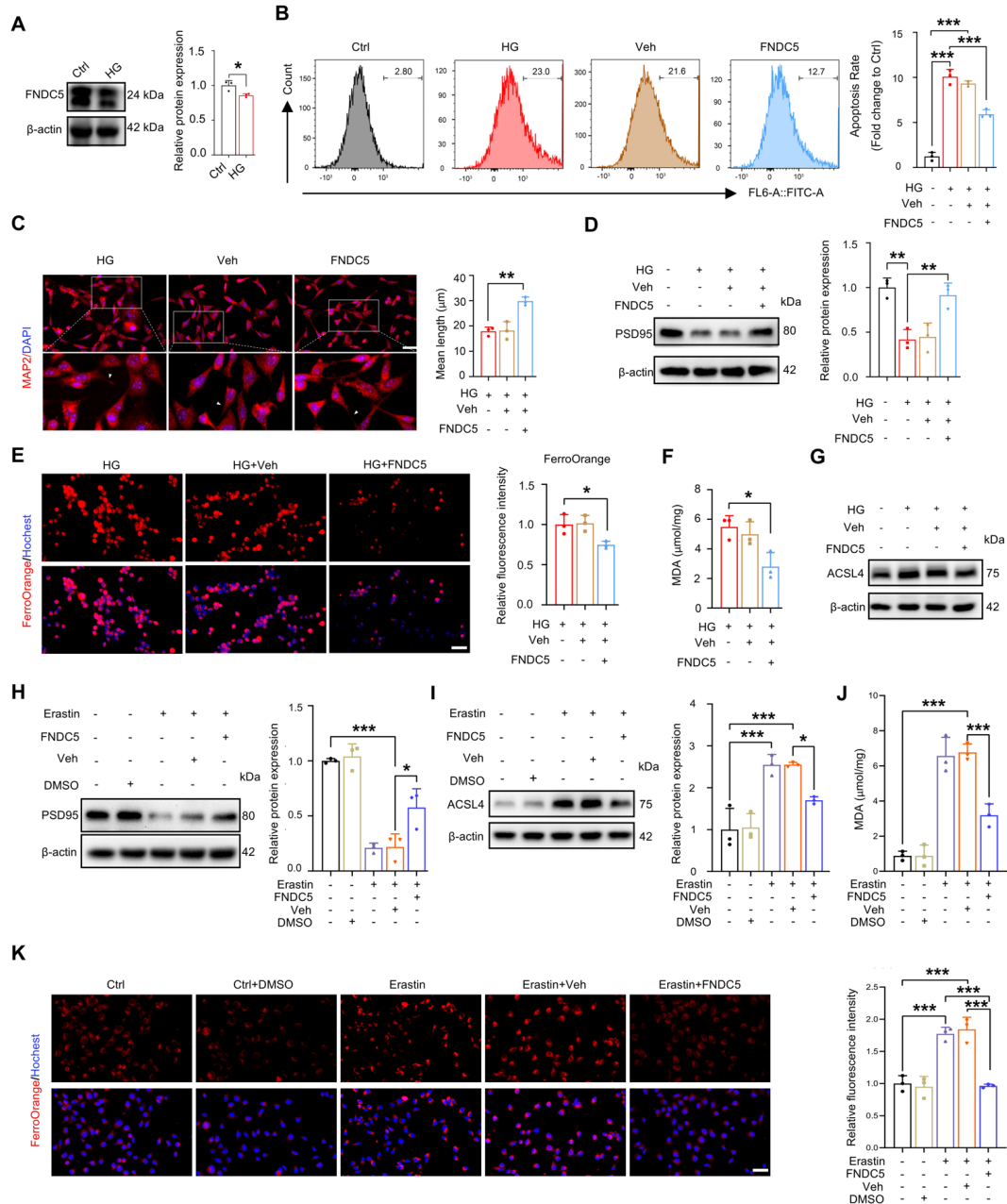


Figure 4. FNDC5 overexpression ameliorated high glucose-induced neurotoxicity and ferroptosis. (A) Endogenous FNDC5 protein expression levels in HT22 cells under high glucose. (B) Apoptosis rate in HT22 cells under high glucose conditions following FNDC5 overexpression, as measured by flow cytometry. (C) Representative images of immunofluorescence staining of MAP2 (red) and DAPI (blue). Scale bar = 50 μ m. The mean neurite length, as indicated by MAP2 staining, was quantified. (D) Protein levels of PSD95 in HT22 cells under high glucose conditions following FNDC5 overexpression. (E) Intracellular ferrous fluorescence intensity of HT22 cells under high glucose conditions following FNDC5 overexpression. Intracellular ferrous ions (FerroOrange, red) and nuclei (Hoechst, blue) was performed to count the average fluorescence intensity. Scale bar 50 = μ m. (F) Quantitative intracellular MDA levels. (G) Intracellular ACSL4 protein expression levels. (H) Intracellular PSD95 protein expression levels in erastin-treated HT22 cells with FNDC5 overexpression. (I) Intracellular ACSL4 protein expression levels. (J) Intracellular MDA levels. (K) Intracellular ferrous fluorescence intensity. Each experiment was conducted in triplicate, data are expressed as mean \pm SD. Statistical analyses were performed including unpaired Student's *t*-tests and one-way ANOVA with Tukey's post hoc tests. * ($P < 0.05$), ** ($P < 0.01$), and *** ($P < 0.001$).

of PSD95 (Figure 4D).

In addition, we observed that overexpression of FNDC5 effectively reduced the intracellular ferrous ions (Figure 4E), MDA level (Figure 4F), and protein expression of ACSL4 (Figure 4G) in HT22 cells under high glucose conditions. These results suggest that overexpression of FNDC5 attenuates high glucose-

induced neurotoxicity and ferroptosis. To further validate the effect of FNDC5 on ferroptosis, we tested the impact of FNDC5 overexpression using the ferroptosis inducer Erastin, which promotes ferroptosis through multiple mechanisms (24). We treated cells with 0.5 μ M Erastin to induce ferroptosis and found that Erastin treatment inhibited the protein expression of PSD95 and increased

the protein expression of ACSL4, a marker of ferroptosis, in HT22 cells compared to controls. Overexpression of FNDC5 effectively increased PSD95 protein expression and decreased ACSL4 protein levels (Figure 4H-I). Additionally, we observed that Erastin-induced MDA levels and ferrous ion accumulation were alleviated by FNDC5 overexpression (Figure 4J-K). Taken together, these findings suggest that overexpression of FNDC5 in a high glucose environment attenuates neurotoxicity through the inhibition of ferroptosis.

3.5. Exogenous irisin attenuates high glucose-induced neurotoxicity under conditions of reduced FNDC5 expression

Due to the decreased expression of FNDC5 in a high glucose environment, leading to reduced endogenous irisin production, we aimed to investigate whether exogenous irisin could exert neuroprotective effects when FNDC5 expression is significantly reduced. We further knocked down FNDC5 expression in HT22 cells under high glucose conditions (Supplementary Figure S1. E-F, <https://www.biosciencetrends.com/action/getSupplementalData.php?ID=216>) and then treated the cells with exogenous irisin. The results showed that irisin treatment effectively reduced the apoptosis rate in the FNDC5 knockdown group under high glucose conditions (Figure 5A), prolonged the average neurite length (Figure 5B), and increased the PSD95 protein expression level

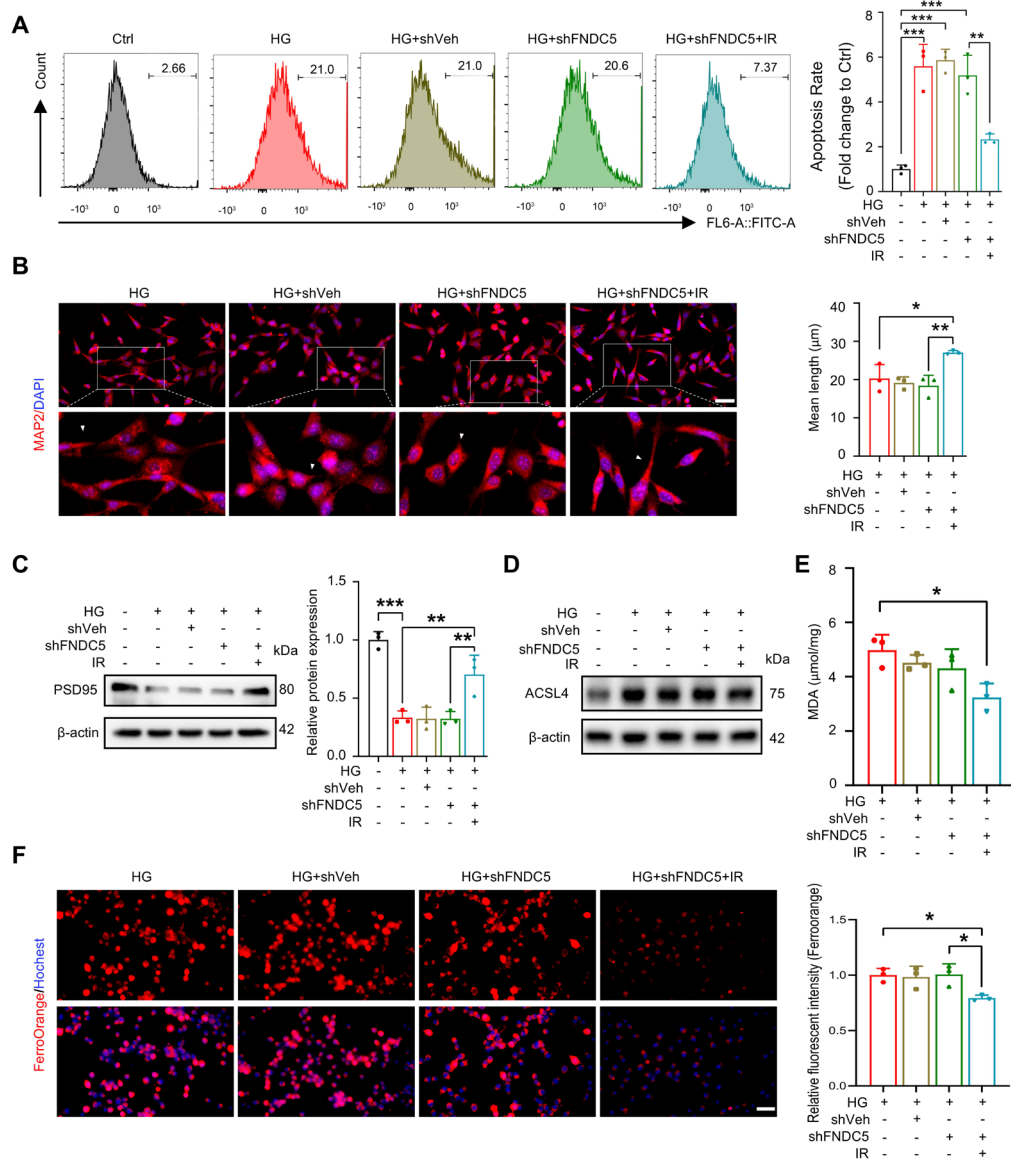


Figure 5. Exogenous Irisin administration after FNDC5 knockdown ameliorated high glucose-induced neurotoxicity. (A) Apoptosis detection by flow cytometry in HT22 cells with FNDC5 knockdown following irisin intervention. **(B)** Representative images of immunofluorescence staining of MAP2 (red) and DAPI (blue). Scale bar = 50 μm. The mean neurite length, as indicated by MAP2 staining, was quantified. **(C)** Protein levels of PSD95. **(D)** Intracellular ACSL4 protein expression levels. **(E)** Quantitative intracellular MDA levels. **(F)** Intracellular ferrous fluorescence intensity of HT22 cells with FNDC5 knockdown following irisin intervention. Ferrous ions (FerroOrange, red) and nuclei (Hoechst, blue). Scale bar = 50 μm. Each experiment was conducted in triplicate, data are expressed as mean ± SD. Statistical analyses were performed including unpaired Student's *t*-tests and one-way ANOVA with Tukey's post hoc tests. *(*P* < 0.05), **(*P* < 0.01), and ***(*P* < 0.001).

(Figure 5C). Similarly, irisin treatment also inhibited ferroptosis-related markers in FNDC5 knockdown HT22 cells under high glucose conditions, including ACSL4 expression (Figure 5D), MDA levels (Figure 5E), and intracellular ferrous ion levels (Figure 5F). In conclusion, with endogenous FNDC5 knockdown, irisin effectively alleviated high glucose-induced neurotoxicity and ferroptosis in HT22 cells. These results further underscore the effectiveness of irisin in mitigating high glucose-induced neurotoxicity.

4. Discussion

With the aging population, diabetes has emerged as a major global health concern, particularly in the elderly. Diabetic neuropathy represents a critical complication of diabetes, underscoring the importance of elucidating the mechanisms linking hyperglycemia to nerve damage and identifying potential therapeutic interventions.

In this study, we demonstrated that high glucose exerts neurotoxic effects on HT22 cells, as evidenced by reduced cellular viability, increased apoptosis, shortened neurite length, and decreased expression of the synaptic marker protein PSD95. Furthermore, we observed activation of the ferroptosis pathway in high-glucose-treated HT22 cells, characterized by iron overload, oxidative stress, lipid peroxidation, and elevated expression of the ferroptosis marker ACSL4. Notably, irisin treatment effectively suppressed high-glucose-induced neurotoxicity and ferroptosis in these cells. Additionally, high glucose reduced the expression of FNDC5, the precursor protein of irisin. Overexpression of FNDC5 increased endogenous irisin levels, resulting in neuroprotection and inhibition of ferroptosis. To further explore this mechanism, we knocked down FNDC5 expression and treated the cells with exogenous irisin. Remarkably, exogenous irisin supplementation attenuated neurotoxicity and inhibited ferroptosis, even in the context of reduced endogenous FNDC5 expression. In conclusion, our findings indicate that FNDC5/irisin mitigates high-glucose-induced neurotoxicity by inhibiting ferroptosis in HT22 cells, offering new insights and potential therapeutic strategies for diabetic neuropathy.

The expression of ferroptosis-related markers, including glutathione peroxidase 4 (GPX4) and the cystine/glutamate antiporter (SLC7A11), was markedly downregulated in a high-glucose environment. In contrast, ferritin levels and lipid peroxidation were significantly elevated (25,26), indicating that ferroptosis is a key mechanism underlying high-glucose-induced cytotoxicity. Our experimental findings demonstrated that FNDC5/Irisin significantly attenuated lipid peroxidation and intracellular iron accumulation, thereby inhibiting ferroptosis. In line with previous studies, FNDC5/Irisin was also shown to suppress the expression of inducible nitric oxide synthase (iNOS) and NADPH oxidase 2

(NOX2), reducing ROS production under high-glucose conditions (27). Moreover, Irisin reduced ferroptosis by downregulating elevated levels of superoxide dismutase (SOD), glutathione peroxidase 1 (GPX-1), catalase (CAT), and Nrf2, thereby mitigating oxidative stress induced by high glucose (28). These findings suggest that FNDC5/Irisin may represent a promising therapeutic target for diabetes-associated neuropathy and other ferroptosis-related pathologies. Further research is warranted to elucidate the precise regulatory mechanisms of FNDC5/Irisin in ferroptosis and explore its potential clinical applications.

In addition, we observed a reduction in FNDC5 expression in HT22 cells under high-glucose conditions. Previous studies have shown that FNDC5 expression in subcutaneous adipose tissue of type II diabetic patients is reduced by 40–45%, while circulating irisin levels decrease by 40%. Furthermore, circulating irisin levels are negatively correlated with fasting blood glucose (27,29,30) and diabetic complications (29,31). Similarly, an *in vitro* study demonstrated that high glucose suppresses FNDC5 mRNA and protein expression in a concentration-dependent manner (32); however, the underlying mechanism for this reduction remains unclear. In a related study, decreased expression of cystathionine γ -lyase in high-glucose mice led to H₂S deficiency, which triggers excessive oxidative stress and impairs PGC-1 α expression (18). As FNDC5 expression in neurons is heavily dependent on PGC-1 α activity (33), it is plausible that downregulation of PGC-1 α in high-glucose environments contributes to the reduced expression of FNDC5/irisin. Additionally, inflammatory factors and oxidative stress have been shown to influence FNDC5 expression; for example, IL-1 β and TNF α reduce FNDC5 protein synthesis and lower irisin levels (31,34). Previous research suggests that high glucose inhibits the ERK/MAPK signaling pathway (35), which is known to positively regulate PGC-1 α /FNDC5/irisin expression during neuronal differentiation (36). Thus, downregulation of the ERK/MAPK pathway may represent an additional mechanism contributing to the reduction in FNDC5/irisin expression.

Given the reduction in FNDC5/irisin expression under high-glucose conditions, and its established neuroprotective effects, restoring FNDC5/irisin levels is crucial for mitigating high-glucose-induced neurological damage. Our findings indicate that exogenous irisin supplementation, despite reduced FNDC5 expression, attenuated high-glucose-induced neurotoxicity and ferroptosis. Previous studies have shown that adenovirus-mediated delivery of FNDC5 to the liver increases circulating irisin levels, which, in turn, induces the expression of neuroprotective factors in the hippocampus (33). Thus, therapeutic strategies centered on injectable peptides targeting FNDC5/irisin may represent a promising approach to mitigate diabetic neurotoxicity. However, further studies are required to evaluate the

clinical efficacy of FNDC5/irisin in preventing diabetic neurotoxicity and cognitive impairment. While this study focuses on the role of FNDC5/irisin in neuronal cells, the significance of myogenic FNDC5/irisin should not be underestimated. FNDC5/irisin, a myokine, is highly expressed in skeletal muscle, and approximately 70% of circulating irisin in mice originates from muscle tissue (18). Its secretion is significantly elevated in response to exercise (37), and muscle-derived irisin can cross the blood-brain barrier, enabling it to influence the central nervous system. Moreover, exercise has been shown to upregulate FNDC5 expression in the hippocampus, subsequently increasing the levels of brain-derived neurotrophic factor (BDNF) and providing neuroprotection (33). These observations suggest that exercise-induced upregulation of FNDC5/irisin could represent a promising intervention to mitigate the cognitive dysfunction associated with diabetes mellitus.

Furthermore, although our study provides strong evidence that FNDC5/Irisin alleviates high glucose-induced neurotoxicity in HT22 cells, several limitations remain. First, our study was conducted primarily at the cellular level and lacked validation in animal models. Second, it is unclear whether FNDC5/Irisin exerts consistent effects across different types of neuronal cells, necessitating further investigation. Additionally, other potential mechanisms, such as the interaction of FNDC5/Irisin with other signaling pathways, warrant further exploration.

In conclusion, our findings highlight the role of FNDC5/irisin in alleviating high glucose-induced neurotoxicity and ferroptosis, presenting a novel target for the treatment of diabetes-associated neurodegenerative diseases and providing a foundation for future clinical studies.

Acknowledgements

We express our gratitude to the Chongqing Key Laboratory of Translational Medicine for Cognitive Development and Learning and Memory Disorders, Institute of Paediatrics, Affiliated Children's Hospital of Chongqing Medical University for generously providing the HT22 mouse hippocampal cells. We extend our gratitude to the research platform of the Second Affiliated Hospital of Chongqing Medical University for their invaluable support and assistance. We acknowledge the Gene Expression Omnibus (GEO) for providing public access to its data.

Funding: This work was funded by the National Natural Science Foundation of China (Grant No.82371427, Grant No.82401656), Natural Science Foundation of Chongqing, China (CSTB2023NSCQBHX0018, CSTB2023NSCQ-MSX0323), Kuanren Talents Program of the Second Affiliated Hospital of Chongqing Medical University (Grant No. kryc-lj-2105) and Postgraduate

Research and Innovation Project of Chongqing Province (Grant No. CYB240199).

Conflict of Interest: The authors have no conflicts of interest to disclose.

References

1. GBD 2021 Diabetes Collaborators. Global, regional, and national burden of diabetes from 1990 to 2021, with projections of prevalence to 2050: a systematic analysis for the Global Burden of Disease Study 2021. *Lancet*. 2023; 402:203-234.
2. Stumvoll M, Goldstein BJ, van Haeften TW. Type 2 diabetes: principles of pathogenesis and therapy. *Lancet*. 2005; 365:1333-46.
3. Taylor R. Type 2 diabetes: etiology and reversibility. *Diabetes Care*. 2013; 36:1047-55.
4. Xu L, Li Y, Dai Y, Peng J. Natural products for the treatment of type 2 diabetes mellitus: Pharmacology and mechanisms. *Pharmacol Res*. 2018; 130:451-465.
5. You Y, Liu Z, Chen Y, Xu Y, Qin J, Guo S, Huang J, Tao J. The prevalence of mild cognitive impairment in type 2 diabetes mellitus patients: a systematic review and meta-analysis. *Acta Diabetol*. 2021; 58:671-685.
6. Xue M, Xu W, Ou YN, Cao XP, Tan MS, Tan L, Yu JT. Diabetes mellitus and risks of cognitive impairment and dementia: A systematic review and meta-analysis of 144 prospective studies. *Ageing Res Rev*. 2019; 55:100944.
7. Yang Q, Zhou L, Liu C, Liu D, Zhang Y, Li C, Shang Y, Wei X, Li C, Wang J. Brain iron deposition in type 2 diabetes mellitus with and without mild cognitive impairment-an in vivo susceptibility mapping study. *Brain Imaging Behav*. 2018; 12:1479-1487.
8. An JR, Su JN, Sun GY, Wang QF, Fan YD, Jiang N, Yang YF, Shi Y. Liraglutide Alleviates Cognitive Deficit in db/db Mice: Involvement in Oxidative Stress, Iron Overload, and Ferroptosis. *Neurochem Res*. 2022; 47:279-294.
9. Wang Z, Feng S, Li Q, Song Z, He J, Yang S, Yan C, Ling H. Dihydropyridin alleviates hippocampal ferroptosis in type 2 diabetic cognitive impairment rats via inhibiting the JNK-inflammatory factor pathway. *Neurosci Lett*. 2023; 812:137404.
10. Xie Z, Wang X, Luo X, Yan J, Zhang J, Sun R, Luo A, Li S. Activated AMPK mitigates diabetes-related cognitive dysfunction by inhibiting hippocampal ferroptosis. *Biochem Pharmacol*. 2023; 207:115374.
11. Guo T, Yu Y, Yan W, Zhang M, Yi X, Liu N, Cui X, Wei X, Sun Y, Wang Z, Shang J, Cui W, Chen L. Erythropoietin ameliorates cognitive dysfunction in mice with type 2 diabetes mellitus via inhibiting iron overload and ferroptosis. *Exp Neurol*. 2023; 365:114414.
12. Dun SL, Lyu RM, Chen YH, Chang JK, Luo JJ, Dun NJ. Irisin-immunoreactivity in neural and non-neural cells of the rodent. *Neuroscience*. 2013; 240:155-62.
13. Piya MK, Harte AL, Sivakumar K, Tripathi G, Voyias PD, James S, Sabico S, Al-Daghri NM, Saravanan P, Barber TM, Kumar S, Vatish M, McTernan PG. The identification of irisin in human cerebrospinal fluid: influence of adiposity, metabolic markers, and gestational diabetes. *Am J Physiol Endocrinol Metab*. 2014; 306:E512-8.
14. Lourenco MV, Frozza RL, de Freitas GB, *et al*. Exercise-linked FNDC5/irisin rescues synaptic plasticity and memory defects in Alzheimer's models. *Nat Med*. 2019;

- 25:165-175.
15. Islam MR, Valaris S, Young MF, *et al.* Exercise hormone irisin is a critical regulator of cognitive function. *Nat Metab.* 2021; 3:1058-1070.
 16. Wang J, Zhao YT, Zhang LX, Dubielecka PM, Qin G, Chin YE, Gower AC, Zhuang S, Liu PY, Zhao TC. Irisin deficiency exacerbates diet-induced insulin resistance and cardiac dysfunction in type II diabetes in mice. *Am J Physiol Cell Physiol.* 2023; 325:C1085-C1096.
 17. Yano N, Zhang L, Wei D, Dubielecka PM, Wei L, Zhuang S, Zhu P, Qin G, Liu PY, Chin YE, Zhao TC. Irisin counteracts high glucose and fatty acid-induced cytotoxicity by preserving the AMPK-insulin receptor signaling axis in C2C12 myoblasts. *Am J Physiol Endocrinol Metab.* 2020; 318:E791-E805.
 18. Boström P, Wu J, Jedrychowski MP, *et al.* A PGC1- α -dependent myokine that drives brown-fat-like development of white fat and thermogenesis. *Nature.* 2012; 481:463-8.
 19. Wang J, Zhu Q, Wang Y, Peng J, Shao L, Li X. Irisin protects against sepsis-associated encephalopathy by suppressing ferroptosis via activation of the Nrf2/GPX4 signal axis. *Free Radic Biol Med.* 2022; 187:171-184.
 20. Yoon G, Cho KA, Song J, Kim YK. Transcriptomic Analysis of High Fat Diet Fed Mouse Brain Cortex. *Front Genet.* 2019; 10:83.
 21. Yu J, Zhang Y, Zhu Q, Ren Z, Wang M, Kong S, Lv H, Xu T, Xie Z, Meng H, Han J, Che H. A mechanism linking ferroptosis and ferritinophagy in melatonin-related improvement of diabetic brain injury. *iScience.* 2024; 27:109511.
 22. Chen Y, He W, Wei H, Chang C, Yang L, Meng J, Long T, Xu Q, Zhang C. Srs11-92, a ferostatin-1 analog, improves oxidative stress and neuroinflammation via Nrf2 signal following cerebral ischemia/reperfusion injury. *CNS Neurosci Ther.* 2023; 29:1667-1677.
 23. Perakakis N, Triantafyllou GA, Fernández-Real JM, Huh JY, Park KH, Seufert J, Mantzoros CS. Physiology and role of irisin in glucose homeostasis. *Nat Rev Endocrinol.* 2017; 13:324-337.
 24. Zhao Y, Li Y, Zhang R, Wang F, Wang T, Jiao Y. The Role of Erastin in Ferroptosis and Its Prospects in Cancer Therapy. *Onco Targets Ther.* 2020; 13:5429-5441
 25. Feng S, Tang D, Wang Y, *et al.* The mechanism of ferroptosis and its related diseases. *Mol Biomed.* 2023; 4:33.
 26. Miao R, Fang X, Zhang Y, Wei J, Zhang Y, Tian J. Iron metabolism and ferroptosis in type 2 diabetes mellitus and complications: mechanisms and therapeutic opportunities. *Cell Death Dis.* 2023; 14:186.
 27. Lin C, Guo Y, Xia Y, Li C, Xu X, Qi T, Zhang F, Fan M, Hu G, Zhao H, Zhao H, Liu R, Gao E, Yan W, Tao L. FNDC5/Irisin attenuates diabetic cardiomyopathy in a type 2 diabetes mouse model by activation of integrin α V/ β 5-AKT signaling and reduction of oxidative/nitrosative stress. *J Mol Cell Cardiol.* 2021; 160:27-41.
 28. Fu J, Li F, Tang Y, Cai L, Zeng C, Yang Y, Yang J. The Emerging Role of Irisin in Cardiovascular Diseases. *J Am Heart Assoc.* 2021; 10:e022453.
 29. Kurdiova T, Balaz M, Vician M, *et al.* Effects of obesity, diabetes and exercise on Fndc5 gene expression and irisin release in human skeletal muscle and adipose tissue: in vivo and in vitro studies. *J Physiol.* 2014; 592:1091-107.
 30. Moreno-Navarrete JM, Ortega F, Serrano M, Guerra E, Pardo G, Tinahones F, Ricart W, Fernández-Real JM. Irisin is expressed and produced by human muscle and adipose tissue in association with obesity and insulin resistance. *J Clin Endocrinol Metab.* 2013; 98:E769-78.
 31. Parsanathan R, Jain SK. Hydrogen Sulfide Regulates Irisin and Glucose Metabolism in Myotubes and Muscle of HFD-Fed Diabetic Mice. *Antioxidants (Basel).* 2022; 11:1369.
 32. Deng J, Zhang N, Chen F, Yang C, Ning H, Xiao C, Sun K, Liu Y, Yang M, Hu T, Zhang Z, Jiang W. Irisin ameliorates high glucose-induced cardiomyocytes injury via AMPK/mTOR signal pathway. *Cell Biol Int.* 2020; 44:2315-2325.
 33. Wrann CD, White JP, Salogiannis J, Laznik-Bogoslavski D, Wu J, Ma D, Lin JD, Greenberg ME, Spiegelman BM. Exercise induces hippocampal BDNF through a PGC-1 α /FNDC5 pathway. *Cell Metab.* 2013; 18:649-59.
 34. Matsuo Y, Gleitsmann K, Mangner N, Werner S, Fischer T, Bowen TS, Kricke A, Matsumoto Y, Kurabayashi M, Schuler G, Linke A, Adams V. Fibronectin type III domain containing 5 expression in skeletal muscle in chronic heart failure-relevance of inflammatory cytokines. *J Cachexia Sarcopenia Muscle.* 2015; 6:62-72.
 35. Kumar P, Rao GN, Pal BB, Pal A. Hyperglycemia-induced oxidative stress induces apoptosis by inhibiting PI3-kinase/Akt and ERK1/2 MAPK mediated signaling pathway causing downregulation of 8-oxoG-DNA glycosylase levels in glial cells. *Int J Biochem Cell Biol.* 2014; 53:302-19.
 36. Hosseini Farahabadi SS, Ghaedi K, Ghazvini Zadegan F, Karbalaie K, Rabiee F, Nematollahi M, Baharvand H, Nasr-Esfahani MH. ERK1/2 is a key regulator of Fndc5 and PGC1 α expression during neural differentiation of mESCs. *Neuroscience.* 2015; 297:252-61.
 37. Löffler D, Müller U, Scheuermann K, Friebe D, Gesing J, Bielitz J, Erbs S, Landgraf K, Wagner IV, Kiess W, Körner A. Serum irisin levels are regulated by acute strenuous exercise. *J Clin Endocrinol Metab.* 2015; 100:1289-99.

Received August 28, 2024; Revised October 8, 2024; Accepted October 14, 2024.

[§]These authors contributed equally to this work.

*Address correspondence to:

Xiuqing Yao and Yaxi Luo, Department of Rehabilitation, The Second Affiliated Hospital of Chongqing Medical University, Chongqing, China.

E-mail: dryaoxq@cqmu.edu.cn (XY), luoyaxi@hospital.cqmu.edu.cn (YL)

Released online in J-STAGE as advance publication October 17, 2024.

Imaging of pulmonary cryptococcosis with consolidations or diffuse infiltrates suggests longer clinical treatment in non-HIV patients

Yi Su, Yao Zhang, Qingqing Wang, Bijie Hu, Jue Pan*

Department of Infectious Diseases, Zhongshan Hospital, Fudan University, Shanghai 200032, China.

SUMMARY This article was to summarize the clinical features and treatment course in patients with pulmonary cryptococcal infections with different imaging manifestations and to analyse the relevant factors. Categorical variables are described in this paper as percentages, and continuous variables are expressed as medians and quartiles or means and standard deviations. Factors associated with prolonged treatment of pulmonary cryptococcosis with different imaging manifestations were estimated via multivariable analyses with the Cox proportional hazards model. A total of 238 patients were analysed. A significant proportion of patients with diabetes mellitus constituted 18% to 25% of patients with multiple nodules and diffuse infiltrates ($p = 0.026$). The serum antigen level was markedly elevated in patients with diffuse infiltrates and consolidation ($p < 0.001$). A significant proportion of patients who presented with solitary nodules were initially diagnosed through thoracic surgery conducted to remove the lesion ($p < 0.001$). The treatment duration for patients with pulmonary cryptococcosis presenting as single or multiple nodules on imaging was shorter than the traditionally considered 6 months ($p < 0.001$). Imaging revealed that pulmonary cryptococcosis most commonly involved the right lower lung. Serum antigen assays, the number of infectious lobes, the presence of extrapulmonary lesions and the presence of lesions in the lower right lobe were suggested to be predictive indicators for a longer treatment duration. There was no significant difference in the percentage of patients who used amphotericin B or amphotericin B liposomes among patients with the four different types of imaging presentations.

Keywords pulmonary cryptococcosis, imaging characteristics, treatment, prognosis

1. Introduction

Cryptococcus can infect any tissue or organ of the human body. The respiratory system is the most common site of infection, followed by the central nervous system and skin (1,2). Chest imaging, which uses high-resolution computed tomography (HRCT), forms a cornerstone of the diagnostic toolkit for pulmonary cryptococcosis. Patients may have single or multiple parenchymal nodules, which are often subpleural (3); moreover, cavitation may be observed, particularly in immunocompromised patients (4).

Although the imaging features of pulmonary cryptococcosis have been previously reported in the literature, there are few studies on the relationship between imaging and clinical manifestations of pulmonary cryptococcosis (5-7). In this investigation, we analysed the pulmonary imaging characteristics of 216 patients with cryptococcosis. This is the

first study to evaluate the different clinical features presented by different imaging manifestations, and it is also the first to investigate the response of different imaging manifestations to therapeutic drugs and the role of imaging manifestations in determining patient prognosis.

2. Patients and Methods

2.1. Case series

Patients were deemed eligible if they were admitted to the Infectious Diseases Department at Zhongshan Hospital, Fudan University, between January 1, 2012, and December 31, 2021. Data regarding patient demographics, clinical features, laboratory results, pathogenic findings, treatments, and outcomes were obtained from the Zhongshan Hospital Information System. This project received approval from the Ethics

Committee of Zhongshan Hospital (Ethics approval number B2024-276), and informed consent was obtained from all the subjects or their legal guardians. All research was performed in accordance with relevant guidelines and the Declaration of Helsinki. All the data were reviewed by two physicians (QQW and YS), and any discrepancies in interpretation between the primary reviewers were resolved by a third researcher (JP and BJH). The data that support the findings of this study are available from the corresponding author.

2.2. Case definition

Cryptococcosis patients include confirmed and clinical patients. Confirmed cryptococcosis was identified as a positive result of *Cryptococcus* culture from any site. Clinical cryptococcosis can be identified by positive histopathology or cryptococcal antigen results, together with clinical or radiographic evidence of disease (8). The treatment duration refers to the period between starting the medication and discontinuing it. Improvement days denote the period between the initiation of medication and the improvements seen on chest imaging. The morphological features on CT scans can be categorized as solitary nodules/masses, multiple nodules/masses, consolidation, or diffuse infiltrates (nodules/masses with consolidation) (3) (Figure 1).

2.3. Statistical analysis of data

Depending on the data distribution, categorical variables are described herein as percentages, and continuous variables, including age, serum antigen assay, improvement days and treatment days, are described as medians and quartiles. Continuous variables, including laboratory results, are described as the means and standard deviations. The chi-square test was used to screen for differences in sex, immune status, chronic disease, clinical symptoms at onset, medical or surgical treatment, extrapulmonary involvement, lesions that improved but remained nonresorbed, CT characteristics, the number of involved lung lobes and treatment. A median comparison of nonparametric tests was used to compare age, serum antigen assay, improvement

days and treatment days. Independent sample Kruskal–Wallis tests of nonparametric tests were used to compare laboratory results. Factors associated with prolonged treatment of pulmonary cryptococcosis with different imaging manifestations were estimated *via* multivariable analyses with the Cox proportional hazards model. A probability (*P*) value < 0.05 indicated a statistically significant difference. Statistical analyses were performed *via* SPSS software (version 23). The figures were created through GRAPHPAD PRISM 8.0.

3. Results

3.1. Patient selection and classification

A total of 238 patients were included in this analysis. Of these, 216 patients with pulmonary *Cryptococcus* infection (15 cases with positive culture) and other site infections in combination with pulmonary infection were subjected to further analysis (Figure 2).

3.2. Clinical manifestations and laboratory results

A significant proportion of patients with diabetes mellitus constituted 18% to 25% of patients with multiple nodules and diffuse infiltrates ($p = 0.026$). As seen in Table 1, over half of the patients with solitary nodules and diffuse infiltrates presented with clinical manifestations, the most prevalent of which was cough ($p < 0.001$). Compared with that in patients with solitary nodules and multiple nodules, the serum antigen level was markedly elevated in patients with diffuse infiltrates and consolidation ($p < 0.001$). A significant proportion of patients who presented with solitary nodules were initially diagnosed with thoracic surgery to remove the lesion ($p < 0.001$). The treatment duration for patients with pulmonary cryptococcosis presenting as single or multiple nodules on imaging was shorter than the traditionally considered 6 months ($p < 0.001$). The proportion of patients who exhibited lesion improvement but persistent lesion nonresorption was significantly greater in patients who presented with consolidation and diffuse pulmonary infiltrates ($p < 0.001$).

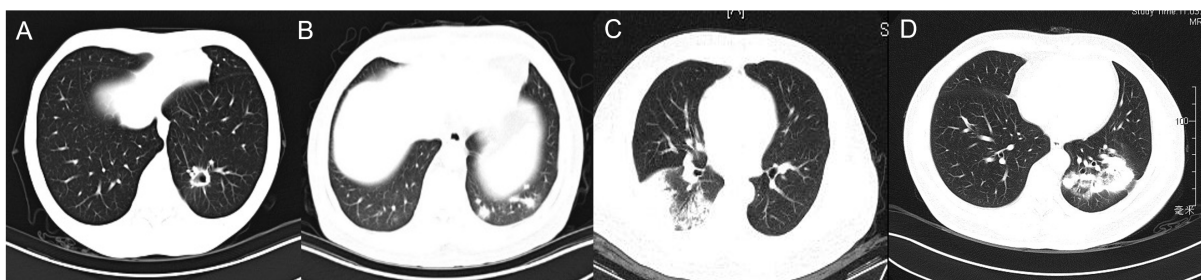


Figure 1. Classification of the imaging manifestations of *Cryptococcus pneumoniae*. A: Solitary nodule. B: Multiple nodules. C: Consolidation. D: Diffuse infiltrates (nodules/mass with consolidation).

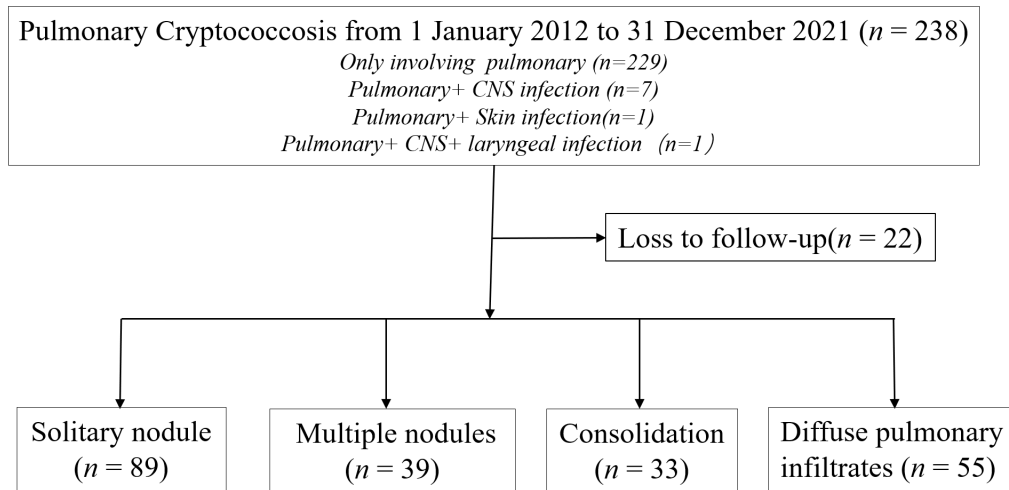


Figure 2. Flow chart of case selection and chest imaging classification. CNS: central nervous system.

Table 1. Clinical manifestations and laboratory results

Items	Solitary nodule (n = 89)	Multiple nodules (n = 39)	Consolidation (n = 33)	Diffuse pulmonary infiltrates (n = 55)	Chi-square Value	p
Male/female	50 (56.18)	27 (69.23)	20 (60.61)	32 (58.18)	1.995	0.573
Age, years	49 (42,59)	52 (44,64)	48 (39,64)	52 (42,63)	/	0.376
Immunocompetent/ Immunocompromised	70 (78.65)	31 (79.49)	26 (78.79)	40 (72.73)	0.896	0.826
Chronic disease						
Diabetes	6 (6.74)	10 (25.64)	4 (12.12)	10 (18.18)	9.239	0.026*
Chronic kidney disease	0 (0.00)	1 (2.56)	0 (0.00)	0 (0.00)	4.560	0.207
Solid organ transplantation	1 (0.00)	0 (0.00)	0 (0.00)	0 (0.00)	1.434	0.698
Rheumatologic disease	1 (1.12)	0 (0.00)	0 (0.00)	1 (1.82)	1.188	0.756
Solid tumours	8 (8.99)	2 (5.13)	2 (6.06)	1 (1.82)	3.158	0.368
Haematologic malignancy	0 (0.00)	1 (2.56)	2 (6.06)	3 (5.45)	5.326	0.149
Chronic steroid or immunosuppressive drug use	7 (7.87)	6 (15.38)	3 (9.09)	8 (14.55)	2.464	0.482
Chronic liver disease	2 (2.25)	1 (2.56)	2 (6.06)	4 (7.27)	2.697	0.441
Clinical symptoms at onset	20 (22.47)	14 (35.90)	19 (57.58)	30 (54.55)	20.835	< 0.001*
Fever	7 (7.87)	4 (4.49)	8 (24.24)	11 (20.00)	7.806	0.050
Cough	13 (14.61)	10 (11.24)	14 (42.42)	26 (47.27)	20.902	< 0.001*
Expectoration	10 (11.24)	10 (11.24)	9 (27.27)	20 (36.36)	13.109	0.004*
Shortness of breath	2 (2.25)	0 (0.00)	1 (3.03)	2 (3.64)	1.455	0.693
Chest pain	3 (3.37)	1 (2.56)	4 (12.12)	5 (20.00)	5.017	0.171
Serum antigen assay	7.5 (0,20)	20 (15,40)	40 (10,320)	80 (20,320)	/	< 0.001*
Leukocytes *10 ⁹ /L	6.66 ± 1.89	6.70 ± 2.74	7.30 ± 3.81	6.87 ± 2.52	/	0.781
Neutrophils *10 ⁹ /L	4.43 ± 1.74	4.50 ± 2.70	4.91 ± 3.55	4.73 ± 2.40	/	0.700
Lymphocytes *10 ⁹ /L	1.34 ± 0.71	1.60 ± 0.74	1.58 ± 0.57	1.41 ± 0.61	/	0.357
CD4 (cells/μL)	462.28 ± 369.48	479.88 ± 365.03	435.04 ± 416.97	496.41 ± 311.28	/	0.838
ESR (mm/H)	14.69 ± 12.99	17.36 ± 18.30	28.12 ± 30.89	21.27 ± 19.95	/	0.239
CRP (mg/L)	4.88 ± 7.40	8.08 ± 16.48	13.71 ± 29.63	10.48 ± 20.10	/	0.534
IL-2 (U/mL)	204.54 ± 251.84	369.57 ± 231.64	378.45 ± 160.56	659.20 ± 663.65	/	0.062
IL-6 (pg/mL)	2.26 ± 3.30	4.02 ± 3.79	3.29 ± 2.56	5.06 ± 5.78	/	0.022
INF-γ (pg/mL)	6.63 ± 7.32	8.52 ± 7.97	32.49 ± 96.91	11.26 ± 9.20	/	0.106
Initial treatment: Medication/ surgery	47 (52.81)	29 (74.36)	33 (100.00)	54 (98.18)	50.754	< 0.001*
Involvement of other sites	3 (3.37)	2 (5.13)	1 (3.03)	2 (3.64)	0.292	0.961
Improvement days	33 (27,58)	40 (33,58)	32 (16,62)	30 (14,45)	/	0.149
Treatment days	111 (31,199)	150 (90,307)	207 (134,323)	280 (163,364)	/	< 0.001*
Improved but nonresorbed lesions	40 (44.94)	24 (61.54)	29 (87.88)	47 (85.45)	60.076	< 0.001*

The values in brackets for chronic disease, clinical symptoms at onset, medication, other parts involved and lesions that improved but remained nonresorbed are percentages, and the values in brackets for age, serum antigen assay, improvement days and treatment days are quartiles. Bolded text and asterisks (*) indicate significant differences. ESR: erythrocyte sedimentation rate, CRP: high-sensitivity C-reactive protein, IL-2: interleukin-2, IL-6: interleukin-6, INF-γ: interferon-gamma. Involvement of other sites: 9 cases are shown in Figure 2.

3.3. Imaging manifestations

Burrs were most commonly observed in solitary nodules or multiple nodules, followed by lobulation ($p = 0.031^*$) and cavitation. The air bronchial sign was the predominant manifestation on imaging of consolidation and diffuse pulmonary infiltrates ($p < 0.001^*$). Imaging of single nodules, multiple nodules, and consolidation of pulmonary cryptococcosis most commonly involved the right lower lung, followed by the left lower lung in Table 2.

3.4. Factors related to the treatment course

It was proposed that the serum antigen assay, the

number of infectious lobes, and the involvement of extrapulmonary lesions and lower right lobes be employed as predictive indicators for a longer treatment duration than the median treatment duration for patients with different imaging manifestations (Figure 3).

3.5. Treatment for different imaging manifestations and prognoses

There was no significant difference in the percentage of patients who used amphotericin B or amphotericin B liposomes among patients with four different types of imaging presentations. Only one patient who underwent imaging for consolidation died because of

Table 2. Imaging manifestations

Items	Solitary nodule (n = 89)	Multiple nodules (n = 39)	Consolidation (n = 33)	Diffuse pulmonary infiltrates (n = 55)	Chi-square Value	P
CT characteristic						
<i>lobulation</i>	13 (14.61)	4 (10.27)	0 (0.00)	2 (3.64)	8.857	0.031*
<i>burr</i>	17 (19.10)	9 (23.08)	2 (6.06)	5 (9.09)	6.630	0.085
<i>cavitation</i>	11 (12.36)	5 (12.82)	3 (9.09)	10 (1.82)	1.703	0.636
<i>halo sign</i>	1 (1.12)	2 (5.13)	1 (3.03)	5 (9.09)	5.601	0.133
<i>air bronchial sign</i>	1 (1.12)	4 (10.26)	8 (24.24)	17 (30.91)	28.836	< 0.001*
<i>mediastinal lymph nodes</i>	2 (2.24)	4 (10.26)	1 (3.03)	2 (3.64)	4.589	0.205
<i>pleural effusion</i>	0 (0.00)	0 (0.00)	1 (3.03)	0 (0.00)	5.571	0.135
Involvement of lung lobes						
<i>upper left lobe</i>	10 (11.24)	14 (35.90)	6 (18.18)	22 (40.00)	106.481	< 0.001*
<i>lower left lobe</i>	24 (26.97)	18 (46.15)	10 (30.30)	10 (18.18)	160.782	0.005*
<i>upper right lobe</i>	17 (19.10)	16 (41.02)	5 (15.15)	19 (34.55)	119.555	0.013*
<i>middle right lobe</i>	4 (4.49)	17 (43.59)	7 (21.21)	10 (18.18)	69.319	< 0.001*
<i>lower right lobe</i>	34 (38.20)	25 (64.10)	17 (51.52)	31 (56.36)	208.152	0.030*

The values in brackets are percentages, and the values in bold and * indicate significant differences.

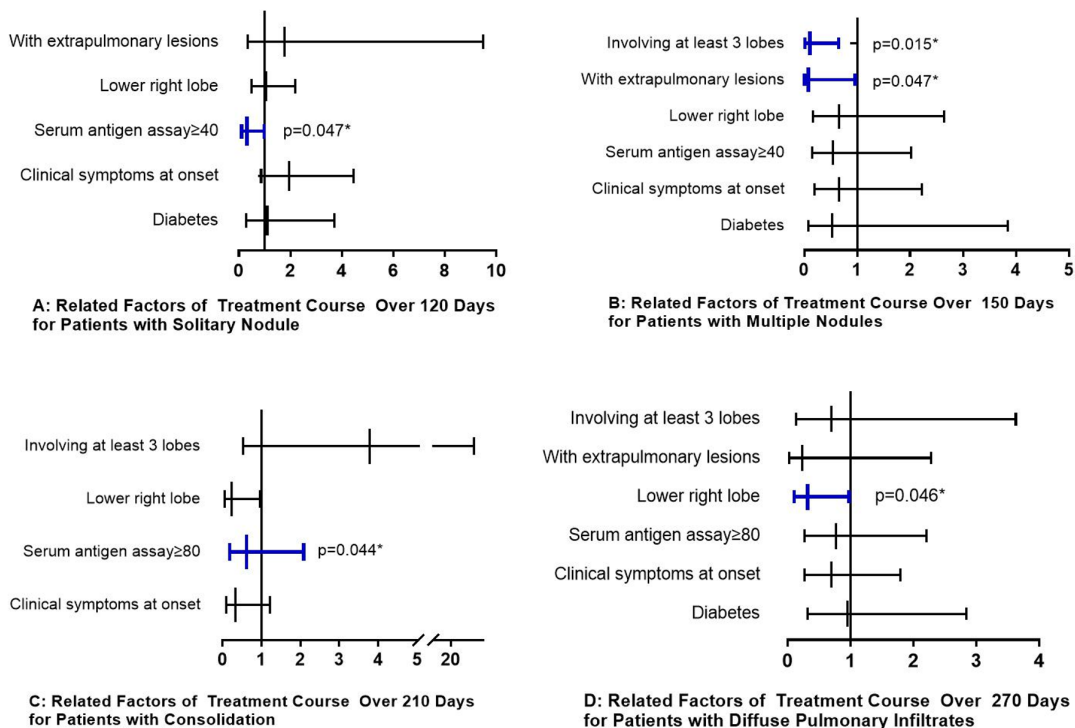


Figure 3. Factors associated with prolonged treatment of pulmonary cryptococcosis with different imaging manifestations.

Table 3. Treatments for the different imaging manifestations

Treatment	Solitary nodule (n = 89)	Multiple nodules (n = 39)	Consolidation (n = 33)	Diffuse pulmonary infiltrates (n = 55)	Chi-square Value	P
No medicine	23 (25.84)	6 (15.38)	0 (0.00)	0 (0.00)	25.581	< 0.001*
Triazoles ± Fluorocytosine	54 (60.67)	27 (69.23)	28 (84.85)	50 (90.91)	18.671	< 0.001*
Amphotericin B/ Amphotericin B Liposome after Fluconazole	6 (6.90)	5 (12.82)	5 (15.15)	4 (7.27)	2.882	0.410
Amphotericin B/ Amphotericin B Liposome ± Fluorocytosine	4 (4.49)	1 (2.56)	0 (0.00)	1 (1.82)	2.108	0.550
Surgery after medication	2 (2.25)	0 (0.00)	0 (0.00)	0 (0.00)	2.881	0.410

The values in brackets are percentages. Bold and * indicate significant differences. Triazoles include fluconazole, voriconazole and itraconazole. Amphotericin B/amphotericin B Liposome after fluconazole: Fluconazole was ineffective at treating this condition; thus, the treatment was switched to amphotericin B/amphotericin B Liposome.

myelodysplastic syndrome in Table 3.

4. Discussion

Consideration of imaging changes is highly important when evaluating the efficacy of pulmonary cryptococcosis treatment. This paper presents an inaugural examination of the time to improvement in patients exhibiting pulmonary cryptococcosis with varying imaging manifestations. Our findings contrast with our initial hypothesis that the time to improvement on imaging would be dependent on the lesion size. However, the time to improvement was approximately four weeks for both the nodular and diffuse lesions. These results suggest that a period of approximately four weeks should be allowed for follow-up imaging to assess improvement following the use of antifungal drugs.

The global guidelines for diagnosing and managing cryptococcosis indicate that the recommended course of treatment for pulmonary cryptococcosis is 6–12 months, with the possibility of a shorter duration (*e.g.*, 3 months) in immunocompetent individuals with mild isolated pulmonary cryptococcosis (9). This conclusion is generally consistent with the findings of our study. We aimed to further prognosticate the treatment time that may be required for different imaging presentations. Our findings indicate that the treatment of a single nodule or multiple nodules may take less than six months, whereas the treatment of patients showing consolidation and diffuse pulmonary infiltrates upon imaging may require six to twelve months.

The question of when treatment for pulmonary cryptococcosis can be discontinued has always been of great interest to clinicians. Only 12–55% of patients with pulmonary cryptococcosis achieve complete resolution of their intrapulmonary lesions, and the majority of patients will have long-term residual intrapulmonary lesions. In our study, lesions extending to a single nodule

stabilized after approximately four months of treatment, whereas other imaging manifestations of pulmonary cryptococcosis stabilized with no lesion resorption after seven to nine months of treatment. Therefore, the persistence of nonresorption assessed by imaging does not constitute an indication for the long-term use of drugs.

Recent studies have reported a 10%-30% incidence of fluconazole-resistant *Cryptococcus* isolates in patients (10,11); moreover, *Cryptococcus* has the potential to acquire fluconazole resistance during long-term treatment with this drug (12-14). The finding that the proportion of pathologies requiring amphotericin B or amphotericin B liposome therapy after ineffective fluconazole treatment did not increase with consolidation or diffuse pulmonary infiltrates in patients with cryptococcosis compared with those with nodular forms of cryptococcosis is not entirely consistent with our conventional knowledge (9,15). These results indicate that imaging findings are not indicative of the therapeutic efficacy of fluconazole in patients. Consequently, active drug sensitivity testing is essential in diagnostic and therapeutic processes.

The detection of cryptococcal antigen (CrAg) may prove to be an efficacious diagnostic tool for pulmonary cryptococcosis that facilitates the prompt commencement of antifungal therapy (16,17). The patient's immune status and imaging modality affect the detection of cryptococcal antigens (18,19). In our study, cryptococcal antigen titres were found to be significantly greater in patients with imaging manifestations of consolidation and diffuse infiltrates than in those with nodular phenotypes. Additionally, elevated antigen titres were observed to predict higher fungal loads and longer treatment times.

Because of the retrospective study design, certain preliminary laboratory data were absent for the evaluation of cellular immunity (CD4) and cytokines (IL-2, IL-6, INF- γ). Additionally, the comparison of follow-up chest imaging intervals and discontinuation times

among various physicians was subjective and lacked a standardized and rigorous definition were the limitations.

In conclusion, the duration of the treatment regimen for pulmonary cryptococcosis is contingent upon the imaging presentation. The serum antigen level, number of infectious lung lobes, presence of extrapulmonary lesions and presence of lesions in the lower right lobe are predictive indicators for a longer treatment duration. Antifungal treatment is recommended for approximately one month. Follow-up imaging should also be performed.

Acknowledgements

We would like to thank all the study participants whose data were used in this study. Furthermore, we are most grateful for the assistance and support of clinicians, laboratory technicians and radiologists at Zhongshan Hospital, Fudan University.

Funding: This work was supported by grants from the National Key Research and Development Program of China (2021YFC 2300400) and the Fund of Zhongshan Hospital Fudan University (2021ZSFZ15).

Conflict of Interest: The authors have no conflicts of interest to disclose.

References

- Smith RM, Mba-Jonas A, Tourdjman M, Schimek T, DeBess E, Marsden-Haug N, Harris JR. Treatment and outcomes among patients with *Cryptococcus gattii* infections in the United States Pacific Northwest. *PLoS One*. 2014; 9:e88875.
- Ye F, Xie JX, Zeng QS, Chen GQ, Zhong SQ, Zhong NS. Retrospective analysis of 76 immunocompetent patients with primary pulmonary cryptococcosis. *Lung*. 2012; 190:339-46.
- Kohno S, Kakeya H, Izumikawa K, Miyazaki T, Yamamoto Y, Yanagihara K, Mitsutake K, Miyazaki Y, Maesaki S, Yasuoka A, Tashiro T, Mine M, Uetani M, Ashizawa K. Clinical features of pulmonary cryptococcosis in non-HIV patients in Japan. *J Infect Chemother*. 2015; 21:23-30.
- Kishi K, Homma S, Kurosaki A, Kohno T, Motoi N, Yoshimura K. Clinical features and high-resolution CT findings of pulmonary cryptococcosis in non-AIDS patients. *Respir Med*. 2006; 100:807-812.
- Obmann VC, Bickel F, Hosek N, Ebner L, Huber AT, Damonti L, Zimmerli S, Christe A. Radiological CT Patterns and Distribution of Invasive Pulmonary Aspergillus, Non-Aspergillus, Cryptococcus and Pneumocystis Jirovecii Mold Infections - A Multicenter Study. *Rofo*. 2021; 193:1304-1314.
- Wang DX, Zhang Q, Wen QT, *et al.* Comparison of CT findings and histopathological characteristics of pulmonary cryptococcosis in immunocompetent and immunocompromised patients. *Sci Rep*. 2022 Apr 5;12(1):5712. doi: 10.1038/s41598-022-09794-6.
- Wang D, Wu C, Gao J, Zhao S, Ma X, Wei B, Feng L, Wang Y, Xue X. Comparative study of primary pulmonary cryptococcosis with multiple nodules or masses by CT and pathology. *Exp Ther Med*. 2018; 16:4437-4444.
- Baddley JW, Perfect JR, Oster RA, Larsen RA, Pankey GA, Henderson H, Haas DW, Kauffman CA, Patel R, Zaas AK, Pappas PG. Pulmonary cryptococcosis in patients without HIV infection: factors associated with disseminated disease. *Eur J Clin Microbiol Infect Dis*. 2008; 27:937-943.
- Chang CC, Harrison TS, Bicanic TA, *et al.* Global guideline for the diagnosis and management of cryptococcosis: An initiative of the ECMM and ISHAM in cooperation with the ASM. *Lancet Infect Dis*. 2024; 24:e495-e512.
- Cheong JWS, McCormack J. Fluconazole resistance in cryptococcal disease: Emerging or intrinsic? *Med Mycol*. 2013; 51:261-269.
- Bongomin F, Oladele RO, Gago S, Moore CB, Richardson MD. A systematic review of fluconazole resistance in clinical isolates of *Cryptococcus* species. *Mycoses*. 2018; 61:290-297.
- Lee Y, Puumala E, Robbins N, Cowen LE. Antifungal Drug Resistance: Molecular Mechanisms in *Candida albicans* and Beyond. *Chem Rev*. 2021; 121:3390-3411.
- Robbins N, Caplan T, Cowen LE. Molecular evolution of antifungal drug resistance. *Annu Rev Microbiol*. 2017; 71:753-775.
- Skolnik K, Huston S, Mody CH. Cryptococcal lung infections. *Clin Chest Med*. 2017; 38:451-464.
- Stone NR, Bicanic T, Salim R, Hope W. Liposomal amphotericin B (AmBisome®): A review of the pharmacokinetics, pharmacodynamics, clinical experience and future directions. *Drugs*. 2016; 76:485-500.
- Temfack E, Rim JJB, Spijker R, Loyse A, Chiller T, Pappas PG, Perfect J, Sorell TC, Harrison TS, Cohen JF, Lortholary O. Cryptococcal Antigen in Serum and Cerebrospinal Fluid for Detecting Cryptococcal Meningitis in Adults Living With Human Immunodeficiency Virus: Systematic Review and Meta-Analysis of Diagnostic Test Accuracy Studies. *Clin Infect Dis*. 2021; 72:1268-1278.
- Schub T, Forster J, Suerbaum S, Wagener J, Dichtl K. Comparison of a Lateral Flow Assay and a Latex Agglutination Test for the Diagnosis of *Cryptococcus Neoformans* Infection. *Curr Microbiol*. 2021; 78:3989-3995.
- Min J, Huang K, Shi C, Li L, Li F, Zhu T, Deng H. Pulmonary Cryptococcosis: comparison of Cryptococcal antigen detection and radiography in Immunocompetent and Immunocompromised patients. *BMC Infect Dis*. 2020; 20:91.
- Singh N, Alexander BD, Lortholary O, *et al.* Pulmonary cryptococcosis in solid organ transplant recipients: clinical relevance of serum cryptococcal antigen. *Clin Infect Dis*. 2008; 46:e12-18.

Received September 18, 2024; Revised October 14, 2024; Accepted October 17, 2024.

*Address correspondence to:

Jue Pan, Department of Infectious Diseases, Zhongshan Hospital of Fudan University, 180 Fenglin Road, Shanghai 200032, China.
E-mail: pjzzy@163.com

Released online in J-STAGE as advance publication October 23, 2024.

Ligustrazine alleviates the progression of coronary artery calcification by inhibiting caspase-3/GSDME mediated pyroptosis

Honghui Yang*, Guian Xu, Qingman Li, Lijie Zhu

Department of Cardiology, Zhengzhou University, Central China Fuwai Hospital, Zhengzhou, China.

SUMMARY Coronary artery calcification (CAC) is an early marker for atherosclerosis and is mainly induced by the osteoblast-like phenotype conversion of vascular smooth muscle cells (VSMCs). Recent reports indicate that NOD-like receptor protein 3 (NLRP3)-mediated pyroptosis plays a significant role in the calcification of vascular smooth muscle cells (VSMCs), making it a promising target for treating calcific aortic valve disease (CAC). Ligustrazine, or tetramethylpyrazine (TMP), has been found effective in various cardiovascular and cerebrovascular diseases and is suggested to inhibit NLRP3-mediated pyroptosis. However, the function of TMP in CAC is unknown. Herein, influences of TMP on β -glycerophosphate (β -GP)-stimulated VSMCs and OPG^{-/-} mice were explored. Mouse Aortic Vascular Smooth Muscle (MOVAS-1) cells were stimulated by β -GP with si-caspase-3, si-Gasdermin E (GSDME) or TMP. Increased calcification, reactive oxygen species (ROS) level, Interleukin-1 β (IL-1 β) and Interleukin-18 (IL-18) levels, lactate dehydrogenase (LDH) release, enhanced apoptosis, and activated cysteine-aspartic acid protease-3 (caspase-3)/GSDME signaling were observed in β -GP-stimulated MOVAS-1 cells, which was sharply alleviated by si-caspase-3, si-GSDME or TMP. Furthermore, the impact of TMP on the β -GP-induced calcification and injury in MOVAS-1 cells was abolished by raptinal, an activator of caspase-3. Subsequently, OPG^{-/-} mice were dosed with TMP or TMP combined with raptinal. Calcium deposition, increased nodules, elevated IL-1 β and IL-18 levels, upregulated CASP3 and actin alpha 2, smooth muscle (ACTA2), and activated caspase-3/GSDME signaling in OPG^{-/-} mice were markedly alleviated by TMP, which were notably reversed by the co-administration of raptinal. Collectively, TMP mitigated CAC by inhibiting caspase-3/GSDME mediated pyroptosis.

Keywords coronary artery calcification, Ligustrazine, caspase-3, GSDME, vascular smooth muscle cells

1. Introduction

Cardiovascular disease ranks first in morbidity and mortality in the world, which is one of the most common chronic diseases and one of the most susceptible diseases in the elderly. Despite advances in the diagnosis and treatment of cardiovascular disease, the incidence is still increasing (1). CAC is an important marker of the late development of coronary atherosclerosis (CAS). CAC is a common type of arterial calcification, which contributes to the reduction of coronary vessel compliance. Abnormal vasoconstrictor response and impaired myocardial perfusion are risk factors for poor prognosis in patients with revascularization and coronary heart diseases (2,3). The degree of CAC has a certain impact on the stability of plaque. For example, microcalcifications within the fibrous cap may lead to plaque rupture (4), while the fibrous cap will be

disrupted by calcified nodules to expose collagen fibers and induce thrombosis (5). In addition, recurrent plaque rupture and healing after hemorrhage may lead to the development of obstructive fibrocalcific lesions, causing the occurrence of angina and sudden death (6). Currently, no effective agents for treating CAC are available in the clinic. Several reported treatment strategies, such as statins and RAAS system inhibitors, are reported with non-ideal results (7), and some studies even show that statins aggravate the development of calcification (8). As the pathogenesis of CAC is complex and the clinical therapeutic methods are lacking, studying the pathogenesis of vascular calcification and developing novel therapeutic drugs are of great significance.

VSMCs are contractile cells located in the vascular wall, and secrete pro- or anti-calcification factors. The osteoblast-like phenotype conversion of VSMCs is claimed to be the most important inducer in vascular

calcification. Following the stimulation of factors, such as oxidative stress, inflammation, calcium and phosphorus internal environment disorders, the phenotype conversion of VSMCs to osteoblast-like cells is induced. By secreting bone-related transcription factors and upregulating bone-related proteins, osteoblasts promote the formation of vascular calcification (9). Matrix vesicles will be released by apoptotic VSMCs or osteoblast-like cells. These matrix vesicles are rich in phospholipids and convert calcium ions to amorphous calcium phosphate, which is further converted to hydroxyapatite. The process of calcification starts on the surface of the vesicle or inside the vesicle, and contributes to the initiation of calcification (10). Recently, the role of NLRP3-mediated pyroptosis in the calcification of VSMCs has been widely reported (11,12). Regulating the pyroptosis of VSMCs will be a promising method for treating CAC.

In 2017, Wang *et al.* (13) reported that Gasdermin E (GSDME), a member of the Gasdermin protein family, can be cleaved by caspase-3 and mediates development of pyroptosis, which is consistent with the results of Shao Feng's team (14) in the same year. GSDME and GSDMD belong to the Gasdermin family and share a pore forming structure (15). Unlike GSDMD, cleavage of GSDME does not involve caspase-1 or caspase-4/5/11 pathways. Instead, GSDME relies on caspase-3, another member of the caspase protein family. In contrast to other members of the caspase protein family, caspase-3 is located at the end of the caspase cascade and is a major effector enzyme. Upon activation by upstream caspases, caspase-3 is involved in the execution of apoptosis and the activation of other inflammatory mediators (16,17).

The research team at Amgen in the United States first found OPG in the cDNA library of rat small intestine in 1997 (18). In the same year, Tsuda *et al.* also found a cytokine that could inhibit the formation of osteoclasts in the culture medium of human embryonic fibroblasts, which was named as osteoclast formation inhibitory factor (OCIF) (19). In subsequent studies, Ten *et al.* inferred and analyzed the amino acid sequences of OPG and OCIF, and finally confirmed that OCIF and OPG were the same protein (20). It is widely reported that the OPG/RANKL/RANK system participates in vascular calcification. Price *et al.* found that in the mouse model of vascular calcification established by the induction of warfarin and toxic doses of VitD, supplementation of OPG significantly inhibited progression of vascular calcification (21). The OPG^{-/-} mice established by Bucay developed progressively aggravated systemic osteoporosis after birth, accompanied by medial calcification of the aorta and/or renal artery (22). Min *et al.* confirmed that intravenous injection of recombinant OPG protein or transgenic overexpression of OPG inhibited occurrence of vascular calcification and osteoporosis in OPG^{-/-} mice (23). These data indicate that OPG is associated with osteoporosis and vascular

calcification, and is a protective factor for vascular calcification. The OPG^{-/-} mouse is a recognized animal model of arterial calcification and has incomparable advantages in studying the role of the OPG/RANKL/RANK system in arterial calcification (24).

Ligustrazine, also named as 2, 3, 5, 6-tetramethylpyrazine (TMP), mainly extracted from the root of Chuanxiong rhizoma, is a non-volatile alkaloid with anti-ischemia-reperfusion injury and protective effects against cell damage, which provides a foundation for the clinical application of TMP in the treatment of various cardiovascular and cerebrovascular diseases (25). Furthermore, TMP is reported to have promising antioxidant effects (26). The previous study has confirmed the therapeutic function of TMP against atherosclerosis (27). Moreover, several reports have claimed the inhibitory effect of TMP on NLRP3-mediated pyroptosis (28,29). However, the potential therapeutic function of TMP against CAC remains uncertain. Herein, the regulatory effect of TMP on β -GP-treated VSMCs and OPG^{-/-} mice was explored.

2. Materials and Methods

2.1. Cells and treatments

Mouse vascular smooth muscle cell line, MOVAS-1 cells, was obtained from ATCC (USA) and cultured in DMEM medium involving penicillin/streptomycin and 10% FBS at 5% CO₂ and 37°C. To establish the *in vitro* vascular calcification model, MOVAS-1 cells were treated with 2.5 mM β -glycerophosphate (β -GP, Sigma, UK) for 21 days.

2.2. Transfection

To knockdown the caspase-3 and GSDME level in MOVAS-1 cells, cells were transfected with the siRNA targeting caspase-3 (si-caspase-3) and the siRNA targeting GSDME (si-GSDME) with lipofectamine3000 (Thermo Fisher, USA). Si-NC was used as a negative control for siRNAs. After culturing lipofectamine3000 and siRNAs separately in serum-free medium for 5 min, 2 solutions were mixed and incubated for 20 min, followed by being introduced into MOVAS-1 cells and incubating for 48 h. All siRNAs were synthesized by Genscript (Nanjing, China). Sequences of siRNAs are shown in Table 1.

2.3. RT-PCR

MOVAS-1 cells were collected to extract total RNAs using the Trizol reagent (15596026, Invitrogen, USA). Subsequently, cDNA synthesis was performed utilizing the RT-PCR reverse transcription kit (205311, QIAGEN, USA), followed by PCR amplification in the PCR instrument (Quant Studio5, Thermo Fisher, USA). The

Table 1. Sequences of siRNAs

SiRNAs	Sense (5'-3')	Antisense (5'-3')
Si-GSDME	GGAUCAGGAUCUAUUACCU	AGGUAUUAGAUCUGAUCCTT
Si-caspase-3	TGACATCTCGGTCTGGTAC	TACCAGTGGAGGCCGACTT
Si-NC	CCAAGAACTTCCAGAACATAT	ATATGTTCTGGAAGTCTTGG

internal reference gene was GAPDH and gene levels were determined utilizing the $2^{-\Delta\Delta Ct}$ method.

2.4. Alizarin red staining

After fixing with 4% paraformaldehyde for 10 min, MOVAS-1 cells were stained with alizarin red solution (2003999, Sigma, USA) in the dark for half an hour. Then, cells were washed with ddH₂O 3 times, followed by observation under the optical microscope (SP8, Leica, Germany).

2.5. ROS detection using the flow cytometry

MOVAS-1 cells were centrifuged at 300 g for 10 min and collected, followed by resuspension using serum-free medium containing 10 μ M DCFH-DA. After incubating at 37 °C for 20 min, cells were rinsed with PBS and loaded onto flow cytometry (CytoFLEX3, Beckman, USA) to detect the ROS level.

2.6. The detection of LDH release

After plating on 96-well plates, MOVAS-1 cells were exposed to LDH reagent (11644793001, Sigma, USA), followed by 90 min incubation in the dark. Then, the optical density was determined utilizing a microplate reader (EnSpire, PerkinElmer, USA) at 490 nm, followed by calculating LDH release according to the standard curve.

2.7. ELISA assay for cytokine level detection

The IL-1 β (E-EL-M0037c, eBioScience, USA) and IL-18 level (BMS618-3, eBioScience, USA) were detected using commercial kits. The coronary artery tissues were collected and homogenized, followed by centrifugation and collecting the supernatant. For cell samples, MOVAS-1 cells were centrifuged at 300 g for 10 min and supernatant was collected. 50 μ L supernatant was diluted to a 1:1 ratio, which was loaded into the wells. Then, 50 μ L Biotin-labeled antibody was introduced and cultured for 60 min at 37°C, followed by removing the reagent and adding 80 μ L HRP-loaded secondary antibody. Following half an hour culture at 37°C, 50 μ L TMB substrates were added and cultured at 37°C for 10 min, followed by loading 50 μ L stop solution. Lastly, the OD value was measured utilizing a microplate reader (EnSpire, PerkinElmer, USA).

2.8. Hoechst/PI staining

MOVAS-1 cells were loaded into 6-well plates and cultured overnight, followed by discarding the medium and introducing 10 μ L Heochst staining reagent at 37°C in the dark for 12 min. Cells were then centrifuged at 300 g at 4°C for 5 min and the medium was discarded, followed by introducing 5 μ L PI solution and placement in the dark for 6 min. 50 μ L stained cells were dropped onto a cover glass and observed under the fluorescence microscope (DM2500, Leica, Germany).

2.9. Animals and grouping

Thirty male OPG^{-/-} mice (7-9 weeks, 18-22 g) and 12 male wide type mice (WT, 7-9 weeks, 18-22 g) were purchased from Shanghai Model Organisms Center, Inc (China) and raised in the SPF laboratory with controlled humidity, temperature and a 12/12 light/dark cycle. After 1-week of adaption, animals were divided into 3 groups (n=6/group): Control, Model, and TMP. In the Model and TMP groups, OPG^{-/-} mice were orally administered 200 μ L/day normal saline and 80 mg/kg/day TMP for 4 weeks. In the control group, WT mice were orally administered 200 μ L/day normal saline for 4 weeks. To verify the potential mechanism of TMP in calcification, animals were divided into 4 groups (n=6/group): Control, Model, TMP, and TMP+raptinal. Administrations of the control, model, and TMP groups are listed above. In the TMP+raptinal group, OPG^{-/-} mice were orally administered 80 mg/kg/day TMP for 4 weeks and 20 mg/kg/day raptinal for 3 consecutive days in the beginning.

All animal experiments were authorized by the ethics committee of Central China Fuwai Hospital, Zhengzhou University (No.2021032).

2.10. HE staining assay

Coronary artery tissues were fixed in 4% paraformaldehyde solution for 90 min, dehydrated in a gradient of 70% to 100% ethanol, transparent in xylene, embedded in paraffin, and sectioned. Paraffin sections were deparaffinized with xylene and eluted in xylene for 10 min, 100% ethanol for 5 min, 90% ethanol for 5 min, 80% ethanol for 5 min, 70% ethanol for 5 min, and distilled water for 5 min, followed by staining with hematoxylin for 10 min, washed with distilled water for 10 min, differentiated in 1% hydrochloric acid for several seconds, and counterstained with eosin. Slices

were dehydrated, dried, and sealed with neutral gum, and observed under a microscope (SP8, Leica, Germany).

2.11. Von Kossa staining assay

After deparaffinization and dehydration, sections were exposed to nitrate solution for 30 min for staining. After washing with distilled water three times, sections were fixed with sodium thiosulfate solution and counterstained with neutral fuchsin. Calcium deposition was observed under a microscope (SP8, Leica, Germany) after rinsing again with distilled water.

2.12. Western blotting assay

Coronary artery tissues or MOVAS-1 cells were collected to extract total proteins using the RIPA lysis buffer, followed by quantification with the BCA method (23227, Elabscience, USA). The separation of proteins was conducted using SDS-PAGE, followed by transferring the separated proteins onto a PVDF membrane. Blocking was conducted using 5% skim milk and primary antibodies against pro-caspase-3 (1/1000, ab32150, Abcam, USA), cleaved-caspase-3 (1/500, ab32042, Abcam, USA), GSDME-N (1:1000, ab215191, Abcam, USA), NLRP3 (1:1000, ab263899, Abcam, USA), and GAPDH (1:2000, ab8245, Abcam, USA). Subsequently, the secondary antibody (1:4000, ab288151, Abcam, USA) was introduced and cultured for 60 min. ECL solution was loaded for exposure and the protein level was quantified with Image J software.

2.13. Immunofluorescence assay

Sections of coronary artery tissues were rinsed utilizing distilled water and incubated using 10% goat serum for blocking, followed by introducing the primary antibody against CASP3 (1:25, ab32351, Abcam, USA) and ACTA2 (1:25, ab7817, Abcam, USA) overnight at 4°C. After washing several times, sections were incubated with secondary antibody (1:200, ab150077, Abcam, USA) for 90 min at 37°C and then stained with DAB dye, followed by observing the images using the fluorescence microscope (DM2500, Leica, Germany).

2.14. Statistical analysis

Data was expressed as Mean \pm SD. The comparison among three or more groups was analyzed using the one-way ANOVA (Tukey's method). The analysis was conducted using GraphPad software (GraphPad Prism 8) and $p < 0.05$ was taken as a significant difference.

3. Results

3.1. Caspase-3/GSDME axis participated in β -GP-induced calcification in MOVAS-1 cells

To explore the function of the caspase-3/GSDME axis in β -GP-induced calcification in MOVAS-1 cells, MOVAS-1 cells were stimulated by β -GP with si-caspase-3 or si-GSDME. First, the knockdown efficacy of caspase-3 and GSDME in MOVAS-1 cells was verified using the RT-PCR assay. Compared to β -GP+si-NC, caspase-3 was markedly downregulated in the β -GP+si-caspase-3 group, while the GSDME level was notably decreased in the β -GP+si-GSDME group (Figure 1A). As visualized by the Alizarin red staining assay, the percentage of calcification was sharply increased in β -GP-stimulated MOVAS-1 cells, which was markedly reduced by si-caspase-3 and si-GSDME (Figure 1B). The IL-1 β level was found increased from 34.4 to 151.0 ng/L in β -GP-stimulated MOVAS-1 cells, which was reduced to 94.1 and 98.5 ng/L by si-caspase-3 and si-GSDME, respectively. Moreover, the IL-18 level in the control, β -GP, β -GP+si-caspase-3, and β -GP+si-GSDME groups was 92.5, 347.3, 221.2, and 216.3 ng/L, respectively (Figure 1C). The dramatically elevated LDH release observed in the β -GP group was markedly repressed by si-caspase-3 and si-GSDME (Figure 1D). Furthermore, the increased percentage of Hoechst-positive cells in β -GP-stimulated MOVAS-1 cells was notably reduced by si-caspase-3 and si-GSDME (Fig 1E). More importantly, levels of cleaved-caspase-3, GSDME-N, and NLRP3 were sharply increased in the β -GP group, which was markedly repressed by si-caspase-3 and si-GSDME (Figure 1F).

3.2. TMP alleviated the β -GP-induced calcification in MOVAS-1 cells

To explore the impact of TMP on β -GP-induced calcification in MOVAS-1 cells, MOVAS-1 cells were stimulated by β -GP, followed by treatment with 25 μ M TMP for 24 h. The increased percentage of calcification in β -GP-stimulated MOVAS-1 cells was suppressed by TMP (Figure 2A). Furthermore, the elevated ROS level in β -GP-stimulated MOVAS-1 cells was reduced by TMP (Figure 2B). The IL-1 β level in the control, β -GP, and β -GP+TMP groups was 49.4, 139.1, and 100.0 ng/L, respectively. In addition, the IL-18 level was found increased from 68.3 to 230.7 ng/L in β -GP-stimulated MOVAS-1 cells, which was reduced to 157.2 ng/L by TMP (Figure 2C). LDH release in the control, β -GP, and β -GP+TMP groups was 0.67, 2.25, and 1.29 mM, respectively (Figure 2D). The increased percentage of Hoechst-positive cells in β -GP-stimulated MOVAS-1 cells was greatly reduced by TMP (Fig 2E). Moreover, cleaved-caspase-3, GSDME-N, and NLRP3 were markedly upregulated in the β -GP group, which were greatly downregulated by TMP (Figure 2F).

3.3. The influence of TMP on β -GP-induced calcification in MOVAS-1 cells was abolished by the activation of caspase-3

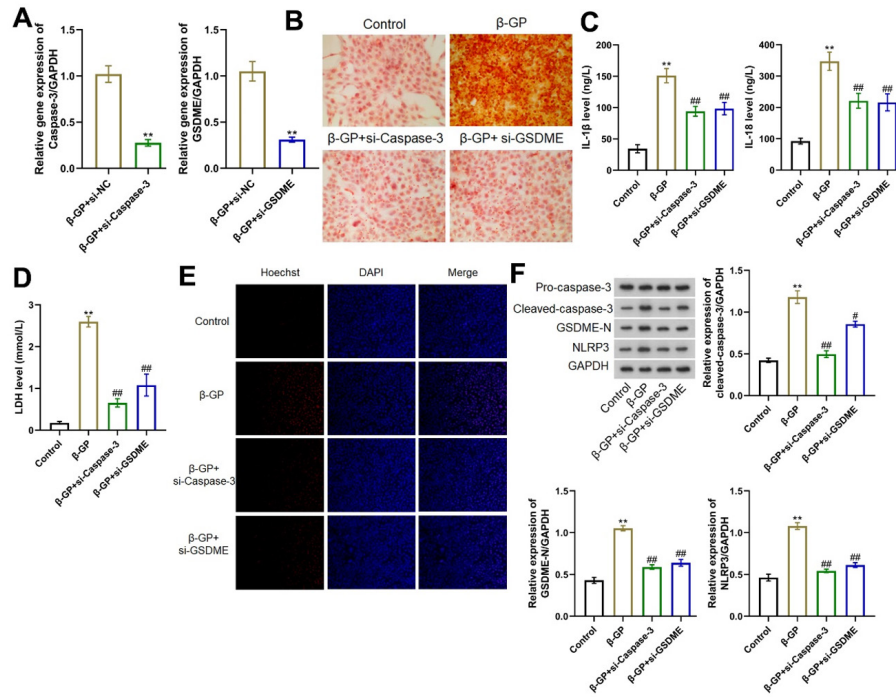


Figure 1. Caspase-3/GSDME axis was involved in β -GP-induced calcification in MOVAS-1 cells. (A) Knockdown efficacy of caspase-3 and GSDME in MOVAS-1 cells was verified using the RT-PCR assay (** $p < 0.01$ vs. β -GP+si-NC); (B) Calcification in MOVAS-1 cells was visualized using the Alizarin red staining assay; (C) ELISA assay was utilized for the detection of IL-1 β and IL-18 levels in MOVAS-1 cells; (D) LDH release in MOVAS-1 cells was determined using a commercial kit; (E) Apoptosis of MOVAS-1 cells was evaluated using the Hoechst/PI staining assay; (F) Levels of cleaved-caspase-3, GSDME-N, and NLRP3 were detected using Western blotting (** $p < 0.01$ vs. Control, $^{###}p < 0.01$ vs. β -GP).

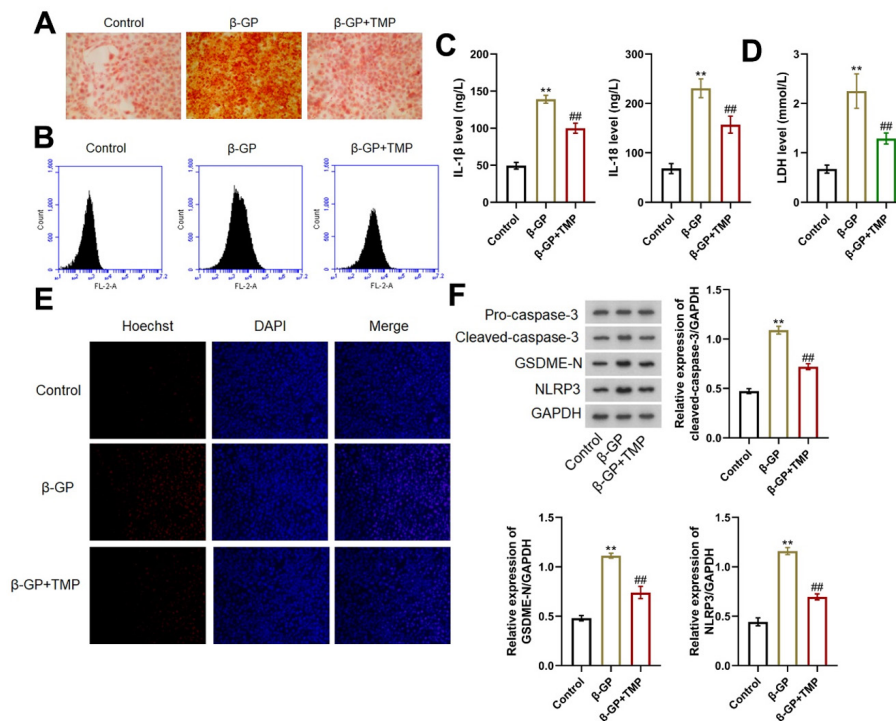


Figure 2. The β -GP-induced calcification in MOVAS-1 cells was alleviated by TMP. (A) Calcification in MOVAS-1 cells was determined using the Alizarin red staining assay; (B) ROS level was measured using flow cytometry; (C) ELISA assay was utilized for the detection of IL-1 β and IL-18 levels; (D) LDH release in MOVAS-1 cells was detected using a commercial kit; (E) Apoptosis of MOVAS-1 cells was determined using the Hoechst/PI staining assay; (F) Expressions of cleaved-caspase-3, GSDME-N, and NLRP3 were detected using Western blotting (** $p < 0.01$ vs. Control, $^{###}p < 0.01$ vs. β -GP).

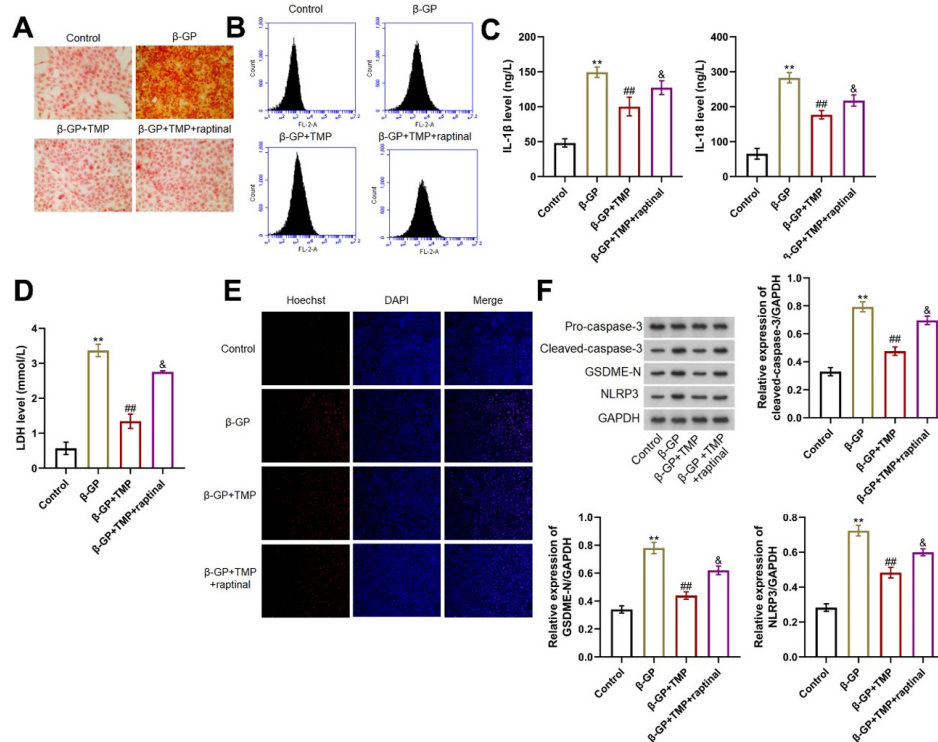


Figure 3. Activation of caspase-3 abolished the influence of TMP on the β -GP-induced calcification in MOVAS-1 cells. (A) Alizarin red staining assay was utilized to detect the calcification in MOVAS-1 cells; (B) Flow cytometry was used to measure the ROS level; (C) The IL-1 β and IL-18 level in MOVAS-1 cells was determined by ELISA assay; (D) A commercial kit was used for the detection of LDH release in MOVAS-1 cells; (E) The Hoechst/PI staining assay was used for detecting the apoptosis of MOVAS-1 cells; (F) Western blotting was utilized to determine the cleaved-caspase-3, GSDME-N, and NLRP3 levels (** $p < 0.01$ vs. Control, ## $p < 0.01$ vs. β -GP, & $p < 0.05$ vs. β -GP+TMP).

To identify whether TMP exerted anti-calcification function by inhibiting caspase-3, MOVAS-1 cells were stimulated by β -GP, followed by treatment with 25 μ M TMP with or without 10 μ M raptinal, an agonist of caspase-3. The increased percentage of calcification in β -GP-stimulated MOVAS-1 cells was reduced by TMP, which was elevated by the co-culture with raptinal (Figure 3A). Furthermore, the promoted ROS level observed in the β -GP group was decreased by TMP, which was reversed in the β -GP+TMP+ raptinal group (Figure 3B). IL-1 β level in the control, β -GP, β -GP+TMP, and β -GP+TMP+ raptinal groups was 48.1, 149.2, 100.2, and 127.3 ng/L, respectively. IL-18 level in the control, β -GP, β -GP+TMP, and β -GP+TMP+ raptinal groups was 65.1, 282.6, 176.8, and 217.3 ng/L, respectively (Figure 3C). LDH release in MOVAS-1 cells was increased from 0.57 to 3.37 mM by β -GP, and was markedly reduced to 1.35 mM in the β -GP+TMP group, which was greatly reversed to 2.75 mM in the β -GP+TMP+ raptinal group (Figure 3D). The increased percentage of Hoechst-positive cells in the β -GP group was repressed by TMP, which was markedly reversed by the co-culture with raptinal (Figure 3E). Moreover, the elevated levels of cleaved-caspase-3, GSDME-N, and NLRP3 in β -GP-stimulated MOVAS-1 cells were notably reduced by TMP, which were markedly reversed in the β -GP+TMP+ raptinal group (Figure 3F).

3.4. TMP ameliorated the progression of CAC in OPG^{-/-} mice

To identify the function of TMP against CAC, OPG^{-/-} mice were used to mimic the clinical symptom of CAC, which were orally administered with TMP. Calcium deposition was obviously observed in OPG^{-/-} mice, which was markedly alleviated by TMP (Figure 4A). Moreover, HE staining showed that the number of nodules was markedly increased in the model group, which was sharply reduced by TMP (Figure 4B). In coronary artery tissues, the IL-1 β level was sharply increased from 44.1 to 142.4 ng/L in OPG^{-/-} mice, which was greatly repressed to 77.1 ng/L by TMP. The IL-18 level in the control, model, and TMP groups was 52.8, 180.7, and 112.5 ng/L, respectively (Figure 4C). Increased levels of cleaved-caspase-3, GSDME-N, and NLRP3 in OPG^{-/-} mice were markedly decreased by TMP (Figure 4D). Moreover, the upregulated CASP3 and ACTA2 in OPG^{-/-} mice were downregulated by TMP (Figure 4E).

3.5. Inhibition of TMP on progression of CAC in OPG^{-/-} mice was abolished by activation of caspase-3

To identify whether TMP exerted anti-CAC function by suppressing caspase-3, OPG^{-/-} mice were administered TMP with or without raptinal, an agonist of caspase-3. The increased calcium deposition (Figure 5A) and

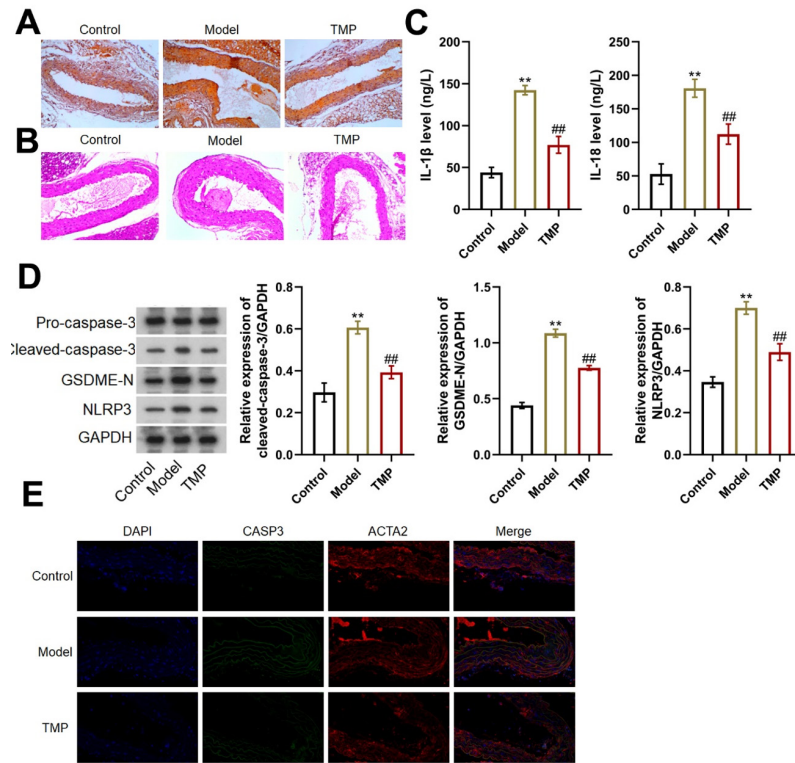


Figure 4. Progression of CAC in OPG^{-/-} mice was ameliorated by TMP. (A) Calcification in coronary artery tissues was evaluated using the Von Kossa staining assay; (B) The pathological state in coronary artery tissues was evaluated using HE staining; (C) The IL-1 β and IL-18 level in coronary artery tissues was detected using ELISA; (D) Expressions of cleaved-caspase-3, GSDME-N, and NLRP3 in coronary artery tissues were detected using Western blotting (** $p < 0.01$ vs. Control, ## $p < 0.01$ vs. Model); (E) The expression of CASP3 and ACTA2 in coronary artery tissues was evaluated by immunofluorescence.

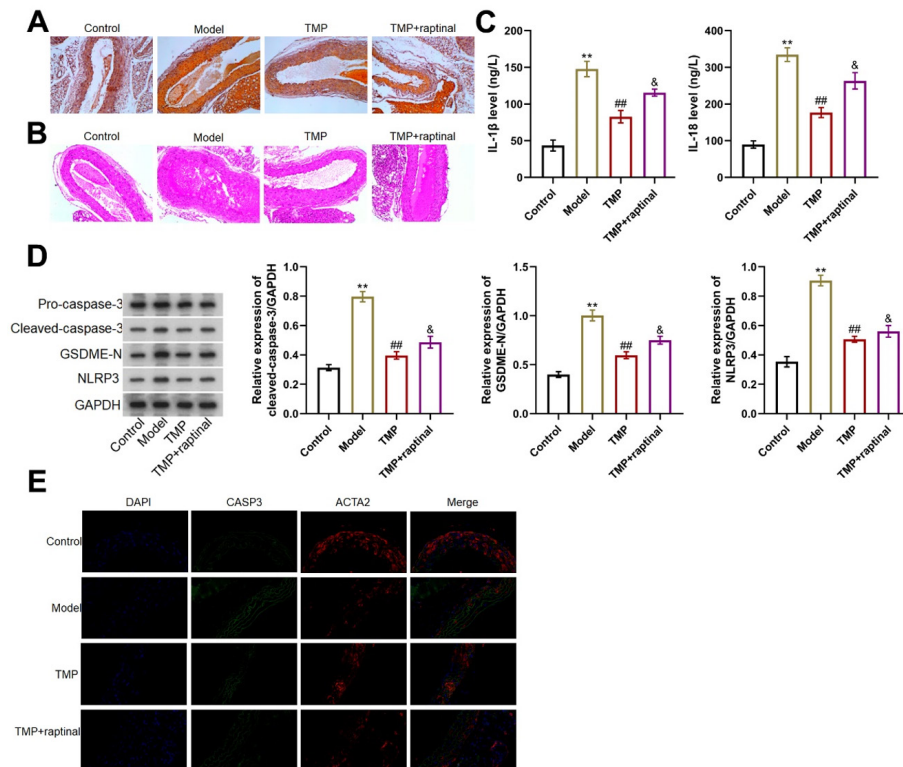


Figure 5. Activation of caspase-3 abolished the inhibition of TMP on the progression of CAC in OPG^{-/-} mice. (A) Calcification in coronary artery tissues was determined using the Von Kossa staining assay; (B) HE staining was used to evaluate the pathological state in coronary artery tissues; (C) The IL-1 β and IL-18 level in coronary artery tissues was measured using ELISA; (D) Western blotting was utilized to determine the cleaved-caspase-3, GSDME-N, and NLRP3 levels in coronary artery tissues (** $p < 0.01$ vs. Control, ## $p < 0.01$ vs. Model, & $p < 0.05$ vs. TMP); (E) Expression of CASP3 and ACTA2 in coronary artery tissues was determined using immunofluorescence.

elevated number of nodules (Figure 5B) observed in OPG^{-/-} mice were markedly repressed by TMP, which were signally reversed by the co-administration of raptinal. The IL-1 β level in the control, model, TMP, and TMP+ raptinal groups was 43.5, 147.8, 82.7, and 115.5 ng/L, respectively. The IL-18 level in the control, model, TMP, and TMP+ raptinal groups was 89.6, 334.6, 176.8, and 263.2 ng/L, respectively (Figure 5C). The elevated cleaved-caspase-3, GSDME-N, and NLRP3 levels in OPG^{-/-} mice were markedly reduced by TMP, which were sharply increased by the co-administration of raptinal (Figure 5D). The upregulated CASP3 and ACTA2 in OPG^{-/-} mice were downregulated by TMP, the expression of which was notably increased in the TMP+ raptinal group (Figure 5E).

4. Discussion

Pyroptosis is a newly discovered cell death mode with a high degree of inflammation in recent years, which is programmed and controlled with the dual characteristics of necrosis and apoptosis, and finally triggers a secondary inflammatory response (30). Originally misclassified as apoptosis, pyroptosis was subsequently found to be a form of programmed cell death dependent on the Caspase family and mediated by the Gasdermin protein (31). Herein, as described in other research (11,32), β -GP was used to induce calcification in VSMCs, which was verified by increased calcification, enhanced inflammation, promoted LDH release, and aggravated apoptosis, accompanied by an activation of caspase-3/GSDME signaling. Furthermore, these pathological changes in β -GP-stimulated VSMCs were sharply alleviated by the knockdown of caspase-3 or GSDME, implying that caspase-3/GSDME axis mediated pyroptosis might participate in the progression of calcification in β -GP-stimulated VSMCs.

The present study investigates the molecular mechanisms underlying the protective effects of tetramethylpyrazine (TMP) on β -glycerophosphate (β -GP)-induced calcification and inflammation in MOVAS-1 cells and OPG^{-/-} mice. The findings reveal that TMP significantly mitigates various pathological processes induced by β -GP, including increased calcification, elevated levels of reactive oxygen species (ROS), inflammatory cytokines such as Interleukin-1 β (IL-1 β) and Interleukin-18 (IL-18), lactate dehydrogenase (LDH) release, enhanced apoptosis, and the activation of caspase-3/GSDME signaling. These effects were further corroborated *in vivo*, where TMP administration in OPG^{-/-} mice significantly reduced calcium deposition and inflammation, effects that were reversed by raptinal, a caspase-3 activator. In addition, the increased calcification observed in β -GP-stimulated MOVAS-1 cells highlights the pro-osteogenic environment created by β -GP, a well-known calcification inducer. The concurrent elevation in ROS

levels indicates oxidative stress as a critical mediator of this process. ROS are known to exacerbate vascular calcification by promoting the differentiation of vascular smooth muscle cells (VSMCs) into osteoblast-like cells. TMP's ability to reduce ROS levels suggests that it may exert its protective effects through antioxidant properties, thus preventing oxidative damage that contributes to calcification.

Inflammatory cytokines such as IL-1 β and IL-18 play pivotal roles in vascular inflammation and calcification. The significant reduction of these cytokines by TMP treatment indicates its potent anti-inflammatory effects. This reduction may be attributed to the suppression of the NF- κ B signaling pathway, which is a central regulator of inflammation. By inhibiting this pathway, TMP likely decreases the transcription of pro-inflammatory genes, thereby reducing the levels of IL-1 β and IL-18.

The enhanced apoptosis and LDH release in β -GP-stimulated MOVAS-1 cells indicate cellular injury and membrane damage. LDH is a marker of cell membrane integrity, and its release signifies cell death. TMP's ability to attenuate these effects suggests that it may enhance cell survival by inhibiting apoptotic pathways. The involvement of caspase-3 in apoptosis is well-documented, and TMP's inhibitory effect on caspase-3 activation further supports its role in promoting cell survival. Pyroptosis, a form of programmed cell death distinct from apoptosis, involves activation of caspase-3 and GSDME. This study shows that TMP mitigates β -GP-induced pyroptosis by inhibiting the caspase-3/GSDME pathway. This inhibition is crucial, as pyroptosis contributes to inflammatory responses and calcification. The reversal of TMP's protective effects by raptinal, a caspase-3 activator, underscores the central role of caspase-3 in this process. Thus, TMP's ability to prevent pyroptosis may be a key mechanism through which it exerts its protective effects.

In OPG^{-/-} mice, TMP administration significantly alleviated calcium deposition and reduced the number of calcified nodules. This model is particularly relevant as OPG deficiency is associated with increased vascular calcification, mimicking clinical conditions of enhanced calcification risk. The observed reductions in IL-1 β and IL-18 levels, along with decreased expression of CASP3 and ACTA2, highlight TMP's broad anti-inflammatory and anti-calcification effects. Reversal of these protective effects by co-administration of raptinal further validates the role of caspase-3 in TMP's mechanism of action. The findings from the OPG^{-/-} mouse model suggest that TMP may have significant therapeutic potential in treating vascular calcification and associated inflammatory conditions. By targeting multiple pathways involved in calcification, oxidative stress, and inflammation, TMP provides a comprehensive protective effect. This multi-target approach is advantageous in treating complex diseases like vascular calcification, where multiple pathological processes are involved. Herein, in line with

data presented by Osako (33), vascular calcification was observed in coronary artery tissues of OPG^{-/-} mice, accompanied by enhanced inflammation and activated caspase-3/GSDME signaling, which were also observed in β -GP-stimulated VSMCs. After administration of TMP, vascular calcification and inflammation were markedly alleviated, implying a promising anti-CAC property of TMP. The *in vivo* efficacy of TMP was in line with the observation in β -GP-stimulated VSMCs after the incubation with TMP, especially the repressive effect of TMP against the caspase-3/GSDME signaling, suggesting that TMP might exert the anti-CAC property by inhibiting the caspase-3/GSDME axis mediated VSMCs pyroptosis. Raptinal, the specific activator of caspase-3, was used to identify the function of caspase-3/GSDME signaling in melanoma previously (34). Herein, suppressive effects of TMP on calcification in both β -GP-stimulated VSMCs and OPG^{-/-} mice were abolished by raptinal, accompanied by enhanced inflammation and activated caspase-3/GSDME signaling, suggesting that TMP exerted the anti-CAC function by inhibiting the caspase-3/GSDME pathway. In future work, the relationship between the efficacy and doses of TMP will be explored to better support the therapy treating CAC using TMP. Collectively, TMP alleviated the progression of CAC by inhibiting caspase-3/GSDME mediated pyroptosis.

5. Conclusion

In summary, this study elucidates the protective mechanisms of TMP against β -GP-induced vascular calcification and inflammation. By inhibiting ROS production, reducing inflammatory cytokine release, preventing apoptosis, and blocking caspase-3/GSDME-mediated pyroptosis, TMP effectively mitigates the pathological processes associated with calcification. These findings provide a strong basis for further exploration of TMP as a therapeutic agent for vascular calcification and related inflammatory disorders. Future studies should focus on clinical trials to evaluate the efficacy and safety of TMP in human subjects, as well as exploring its potential synergistic effects with other therapeutic agents.

Funding: None.

Conflict of Interest: The authors have no conflicts of interest to disclose.

References

- Soppert J, Lehrke M, Marx N, Jankowski J, Noels H. Lipoproteins and lipids in cardiovascular disease: From mechanistic insights to therapeutic targeting. *Adv Drug Deliv Rev.* 2020; 159:4-33.
- Anzaki K, Kanda D, Ikeda Y, Takumi T, Tokushige A, Ohmure K, Sonoda T, Arikawa R, Ohishi M. Impact of malnutrition on prognosis and coronary artery calcification in patients with stable coronary artery disease. *Curr Probl Cardiol.* 2023; 48:101185.
- Samadi S, Sadeghi M, Dashtbayaz RJ, Nezamdoost S, Mohammadpour AH, Jomehzadeh V. Prognostic role of osteoprotegerin and risk of coronary artery calcification: A systematic review and meta-analysis. *Biomark Med.* 2023; 17:171-180.
- Kelly-Arnold A, Maldonado N, Laudier D, Aikawa E, Cardoso L, Weinbaum S. Revised microcalcification hypothesis for fibrous cap rupture in human coronary arteries. *Proc Natl Acad Sci U S A.* 2013; 110:10741-10746.
- Narula N, Olin JW, Narula N. Pathologic disparities between peripheral artery disease and coronary artery disease. *Arterioscler Thromb Vasc Biol.* 2020; 40:1982-1989.
- Opdebeeck B, D'Haese PC, Verhulst A. Molecular and cellular mechanisms that induce arterial calcification by indoxyl sulfate and p-cresyl sulfate. *Toxins (Basel).* 2020; 12:58.
- Demola P, Ristalli F, Hamiti B, Meucci F, Di Mario C, Mattesini A. New advances in the treatment of severe coronary artery calcifications. *Cardiol Clin.* 2020; 38:619-627.
- Henein M, Granasen G, Wiklund U, Schermund A, Guerci A, Erbel R, Raggi P. High dose and long-term statin therapy accelerate coronary artery calcification. *Int J Cardiol.* 2015; 184:581-586.
- Leopold JA. Vascular calcification: Mechanisms of vascular smooth muscle cell calcification. *Trends Cardiovasc Med.* 2015; 25:267-274.
- Demer LL, Tintut Y. Inflammatory, metabolic, and genetic mechanisms of vascular calcification. *Arterioscler Thromb Vasc Biol.* 2014; 34:715-723.
- Pang Q, Wang P, Pan Y, Dong X, Zhou T, Song X, Zhang A. Irisin protects against vascular calcification by activating autophagy and inhibiting NLRP3-mediated vascular smooth muscle cell pyroptosis in chronic kidney disease. *Cell Death Dis.* 2022; 13:283.
- Wen C, Yang X, Yan Z, Zhao M, Yue X, Cheng X, Zheng Z, Guan K, Dou J, Xu T, Zhang Y, Song T, Wei C, Zhong H. Nalp3 inflammasome is activated and required for vascular smooth muscle cell calcification. *Int J Cardiol.* 2013; 168:2242-2247.
- Wang Y, Gao W, Shi X, Ding J, Liu W, He H, Wang K, Shao F. Chemotherapy drugs induce pyroptosis through caspase-3 cleavage of a gasdermin. *Nature.* 2017; 547:99-103.
- Shi J, Gao W, Shao F. Pyroptosis: Gasdermin-mediated programmed necrotic cell death. *Trends Biochem Sci.* 2017; 42:245-254.
- Zhang Z, Zhang Y, Xia S, Kong Q, Li S, Liu X, Junqueira C, Meza-Sosa KF, Mok TMY, Ansara J, Sengupta S, Yao Y, Wu H, Lieberman J. Gasdermin E suppresses tumour growth by activating anti-tumour immunity. *Nature.* 2020; 579:415-420.
- Jiang M, Qi L, Li L, Li Y. The caspase-3/GSDME signal pathway as a switch between apoptosis and pyroptosis in cancer. *Cell Death Discov.* 2020; 6:112.
- Kayacan S, Sener LT, Melikoglu G, Kultur S, Albeniz I, Ozturk M. Induction of apoptosis by *Centaurea nerimaniae* extract in HeLa and MDA-MB-231 cells by a caspase-3 pathway. *Biotech Histochem.* 2018; 93:311-319.
- Simonet WS, Lacey DL, Dunstan CR, *et al.*

- Osteoprotegerin: A novel secreted protein involved in the regulation of bone density. *Cell*. 1997; 89:309-319.
19. Tsuda E, Goto M, Mochizuki S, Yano K, Kobayashi F, Morinaga T, Higashio K. Isolation of a novel cytokine from human fibroblasts that specifically inhibits osteoclastogenesis. *Biochem Biophys Res Commun*. 1997; 234:137-142.
 20. Tan KB, Harrop J, Reddy M, Young P, Terrett J, Emery J, Moore G, Truneh A. Characterization of a novel TNF-like ligand and recently described TNF ligand and TNF receptor superfamily genes and their constitutive and inducible expression in hematopoietic and non-hematopoietic cells. *Gene*. 1997; 204:35-46.
 21. Price PA, June HH, Buckley JR, Williamson MK. Osteoprotegerin inhibits artery calcification induced by warfarin and by vitamin D. *Arterioscler Thromb Vasc Biol*. 2001; 21:1610-1616.
 22. Bucay N, Sarosi I, Dunstan CR, Morony S, Tarpley J, Capparelli C, Scully S, Tan HL, Xu W, Lacey DL, Boyle WJ, Simonet WS. Osteoprotegerin-deficient mice develop early onset osteoporosis and arterial calcification. *Genes Dev*. 1998; 12:1260-1268.
 23. Min H, Morony S, Sarosi I, Dunstan CR, Capparelli C, Scully S, Van G, Kaufman S, Kostenuik PJ, Lacey DL, Boyle WJ, Simonet WS. Osteoprotegerin reverses osteoporosis by inhibiting endosteal osteoclasts and prevents vascular calcification by blocking a process resembling osteoclastogenesis. *J Exp Med*. 2000; 192:463-474.
 24. Orita Y, Yamamoto H, Kohno N, Sugihara M, Honda H, Kawamata S, Mito S, Soe NN, Yoshizumi M. Role of osteoprotegerin in arterial calcification: Development of new animal model. *Arterioscler Thromb Vasc Biol*. 2007; 27:2058-2064.
 25. Lin J, Wang Q, Zhou S, Xu S, Yao K. Tetramethylpyrazine: A review of its mechanisms and functions. *Biomed Pharmacother*. 2022; 150:113005.
 26. Lu C, Jiang Y, Zhang F, Shao J, Wu L, Wu X, Lian N, Chen L, Jin H, Chen Q, Lu Y, Zheng S. Tetramethylpyrazine prevents ethanol-induced hepatocyte injury *via* activation of nuclear factor erythroid 2-related factor 2. *Life Sci*. 2015; 141:119-127.
 27. Jiang F, Qian J, Chen S, Zhang W, Liu C. Ligustrazine improves atherosclerosis in rat *via* attenuation of oxidative stress. *Pharm Biol*. 2011; 49:856-863.
 28. Jiang R, Xu J, Zhang Y, Zhu X, Liu J, Tan Y. Ligustrazine alleviates acute lung injury through suppressing pyroptosis and apoptosis of alveolar macrophages. *Front Pharmacol*. 2021; 12:680512.
 29. Zhang F, Jin H, Wu L, Shao J, Wu X, Lu Y, Zheng S. Ligustrazine disrupts lipopolysaccharide-activated NLRP3 inflammasome pathway associated with inhibition of Toll-like receptor 4 in hepatocytes. *Biomed Pharmacother*. 2016; 78:204-209.
 30. Yu P, Zhang X, Liu N, Tang L, Peng C, Chen X. Pyroptosis: Mechanisms and diseases. *Signal Transduct Target Ther*. 2021; 6:128.
 31. Wang YY, Liu XL, Zhao R. Induction of pyroptosis and its implications in cancer management. *Front Oncol*. 2019; 9:971.
 32. Ma WQ, Sun XJ, Wang Y, Zhu Y, Han XQ, Liu NF. Restoring mitochondrial biogenesis with metformin attenuates beta-GP-induced phenotypic transformation of VSMCs into an osteogenic phenotype *via* inhibition of PDK4/oxidative stress-mediated apoptosis. *Mol Cell Endocrinol*. 2019; 479:39-53.
 33. Osako MK, Nakagami H, Shimamura M, Koriyama H, Nakagami F, Shimizu H, Miyake T, Yoshizumi M, Rakugi H, Morishita R. Cross-talk of receptor activator of nuclear factor-kappaB ligand signaling with renin-angiotensin system in vascular calcification. *Arterioscler Thromb Vasc Biol* 2013; 33:1287-1296.
 34. Vernon M, Wilski NA, Kotas D, Cai W, Pomante D, Tiago M, Alnemri ES, Aplin AE. Raptinal induces gasdermin e-dependent pyroptosis in naive and therapy-resistant melanoma. *Mol Cancer Res*. 2022; 20:1811-1821.

Received April 15, 2024; Revised June 18, 2024; Accepted June 22, 2024.

*Address correspondence to:

Honghui Yang, Department of Cardiology, Zhengzhou University, Central China Fuwai Hospital, No. 1, Fuwai Road, Zhengzhou 451464, China.
E-mail: 19503809999@163.com

Released online in J-STAGE as advance publication July 6, 2024.

Financial inclusion and financial gerontology in Japan's aging society

Shotaro Kinoshita^{1,2}, Kohei Komamura^{3,4}, Taishiro Kishimoto^{1,*}

¹Hills Joint Research Laboratory for Future Preventive Medicine and Wellness, Keio University School of Medicine, Tokyo, Japan;

²Graduate School of Interdisciplinary Information Studies, The University of Tokyo, Tokyo, Japan;

³Research Center for Financial Gerontology, Keio University, Tokyo, Japan;

⁴Faculty of Economics, Keio University, Tokyo, Japan.

SUMMARY Japan, the world's most rapidly aging society, faces increasing financial strains related to personalized dementia care. The government has shifted its focus from prevention to coexistence with dementia, as outlined in the 2023 Basic Act on Dementia. Emphasis on financial inclusion aligns with the G20's 2019 "Fukuoka Policy Priorities on Aging and Financial Inclusion", which addresses financial exclusion due to cognitive decline and poor financial literacy. While economic activity among older adults is already hampered by legal challenges and risks associated with dementia, outcomes are expected to worsen as the assets of older adults with dementia are projected to reach 215 trillion JPY (\$1.4 trillion USD) by 2030. Government measures and research in financial gerontology advocate for protecting older adults and promoting flexible financial practices. Enhanced efforts and shared research outcomes are crucial for Japan to be a leader as an advanced aging society.

Keywords dementia, policy, aging

To the Editor,

Japan has the highest aging rate worldwide, with 29.0% of the population aged 65 and over in 2022 (1). Given this situation, Japan has implemented various policy responses to address aging, as well as encouraged conducting research on the aging society (1). The number of patients with dementia is also on the rise: it is estimated to reach 7 million by 2025, which, coupled with Japan's declining birthrate, has created an increasingly difficult financial situation for healthcare insurers and providers (2,3). Providing personalized medical care to prevent dementia in all citizens is not considered a realistic solution. Therefore, in recent years, the Japanese government has focused on coexistence with dementia, rather than prevention. In the deliberative process of the Basic Act on Dementia of 2023, the phrase "the people should strive for prevention" was deleted from the law (3).

Under these circumstances, Japan has recently emphasized "financial inclusion" of older adults and people with dementia. Financial inclusion refers to the concept of ensuring everyone is able to access and benefit from financial services, and is consistent with the United Nations Sustainable Development Goals (SDGs). Financial inclusion of older adults, in particular, has

gained attention since the release of the "G20 Fukuoka Policy Priorities on Aging and Financial Inclusion" from the subordinate organizations of G20 in Japan during June 2019 (4). This Policy Priority proposes strategies to address "financial exclusion", a concept that prevents older adults from accessing financial services due to limited financial literacy, cognitive decline, and social isolation (4) (Figure 1). The challenge is to prevent such financial exclusion among older adults in Japan.

In fact, financial literacy has been observed to decline from the late 60s onward in this population (5). In addition, if a person's cognitive function declines beyond a certain level, he or she is legally considered incapable of performing contractual acts in Japan. Therefore, the purchase or sale of goods or services may become legally invalid if the customer is discovered after the transaction to have dementia. Such lawsuits are on the rise in Japan, causing companies to refrain from high value transactions with older adults for fear of the risk of dementia (3). Given that in Japan, people with lower incomes are reported to be at higher risk of dementia, among other conditions (6), those who need financial services may be excluded from transactions due to cognitive decline.

Indeed, several older adults are financially insecure,

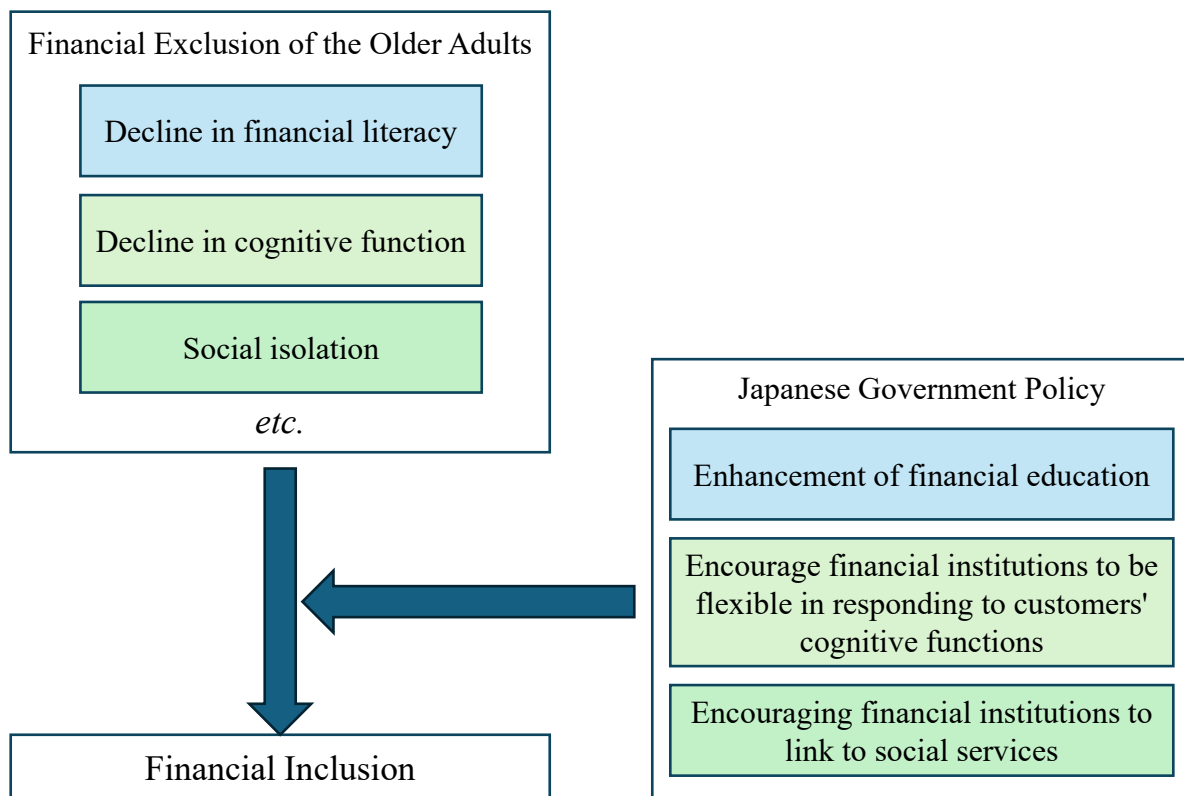


Figure 1. Japanese government policies for financial inclusion of older adults.

and are concerned about their inability to properly manage their assets due to dementia or cognitive dysfunction (7). Moreover, the assets held by older adults with dementia in Japan are projected to reach approximately 215 trillion JPY (\$1.4 trillion USD) by 2030 (3). While ensuring the protection of these assets, the private sector should be prevented from applying excessive brakes on the economic activities of the elderly with residual cognitive functions. Several government measures and research activities in the field of financial gerontology are underway to address the financial inclusion of older adults in Japan.

The first mention of cognitive decline and finance among this population, as well as the first use of financial gerontology in a government document can be found in the Outline of Measures for an Aging Society, a policy package formulated in 2018 (8). Subsequently, the Financial Services Agency's Financial System Council issued a report in 2019 stating that older adult customers should be treated according to their respective cognitive functions rather than their age, and that protections for these customers should be reviewed in light of developments in financial gerontology (9). Furthermore, the Council issued a report in 2020 that calls for financial institutions to be more flexible when dealing with older adult customers with cognitive decline over the counter (10).

Following this, in April 2023, a public call was made requesting up to 350 million JPY (\$2.3 million USD) in research support under the direct control of the Cabinet Office for the purpose of "developing social technologies to support autonomous economic activities based on residents' cognitive functions" (3). In light of these trends, the new Outline of Measures for an Aging Society, formulated in September 2024, further incorporates content related to the financial inclusion of older adults. Specifically, it includes the promotion of understanding of finance and economics among older adults in conjunction with consumer education, the promotion of the development of AI technology to support financial transactions based on cognitive function, and the promotion of financial institutions' cooperation with protection and welfare agencies for the elderly with cognitive decline (11).

In order for Japan to become a role model for the world as an advanced aging society, government initiatives on financial inclusion and research in the field of financial gerontology should be further promoted and the results widely shared.

Funding: None.

Conflict of Interest: The authors have no conflicts of interest to disclose.

References

1. Liu Y, Kobayashi S, Karako K, Song P, Tang W. The latest policies, practices, and hotspots in research in conjunction with the aging of Japan's population. *Biosci Trends*. 2024; 18:219-223.
2. Kinoshita S, Kishimoto T. Ageing population in Japan: Immediate shake-up in healthcare required. *QJM*. 2024; hcae097.
3. Kinoshita S, Kishimoto T. Dementia in Japan: A societal focus. *Lancet Neurol*. 2024; 22:1101-1102.
4. Global Partnership for Financial Inclusion. G20 Fukuoka Policy Priorities on Aging and Financial Inclusion. <https://www.fsa.go.jp/en/news/2019/20190606/engfukuoka.pdf> (accessed July 30, 2024).
5. Okamoto S, Komamura K. Age, gender, and financial literacy in Japan. *PLoS One*. 2021; 16:e0259393.
6. Okamoto S. Socioeconomic factors and the risk of cognitive decline among the elderly population in Japan. *Int J Geriatr Psychiatry*. 2019; 34:265-271.
7. Sano J, Hirazawa Y, Komamura K, Okamoto S. An overview of systems for providing integrated and comprehensive care for older people in Japan. *Arch Pub Health*. 2023; 81:81.
8. Cabinet Office. Outline of Measures for an Aging Society. <https://www8.cao.go.jp/kourei/measure/taikou/h29/hon-index.html> (accessed July 30, 2024). (in Japanese)
9. Financial Services Agency. Report by the Working Group on Financial Markets under the Financial System Council "Asset Formation and Management in an Aging Society". https://www.fsa.go.jp/singi/singi_kinyu/tosin/20190603/01.pdf (accessed July 30, 2024). (in Japanese)
10. Financial Services Agency. Report by the Working Group on Financial Markets under the Financial System Council "Toward the Enhancement of Financial Institutions' Customer-Oriented Business Conduct". https://www.fsa.go.jp/singi/singi_kinyu/tosin/20200805/houkoku.pdf (accessed July 30, 2024). (in Japanese)
11. Cabinet Office. Outline of Measures for an Aging Society. https://www8.cao.go.jp/kourei/measure/taikou/pdf/p_honbun_r06.pdf (accessed September 13, 2024). (in Japanese)

Received August 1, 2024; Revised September 20, 2024; Accepted September 26, 2024.

*Address correspondence to:

Taishiro Kishimoto, Hills Joint Research Laboratory for Future Preventive Medicine and Wellness, Keio University School of Medicine, #7F Azabudai Hills Mori JP Tower 1-3-1 Azabudai, Minato-ku, Tokyo 106-0041, Japan.
E-mail: tkishimoto@keio.jp

Released online in J-STAGE as advance publication October 2, 2024.



Guide for Authors

1. Scope of Articles

BioScience Trends (Print ISSN 1881-7815, Online ISSN 1881-7823) is an international peer-reviewed journal. *BioScience Trends* devotes to publishing the latest and most exciting advances in scientific research. Articles cover fields of life science such as biochemistry, molecular biology, clinical research, public health, medical care system, and social science in order to encourage cooperation and exchange among scientists and clinical researchers.

2. Submission Types

Original Articles should be well-documented, novel, and significant to the field as a whole. An Original Article should be arranged into the following sections: Title page, Abstract, Introduction, Materials and Methods, Results, Discussion, Acknowledgments, and References. Original articles should not exceed 5,000 words in length (excluding references) and should be limited to a maximum of 50 references. Articles may contain a maximum of 10 figures and/or tables. Supplementary Data are permitted but should be limited to information that is not essential to the general understanding of the research presented in the main text, such as unaltered blots and source data as well as other file types.

Brief Reports definitively documenting either experimental results or informative clinical observations will be considered for publication in this category. Brief Reports are not intended for publication of incomplete or preliminary findings. Brief Reports should not exceed 3,000 words in length (excluding references) and should be limited to a maximum of 4 figures and/or tables and 30 references. A Brief Report contains the same sections as an Original Article, but the Results and Discussion sections should be combined.

Reviews should present a full and up-to-date account of recent developments within an area of research. Normally, reviews should not exceed 8,000 words in length (excluding references) and should be limited to a maximum of 10 figures and/or tables and 100 references. Mini reviews are also accepted, which should not exceed 4,000 words in length (excluding references) and should be limited to a maximum of 5 figures and/or tables and 50 references.

Policy Forum articles discuss research and policy issues in areas related to life science such as public health, the medical care system, and social science and may address governmental issues at district, national, and international levels of discourse. Policy Forum articles should not exceed 3,000 words in length (excluding references) and should be limited to a maximum of 5 figures and/or tables and 30 references.

Communications are short, timely pieces that spotlight new research findings or policy issues of interest to the field of global health and medical practice that are of immediate importance. Depending on their content, Communications will be published as "Comments" or "Correspondence". Communications should not exceed 1,500 words in length (excluding references) and should be limited to a maximum of 2 figures and/or tables and 20 references.

Editorials are short, invited opinion pieces that discuss an issue of immediate importance to the fields of global health, medical practice, and basic science oriented for clinical application. Editorials should not exceed 1,000 words in length (excluding references) and should be limited to a maximum of 10 references. Editorials may contain one figure or table.

News articles should report the latest events in health sciences and medical research from around the world. News should not exceed 500 words in length.

Letters should present considered opinions in response to articles published in *BioScience Trends* in the last 6 months or issues of general interest. Letters should not exceed 800 words in length and may contain a maximum of 10 references. Letters may contain one figure or table.

3. Editorial Policies

For publishing and ethical standards, *BioScience Trends* follows the Recommendations for the Conduct, Reporting, Editing, and Publication of Scholarly Work in Medical Journals issued by the International Committee of Medical Journal Editors (ICMJE, <https://icmje.org/recommendations>), and the Principles of Transparency and Best Practice in Scholarly Publishing jointly issued by the Committee on Publication Ethics (COPE, <https://publicationethics.org/resources/guidelines-new/principles-transparency-and-best-practice-scholarly-publishing>), the Directory of Open Access Journals (DOAJ, <https://doaj.org/apply/transparency>), the Open Access Scholarly Publishers Association (OASPA, <https://oaspa.org/principles-of-transparency-and-best-practice-in-scholarly-publishing-4>), and the World Association of Medical Editors (WAME, <https://wame.org/principles-of-transparency-and-best-practice-in-scholarly-publishing>).

BioScience Trends will perform an especially prompt review to encourage innovative work. All original research will be subjected to a rigorous standard of peer review and will be edited by experienced copy editors to the highest standards.

Ethical Approval of Studies and Informed Consent: For all manuscripts reporting data from studies involving human participants or animals, formal review and approval, or formal review and waiver, by an appropriate institutional review board or ethics committee is required and should be described in the Methods section. When your manuscript contains any case details, personal information and/or images of patients or other individuals, authors must obtain appropriate written consent, permission and release in order to comply with all applicable laws and regulations concerning privacy and/or security of personal information. The consent form needs to comply with the relevant legal requirements of your particular jurisdiction, and please do not send signed consent form to *BioScience Trends* to respect your patient's and any other individual's privacy. Please instead describe the information clearly in the Methods (patient consent) section of your manuscript while retaining copies of the signed forms in the event they should be needed. Authors should also state that the study conformed to the provisions of the Declaration of Helsinki (as revised in 2013, <https://wma.net/what-we-do/medical-ethics/declaration-of-helsinki>). When reporting experiments on animals, authors should indicate whether the institutional and national guide for the care and use of laboratory animals was followed.

Reporting Clinical Trials: The ICMJE (<https://icmje.org/recommendations/browse/publishing-and-editorial-issues/clinical-trial-registration.html>) defines a clinical trial as any research project that prospectively assigns people or a group of people to an intervention, with or without concurrent comparison or control groups, to study the relationship between a health-related intervention and a health outcome. Registration of clinical trials in a public trial registry at or before the time of first patient enrollment is a condition of consideration for publication in *BioScience Trends*, and the trial registration number will be published at the end of the Abstract. The registry must be independent of for-profit interest and publicly accessible. Reports of trials must conform to CONSORT 2010 guidelines (<https://consort-statement.org/consort-2010>). Articles reporting the results of randomized trials must include the CONSORT flow diagram showing the progress of patients throughout the trial.

Conflict of Interest: All authors are required to disclose any actual or potential conflict of interest including financial interests or relationships with other people or organizations that might raise questions of bias

in the work reported. If no conflict of interest exists for each author, please state "There is no conflict of interest to disclose".

Submission Declaration: When a manuscript is considered for submission to *BioScience Trends*, the authors should confirm that 1) no part of this manuscript is currently under consideration for publication elsewhere; 2) this manuscript does not contain the same information in whole or in part as manuscripts that have been published, accepted, or are under review elsewhere, except in the form of an abstract, a letter to the editor, or part of a published lecture or academic thesis; 3) authorization for publication has been obtained from the authors' employer or institution; and 4) all contributing authors have agreed to submit this manuscript.

Initial Editorial Check: Immediately after submission, the journal's managing editor will perform an initial check of the manuscript. A suitable academic editor will be notified of the submission and invited to check the manuscript and recommend reviewers. Academic editors will check for plagiarism and duplicate publication at this stage. The journal has a formal recusal process in place to help manage potential conflicts of interest of editors. In the event that an editor has a conflict of interest with a submitted manuscript or with the authors, the manuscript, review, and editorial decisions are managed by another designated editor without a conflict of interest related to the manuscript.

Peer Review: *BioScience Trends* operates a single-anonymized review process, which means that reviewers know the names of the authors, but the authors do not know who reviewed their manuscript. All articles are evaluated objectively based on academic content. External peer review of research articles is performed by at least two reviewers, and sometimes the opinions of more reviewers are sought. Peer reviewers are selected based on their expertise and ability to provide quality, constructive, and fair reviews. For research manuscripts, the editors may, in addition, seek the opinion of a statistical reviewer. Every reviewer is expected to evaluate the manuscript in a timely, transparent, and ethical manner, following the COPE guidelines (https://publicationethics.org/files/cope-ethical-guidelines-peer-reviewers-v2_0.pdf). We ask authors for sufficient revisions (with a second round of peer review, when necessary) before a final decision is made. Consideration for publication is based on the article's originality, novelty, and scientific soundness, and the appropriateness of its analysis.

Suggested Reviewers: A list of up to 3 reviewers who are qualified to assess the scientific merit of the study is welcomed. Reviewer information including names, affiliations, addresses, and e-mail should be provided at the same time the manuscript is submitted online. Please do not suggest reviewers with known conflicts of interest, including participants or anyone with a stake in the proposed research; anyone from the same institution; former students, advisors, or research collaborators (within the last three years); or close personal contacts. Please note that the Editor-in-Chief may accept one or more of the proposed reviewers or may request a review by other qualified persons.

Language Editing: Manuscripts prepared by authors whose native language is not English should have their work proofread by a native English speaker before submission. If not, this might delay the publication of your manuscript in *BioScience Trends*.

The Editing Support Organization can provide English proofreading, Japanese-English translation, and Chinese-English translation services to authors who want to publish in *BioScience Trends* and need assistance before submitting a manuscript. Authors can visit this organization directly at <https://www.iacmhr.com/iac-eso/support.php?lang=en>. IAC-ESO was established to facilitate manuscript preparation by researchers whose native language is not English and to help edit works intended for international academic journals.

Copyright and Reuse: Before a manuscript is accepted for publication in *BioScience Trends*, authors will be asked to sign a transfer of copyright agreement, which recognizes the common

interest that both the journal and author(s) have in the protection of copyright. We accept that some authors (e.g., government employees in some countries) are unable to transfer copyright. A JOURNAL PUBLISHING AGREEMENT (JPA) form will be e-mailed to the authors by the Editorial Office and must be returned by the authors by mail, fax, or as a scan. Only forms with a hand-written signature from the corresponding author are accepted. This copyright will ensure the widest possible dissemination of information. Please note that the manuscript will not proceed to the next step in publication until the JPA Form is received. In addition, if excerpts from other copyrighted works are included, the author(s) must obtain written permission from the copyright owners and credit the source(s) in the article.

4. Cover Letter

The manuscript must be accompanied by a cover letter prepared by the corresponding author on behalf of all authors. The letter should indicate the basic findings of the work and their significance. The letter should also include a statement affirming that all authors concur with the submission and that the material submitted for publication has not been published previously or is not under consideration for publication elsewhere. The cover letter should be submitted in PDF format. For an example of Cover Letter, please visit: <https://www.biosciencetrends.com/downcentre> (Download Centre).

5. Submission Checklist

The Submission Checklist should be submitted when submitting a manuscript through the Online Submission System. Please visit Download Centre (<https://www.biosciencetrends.com/downcentre>) and download the Submission Checklist file. We recommend that authors use this checklist when preparing your manuscript to check that all the necessary information is included in your article (if applicable), especially with regard to Ethics Statements.

6. Manuscript Preparation

Manuscripts are suggested to be prepared in accordance with the "Recommendations for the Conduct, Reporting, Editing, and Publication of Scholarly Work in Medical Journals", as presented at <https://www.ICMJE.org>.

Manuscripts should be written in clear, grammatically correct English and submitted as a Microsoft Word file in a single-column format. Manuscripts must be paginated and typed in 12-point Times New Roman font with 24-point line spacing. Please do not embed figures in the text. Abbreviations should be used as little as possible and should be explained at first mention unless the term is a well-known abbreviation (e.g. DNA). Single words should not be abbreviated.

Title page: The title page must include 1) the title of the paper (Please note the title should be short, informative, and contain the major key words); 2) full name(s) and affiliation(s) of the author(s), 3) abbreviated names of the author(s), 4) full name, mailing address, telephone/fax numbers, and e-mail address of the corresponding author; 5) author contribution statements to specify the individual contributions of all authors to this manuscript, and 6) conflicts of interest (if you have an actual or potential conflict of interest to disclose, it must be included as a footnote on the title page of the manuscript; if no conflict of interest exists for each author, please state "There is no conflict of interest to disclose").

Abstract: The abstract should briefly state the purpose of the study, methods, main findings, and conclusions. For articles that are Original Articles, Brief Reports, Reviews, or Policy Forum articles, a one-paragraph abstract consisting of no more than 250 words must be included in the manuscript. For Communications, Editorials, News, or Letters, a brief summary of main content in 150 words or fewer should be included in the manuscript. For articles reporting clinical trials, the trial registration number should be stated at the end of the Abstract. Abbreviations must be kept to a minimum and non-standard

abbreviations explained in brackets at first mention. References should be avoided in the abstract. Three to six key words or phrases that do not occur in the title should be included in the Abstract page.

Introduction: The introduction should provide sufficient background information to make the article intelligible to readers in other disciplines and sufficient context clarifying the significance of the experimental findings

Materials/Patients and Methods: The description should be brief but with sufficient detail to enable others to reproduce the experiments. Procedures that have been published previously should not be described in detail but appropriate references should simply be cited. Only new and significant modifications of previously published procedures require complete description. Names of products and manufacturers with their locations (city and state/country) should be given and sources of animals and cell lines should always be indicated. All clinical investigations must have been conducted in accordance Materials/Patients and Methods.

Results: The description of the experimental results should be succinct but in sufficient detail to allow the experiments to be analyzed and interpreted by an independent reader. If necessary, subheadings may be used for an orderly presentation. All Figures and Tables should be referred to in the text in order, including those in the Supplementary Data.

Discussion: The data should be interpreted concisely without repeating material already presented in the Results section. Speculation is permissible, but it must be well-founded, and discussion of the wider implications of the findings is encouraged. Conclusions derived from the study should be included in this section.

Acknowledgments: All funding sources (including grant identification) should be credited in the Acknowledgments section. Authors should also describe the role of the study sponsor(s), if any, in study design; in the collection, analysis, and interpretation of data; in the writing of the report; and in the decision to submit the paper for publication. If the funding source had no such involvement, the authors should so state.

In addition, people who contributed to the work but who do not meet the criteria for authors should be listed along with their contributions.

References: References should be numbered in the order in which they appear in the text. Citing of unpublished results, personal communications, conference abstracts, and theses in the reference list is not recommended but these sources may be mentioned in the text. In the reference list, cite the names of all authors when there are fifteen or fewer authors; if there are sixteen or more authors, list the first three followed by *et al.* Names of journals should be abbreviated in the style used in PubMed. Authors are responsible for the accuracy of the references. The EndNote Style of *BioScience Trends* could be downloaded at **EndNote** (https://ircabssagroup.com/examples/BioScience_Trends.ens).

Examples are given below:

Example 1 (Sample journal reference):

Inagaki Y, Tang W, Zhang L, Du GH, Xu WF, Kokudo N. Novel aminopeptidase N (APN/CD13) inhibitor 24F can suppress invasion of hepatocellular carcinoma cells as well as angiogenesis. *Biosci Trends*. 2010; 4:56-60.

Example 2 (Sample journal reference with more than 15 authors):

Darby S, Hill D, Auvinen A, *et al.* Radon in homes and risk of lung cancer: Collaborative analysis of individual data from 13 European case-control studies. *BMJ*. 2005; 330:223.

Example 3 (Sample book reference):

Shalev AY. Post-traumatic stress disorder: Diagnosis, history and life course. In: *Post-traumatic Stress Disorder, Diagnosis, Management and Treatment* (Nutt DJ, Davidson JR, Zohar J, eds.). Martin Dunitz, London, UK, 2000; pp. 1-15.

Example 4 (Sample web page reference):

World Health Organization. The World Health Report 2008 – primary health care: Now more than ever. http://www.who.int/whr/2008/whr08_en.pdf (accessed September 23, 2022).

Tables: All tables should be prepared in Microsoft Word or Excel and should be arranged at the end of the manuscript after the References section. Please note that tables should not in image format. All tables should have a concise title and should be numbered consecutively with Arabic numerals. If necessary, additional information should be given below the table.

Figure Legend: The figure legend should be typed on a separate page of the main manuscript and should include a short title and explanation. The legend should be concise but comprehensive and should be understood without referring to the text. Symbols used in figures must be explained. Any individually labeled figure parts or panels (A, B, *etc.*) should be specifically described by part name within the legend.

Figure Preparation: All figures should be clear and cited in numerical order in the text. Figures must fit a one- or two-column format on the journal page: 8.3 cm (3.3 in.) wide for a single column, 17.3 cm (6.8 in.) wide for a double column; maximum height: 24.0 cm (9.5 in.). Please make sure that the symbols and numbers appeared in the figures should be clear. Please make sure that artwork files are in an acceptable format (TIFF or JPEG) at minimum resolution (600 dpi for illustrations, graphs, and annotated artwork, and 300 dpi for micrographs and photographs). Please provide all figures as separate files. Please note that low-resolution images are one of the leading causes of article resubmission and schedule delays.

Units and Symbols: Units and symbols conforming to the International System of Units (SI) should be used for physicochemical quantities. Solidus notation (*e.g.* mg/kg, mg/mL, mol/mm²/min) should be used. Please refer to the SI Guide www.bipm.org/en/si/ for standard units.

Supplemental data: Supplemental data might be useful for supporting and enhancing your scientific research and *BioScience Trends* accepts the submission of these materials which will be only published online alongside the electronic version of your article. Supplemental files (figures, tables, and other text materials) should be prepared according to the above guidelines, numbered in Arabic numerals (*e.g.*, Figure S1, Figure S2, and Table S1, Table S2) and referred to in the text. All figures and tables should have titles and legends. All figure legends, tables and supplemental text materials should be placed at the end of the paper. Please note all of these supplemental data should be provided at the time of initial submission and note that the editors reserve the right to limit the size and length of Supplemental Data.

5. Submission Checklist

The Submission Checklist will be useful during the final checking of a manuscript prior to sending it to *BioScience Trends* for review. Please visit Download Centre and download the Submission Checklist file.

6. Online Submission

Manuscripts should be submitted to *BioScience Trends* online at <https://www.biosciencetrends.com/login>. Receipt of your manuscripts submitted online will be acknowledged by an e-mail from Editorial Office containing a reference number, which should be used in all future communications. If for any reason you are unable to submit a file online, please contact the Editorial Office by e-mail at office@biosciencetrends.com

8. Accepted Manuscripts

Page Charge: Page charges will be levied on all manuscripts accepted for publication in *BioScience Trends* (Original Articles / Brief Reports / Reviews / Policy Forum / Communications: \$140 per page for black white pages, \$340 per page for color pages; News / Letters: a total cost of \$600). Under exceptional circumstances, the author(s) may apply to the editorial office for a waiver of the publication charges by stating the reason in the Cover Letter when the manuscript online.

Misconduct: *BioScience Trends* takes seriously all allegations of potential misconduct and adhere to the ICMJE Guideline (<https://icmje.org/recommendations>) and COPE Guideline (https://publicationethics.org/files/Code_of_conduct_for_journal_editors.pdf). In cases of

suspected research or publication misconduct, it may be necessary for the Editor or Publisher to contact and share submission details with third parties including authors' institutions and ethics committees. The corrections, retractions, or editorial expressions of concern will be performed in line with above guidelines.

(As of December 2022)

BioScience Trends
Editorial and Head Office
Pearl City Koishikawa 603,
2-4-5 Kasuga, Bunkyo-ku,
Tokyo 112-0003, Japan.
E-mail: office@biosciencetrends.com

